

University of Bath



**PHD**

**Developing a marine biorefinery for the production of fuels and fertilizer from the hydrothermal liquefaction of macroalgae**

Raikova, Sofia

*Award date:*  
2019

[Link to publication](#)

**General rights**

Copyright and moral rights for the publications made accessible in the public portal are retained by the authors and/or other copyright owners and it is a condition of accessing publications that users recognise and abide by the legal requirements associated with these rights.

- Users may download and print one copy of any publication from the public portal for the purpose of private study or research.
- You may not further distribute the material or use it for any profit-making activity or commercial gain
- You may freely distribute the URL identifying the publication in the public portal ?

**Take down policy**

If you believe that this document breaches copyright please contact us providing details, and we will remove access to the work immediately and investigate your claim.

University of Bath



**PHD**

**Developing a marine biorefinery for the production of fuels and fertilizer from the hydrothermal liquefaction of macroalgae**

Raikova, Sofia

*Award date:*  
2019

[Link to publication](#)

**General rights**

Copyright and moral rights for the publications made accessible in the public portal are retained by the authors and/or other copyright owners and it is a condition of accessing publications that users recognise and abide by the legal requirements associated with these rights.

- Users may download and print one copy of any publication from the public portal for the purpose of private study or research.
- You may not further distribute the material or use it for any profit-making activity or commercial gain
- You may freely distribute the URL identifying the publication in the public portal ?

**Take down policy**

If you believe that this document breaches copyright please contact us providing details, and we will remove access to the work immediately and investigate your claim.

Download date: 13. Jun. 2019

# Developing a marine biorefinery for the production of fuels and fertilizer from the hydrothermal liquefaction of macroalgae

---

Sofia Raikova

A thesis submitted for the degree of Doctor of Philosophy

University of Bath

Department of Chemical Engineering

September 2018

Attention is drawn to the fact that copyright of this report rests with the author. A copy of this thesis has been supplied on condition that anyone who consults it is understood to recognise that its copyright rests with the author and that they must not copy it or use material from it except as permitted by law or with the consent of the author.

This thesis may be made available for consultation within the University Library and may be photocopied or lent to other libraries for the purposes of consultation with effect from

.....  
Signed on behalf of the Faculty of Engineering

.....

*This thesis is dedicated to Georgina Paterson – you deserve ballads of praise and epic poetry, but you get a book about seaweed instead.*

# Abstract

Hydrothermal liquefaction (HTL) is a promising, low-energy route for the conversion of wet biomass, such as macroalgae, to bio-crude oils, which can be upgraded to advanced biofuels. Co-products of HTL, such as the nutrient-rich aqueous phase, can also be valorised within a biorefinery paradigm. This project sought to explore the effects of feedstock variation and quality on the products from the HTL process.

Initially, a comprehensive screen of a wide range of species of UK macroalgae specific to the South West was undertaken, encompassing all three major macroalgae classes and the correlation between biomass biochemical composition and HTL reactivity was assessed. The complexity of interactions occurring under HTL conditions meant that a simple additive model based on crude biochemical breakdown was insufficient to account for reactivity across all species and predict bio-crude yields. Macroalgae belonging to the genus *Ulva* gave the highest yields of bio-crude, and would be expected to be a promising feedstock for an HTL biorefinery based in the South West of the UK.

Although *Ulva* presented a promising HTL feedstock in the UK, geographical and environmental effects are known to affect the biochemical composition of macroalgae. As such, the impact of geographical variability on the production of bio-crude from a single species of macroalgae was assessed. One of the highest bio-crude producers from the UK, *Ulva intestinalis*, was selected and sampled across a 1,200 km stretch of Swedish coastline before being processed using HTL. Geographical variability in macroalgae composition was substantial across the sampling spectrum, including between sites a short distance apart, resulting in significant levels of variation in bio-crude yield and aqueous phase product composition. As such, suitable feedstock species for future biorefineries will need to be individually assessed for each location, even for locations within relatively close proximity.

A functioning macroalgal biorefinery will also need to have the capacity to handle multiple marine pollutants, including marine plastics. In order to understand the effect of plastics on HTL processing, the effect of simultaneous processing of UK macroalgae with common marine plastic pollutants was assessed. Thermally stable plastics polyethylene and polypropylene were unreactive under the conditions tested, but were more readily degraded under HTL conditions in the presence of macroalgae, and synergistic effects between biomass and plastic conversion were observed. Synergistic effects were also observed for nylon 6, which almost completely depolymerised under HTL conditions to

generate the caprolactam monomer, which may constitute an additional revenue source within a marine biorefinery.

Finally, the concept of implementing HTL as a route to simultaneous remediation of marine plastics and algal blooms in the developing world was investigated. Bloom-forming macro- and microalgae harvested in Vietnam were co-liquefied with plastics using similar protocols to those implemented for the UK macroalgae. Due to geographical variation in macroalgae composition, synergistic effects between macroalgae and plastic conversion were stronger than those observed for UK biomass, producing bio-crudes in higher yields and with better fuel properties.

Geographical variability plays a substantial role in dictating feedstock quality and influencing HTL outcomes, and different species are likely to be optimal for different biorefinery locations. The inevitable presence of marine plastic pollutants can affect HTL, but can, in some cases, be beneficial for bio-crude yields and properties. Ultimately, HTL has been demonstrated to be a highly promising route to generating value from marine macroalgal resources, including marine plastic pollutants.

# Acknowledgements

I would like to express my gratitude first and foremost to my supervisor, Dr. Chris Chuck, for his infectious enthusiasm, insightful advice, fruitful discussions, career guidance, endless patience, coffee breaks, questionable puns, and, crucially, his ability to always look on the bright side. Without his unrelenting support and constant encouragement, this PhD would certainly not have been possible. A huge thank you is also due to Dr. Mike Allen for his guidance, creativity, and, in no small measure, for all the seaweed. And also the jellyfish.

Many of the successes of my PhD have undoubtedly been due to Dr. Jon Wagner's training at the early stages of my research and his work in setting up the running of HTL within our department. Having never been much of a Lego enthusiast as a child, the discovery of Swagelok has been, to my surprise, one of the most enjoyable aspects of my lab work, and Jon's engineering insights have been instrumental to my understanding of the principles of reactor design and construction.

The Chuck Group in its many manifestations has been a pleasure to work with – special thanks to Dr. Rhod Jenkins, Dr. Joe Donnelly and Dr. Sophie Parsons for their wise life and career advice. None of it has been taken on board, obviously.

I would also like to express my gratitude to the Centre for Sustainable Chemical Technologies for generously funding this PhD, and giving me the opportunity to develop my skills and to travel. In particular, thank you to Suslab '14 for always taking the belt and braces approach.

On that note, I must acknowledge Dr. Oli Weber, Dr. Emma Sackville, Dr. Jemma Rowlandson and Dr. James Coombs OBrien, for convincing me to do a PhD during that fateful dinner one night in late 2013, and for all their support in the years since, in a poorly disguised attempt to atone for this.

I would be nowhere without my family and friends. To my family, and especially to Niall, Pixie, Yana, Jackie, the Lunchables, the occupants of Illuminati HQ, and to everyone else that has had my back and supported and encouraged me through the good times and the downright woeful times, I offer an absolute mountain of gratitude.

A final shout out to the well-dressed man in the café I worked in at the age of sixteen, for kindly informing me that Chemical Engineering “wasn't really a woman's subject”. I must admit, as I submit my PhD thesis to the Department of Chemical Engineering, the memory is pretty gratifying.

# Dissemination

## Journal articles

Arising primarily from work presented in this thesis

**Raikova, S.**, Le, C.D., Beacham, T.A., Jenkins, R.W., Allen, M.J., Chuck, C.J., 2017. *Towards a marine biorefinery through the hydrothermal liquefaction of macroalgae native to the United Kingdom*. *Biomass and Bioenergy*, **107**, 244–253. doi:10.1016/j.biombioe.2017.10.010

**Raikova, S.**, Olsson, J., Mayers, J., Nylund, G., Albers, E., Chuck, C.J., 2018. *Effect of geographical location on the variation in products formed from the hydrothermal liquefaction of *Ulva intestinalis**. *Energy & Fuels*, **Accepted manuscript**. doi:10.1021/acs.energyfuels.8b02374

**Raikova, S.**, Knowles, T., Allen, M.J., Chuck, C.J., *Co-liquefaction of macroalgae with common marine plastic pollutants*, *ACS Sustainable Chemistry & Engineering*, **Submitted manuscript**

**Raikova, S.**, Allen, M.J., Chuck, C.J., *Thermochemical processing of macroalgae for renewable fuels and chemicals*, *Biofuels, Bioproducts and Biorefining*, **Submitted manuscript**

## Co-authored publications

Coma, M., Martinez Hernandez, E., Abeln, F., **Raikova, S.**, Donnelly, J., Arnot, T.C., Allen, M., Hong, D.D., Chuck, C.J., 2017. *Organic waste as a sustainable feedstock for platform chemicals*. *Faraday Discussions*. **202**, 175–195. doi:10.1039/C7FD00070G

Piccini, M., **Raikova, S.**, Brigden, K., Allen, M. J., Chuck, C., *A synergistic use of microalgae and macroalgae for heavy metal bioremediation and bioenergy production through hydrothermal liquefaction*, *Sustainable Energy and Fuels*, **Accepted manuscript**

Landels, A., Beacham, T.A., Evans, C.T., Carnovale, G., **Raikova, S.**, Cole, I.S., Goddard, P., Chuck, C.J., Allen, M., *Improving electrocoagulation floatation for harvesting microalgae*, *Algal Research*, **Submitted manuscript**



## **Conference contributions**

255<sup>th</sup> ACS National Meeting: Nexus of Food, Energy and Water (New Orleans, LA, USA) March 2018, Oral presentation, “Hydrothermal liquefaction for marine macroalgal biorefinery”

International Workshop on Vietnamese Algae Conversion (Hanoi University of Mining and Geology, Vietnam) January 2017, Oral presentation, “HTL for the production of fuels and chemicals from Vietnamese algae”

ChemEngDay UK (University of Bath, Bath, UK) March 2016, Poster presentation, “Exploring a range of UK seaweed species for the production of fuels and fertiliser”

# Abbreviations

ANOVA	Analysis of Variance	ICP-MS	Inductively-coupled plasma mass spectrometry
ÅHS	Åhus, Sweden	ICP-OES	Inductively-coupled plasma optical emission spectrometry
AMS	Accelerator mass spectrometry	KKR	Karlskrona, Sweden
AN	<i>Ascophyllum nodosum</i>	LCA	Life cycle assessment
AP	Aqueous phase	LD	<i>Laminaria digitata</i>
CC	<i>Chondrus crispus</i>	LH	<i>Laminaria hyperborea</i>
CHG	Catalytic hydrothermal gasification	NMR	Nuclear magnetic resonance (spectroscopy)
CHN	Carbon, hydrogen and nitrogen (when referring to elemental analysis)	NY	Nylon 6
CSTR	Continuous stirred tank reactor	PC	<i>Pelvetia canaliculata</i>
daf	Dry, ash free	PE	Polyethylene
DHPAEC-PAD	High performance anion exchange chromatography with pulsed amperometric detection	PFR	Plug flow reactor
E2E	Environment-Enhancing Energy	PP	Polypropylene
ER	Energy ratio	PUFA	Polyunsaturated fatty acid(s)

EROI	Energy Return on Energy Invested	RR	<i>Rhizoclonium riparium</i>
FC	<i>Fucus ceranoides</i>	SC	<i>Solieria chordalis</i>
FTIR	Fourier-transform infrared spectrometry	SM	<i>Sargassum muticum</i>
FV	<i>Fucus vesiculosus</i>	STH	Stockholm, Sweden
GBG	Tjörn, Sweden	TBG	Trelleborg, Sweden
GC-FID	Gas chromatography with flame ionisation detection	TC	Total carbon
GC/MS	Gas chromatography/mass spectrometry	TGA	Thermogravimetric analysis
GHG	Greenhouse gas	TJÖ	Tjärnö, Sweden
HBG	Helsingborg, Sweden	TN	Total nitrogen
HE	<i>Himantalia elongata</i>	UI	<i>Ulva intestinalis</i>
HHV	Higher heating value	UL	<i>Ulva lactuca</i>
HTG	Hydrothermal gasification	UV	Ultraviolet
HTL	Hydrothermal liquefaction	VSV	Västervik, Sweden
HUMG	Hanoi University of Mining and Geology		

# Table of contents

## **Preliminary pages**

Abstract .....	i
Acknowledgements.....	iii
Dissemination .....	iv
Abbreviations.....	vi
Table of contents .....	viii
List of figures .....	xiii
List of tables .....	xviii

## **Chapter 1 – Literature review .....**

1.1	Context.....	2
1.2	Biomass utilisation.....	2
1.2.1	Advanced biofuel feedstocks in the UK.....	4
1.2.2	Third generation feedstocks: marine biomass.....	4
1.3	Thermochemical processing.....	5
1.3.1	Hydrothermal liquefaction .....	6
1.4	HTL of macroalgal biomass .....	11
1.4.1	Feedstocks examined to date .....	11
1.4.2	Process parameters .....	15
1.4.3	Continuous processing .....	19
1.5	HTL products.....	21
1.5.1	Bio-crude.....	21
1.5.2	Aqueous phase products .....	25
1.5.3	Solid phase products .....	27
1.5.4	Gaseous products .....	28

1.6	The biorefinery concept .....	28
1.6.1	Macroalgae cultivation .....	29
1.6.2	Integration with environmental services .....	32
1.6.3	Biorefinery model.....	34
1.6.4	Technoeconomics and life cycle assessment .....	35
1.7	Concluding remarks.....	36
1.8	Aims and objectives.....	37
1.9	References .....	39

## **Chapter 2 - Towards a marine biorefinery through the hydrothermal liquefaction of macroalgae native to the United Kingdom .....**

2.1	Context.....	58
2.2	Biomass and Bioenergy paper.....	60
2.2.1	Keywords .....	60
2.2.2	Abbreviations.....	60
2.2.3	Highlights .....	61
2.2.4	Abstract.....	61
2.2.5	Introduction.....	62
2.2.6	Methods .....	64
2.2.7	Results and Discussion .....	67
2.2.8	Conclusions.....	81
2.2.9	Acknowledgements .....	82
2.2.10	References.....	83
2.3	Supplementary information.....	90
2.3.1	Collection and preparation of macroalgal biomass.....	90
2.4	Appendices.....	92
2.4.1	Appendix 2A.....	92

2.4.2	Appendix 2B .....	92
2.4.3	Appendix 2C .....	93
2.5	Context and appendix references .....	94

**Chapter 3 – Effect of geographical location on the variation in products formed from the hydrothermal liquefaction of *Ulva intestinalis* .....**

3.1	Context.....	96
3.2	Energy and Fuels paper .....	98
3.2.1	Abstract.....	98
3.2.2	Introduction.....	99
3.2.3	Methods .....	101
3.2.4	Results and discussion .....	104
3.2.5	Conclusions.....	118
3.2.6	Acknowledgements .....	119
3.2.7	Dedication .....	119
3.2.8	References.....	120
3.3	Supporting information.....	129
3.4	Context references .....	140

**Chapter 4 – Co-liquefaction of UK macroalgae with common marine plastic pollutants .....**

4.1	Context.....	142
4.2	Sustainable Chemistry and Engineering paper .....	144
4.2.1	Abstract.....	144
4.2.2	Introduction.....	145
4.2.3	Methods .....	147

4.2.4	Results and discussion .....	150
4.2.5	Conclusions.....	171
4.2.6	Conflicts of interest.....	171
4.2.7	Acknowledgments .....	172
4.2.8	References.....	173
4.3	Supplementary information.....	179
4.4	Appendices.....	188
4.4.1	Appendix 4A.....	188
4.4.2	Appendix 4B.....	188
4.5	Context and appendix references.....	189

## **Chapter 5 – Co-liquefaction of bloom-forming Vietnamese algae with common marine plastic pollutants..... 191**

5.1	Declaration .....	192
5.2	Introduction.....	192
5.3	Aims .....	193
5.4	Experimental .....	193
5.4.1	Materials.....	193
5.4.2	Batch reactions.....	194
5.4.3	Extraction .....	195
5.4.4	Characterisation .....	196
5.5	Results and discussion .....	196
5.5.1	Hydrothermal co-liquefaction of algal and plastic wastes.....	196
5.5.2	Fate of remaining plastics.....	204
5.6	Conclusions.....	205
5.7	References.....	207

<b>Chapter 6 – Conclusions and future work .....</b>	<b>209</b>
6.1 Conclusions.....	210
6.2 Future work .....	212



# List of figures

Figure 1.3-1 – Hydrothermal liquefaction phase diagram [49] .....	6
Figure 1.3-2 – Processes and products in hydrothermal liquefaction of macroalgae .....	8
Figure 1.3-3 – Simplified summary of key reaction pathways in the HTL of macroalgae [60]. .....	10
Figure 1.4-1 – An example of a bench-scale continuous HTL reactor [98] .....	20
Figure 1.5-1 – van Krevelen diagram summarising some macroalgal bio-crudes described in literature to date compared to the approximate elemental composition of crude oil. Data labels are explained in Table 1.5-1.....	22
Figure 1.6-1 – Illustration of three different anchoring structures for kelp aquaculture. Top right: ring system for <i>Laminaria</i> [134]; top left: basic hanging rope curtain cultivation system for the brown seaweed <i>Laminaria</i> ; bottom: nearshore <i>Macrocystis</i> planting system [135]. .....	30
Figure 1.6-2 – Concept multi-use installations for offshore wind and macroalgae cultivation [141].....	31
Figure 1.6-3 – Cradle-to-grave model of hypothetical biorefinery centred around macroalgal HTL .....	34
Figure 1.6-4 – Conceptual design of a floating biorefinery, incorporating cultivation, harvesting and processing [156] .....	35
Figure 2.2-1 – Effect of a) the heating rate on the bio-crude yield from <i>A. nodosum</i> and b) reaction temperature on product distribution from the HTL of <i>A. nodosum</i> (mass fractions on dry basis). Non-closure of the mass balance is predominantly due to loss of some volatiles from the aqueous and bio-crude fractions on work up. ....	68
Figure 2.2-2 – Effect of reaction temperature on a) phosphate and b) ammonia concentration of aqueous phase from HTL of <i>A. nodosum</i> .....	70
Figure 2.2-3 – a) <i>A. nodosum</i> ground particles with from left to right with an average particle size of 62.5, 187.5, 375, 950, 1550 $\mu\text{m}$ . b) Product mass balance from the HTL conversion of <i>A. nodosum</i> over variable particle size, at 345 °C (dry basis). The remaining fraction of the mass is assigned to volatile losses from the aqueous and bio-crude fractions on work up.....	71

Figure 2.2-4 – Product distribution from HTL of 13 macroalgae species (345 °C; ca. 30 K min <sup>-1</sup> ). The remaining fraction of the mass is assigned to volatile losses from the aqueous and bio-crude fractions on work up.....	75
Figure 2.2-5 – Correlation between biomass biochemical composition and bio-crude yields and bio-crude nitrogen from HTL of 13 macroalgae species: a) biomass lipid vs. yield; b) biomass analysed carbohydrate vs. yield; c) biomass protein vs. yield; and d) biomass protein vs. bio-crude nitrogen. ....	76
Figure 2.2-6 – Comparison of experimentally obtained bio-crude yields and yields calculated using the additive model proposed by Biller and Ross for HTL of 13 UK macroalgae species.....	78
Figure 2.2-7 – a) Deposition of carbon and nitrogen from the initial feedstock into the bio-crude for the 13 species of macroalgae b) energy recovery of the bio-crude as a proportion of the biomass HHV.....	79
Figure 2.2-8 – a) Ammonia and phosphate deposition in the aqueous phase for each strain of macroalgae. b) Correlation between biomass protein and ammonia concentration in the aqueous phase from HTL of 13 macroalgae species. ....	81
Figure 2.4-1 – TGA of <i>A. nodosum</i> , used to assess ash and moisture content .....	92
Figure 3.2-1 – Map of sampling sites; Atlantic sites are represented by yellow markers, Baltic sites represented by blue markers. Three samples were obtained at each site, with sampling locations located approx. 50–7000 m apart. ....	101
Figure 3.2-2 – Total biochemical mass balance for <i>U. intestinalis</i> collected from three sampling sites across eight locations around the coast of Sweden. Error bars are derived from duplicate analysis of protein content, and triplicate analysis of total carbohydrate. ....	105
Figure 3.2-3 – Elemental composition of <i>U. intestinalis</i> collected from three sampling sites across eight locations around the coast of Sweden. Carbon, hydrogen and nitrogen analysis was carried out in duplicate; error was negligible. ....	106
Figure 3.2-4 – Mass balance of product fractions obtained from the hydrothermal liquefaction of 24 samples of <i>U. intestinalis</i> from three sampling sites across eight locations around the coast of Sweden. The remaining fraction of the mass is assigned to volatile losses from the aqueous and bio-crude fractions on work up. Mass yields quoted on a dry basis. Error bars represent the standard deviation of the product mass fractions obtained from three repeat runs of HTL using the GBG3 feedstock.....	107

Figure 3.2-5 – Bio-crude nitrogen and sulfur levels. The markers represent average values for each sampling location; the bars represent the highest and lowest values for bio-crude N and S obtained for each location. ....	110
Figure 3.2-6 – Characteristics of the bio-crude produced through HTL processing of <i>U. intestinalis</i> from three sampling sites across eight locations around the coast of Sweden; a) bio-crude H/C ratios, b) higher heating values (HHV), and c) the energy recovery (ER) in the bio-crude products. Bars represent the values obtained for individual bio-crudes; yellow markers denote averages for each location.....	111
Figure 3.2-7 – Carbon distribution (weight %) between the product phases of HTL of <i>U. intestinalis</i> from three sampling sites across eight locations around the coast of Sweden .....	113
Figure 3.2-8 – Partitioning of biomass metals between HTL product phases, presented as a proportion of the total metal content of the macroalgae feedstock.....	113
Figure 3.2-9 – Partitioning of key elements suitable for plant growth in the aqueous phase: a) K and Mg; b) Ca and P; c) N and S.....	115
Figure 3.2-10 – Partitioning of P between the product phases for the HTL of <i>U. intestinalis</i> from three sampling sites across eight locations around the coast of Sweden .....	118
Figure S3.3-1 - Overlaid GC/MS chromatograms for 24 bio-crudes derived from macroalgae harvested across eight locations around the coast of Sweden .....	135
Figure S3.3-2 - Overlaid GC/MS chromatograms for Tjö bio-crudes .....	136
Figure S3.3-3 - Overlaid GC/MS chromatograms for GBG bio-crudes .....	136
Figure S3.3-4 - Overlaid GC/MS chromatograms for HBG bio-crudes .....	137
Figure S3.3-5 - Overlaid GC/MS chromatograms for TBG bio-crudes.....	137
Figure S3.3-6 – Overlaid GC/MS chromatograms for ÅHS bio-crudes.....	138
Figure S3.3-7 – Overlaid GC/MS chromatograms for KKR bio-crudes.....	138
Figure S3.3-8 - Overlaid GC/MS chromatograms for VSV bio-crudes.....	139
Figure S3.3-9 - Overlaid GC/MS chromatograms for STH bio-crudes.....	139
Figure 4.2-1 – Mass balances of HTL products from liquefaction of <i>L. digitata</i> blended with a) polyethylene, b) polypropylene and c) nylon 6.....	152
Figure 4.2-2 – Synergistic effects on bio-crude yields from liquefaction of <i>L. digitata</i> , blended with plastics (PE = polyethylene, PP = polypropylene, NY = nylon 6).....	154

Figure 4.2-3 - Synergistic effects on bio-crude production for co-liquefaction of <i>L. digitata</i> with polyethylene (10 % blend) at a range of heating rates .....	155
Figure 4.2-4 – Bio-crude compositions produced from the co-liquefaction of <i>L. digitata</i> with PE, PP and nylon 6, where a) is carbon wt. %, b) hydrogen wt. % c) nitrogen wt. % and d) is HHV of the bio-crudes .....	156
Figure 4.2-5 – FT-IR spectra of bio-crudes obtained from liquefaction of pure <i>L. digitata</i> and <i>L. digitata</i> blends with polyethylene, polypropylene and nylon 6 .....	158
Figure 4.2-6 – Overlay of GC chromatograms of bio-crudes created from <i>L. digitata</i> /PE feedstocks at PE blend levels of 0, 10, 25 and 50 %. The high-intensity peak at 17.09 min is of solvent origin. ....	160
Figure 4.2-7 – Overlay of GC chromatograms of bio-crudes created from <i>L. digitata</i> /nylon 6 feedstocks at nylon blend levels of 0, 10 and 25 %. The high-intensity peak at 17.09 min is of solvent origin. ....	162
Figure 4.2-8 – Elemental composition of aqueous phases produced from liquefaction of <i>L. digitata</i> blended with a) PE, b) PP and c) nylon 6 .....	163
Figure 4.2-9 – Distribution of biogenic carbon, fossil (plastic) carbon, and other elements in bio-crude oils produced from co-liquefaction of <i>L. digitata</i> with plastics.....	165
Figure 4.2-10 – TGA of pure plastics and solid phase products from co-liquefaction of <i>L. digitata</i> with plastics.....	166
Figure 4.2-11 – Distribution of nylon 6 between HTL product phases .....	167
Figure 4.2-12 – Bio-crude yields from liquefaction of blended macroalgae/plastic feedstocks; a) <i>F. serratus</i> , b) <i>S. muticum</i> , c) <i>U. lactuca</i> . (PE = polyethylene, PP = polypropylene, NY = nylon 6).....	169
Figure 4.2-13 – Synergistic effects on bio-crude yields from liquefaction of blended macroalgae/plastic feedstocks; a) <i>F. serratus</i> , b) <i>S. muticum</i> , c) <i>U. lactuca</i> . (PE = polyethylene, PP = polypropylene, NY = nylon 6). ....	170
Figure S4.3-1 – Proposed radical mechanism of ketone formation from polyethylene under hydrothermal conditions.....	184
Figure S4.3-2 – Mass balances for hydrothermal liquefaction of marine macroalgae with plastics: a) <i>F. serratus</i> , b) <i>S. muticum</i> and c) <i>U. lactuca</i> with polyethylene; d) <i>F. serratus</i> , e) <i>S. muticum</i> and f) <i>U. lactuca</i> with polypropylene; g) <i>F. serratus</i> , h) <i>S. muticum</i> and i) <i>U. lactuca</i> with nylon 6.....	185

Figure 5.4-1 – L: batch reactor used for hydrothermal liquefaction; R: six-port Micromeritics FlowPrep 060 furnace.....	194
Figure 5.5-1 – Mass balance of products from HTL of <i>Spirulina</i> and <i>Ulva</i> (310 °C, 60 min) .....	197
Figure 5.5-2 – Co-liquefaction bio-crude yields with a) increasing PE content, and b) increasing PP content.....	198
Figure 5.5-3 – Extent of synergistic effects on bio-crude production during co-liquefaction of a) <i>Spirulina</i> and b) <i>Ulva</i> with polyethylene (PE) and polypropylene (PP) .....	199
Figure 5.5-4 – H/C ratio and nitrogen content in bio-crudes.....	200
Figure 5.5-5 – Ratio of CH <sub>2</sub> to CH <sub>3</sub> peak areas quantified using <sup>1</sup> H NMR.....	201
Figure 5.5-6 – Overlaid GC/MS chromatogram of bio-crudes produced from pure <i>Ulva</i> and co-processing with polyethylene and polypropylene .....	202
Figure 5.5-7 – Bio-crude yield and biogenic vs. fossil carbon distribution. Overall percentages of fossil carbon are labelled.....	202
Figure 5.5-8 – Analysis of the solid residue from the HTL of <i>Spirulina</i> and <i>Ulva</i> (320 °C, 40 mins) where a) solid residue yield with increasing plastic, b) carbon content (%) of the solid phase products and c) nitrogen content (%) of the solid phase products .....	205

# List of tables

Table 1.3-1 – Properties of liquid water at ambient and subcritical conditions.....	7
Table 1.4-1 – Reports on hydrothermal liquefaction of macroalgae to date (aqueous HTL only presented).....	11
Table 1.5-1 – Feedstocks corresponding to bio-crudes summarised in Fig. 1.5-1.....	22
Table 2.2-1 – Biomass proximate, biochemical and ultimate analysis, and higher heating value (HHV).....	72
Table 2.3-1 – Location and description of macroalgal samples.....	91
Table 3.2-1 – Bio-crude yields from Swedish <i>U. intestinalis</i> , reported on a dry, ash-free basis (DAF %).....	108
Table S3.3-1 – Elemental composition of bio-crudes from HTL of <i>U. intestinalis</i> .....	129
Table S3.3-2 – Elemental composition of aqueous phase products from HTL of <i>U. intestinalis</i> .....	131
Table S3.3-3 – Identities of notable compounds in bio-crude products from the liquefaction of <i>U. intestinalis</i> from multiple locations.....	132
Table 4.2-1 – Identities of notable compounds in bio-crude products from co-liquefaction of <i>L. digitata</i> with polyethylene.....	160
Table 4.2-2 – Distribution of carbon from the initial plastic into the bio-crude phase .	165
Table S4.3-1 – Composition of gas phase products of hydrothermal liquefaction of <i>L. digitata</i> with plastics.....	179
Table S4.3-2 – Identities of compounds identified in volatile portion of bio-crude oils	180
Table 4.4-2 – Thermal characteristics of major components of <i>L. digitata</i> [12].....	188
Table 5.5-1 – Distribution of carbon from the initial plastic into the bio-crude phase .	203

# Chapter 1

---

## Literature review

## **1.1 Context**

The use of fossil resources has allowed humanity to achieve technological progress at an unprecedented rate. Fossil fuels, particularly crude oil, have historically been inexpensive, and their abundance and easy accessibility has led to the development of vast industries and widespread infrastructure for crude oil processing to fuels and commodity chemicals. Currently 88 % of all energy used by the global population is of fossil origin [1], with an estimated 2 L liquid fuel consumed daily by each human being on the planet [2]. However, increases in energy demand associated with rapid population growth and economic development have led to significant depletion of fossil resources, leading to suggestions that the Earth has only enough accessible crude oil in known reserves to meet 53.3 years of global production if consumption continues at current rates [3]. Political and economic uncertainty has also led to extremely volatile oil prices. These factors, coupled with the undisputable contribution of continued fossil fuel consumption to atmospheric CO<sub>2</sub> accumulation and possibly irreversible climate change, has driven research into more sustainable production of energy and chemicals. Although significant developments have been made in the field of alternative energy sources, such as wind and solar energy, not all sectors are easily adaptable. For instance, electrification within the transport sector becomes increasingly difficult to implement with increasing payload, making high-energy density liquid fuels the only viable option for heavier transport, such as commercial aviation and marine freight [4]. Additionally the vast swathes of pre-existing fossil-based infrastructure, from the 700 petroleum refineries [5] to the fleet of existing road vehicles (currently numbering nearly 1.25 billion) [6], should ideally be incorporated into alternative energy and chemical platforms in order to ease the transition to a less fossil-dependent global economy. High-energy density bio-based liquid fuels with properties mimicking crude oil could play a significant role in transitioning away from fossil fuels and towards “greener” and more renewable feedstocks.

## **1.2 Biomass utilisation**

Prior to the development of fossil fuel-based technologies, biomass was the primary global source of energy, and has the potential to displace a significant portion of fossil resources in fuel and chemical production [7]. Biofuels have the potential to provide a low-carbon, sustainable and environmentally benign source of energy compatible with existing transport and refinery infrastructure [8].

In terms of fuel production from biomass, feedstocks are typically subdivided into categories. First-generation biofuels, which are based on the use of existing food crops,



such as corn, sugarcane or soybean, represent a diversion of agricultural land and resources away from the food industry (the “food vs fuel” debate) [9]. Although first-generation biofuels have now displaced 1–1.5 % of the petroleum consumed globally, this has required an estimated 1 % of the world’s total agricultural land [10]. Similarly, it has been estimated that over 19 % of the EU’s arable land would need to be repurposed from food production to first-generation fuel crops in order to replace just 6 % of its petroleum with biofuel [11]. Logistically, a 100 % switch is impossible without significant developments in biofuel production technologies. Although first-generation fuel technologies are currently the best-developed, given the logistical and ethical considerations inherent in first-generation biofuel production, they constitute a medium term solution at best [12]. Much recent research has focused on the utilisation of alternative biomass sources.

Advanced biofuels are those derived from non-agricultural fuel crops, such as cassava and *Miscanthus* (which can be cultivated on marginal land), agricultural or municipal wastes, yeasts, bacteria, or aquatic feedstocks (micro- and macroalgae).<sup>i</sup> These have the potential to overcome a number of sustainability issues associated with use of first-generation biomass feedstocks, and displace a number of petrochemicals in addition to fuels. It is important to note that, although the use of second-generation biofuel feedstocks addresses the impacts of first-generation feedstocks on the food industry, they can have other environmental and economic implications. Second-generation fuels from crop residues, such as corn, can be used to create lignocellulosic bioethanol, but their removal from agricultural land to produce a relatively low-energy-density biofuel can produce high CO<sub>2</sub> emissions per unit energy, ultimately increasing overall CO<sub>2</sub> emissions relative to natural decomposition [13]. Cultivation of dedicated fuel crops on non-arable land, although not in direct competition with food crops, would still require vast amounts of space to cultivate sufficient volumes of biomass to supply global demand [14]. Cultivation of fuel crops without sustainable management could cause significant ecosystem damage, and a number of significant technological developments are necessary for efficiency improvement and cost reductions before second-generation technologies can be implemented on an industrial scale [15]. However, the overall sustainability of biofuel production can be improved by integrating with a number of

---

<sup>i</sup> The terminology varies between sources, and feedstocks are sometimes referred to interchangeably as “second generation” for non-food terrestrial crops and industrial and agricultural wastes and “third generation” for aquatic biomass, although “second generation” is also sometimes used to describe all non-edible biofuel feedstocks.

additional services, such as environmental remediation, to generate added-value fuel production systems in both economic and environmental terms [16].

### **1.2.1 Advanced biofuel feedstocks in the UK**

In the UK, biofuels are crucial to the development of a low-carbon economy and compliance with emissions targets. The UK's Climate Change Act has mapped out a reduction of 80 % GHG emissions from 1990 levels by 2050 [17], with biofuels projected to play a key role [18,19]. Between 2003 and 2011, UK biofuel consumption increased from 0.026 to 3.1 % of all UK transport fuel [20], accounted for predominantly by imported fuels, or fuels manufactured from imported feedstocks [21]. As of August 2016, UK feedstocks accounted for 26 % of total biofuel use, with approximately 50 % of fuels and feedstocks supplied by members of the EU [22]. Development of UK-based biofuel production systems is essential to ensuring biofuel production security.

The UK has a thriving agricultural sector, with over 70 % of land taken up by agriculture [23]. Hence, the large-scale adoption of first-generation biofuels is clearly unfeasible, and second-generation terrestrial crops are likely to be space-limited. However, some second-generation biomass crops such as *Miscanthus* show significant potential to displace up to 10 % of the UK's total energy use without having a negative impact on food production, requiring significantly less fertiliser, while simultaneously improving soil and water quality relative to conventional food and fuel crops [24].

In addition to the potential scope for second-generation fuel crop exploitation, the UK has huge potential for a seaweed production industry.

### **1.2.2 Third generation feedstocks: marine biomass**

Algae are a range of uni- and multicellular aquatic predominantly photosynthetic organisms, although exact definitions of what comprises an alga differ between sources. The chemical compositions of macroalgae and microalgae can vary significantly, influenced in part by species, but also affected significantly by cultivation conditions (temperature, CO<sub>2</sub> and nutrient availability, pH, light levels) [25]. Microalgae are unicellular organisms ranging between several µm to several hundred µm in diameter [26]. They are widely recognised as one of the oldest existing types of microorganism, comprising an estimated 72,500 different species, although some sources have (less conservatively) estimated this number to fall anywhere between 5 and 50 million [27].

It is estimated that approximately 9,000 species of macroalgae exist, falling into three major divisions of Heterokontophyceae, or brown seaweed (ca. 2,000 species), Rhodophyceae, or red seaweed (ca. 6,000 species) and Chlorophyceae, or green

seaweed (*ca.* 1,200 species) [28], giving a rich variety of potential biofuel feedstocks. Nearly 28 million tonnes wet macroalgal biomass is generated annually through aquaculture, with the macroalgae industry currently worth over \$7 bn. [29]. Worldwide utilisation of macroalgae is predominantly accounted for by the food sector (*ca.* 87–90 %) [30], although other applications, such as nutraceuticals, cosmetics, pigments, proteins and other chemicals, also play a significant role [31].

Both micro- and macroalgae typically have higher photosynthetic efficiencies with respect to terrestrial crops (approx. 6–8 %, *c.f.* *ca.* 1.8–2.2 %) [32], giving higher biomass yields per unit area (for instance, a yield of *ca.* 13.1 kg dry biomass m<sup>-2</sup> year<sup>-1</sup> for brown seaweed, *c.f.* *ca.* 10 kg m<sup>-2</sup> year<sup>-1</sup> for sugarcane) [26,33]. Many algae have lower water demands [34], faster growth rates and shorter growth cycles [35] than terrestrial crops. Additionally, the high CO<sub>2</sub> fixation capacity of algae opens a route for algal cultivation to simultaneously mitigate industrial CO<sub>2</sub> emissions. In light of these advantages, algae have been recently considered a promising alternative feedstock for biofuel and chemical production. Investigations into micro- and macroalgae utilisation for biofuel production have spanned anaerobic digestion to biogas [36], fermentation of sugars to bioethanol [37] and conversion of algal lipids to biodiesel [38,39], with thermochemical processing techniques, such as hydrothermal gasification (HTG), pyrolysis and hydrothermal liquefaction (HTL) attracting attention in more recent years [40].

### **1.3 Thermochemical processing**

Thermochemical processing techniques utilise heat to effect the transformation of biomass. These encompass processes such as pyrolysis and hydrothermal liquefaction (HTL) to generate liquid fuels, carbonisation and torrefaction for solid fuel production, and gasification to generate gaseous products [41]. Thermochemical processing is particularly attractive owing to its simplicity and suitability for processing feedstocks with a wide variety of biochemical compositions [28].

Thermochemical processes utilise the entire organic fraction of a biomass feedstock, including lipids, proteins and carbohydrates, lifting the constraint on high-lipid biomass selection for biodiesel production. Pyrolysis and HTL generate high-energy density liquid products, and are hence the most relevant for fuel production for transport systems.

Although pyrolysis has been demonstrated for many types of biomass, it is less suitable for processing wet or high-moisture feedstocks due to the high energy penalties inherent in vapourising water at atmospheric pressure [25] – for biomasses with a high mass fraction of water, such as micro- and macroalgae and some tropical grasses, drying can become prohibitively expensive (both economically and energetically) [41] in a process

with a narrow energy return on investment (EROI) margin. Macroalgal biomass with a moisture content of *ca.* 80 % and a total energy content of 12 MJ kg<sup>-1</sup> (analysed for *L. saccharina*) [32] would require 10.4 MJ kg<sup>-1</sup> to dry fully, constituting 87 % of the total energy content of the biomass [42]. For high-moisture biomass, HTL poses a number of substantial advantages.

### 1.3.1 Hydrothermal liquefaction

The concept of hydrothermal liquefaction had its inception in the 1970s [43], was explored by Shell [44] in the 1980s, and has now been applied to a wide variety of feedstocks, although research interest is dependent on the cost of conventional crude oil [45]. HTL is ideally suited to wet feedstocks such as micro- and macroalgae, significantly lowering the energy requirements associated with feedstock drying [46,47], decreasing oxygen content and boosting the energy content of the resulting liquid products [28] with respect to oils generated through pyrolysis. The comparatively milder temperatures encountered in HTL with respect to pyrolysis also fall comfortably within the operational temperatures of most conventional oil refineries [48], making the process easily scaleable.

In hydrothermal liquefaction, biomass is reacted in a closed system in water at sub-/near-critical conditions (200–374 °C, 50–280 bar).

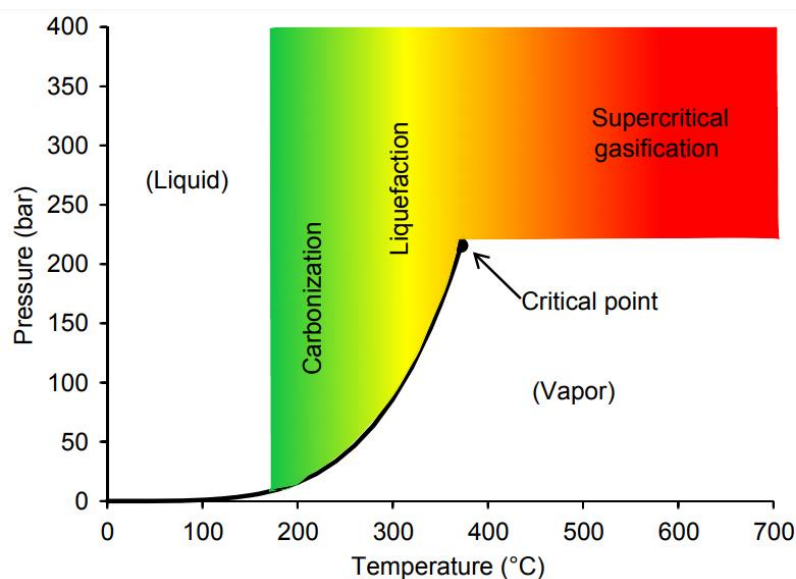


**Figure 1.3-1** – Hydrothermal liquefaction phase diagram [49]

At subcritical conditions, the properties of liquid water (including dielectric constant, density, diffusivity, polarity, viscosity, H-bonding and H<sup>+</sup> donor capabilities) are significantly different to those observed at standard conditions. As a result, subcritical liquid H<sub>2</sub>O begins to exhibit behaviour more typical of a non-polar organic solvent.

*Table 1.3-1 – Properties of liquid water at ambient and subcritical conditions*

	<b>Ambient conditions</b>	<b>Subcritical conditions</b>	<b>Supercritical conditions</b>	
<b>Temperature, <math>T</math> (°C)</b>	25	250	400	400
<b>Pressure, <math>p</math> (MPa)</b>	0.1	5	25	50
<b>Density, <math>\rho</math> (g cm<sup>-3</sup>)</b>	0.997	0.8	0.17	0.58
<b>Dielectric constant, <math>\epsilon</math> (F m<sup>-1</sup>)</b>	78.5	27.1	5.9	10.5
<b>Ionic product, <math>pK_w</math></b>	14.0	11.2	19.4	11.9
<b>Heating capacity, <math>C_p</math> (kJ kg<sup>-1</sup> K<sup>-1</sup>)</b>	4.22	4.86	13	6.8
<b>Viscosity, <math>\gamma</math> (mPa s)</b>	0.89	0.11	0.03	0.07
<b>Thermal conductivity, <math>\lambda</math> (mW m<sup>-1</sup> K<sup>-1</sup>)</b>	608	620	160	438

As water approaches its critical point, the viscosity of water drops dramatically, allowing for increasing rates of reaction, whilst the dielectric constant decreases, allowing the electron shared between the oxygen and hydrogen atoms to be more evenly distributed. This results in the oxygen atom becoming less electronegative, and the water molecule less polar overall, with a greater affinity for organic hydrocarbons – the solvent properties of water at 300 °C are comparable to those of acetone at ambient conditions [50]. Additionally, the cascade of changes in the properties of water means that under hydrothermal conditions, water can also act as a hydrogen source, and participate in hydrolysis, as well as cleavage, condensation and ionic reactions [50]. In this form, it can behave as both an acid and a base, and function simultaneously as a solvent, reactant and catalyst for a cascade of organic reactions, enabling the breakdown of biomass components into reactive fragments, and subsequent repolymerisation.

The most important product from a biofuel perspective is a so-called “bio-crude” oil, consisting of a large number of aliphatic and aromatic hydrocarbons, as well as oxygenates and nitrogenates. Thus named because of its superficial similarity to crude oil, bio-crude has the potential to be similarly refined in existing fossil refineries to generate fuels and other refinery chemicals [51–53].

An aqueous phase containing light polar organics and dissolved minerals is also formed, alongside a solid, metal-rich carbonaceous char and a number of gaseous products (Fig.

1.3-2). Due to differences in polarity between water and the oily products, phase separation occurs spontaneously.

HTL is a relatively low-energy technique, owing to the high pressures generated within the system, which maintain water in the liquid phase, avoiding the large enthalpic penalty of a phase change to steam [43,54]. Additionally, the single-phase fluid system observed in HTL effectively eliminates mass transfer limitations [43].

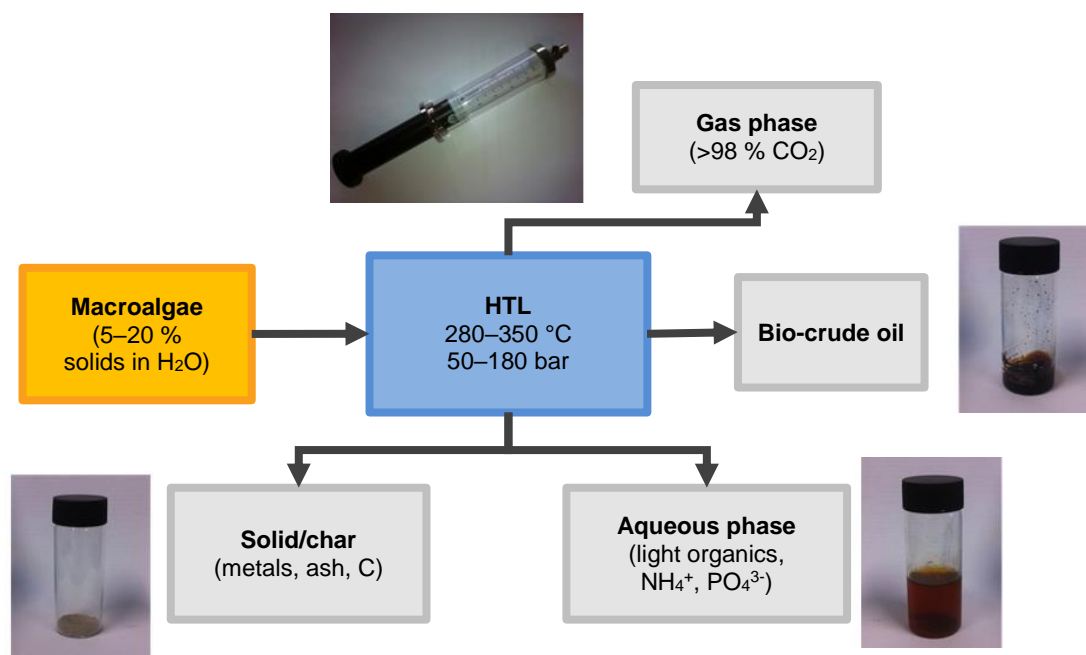


*Figure 1.3-2 – Processes and products in hydrothermal liquefaction of macroalgae*

### **1.3.1.1 HTL mechanisms**

HTL consists of hundreds of simultaneous reactions, the exact pathways of which are not fully understood [50]. Although the complex array of reactions is strongly feedstock-dependent, the process consists of three main stages [55]:

- 1) Biomass depolymerisation
- 2) Monomer degradation (dehydration, decarboxylation, cleavage, deamination)
- 3) Recombination of reactive fragments

Initially, hydrolysis leads to the formation of water-soluble oligomers and monomers. Cellulose undergoes hydrolysis and subsequent decarboxylation to form glucose, in addition to acetic acid, acetaldehyde, glyceraldehyde, glycoaldehyde, furfural derivatives, and a wide range of other species [54]. Hemicellulose can form xylose and mannose monomers, as well as glucose and galactose. Xylose can take one of several forms in an aqueous medium, which can degrade to form different products: its pyranose

ring form can generate furfural, whilst its open chain form can react to form glyceraldehyde, pyruvaldehyde, as well as formic and lactic acids [54]. The degradation of lignin present in woody biomass gives rise to a number of phenolic products [56]. Lipids undergo hydrolysis to free fatty acids and glycerol [55]. Glycerol can degrade further to alcohols and aldehydes, whilst fatty acids, despite their thermal stability, can form long-chain hydrocarbons under HTL conditions [55]. Proteins undergo decarboxylation and deamination; a substantial portion of the nitrogen in proteins is incorporated into the bio-crude products, although ammonia is also formed and incorporated into the aqueous phase products. Maillard reactions between amines and sugars form cyclic and polycyclic nitrogenous species such as pyridines and pyrroles [57], which can act as radical scavengers and inhibit radical chain reactions [55]. Dehydration reactions, leading to oxygen content reduction, also occur. Reactive fragments can undergo repolymerisation [55], forming large, insoluble asphaltenes [58], although it has been suggested that the formation of high-molecular weight products may be suppressed to some degree by the presence of hydrogen or hydrogen radicals [50] generated in subcritical water environments [59]. It has also been suggested that aldol condensation may play a role in hydrothermal reaction mechanisms [50].

A simplified schematic [60] summarising some of the key reactions underpinning hydrothermal liquefaction is presented in Fig. 1.1-3.

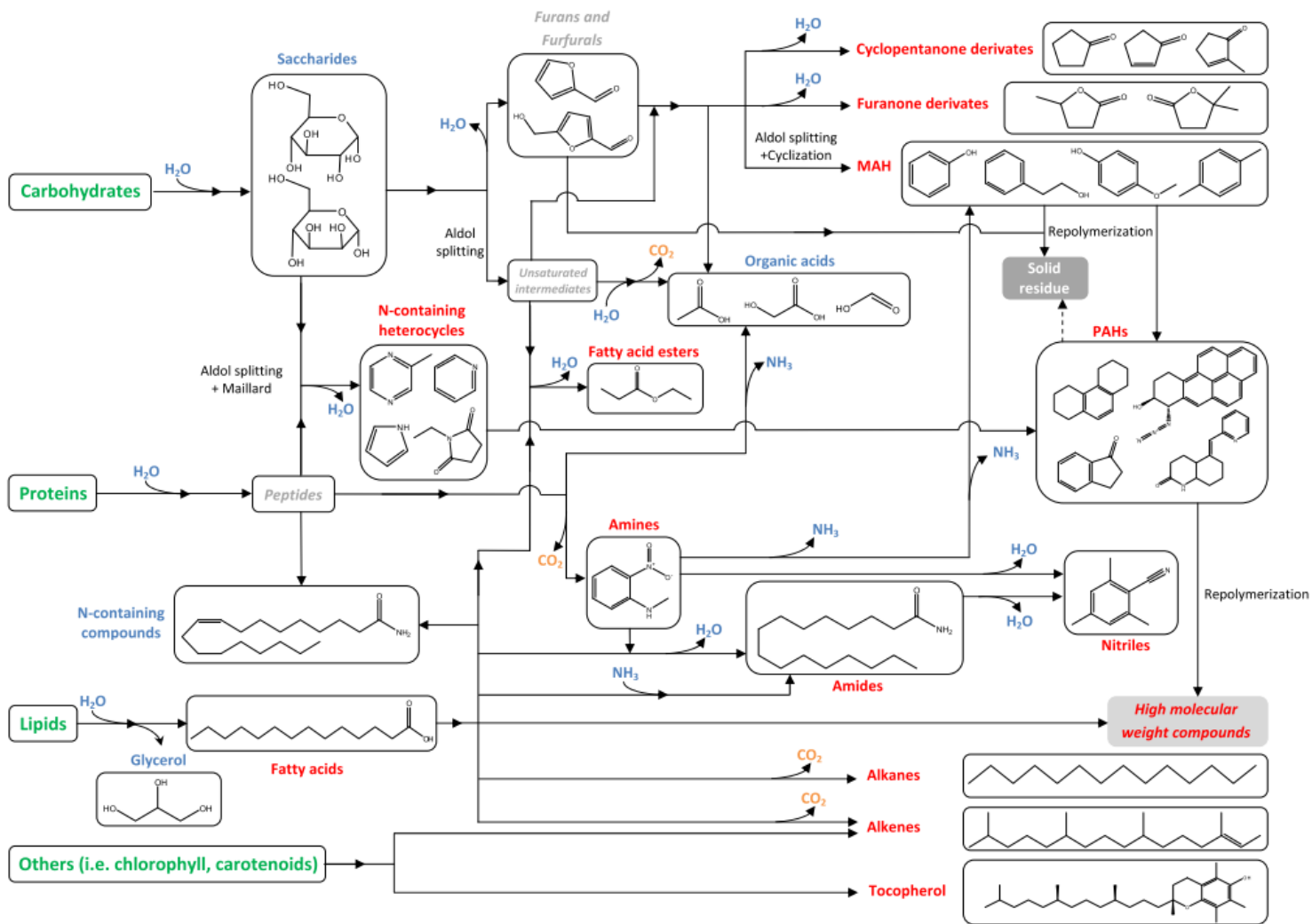


**Figure 1.3-3** – Simplified summary of key reaction pathways in the HTL of macroalgae [60].

(Compounds listed in green represent those present in the initial biomass, blue – in the aqueous phase products, and red – in the bio-crude oil phase.)



## 1.4 HTL of macroalgal biomass

HTL has been used to process a wide variety of biomass and waste types to date, including biowaste (manure, sewage sludge, urban waste, food processing waste), lignocellulose (wood and crop residues) and micro- and macroalgae. Due to its high (10–50 %) inherent ash and moisture content, macroalgae is ideally suited to HTL, particularly due to its high alkali content, which can cause problems of slagging and fouling in pyrolysis and combustion [61], but has been suggested to have a catalytic effect on bio-crude production under HTL conditions [61,62].

The first liquefaction experiments reported for a macroalgal feedstock were carried out by Elliott *et al.* in 1988 [63]. Processing of kelp of the genus *Macrocystis* yielded 19.2 % (on a dry, ash-free basis (daf)) bio-crude oil. They were the first to note that carbohydrates in macroalgal biomass generate oils composed predominantly of phenolic compounds. The idea of macroalgae as a feedstock was subsequently picked up again by Aresta and Dibenedetto in 2005 [38], and has attracted considerable attention in recent years.

### 1.4.1 Feedstocks examined to date

HTL of macroalgae has spanned species across all classifications, as well as across the globe. Liquefaction of macroalgae belonging to the Chlorophyta, Rhodophyta and Heterokontophyta classes has been reported.

**Table 1.4-1** – Reports on hydrothermal liquefaction of macroalgae to date (aqueous HTL only presented)

Year	Macroalgae species	Conditions	Max. bio-crude yield (%)	
1988	<i>Macrocystis</i> sp. (brown)	350 °C, 30 min, 5–10 % TS, CO	19.2 (daf)	[63]
2005	<i>Chaetomorpha linum</i> (green)	395 °C, 1 h, N <sub>2</sub>	8 <sup>a</sup>	[38]
2010	<i>Enteromorpha (Ulva) prolifera</i> (green)	300°C, 30 min, 12 % TS, 5 % Na <sub>2</sub> CO <sub>3</sub>	23.0 <sup>a</sup>	[62]
2011	<i>Laminaria saccharina</i> (brown)	350 °C, 15 min, 10 % TS	19.3 (daf) <sup>a</sup>	[32]

2012	<i>Sargassum patens</i> C. Agardh (brown)	340 °C, 15 min, 10 % TS	32.1 (daf) <sup>a</sup>	[64]
2013	<i>Enteromorpha (Ulva) prolifera</i> (green) with <i>Spirulina</i> microalgae	340 °C, 40 min, 10 % TS	21.6 <sup>a</sup>	[25]
2014	<i>Ulva prolifera</i> (green)	290 °C, 20 min, 25% TS	28.4 <sup>a</sup>	[65]
2014	<i>Derbesia tenuissima</i> (green)	350 °C, 8 min, 6.6 % TS, N <sub>2</sub>	19.7 (33.4 daf) <sup>a</sup>	[66]
2014	<i>Ulva ohnoi</i> (green)	350 °C, 8 min, 6.6 % TS, N <sub>2</sub>	18.7 (30.1 daf) <sup>a</sup>	[66]
2014	<i>Chaetomorpha linum</i> (green)	350 °C, 8 min, 6.6 % TS, N <sub>2</sub>	9.7 (16.6 daf) <sup>a</sup>	[66]
2014	<i>Cladophora coelothrix</i> (green)	350 °C, 8 min, 6.6 % TS, N <sub>2</sub>	13.5 (20.0 daf) <sup>a</sup>	[66]
2014	<i>Oedogonium</i> sp. (green)	350 °C, 8 min, 6.6 % TS, N <sub>2</sub>	26.2 (35.9 daf) <sup>a</sup>	[66]
2014	<i>Cladophora vagabunda</i> (green)	350 °C, 8 min, 6.6 % TS, N <sub>2</sub>	19.7 (25.7) <sup>a</sup>	[66]
2014	<i>Saccharina</i> spp. (brown)	350 °C, continuous system	27.7 (daf)	[67]
2015	<i>Laminaria digitata</i> (brown)	350 °C, 15 min, 21 % TS	13 (17.6 daf) <sup>a</sup>	[61]
2015	<i>Laminaria hyperborea</i> (brown)	350 °C, 15 min, 21 % TS	8.1 (9.8 daf) <sup>a</sup>	[61]
2015	<i>Laminaria saccharina</i> (brown)	350 °C, 15 min, 21 % TS	10 (13 daf) <sup>a</sup>	[61]
2015	<i>Alaria esculenta</i> (brown)	350 °C, 15 min, 21 % TS	13 (17.8 daf) <sup>a</sup>	[61]
2015	<i>Fucus vesiculosus</i> (brown)	350 °C, 15 min, 10 % TS	22.0	[60]

2015	<i>Laminaria saccharina</i> (brown)	350 °C, 15 min, 10 % TS	20.9	[60]
2015	<i>Alaria esculenta</i> (brown)	360 °C, 15 min, 10 % TS	29.4	[60]
2016	<i>Oedogonium</i> spp. (green)	300 °C, 5 min, 5 % TS, continuous system	24 (daf) <sup>a</sup>	[68]
2018	<i>Gracilaria gracilis</i> (green)	350 °C, 15 min, 9 % TS, N <sub>2</sub>	15.7	[69]
2018	<i>Cladophora glomerata</i> (green)	350 °C, 15 min, 9 % TS, N <sub>2</sub>	16.9	[69]
2018	<i>Sargassum tenerrimum</i> (brown)	280 °C, 15 min, 14 % TS	16.3	[70]

<sup>a</sup> Aqueous phase organics extracted

The most well-researched species thus far have been *Enteromorpha* (*Ulva*) [62,65,71–73] and *Laminaria* [32,61]. Anastasakis and Ross described the HTL of three *Laminaria* types, as well as the brown macroalgae *Alaria esculenta*, collected off the coast of Scotland, obtaining the highest yields of 13 % bio-crude for *L. digitata* and *A. esculenta* [61]. Notably high reported bio-crude yields of up to 32.1 % (daf) have been reported for *Sargassum patens* C. Agardh, and 35.9 % (daf) for *Oedogonium* sp. [66], although yields of 10–25 % are more commonly observed [32,38,53,60–62]. These yields are markedly lower than those typically observed for microalgae: this has been attributed to lower lipid levels in macroalgal feedstocks with respect to microalgae, and high carbohydrate contents instead leading to the formation of aqueous phase products [25,54,60]. However, Singh and Balagurumurthy [74] speculated that the higher bio-crude yield produced by *Ulva fasciata* (compared to *Enteromorpha* sp. and *Sargassum muticum*) was due to its higher carbohydrate content.

A comprehensive mechanistic study of algal HTL by Biller and Ross [75] found that biochemical components contributed to bio-crude formation in the order lipids > proteins > carbohydrates. In a similar study examining specifically low-lipid algae, Yang *et al.* [57] confirmed that proteins made a greater contribution to bio-crude oil yields than polysaccharides, albeit at the expense of inflated nitrogen content. Similar results were observed by Yu *et al.* [76]. This serves as a useful proxy for macroalgae, which tend to

contain low lipid and high carbohydrate levels, although no macroalgae-specific verification of this relationship has been published to date. Elliott *et al.* suggested that the oil generated from liquefaction of *Saccharina spp.* is more similar in composition and properties to lignocellulosic HTL bio-crude than the microalgal equivalent [67], despite the almost complete absence of any lignin in the macroalgal feedstock.

A number of other investigations [77,78] have also looked into rationalising HTL reactivity through the use of model compounds (and combinations thereof). Neveux *et al.* [66] attempted to use the model proposed by Biller and Ross [75] to predict the bio-crude yields of marine and freshwater Chlorophyceae, but experimentally obtained bio-crude yields did not fit the proposed additive conversion framework. A satisfactory agreement ( $\pm 5\%$ ) between theoretical and experimental values was obtained for only one of the feedstocks examined, whilst the model underestimated the remaining yields by a significant margin (22–56 %). *Ulva ohnoi* generated 30.1 % (daf) bio-crude, while *Cladophora coelothrix* only yielded 20.0 % (daf), despite containing higher levels of both protein and lipid. The group speculated that Biller and Ross's model falls short due to its failure to account for bio-crude generated through secondary reactions between biochemical compounds, in addition to individual additive conversion yields from each biochemical fraction.

Neveux *et al.* were able to obtain yields of up to 26 % (36 % daf) from liquefaction of freshwater macroalga *Oedogonium sp.* – speculated to be attributable to a high lipid content of 10 %. Six species were examined in total, with significant variation observed in product mass balances, despite belonging to the same class (Chlorophyceae). An attempt to reconcile the frequently conflicting speculations [25,32,61,64] that biomass ash may have a catalytic effect on bio-crude production was unsuccessful: both marine *Derbesia tenuissima* and freshwater *Cladophora vagabunda* yielded 19.7 % bio-crude (daf), despite *Derbesia* having double the ash content.

An investigation into co-liquefaction of micro- and macroalgae (respectively, *Arthrospira platensis* and *Enteromorpha prolifera*) by Jin *et al.* [25] found synergistic effects for both bio-crude yield and quality, obtaining higher yields, HHV and C/H, as well as lower O contents, from a 1:1 mix of the two feedstocks processed at 340 °C. It was speculated that the presence of fatty acids from *Spirulina* catalysed conversion of *Enteromorpha* proteins, leading to a collateral increase in the bio-crude nitrogen levels. The occurrence of secondary reactions between initial liquefaction products was confirmed: a number of peaks were observed in the GC/MS of the bio-crude generated by the feedstock mixture that were not present in the oils formed from the individual algae.

## 1.4.2 Process parameters

As well as feedstock composition, HTL product distributions are influenced by reaction temperature, retention time, initial biomass to water ratio, and the presence and type of catalyst [79]. Optimal conditions are most often identified on the basis of maximising either bio-crude production or bio-crude energy content (higher heating value, or HHV), typically falling in the range 10–20 % solid loading, with 350 °C being the most commonly quoted “ideal” operating temperature for bio-crude yield optimisation [43]. It is generally acknowledged that higher heating rates encourage bio-crude production [80–82].

It must be noted here that yields obtained also depend heavily on the separation methods and solvents used to extract the bio-crude. Chlorinated solvents (DCM, chloroform) are used in most cases, although some studies have reported extraction procedures carried out using acetone [83], toluene [84] or hexane [85].

In addition, “bio-crude” is sometimes defined differently by different researchers: some studies define bio-crude as the sum of all solvent-extractable material from all four product phases, whilst others decant the aqueous phase products (which may contain some solvent-extractable components) before extracting the bio-crude. Extracting the aqueous phase organics can boost bio-crude yields (Xu and Savage calculated aqueous phase organics to comprise 8.4 % of the total bio-crude recovery for the liquefaction of *Nannochloropsis* sp.) [86], but comes at the expense of bio-crude quality and HHV. Aqueous phase organics in the aforementioned study had an HHV of 30.8 MJ kg<sup>-1</sup>, attributable to higher O and N content and depleted C and H, compared to 39.4 MJ kg<sup>-1</sup> for the non-water-soluble bio-crude.

Finally, bio-crude yields are variously calculated on the basis of either total biomass, or “dry, ash-free” (daf) material by different researchers. Although quoting on a daf basis leads to bio-crude yields appearing elevated, yields quoted on the basis of total biomass better serve to represent HTL mass balances in a real-world scenario.

### 1.4.2.1 Reaction temperature

Optimal reaction conditions for bio-crude production are feedstock-dependent, with a variety of conditions reported to be “optimal” by different sources. Reaction temperature has been suggested by some researchers to be the most influential factor influencing HTL product distribution [87]. Temperatures of 340–350 °C are frequently cited to give the highest bio-crude yields [32,60,66], although Zhou *et al.* observed that bio-crude production from *Enteromorpha prolifera* began to decline above 300 °C, obtaining a maximum yield of 23.0 % [62], whilst Yang *et al.* found that a temperature of 290 °C

generated a 28.4 % bio-crude from the same feedstock species [65]. This may potentially be attributed to differences in solid loading (13 % solid used by Zhou *et al.*; 33 % for Yang *et al.*), but could also be due to inherent geographic and seasonal variations in macroalgae composition [88–90] (*E. prolifera* was calculated to contain 30.1 % ash by Zhou and only 15.9 % by Yang).

Paradoxically, the reaction conditions Xu *et al.* [72] identified as producing the highest bio-crude yields from *E. prolifera* (ash content 38.0 %) were almost diametrically opposed to the general trends observed by most other authors. High bio-crude yields (a maximum yield of bio-crude of 31.7 % (daf), corresponding to a total yield of 21.5 %) appeared to be favoured by long reaction times (60 min), high alkali catalyst loadings (20 wt.% K<sub>2</sub>CO<sub>3</sub>), a reaction temperature of 370 °C and an unusually high biomass to water ratio of 3.5:8.4 (48 % total solids). Although employing high solid concentrations in the slurry improves energy efficiency (a smaller volume of water must be heated per unit biomass), it was acknowledged by the authors that this was too high to give processability in a continuous system. The comparatively low water loading contributed to the low oxygen content of the bio-crude oil (6.9 %, compared to 22.4 % obtained by Zhou *et al.* for the same feedstock) [62]. The low oxygen content contributed to the high bio-crude energy content – 39.4 kJ g<sup>-1</sup>, comparable to crude oil. A notably high heating rate – known for encouraging bio-crude yields [91] – was used ( $\geq 75$  °C min<sup>-1</sup>), and approximately 48 % of the original energy content of the starting biomass could be recovered in the bio-crude phase.

More recently, the conversion of *Sargassum tenerrimum* has been described [70]. Bio-crude extraction with a combination of acetone and ether resulted in a maximum bio-crude yield of 16.6 % at 280 °C (residence time 15 min), dropping to 14.7 % when temperature was increased to 300 °C.

#### **1.4.2.2 Residence time**

Residence times have been examined by a number of researchers over the years, although more often in the context of non-macroalgae feedstocks. It is generally acknowledged that long reaction times (beyond *ca.* 15 min) are detrimental to bio-crude yields: longer reaction times tend to favour polymerisation and condensation reactions, leading to increased material partitioning to the solid phase products [30,55], although Zhou *et al.* found that a 30 min reaction time was optimal for bio-crude production from Chlorophyta *Enteromorpha prolifera* [62]. Anastasakis and Ross obtained optimal bio-crude yields from *L. saccharina* after 15 min at 350 °C, although they noted that an

optimal bio-crude HHV was only obtained after 60 min, and required a higher feedstock solid loading (12 % gave optimal HHV, compared to 9 % for yield optimisation) [32].

Extremely rapid heating rates with an associated short residence time of 1 min gave the highest bio-crude production observed to date for the microalga *Nannochloropsis* sp. [92].

### **1.4.2.3 Heating rate**

In essence, heating rates, reaction times and reaction temperatures are closely interlinked and inextricable from one another: slow heating (and cooling) rates inevitably lead to long reaction times, whilst high reaction temperatures necessitate a longer heating period.

Within the literature, the general consensus is that high heating rates are desirable for increasing bio-crude yields [80–82]. This is speculated to be due to the suppression of char and coke formation: char is a product of incomplete biomass conversion, whilst coke is formed from thermal decomposition of bio-crude at extended reaction times [81,82].

It has been suggested that oil-forming HTL reactions can be broken down into beneficial “primary” reactions, including pyrolytic and hydrolytic degradation, and subsequent non-beneficial “secondary” reactions, including recombination and secondary cracking [82]. High heating rates enable both pyrolytic and hydrolytic degradation mechanisms to occur simultaneously, whilst short reaction times ensure that secondary mechanisms are not initiated, although it has also been suggested that overly high heating rates can promote higher gas formation at the expense of bio-crude yield [81].

The maximisation of heating rates [82] and development of “fast HTL” systems [92] has been the focus of a number of recent studies, although Li *et al.* were able to obtain comparatively high yields of 32.1 % bio-crude (daf) from brown macroalga *Sargassum patens* C. Agardh despite extremely slow heating rates of 5 °C min<sup>-1</sup> [64].

### **1.4.2.4 In-situ catalysis**

A range of homo- and heterogeneous catalysts has been employed in hydrothermal liquefaction studies, although catalytic HTL has been reported largely for microalgae, and the use of catalysts with macroalgal feedstocks has thus far been limited.

Although alkali catalysis has been effective for increasing bio-crude yields in the liquefaction of lignocellulosic feedstocks, it was shown to have little impact on bio-crude yields and compositions from marine macroalgae *E. prolifera* and microalgae *D.*

*tortiolecta* [62]. It was speculated that the high levels of sodium already present in the feedstock may have played a role in catalysing conversion [62]. Li *et al.* used 5 % Na<sub>2</sub>CO<sub>3</sub> in the liquefaction of *Sargassum patens* C. Agardh. In this case, the use of an alkali catalyst actually led to depletion of the bio-crude phase in favour of aqueous phase products [64] – also observed by Anastasakis and Ross for KOH catalysis of *L. saccharina* HTL [93]. Xu *et al.* saw only very modest improvements to bio-crude yield from *E. prolifera* on increasing K<sub>2</sub>CO<sub>3</sub> loading from 0 % to 20 % [72].

Sulfuric and acetic acid catalysis was examined by Yang *et al.* in the processing of *E. prolifera*, and found to deplete bio-crude yields relative to uncatalysed HTL, although the acid-catalysed oils were found to have better flow properties [72].

*In-situ* heterogeneous catalysis of algal HTL has precedent only for microalgae. Recently, Duan and Savage examined a wide range of catalysts in the liquefaction of *Nannochloropsis* sp., finding the highest bio-crude yields formed in the presence of Pd/C [94], although as the catalyst had not been pre-sulfided, it has been suggested that its efficiency would be rapidly depleted in the presence of sulfur in the algal feedstock [40]. The presence of high levels of sulfur and alkali may be a barrier to use of heterogeneous catalysts for HTL [95]: this will also be an important consideration for catalytic macroalgal HTL in the future.

#### **1.4.2.5 Particle size**

Post-harvest processing typically involves washing with fresh water to remove salt and debris and milling to a small particle size [61]. Particle size can be crucial for processing, particularly within a continuous industrial context, as the biomass must form an easily pumpable slurry. The need for additional size reduction has been highlighted as one of the drawbacks of macroalgae processing with respect to microalgae [40]. Differences in particle size may potentially affect HTL reactivity for large particles by affecting the rates of mass and heat transport to the particle interior, although these effects are not anticipated to be large due to the high mass transfer within the HTL reaction. HTL was found to be relatively insensitive to particle size for grassland perennials [80], but the effect of particle size has not yet been examined for macroalgal feedstocks.

#### **1.4.2.6 Solvent**

The use of organic co-solvents for macroalgal HTL has been used in a limited number of studies: although overall bio-crude yields from continuous processing of *Oedogonium* sp. were not strongly affected, the presence of *n*-heptane, toluene and anisole facilitated the *in-situ* fractionation of bio-crudes on the basis of polarity [68]. Biswas *et al.* found



increased bio-crude yields from *S. muticum* when HTL was carried out in the presence of ethanol or methanol co-solvent, with marked changes in bio-crude composition [96].

### 1.4.3 Continuous processing

Within a functioning biorefinery, it is likely that processing will be carried out under continuous processing conditions. However, the vast majority of studies to date have been carried out in small batch reactors [55], which give limited insight into a full-scale commercial process. A small number of studies have examined continuous hydrothermal liquefaction of biomass in general [97], and reports on the continuous liquefaction of macroalgae specifically number fewer still. Researchers at Pacific Northwest National Laboratory (PNNL) have recently described the development of continuous systems for processing of macroalgal feedstocks [67] based on their previous set-up for continuous microalgae liquefaction [98]. The majority of lab-scale experiments have used dried feedstocks to accurately calculate solid yields, but the feedstock utilised by Yang *et al.* [65] was used without pre-drying to simulate a real-world system. Bio-crude yields were not compromised, albeit only with the addition of supplementary water in addition to the moisture inherent in the macroalgae.

Factors influencing the economic performance of a biorefinery include biomass pre-processing, feed rate, residence time, reaction temperature, heating rate, heat integration, recycle loops and product separation.

In order to maintain a continuous flow, the biomass feedstock must be in the form of a pumpable aqueous slurry. Although pumping of wet biomass is routine in the pulp and paper industry, biomass pumping at higher pressures is less common, and has not yet been demonstrated for HTL at scale [97]. High water content and low feedstock concentrations can negatively affect HTL product recovery [99], as well as giving rise to unnecessary costs and energetic expenditure as a result of heating and processing excess water [97]. For this reason, biomasses with a particularly high moisture content, such as macroalgae, may require dewatering prior to use. However, within a continuous system, slurry concentrations will be limited by the handling capacity of the pumping system in use. The same holds true for particle sizes, which must be reduced in order to avoid blockages and aid pressure control in continuous systems [99]. Particle size reduction can form a significant energetic expenditure in biomass pre-processing, so must also be carefully optimised. Drying and milling can constitute a substantial portion of the total energy expenditure for liquefaction, so low-energy wet milling techniques are likely to be used in a functioning biorefinery [65]. (Although some macroalgae, such as those of the genus *Ulva*, which possess a less robust and easily degradable cell

structure, do not require pre-milling. [97]) From an economic perspective, higher slurry concentrations and larger particle sizes can lower expenditure, but present numerous operational difficulties in the logistics of pumping. The unavailability of high-pressure pumping systems form one of the key barriers to large-scale implementation of HTL, and these are currently a key research area [100]. Faster pumping and higher pressures can also be used to increase biomass heating rates and decrease residence times, which has been shown to improve bio-crude yields [92,99].

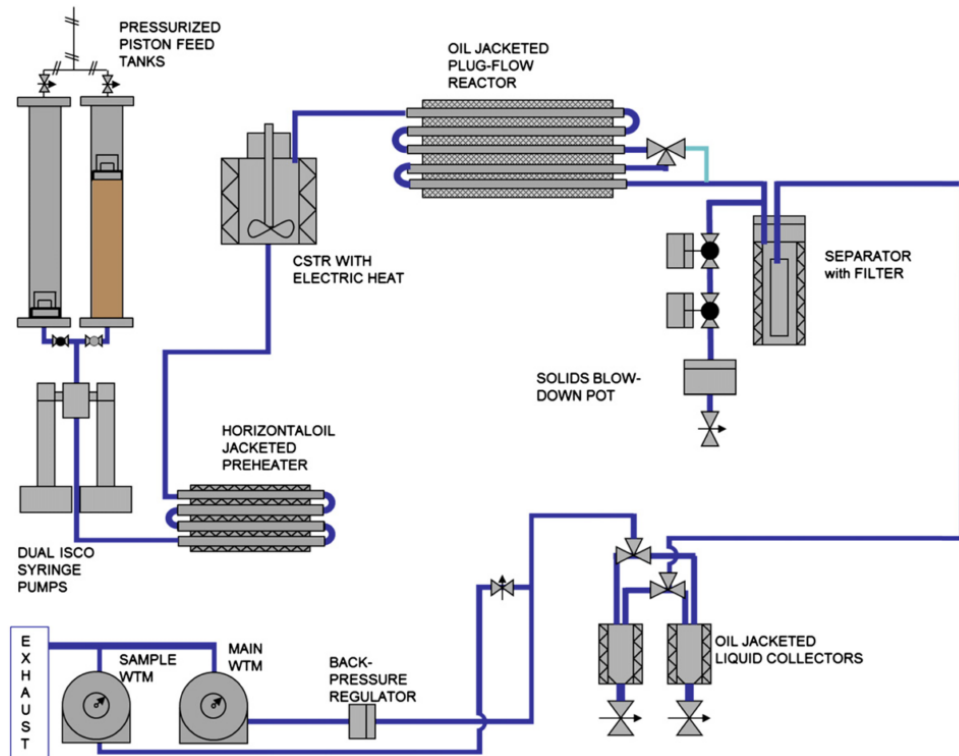


Fig. 2. Process flow configuration for hydrothermal liquefaction.

**Figure 1.4-1** – An example of a bench-scale continuous HTL reactor [98]

Reactor configuration could be in the form of a continuous stirred tank (CSTR) or plug flow reactor (PFR). PFR is likely to give higher heating rates, which have been demonstrated to be conducive to high bio-crude production [91,92], whilst CSTR confers the advantage of mechanical stirring to aid mass transport. A hybrid plug flow and CSTR configuration is also possible, and has been demonstrated to give a favourable return on investment (on a gallon gasoline-equivalent basis) [97]. Heat exchangers recovering energy from the main reactor to a CSTR pre-heater can also improve the overall energy efficiency of the processing plant.

In batch systems, product separation is usually achieved using solvent at the work-up stage, but in a continuous system, solids can be separated *in situ* using a filtration unit with a blow-down pot, leaving the aqueous and bio-crude phases to gravity-separate

[98]. The presence of co-solvents in continuous liquefaction has been shown to give rise to better *in situ* separation of bio-crude and aqueous phase, and enhance bio-crude recovery from the reaction mixture [68]. Incorporating a recycle loop to recirculate the aqueous products can also benefit process efficiency by increasing bio-crude oil yields and improving quality and total process carbon recovery, as well as reducing water consumption and minimising wastewater disposal [67].

Previous studies have shown bio-crude yields and compositions generated in continuous systems to be comparable to those generated in batch. *L. saccharina* (alternatively referred to as *S. latissima*) processed using a continuous protocol by Elliott *et al.* [67] generated at 350 °C with a solid loading of 13 % generated a bio-crude yield of 23.6 % (daf), whilst *L. saccharina* with a near-identical elemental composition processed at similar conditions (13 % solid loading, 350 °C) in a batch system generated ca. 19.3 % (daf) bio-crude [32] with a strikingly similar elemental composition, and hence, HHV. Small-scale batch HTL may, therefore, be assumed to be representative of continuous processing systems.

## 1.5 HTL products

### 1.5.1 Bio-crude

#### 1.5.1.1 Composition

Bio-crudes are typically composed of several hundred individual components, owing to the complex cascade of reactions occurring under hydrothermal conditions. Over 180 compounds have been identified by GC/MS including branched and unbranched hydrocarbons, ketones (often C<sub>15</sub>–C<sub>33</sub>), aldehydes, phenols, alkenes, fatty acids, esters, aromatics and nitrogen and other heterocycles (C<sub>5</sub>–C<sub>16</sub>), although the exact composition of a given bio-crude is strongly feedstock-dependent [101]. Bio-crude composition is influenced by reaction temperatures: bio-crude from *S. tenerrimum* processed at temperatures ranging from 260 to 300 °C contained a significant contribution from *n*-hexadecanoic acid at 260 °C, which decreased steadily with increasing processing temperature, while the content of 3-pyridinol peaked at 280 °C [70].

Owing to the conversion of biomass proteins and carbohydrates, bio-crudes typically have elevated heteroatom (N and O) contents with respect to mineral crudes [54,102,103] (with N contents up to ca. 11 %, compared to 0.1–1 % for mineral crudes),

although the correlation between biomass elemental composition and bio-crude composition is not always linear [101].

Anastasakis and Ross [32] obtained bio-crude oil from the Heterokontophyta *L. saccharina* with a higher weight percentage of carbon than typical macroalgal crudes: up to 82 % carbon was observed, compared to the 65–75 % observed by other authors under similar conditions [72]. Interestingly, although mass balance between the four product phases was strongly temperature-dependent, neither elemental composition, nor, consequently, HHV, were strongly affected. A very slight increase in HHV was observed with increasing temperature, and lower loadings (< 10 %) were found to deplete HHV slightly.

A van Krevelen diagram presenting the elemental compositions of macroalgal bio-crudes produced to date compared to fossil crude is presented in Fig. 1.5-1.

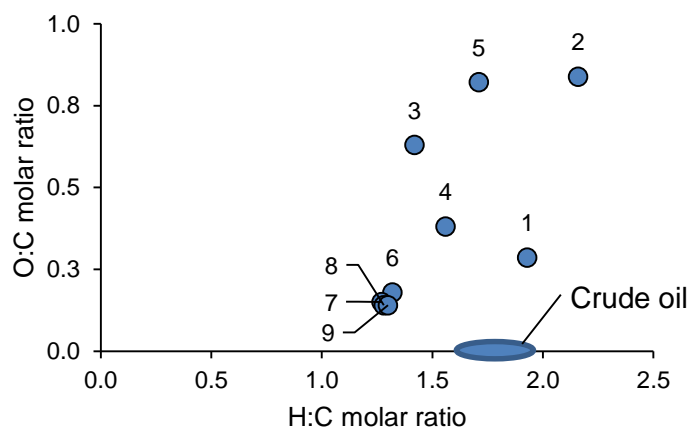


**Figure 1.5-1** – van Krevelen diagram summarising some macroalgal bio-crudes described in literature to date compared to the approximate elemental composition of crude oil. Data labels are explained in Table 1.5-1.

**Table 1.5-1** – Feedstocks corresponding to bio-crudes summarised in Fig. 1.5-1.

	<b>Macroalgae type</b>	<b>Ref.</b>		<b>Macroalgae type</b>	<b>Ref.</b>
1	<i>E. prolifera</i>	[72]	6	<i>L. digitata</i>	[61]
2	<i>E. prolifera</i>	[62]	7	<i>L. hyperborea</i>	[61]
3	<i>L. saccharina</i>	[32]	8	<i>L. saccharina</i>	[61]
4	<i>S. patens</i>	[64]	9	<i>A. esculenta</i>	[61]
5	<i>Saccharina</i> sp.	[67]			

Generally, the energy contents (measured using higher heating value) of macroalgal bio-crudes tend to be relatively high – 25–38 MJ kg<sup>-1</sup> [72]. These HHV values constitute a significant improvement with respect to the HHV of the biomass feedstocks, but fall short of the HHV of typical mineral crudes (ca.41–48 MJ kg<sup>-1</sup>) [104]. It is worth noting that high bio-crude yields do not necessarily correspond to higher bio-crude energy contents: Toor *et al.* obtained 34 % bio-crude from the microalgae *Nannochloropsis* at 350 °C (HHV 38.1 MJ kg<sup>-1</sup>), while an improved yield of 46 % bio-crude, with significantly depleted HHV of 27.7 MJ kg<sup>-1</sup>, was observed at 310 °C [83].

Bio-crudes are highly viscous and acidic. In general, bio-crude properties such as elemental composition and boiling point distribution are more reminiscent of a typical bitumen than a crude oil [32]. A heavy asphaltenic fraction (solid at ambient conditions) makes up a substantial portion of the overall bio-crude, increasing viscosity and heteroatom content with respect to crude oils [105], which can be problematic for bio-crude upgrading.

Macroalgal bio-crudes can also contain elevated quantities of metals – up to 7.5 % of the total magnesium contained in *L. saccharina* processed by HTL at 350 °C for 15 min partitioned to the bio-crude phase (alongside 1.8 % sodium and 3.4 % calcium) although the bulk of the biomass metals distributed between the aqueous and solid phase products [32].

#### ***1.5.1.2 Utilisation of bio-crudes***

As mentioned earlier, macroalgal crudes are more similar in composition and properties to bitumen than crude oil [32]. Their high heteroatom levels, including metals, can be detrimental to fuel properties, giving rise to poor combustion performance and storage stability, high viscosity and acidity [102,106], as well as high NO<sub>x</sub> emissions and potential catalyst poisoning in refineries or catalytic converters. These factors limit the direct usability of bio-crude as a fuel, and further upgrading and hydrotreatment is required to obtain a fuel with similar specifications to petroleum [106].

A number of studies have focused on hydrotreatment, denitrogenation and desulfurization of microalgal bio-crudes [48,107], but macroalgal crudes have thus far attracted little attention. A wide range of catalysts has been considered, ranging from conventional transition metal-based hydrotreatment catalysts (e.g. Pt/γ-Al<sub>2</sub>O<sub>3</sub> [48], Pt/C, Mo<sub>2</sub>C [108]), and Raney-Ni [109], as well as zeolites [53,110], which could be applied to macroalgal bio-crudes in future. Upgraded fuels may be suitable for co-refining with mineral crudes [51–53]; co-refining has been explored for lignocellulosic HTL feedstocks [111,112].

Recently, Cole *et al.* presented a proof-of-concept for the production of usable biofuel from *Oedogonium* macroalgae via continuous HTL. A number of measures were taken to reduce the nitrogen content of the bio-crudes: a) nutrient-starvation to cultivate nitrogen-depleted macroalgal feedstock, b) use of 10 % heptane co-solvent to aid fractionation of the non-polar bio-crude components, c) non-polar bio-crude distillation, d) blending of distilled bio-crude with green feed,<sup>ii</sup> and e) a two-step hydrotreatment of the blended green feed/bio-crude [113]. A two-step procedure was adopted after the initial one-step hydrotreatment utilising commercial Ni-Mo and Ru/C catalysts was found to be ineffective due to poisoning – despite the substantial reduction in nitrogen content prior to hydrotreatment.

An alternative to hydrotreatment may be the simultaneous processing of bio-crudes with fossil crudes in existing refineries. A recent study by Lavanya *et al.* was the first to propose direct blending of microalgal bio-crude with fossil crudes for co-processing to generate biofuels [114]. (This has also previously been explored for bio-crude derived from HTL of lignocellulosic feedstocks [112,115,116]). Simulated distillation of 10 % blends of microalgal marine and freshwater bio-crude with Narimanam petrocrude showed that the kerosene fraction fell within the requirements for sulphur content and smoke point (a proxy for aromaticity) set out by European emissions standard EU II (for heavy commercial vehicles), but fell short of meeting standards for EU III and later standards. Simulated distillation revealed that both blends had elevated N and S levels relative to the pure crude oil, although marine algal bio-crude affected heteroatom levels to a lesser degree. (For reference, the Narimanam petrocrude contained 14 ppm S and <0.01 wt. % N, and the blends contained 100 and 200 ppm S, and 0.04 and 0.07 wt. % N for marine and freshwater-derived algal bio-crudes, respectively). The salt content of marine microalgal bio-crudes also became significant, and, as such, macroalgal bio-crudes may similarly necessitate desalination steps prior to co-refining with fossil crudes. It must be noted that macroalgae tend to have significantly lower protein contents than microalgae, with correspondingly lower N levels carried through to the bio-crude, and as such should be significantly less problematic to co-refine than microalgal bio-crudes.

It has also been suggested that extraction of pentane-soluble bio-crude components prior to upgrading could eliminate the difficult-to-process asphaltenic fractions, thereby reducing the energy consumption of hydrotreatment and extending catalyst lifetimes [105].

---

<sup>ii</sup> Green feed is obtained from the hydrogenation of CO<sub>2</sub> over a potassium-promoted Fe/Al spinel catalyst

### 1.5.2 Aqueous phase products

Alongside the bio-crude fraction, which typically constitutes the focal point of HTL research, the aqueous phase products are diverse in composition, and present a number of opportunities for utilisation and value generation. The aqueous phase contains polar, water-soluble organics, such as organic acids and alcohols, and dissolved ammonia ( $\text{NH}_4^+$ ) originating from the degradation of proteins, alongside dissolved metals (high levels of K, Na, Ca and Mg, as well as Fe and a wide range of other metals) and phosphates. The aqueous phase products of macroalgal HTL can also contain macroalgae-specific sugars, such as laminarin and mannitol, originating from carbohydrate depolymerisation [32].

Total organic content of aqueous phases is variable and species-dependent. Aqueous phase products from macroalgal HTL commonly contain substantial quantities of acetic acid, as well as glycerol originating from algal lipids [60], and a range of pyridinic and pyrrolic compounds generated from the condensation of aldehydes and ketones with ammonia, although the composition can be influenced by the presence of acidic or basic catalysts [65]. Acetic acid can originate from the degradation of glucose, and is stable under HTL conditions due to the formation of acetates with dissolved metals [65]. The aqueous phase products from *E. prolifera* were found to be weakly acidic by Zhou *et al.* [62], with a number of organic acids present besides acetic acid: propanoic, levulinic and benzenepropanoic acids were also present. Acetic acid was also present in aqueous products formed during HTL of *L. saccharina*, although the overall pH was alkaline (pH 7–9), in line with observations from other investigations [60]. Aqueous products were composed largely of sugars, as well as nitrogen-containing compounds (including indole, pyrrole and derivatives, 3-aminophenol) and a substantial contribution from 2-cyclopenten-1-one [32].

Macroalgal HTL aqueous phases contain substantial levels of nitrogen (albeit typically somewhat lower than observed for microalgae, on account of their lower protein content [117]). Although nitrogen is present partly in the form of organic N-containing heterocycles, a significant portion is present in an inorganic form as ammonia, which is a vital nutrient that has the potential to be recovered for further macroalgal cultivation [66].

Phosphorus, recovered in high quantities in microalgal HTL aqueous products, is somewhat lower for macroalgae, and recovered predominantly in the solid products, rather than the aqueous, alongside calcium and magnesium, although sodium and potassium partition predominantly to the aqueous phase [60]. High contents of Ca, Mg

and Fe in feedstocks tend to result in poor recovery of phosphorus in aqueous phase products [118], presumably due to the formation of stable and insoluble phosphates, whilst low-metal biomasses give high phosphorus recoveries in aqueous phase products [119].

#### **1.5.2.1 Utilisation of aqueous phase products**

The carbon- and nutrient-rich aqueous phase cannot be released directly into waterways without treatment to decrease its organic and inorganic content [120], but presents a number of opportunities for valorisation. Aqueous phase utilisation has been examined in greater depth for microalgal HTL aqueous phases than macroalgal, but processes are expected to be comparable.

Direct recycling of the aqueous phase within the HTL system is one potential route to value addition, demonstrated successfully for microalgae [121]. Recycling of aqueous phase carbon was also shown to increase the bio-crude production from *Gracilaria gracilis* and *Cladophora glomerata* macroalgae, although the effect on bio-crude elemental composition was not discussed [69]. However, it is not anticipated that aqueous phases from macroalgal HTL could be recycled indefinitely, due to the build-up of salts (especially chloride) [113], which could damage the structural integrity of the reactor through corrosion.

Organics in process water can also be utilised for further energy recovery. Elliott *et al.* incorporated catalytic hydrothermal gasification (CHG) of the aqueous phase into a continuous system for HTL processing of *Saccharina* spp., resulted in nearly complete conversion of aqueous phase organics to a high-purity carbon dioxide/methane product stream [67]. Methane-rich products could subsequently be used for hydrogen production through steam reforming [122]. Supercritical water gasification of aqueous phases from HTL of a range of macroalgae species was employed by Duan *et al.* to produce a range of light organics (primarily H<sub>2</sub>, CO, CH<sub>4</sub>, CO<sub>2</sub>, and C<sub>2</sub>H<sub>6</sub>). Hydrogen generated in this way could be used as a hydrogen source for bio-crude hydrotreatment further downstream [123].

The recovery of energy from aqueous phase products using anaerobic digestion [124] or fermentation of residual sugars to generate bioethanol [32] has also been suggested, although water-soluble components (such as laminarin and mannitol) could potentially be extracted as a low-volume, high-value product stream.

The HTL aqueous phase is rich in dissolved ammonia and vital micronutrients, such as K, Na, Mg and Ca, and the use of HTL aqueous phases as a growth medium for algae



and other microorganisms [125] has been examined in a number of studies for microalgal feedstocks. High-temperature hydrothermal processing essentially ensures the destruction of all biotic toxins (bacteria, viruses and even prion proteins) in the nutrient-rich aqueous phase [54], leaving a sterile medium with potential for use as a fertiliser. Microalgal HTL aqueous phase, rich in nitrogen, phosphorus and potassium, as well as Fe, Ca, Mg, has been shown to be an effective medium for microalgal cultivation (albeit at high dilutions, due to the presence of organic growth inhibitors) [117,118,126–128]. Certain algal species are capable of mixotrophic growth, and thus utilise carbon, as well as inorganics, present in HTL aqueous phases [117]. Through the consumption of dissolved organics and inorganics, recycling process water for algal cultivation can contribute to reducing its cytotoxicity prior to environmental release by removing organic toxicants [126]. No studies of the suitability of macroalgal HTL aqueous phase as a fertiliser or growth medium have been carried out to date, however.

The recovery of aqueous phase nitrogen and phosphorus in the form of struvite (magnesium ammonium phosphate) has also been proposed – in this way, the extracted material can potentially be used as a fertiliser for agricultural crops. Very recently, Shanmugam *et al.* demonstrated >99 % removal of  $\text{PO}_4^{3-}$  and 40–100 % removal of  $\text{NH}_4^+\text{-N}$  through struvite formation from the aqueous phase products of *Nannochloropsis* sp. microalgae [120]. Struvite crystallisation occurs when the molar ratio of  $\text{NH}_4^+:\text{Mg}^{2+}:\text{PO}_4^{3-}$  is 1:1:1 under basic conditions. HTL aqueous phases tend to contain all three ions, although  $\text{Mg}^{2+}$  tends to be the least abundant of the three: hence, struvite production requires the adjustment of  $\text{Mg}^{2+}$  ion concentration within the solution. The process has the potential to reduce the demand for mining of phosphate rock substantially; there is also scope for utilisation of industrial wastewaters as a magnesium source, further improving the process and environmental economics.

### 1.5.3 Solid phase products

As the bulk of HTL research has centred predominantly on the production of bio-crudes, the solid phase products are less well characterised. The solid phase product is referred to alternately as “solid residue” or “bio-char”, although its composition differs somewhat from that of bio-char generated by pyrolysis. The solid phase tends to contain the majority of the feedstock ash, as well as a portion of the feedstock carbon in the form of insoluble carbonates or asphaltenes. High biomass carbohydrate content has a positive effect on solid formation, so macroalgal HTL tends to generate higher yields of solid products compared to microalgal HTL [69]. Overall, macroalgal HTL solids can have

widely varying compositions [61], and FTIR has demonstrated, variously, an increase or a decrease in oxygenation of HTL solids relative to the starting biomass for different feedstocks [69]. Although energy contents tend to be relatively low (e.g. 13.1 and 10.1 MJ kg<sup>-1</sup> for *C. glomerata* and *G. gracilis*, respectively [69]), HHV of up to 26.2 MJ kg<sup>-1</sup> have been observed for *L. hyperborea* HTL solids [61], opening up potential avenues for value addition through energy recovery. Depending on their exact composition, HTL solids have the potential to be used as a fuel or a fertiliser [129], or carbon sequestration potential and soil enrichment, as for pyrolysis biochar [130]. An integrated energy and nutrient recovery protocol has been suggested by Papadokostantakis *et al.*, incorporating the incineration of HTL solids followed by phosphorus recovery from the resulting ash *via* acid leaching and subsequent struvite production, as described above for aqueous phase phosphorus [122].

#### 1.5.4 Gaseous products

The gaseous products of HTL are composed predominantly of CO<sub>2</sub>, (95–99 % for microalgae [16,99]) most likely originating from decarboxylation reactions, alongside a diverse range of lower-abundance volatile organics, such as hydrogen, methane and C<sub>2</sub>–C<sub>3</sub> gases [60]. The potential of the gas phase products has not yet been fully realised, but a gas stream predominantly composed of CO<sub>2</sub> could potentially be utilised to supplement microalgal cultivation within a biorefinery [117].

### 1.6 The biorefinery concept

The concept of a “biorefinery” is described as a system analogous to a crude oil refinery, which “integrates biomass conversion processes and equipment to produce fuels, power, and chemicals from biomass” [131]. This concept can also be extended to integration with services, such as environmental remediation, or re-use of by-products in other industries.

Although macroalgal biomass has been demonstrated as a promising potential feedstock for fuel production, a number of technological challenges must be overcome before implementation on a larger scale. Among these are cost- and energy-effective cultivation and harvesting, streamlining of pre-processing steps, and development of continuous systems adapted to cope with high solid loadings and ash contents [97].

The major limitations of macroalgal fuel production – high water consumption, energy requirements for harvesting and drying, and pollution from aqueous by-products – could be addressed within a biorefinery model incorporating reuse and recycling of water or

nutrients. The application of this concept for a microalgal biorefinery has been branded “*Environment-Enhancing Energy*” or E2E, but could equally be applied to a macroalgal system [132,133].

Within a fully functional biorefinery, incorporation of heat integration strategies will be necessary to ensure energy-efficient operations. In addition, value recovery from all possible sources will have to be considered. Macroalgae contains a wide range of high-value extractable biochemicals: the market for seaweed hydrocolloids (agar, alginate and carrageenan) is estimated to be worth ca. \$545 million annually [42]. The extraction of these could potentially be incorporated into a macroalgal HTL biorefinery paradigm, in addition to recovery of organic matter (e.g. acetic acid, glycerol, or macroalgal sugars, such as mannitol and laminarin [32]), nutrients (e.g. phosphates, ammonia) or energy (e.g. *via* gasification [98]) from the aqueous phase products.

Alternative valorisation routes must also be considered, such as the value introduced by integration of macroalgae processing with environmental remediation services or secondary biorefineries (e.g. utilisation of CO<sub>2</sub> or aqueous nutrients generated through macroalgal HTL to supplement microalgae cultivation in a connected biorefinery).

Given the high carbon content of the solid char phase products, marine or terrestrial carbon sequestration could also present a viable route to obtaining added environmental value, potentially resulting in “carbon-negative” fuel production.

### **1.6.1 Macroalgae cultivation**

The success of a macroalgal biorefinery crucially depends on economical feedstock production. The main process operations within an algal biorefinery are cultivation and seeding, harvesting, pre-treatment (cleaning, milling, preservation and storage) and finally, energy extraction or other processing [26]. Optimisation of all of these steps is paramount for obtaining a positive energy return on investment (EROI), and improved design of cultivation and harvesting systems will play a key role in overall process sustainability.

Although drift seaweeds (biomass washed up by the tide) are a potentially viable feedstock, their abundance and properties are uncontrolled and unpredictable, so on- or offshore cultivation is required to guarantee a stable supply to support year-round fuel production. Seaweed cultivation in Asia is well-established, but in Europe, macroalgae exploitation is mainly limited to manual or mechanised harvesting of natural stocks [31]. Within Europe, France and Norway harvest the most wild-growing macroalgal biomass, although sustainable harvesting of natural stocks is a significant challenge [31,45].

Cultivation technologies vary depending on the anchoring of the given macroalgae species. In each case, the initial stages of cultivation typically involve manual collection of reproductive samples, extraction of zoospores, and subsequent incubation of young macroalgae plants (thalli) in onshore “hatcheries” for a number of months [134], followed by manual “seeding” of the thalli onto substrates of various configurations. These are typically “longlines” – networks of floating ropes anchored to the seabed or suspended from buoys or boats, although some macroalgae types can be seeded directly onto heavy substrates on the seabed. Different arrangements can be tailored to different macroalgae species, depending on their typical growing depth and light requirements.

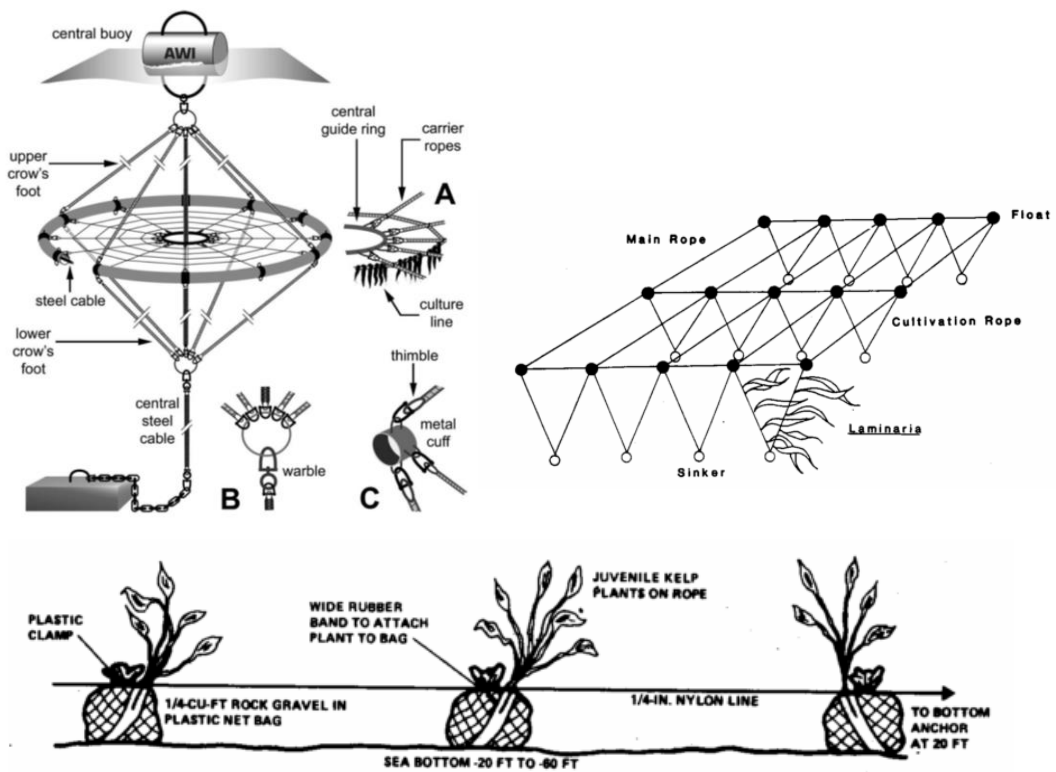


**Figure 1.6-1** – Illustration of three different anchoring structures for kelp aquaculture. Top right: ring system for *Laminaria* [134]; top left: basic hanging rope curtain cultivation system for the brown seaweed *Laminaria*; bottom: nearshore *Macrocyctis* planting system [135].

Cultivation systems can be located nearshore or offshore, with nearshore conferring the advantage of relatively calm and sheltered environments for aquaculture operations [45]. Offshore cultivation systems are more vulnerable to storm damage and strong currents, but integration with existing offshore infrastructure can provide additional shelter and stability [136].

Although mature cultivation technologies are already in place, mechanised harvesting has yet to be implemented on a large scale, due, in part, to the wide availability of cheap

manual labour in many macroalgae-producing nations. A number of technologies have emerged in response to an increased global market for seaweed hydrocolloids: trawlers are used extensively in Norway for harvesting bottom-planted *Laminaria*, removing the adult canopy and leaving smaller plants to regenerate and maintain a stable colony [31]. Although they do not compete for arable land with terrestrial food or energy crops, in order to ensure the economic viability of micro- or macroalgae as a resource, it is imperative that the creation of a new algae-based fuel industry does not compete with an existing food or other product supply chain. In this regard, establishment of an entirely new algae production industry in a country where one does not yet exist would be ideal. In the United Kingdom, cultivation or even large-scale utilisation of algae is virtually unheard of, but its geography and infrastructure lends itself extremely well to wind power and hydroelectricity due to its vast expanses of coastline (11,073 miles) [137], which could potentially be exploited for cultivation of marine bioenergy crops. Integration with offshore wind infrastructure could also play a role in improving the prospects of aqueous crop cultivation [138,139]. As well as providing a potential structural basis for cultivation lines, combinations of offshore wind arrays and macroalgal farms can potentially enhance marine ecosystems by providing a sheltered environment for fish and other aquatic animals [140].

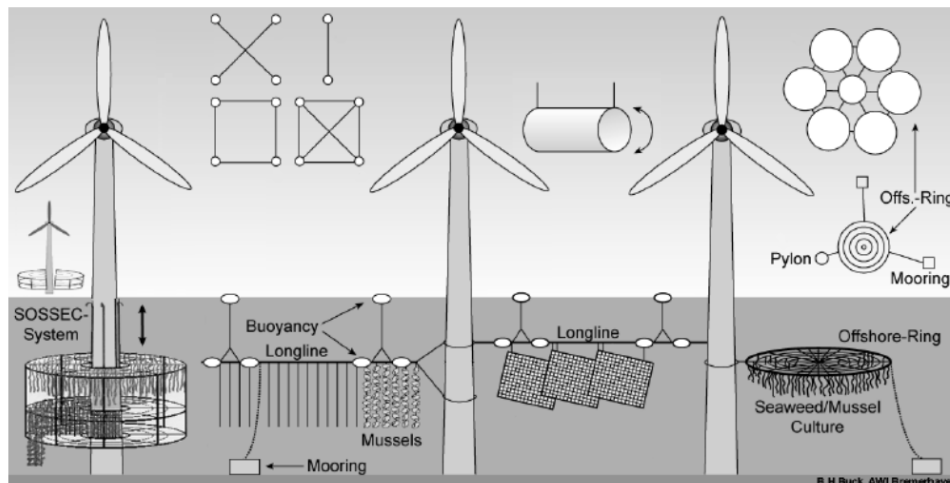


**Figure 1.6-2** – Concept multi-use installations for offshore wind and macroalgae cultivation [141]

Given the seasonal nature of macroalgae growth cycles, judicious selection of several different crops within a rotating annual cultivation cycle may be necessary to ensure a year-round supply of feedstock for fuel production. Multi-crop systems can take advantage of seasonal variation in water temperatures, light conditions and nutrient levels: for example, *Laminaria*, a winter crop, typically harvested between December and February, can be rotated with *Gracillaria*, a summer crop, suited to warmer waters, which

can be seeded onto culture ropes in December and harvested between June and August [135]. Preservation of feedstocks is also important, although little research into this has been published to date [26].

Generally, microalgae have higher areal productivity (158 vs 60–100 tons hectare<sup>-1</sup> year<sup>-1</sup> for microalgae vs macroalage), and significantly shorter harvesting cycles (daily vs 3 or 6 months for macroalgae) [39], but significantly elevated cultivation and harvesting costs. A synergistic combination of micro- and macroalgae processing is a possible route to getting the optimum value out of a third-generation fuel production system.

## **1.6.2 Integration with environmental services**

Within a biorefinery, value can be added not only through the creation of co-products for commercial distribution, but through the incorporation of additional services. One example of an environmental service is industrial and municipal wastewater remediation by micro- or macroalgae.

### ***1.6.2.1 Wastewater remediation***

Recently, Neveux *et al.* demonstrated effective aqueous pollutant removal from municipal wastewater by the freshwater macroalga *Oedogonium* sp. The use of municipal effluents supported high biomass productivity, and nutrient and microbial content in the resulting treated water was reduced by up to 99 %. The composition of the resulting biomass was relatively consistent, and yielded 26–27% bio-crude when processed by HTL. The coupling of a municipal wastewater remediation system with HTL has also been examined by Chen *et al.* [84] for a mixed micro- and macroalgal and bacterial culture.

The remediation of nutrient-rich effluents from seafood aquaculture using macroalgae have also been discussed by a number of researchers [142–145], and have the potential to simultaneously prevent marine eutrophication and generate biomass for processing by HTL.

A recent study has demonstrated the successful uptake of contaminating metals from acid mine drainage (AMD) by microalgae subsequently processed by HTL, resulting in the partitioning of the contaminating metals to the solid phase products, thereby concentrating the dilute aqueous metal pollutants into a solid form substantially simpler to handle and dispose of [16]. Similarly, HTL processing of macroalgae grown in metal-contaminated waters may serve the dual purpose of generating bio-crude and removing dissolved metals from marine environments.

### **1.6.2.2 Marine plastic remediation**

Marine eutrophication by wastewater discharge and aquaculture is a pressing issue that can be addressed through a macroalgal HTL paradigm, but another form of pollution that poses an existential threat to marine water quality worldwide is marine plastic. Reported values vary [146], but approximately 28 million tonnes of plastic are estimated to enter the marine environment annually, including an estimated 10 % of all newly produced plastic, equating to around 6 million tonnes annually for Europe alone [147]. The damage to marine ecosystems caused by ocean plastics is valued at an estimated \$13 billion [148]. This is caused by both plastic litter and microplastics resulting from the physicochemical degradation of larger plastic fragments. Microplastics in particular can adsorb onto marine macroalgal surfaces [149], and may be difficult to eliminate from marine macroalgal feedstocks for an HTL biorefinery. The simultaneous processing of marine macroalgal biomass with marine plastics may provide a valuable environmental service within an HTL biorefinery.

Co-pyrolysis of biomass with plastics has attracted some recent attention [150] and while the co-liquefaction of lignocellulosic biomass with plastics has recently been reported [151,152], no analogous reports exist for macroalgae and plastics. Non-additive synergistic effects on bio-crude production were reported for co-processing of camphor wood sawdust with HDPE, speculated to be the result of hydrogen generated by plastic decomposition stabilising reactive radicals formed from biomass, preventing repolymerisation to insoluble solid-phase products [151]. Few co-liquefaction studies to date have focused on marine biomass: blending *Spirulina* microalgae feedstocks with HDPE in an ethanol medium was shown to have synergistic effects for bio-crude production [153], and, more recently, similar findings were obtained for co-liquefaction of *D. tertiolecta* microalgae with polypropylene in a more typical aqueous HTL medium [154]. However, co-processing of plastics with macroalgae has not, to the author's knowledge, been reported to date.

### **1.6.2.3 Co-processing with alternative wastes**

Co-processing with non-marine pollutants or waste streams is a further opportunity for value addition within a biorefinery. A study of liquefaction of *E. prolifera* in the presence of crude glycerol (a by-product of the biodiesel industry in China) found that synergistic effects between the biomass and glycerol led to increases in bio-crude yield, and a substantial decrease in viscosity and total nitrogen content [155].

### 1.6.3 Biorefinery model

A cradle-to-grave model of a hypothetical biorefinery is presented below, incorporating pre-HTL extraction of valuable components (such as salts), bio-crude upgrading to fuels and other chemicals, and integration of downstream gaseous product recycling to microalgae cultivation, energy recovery from aqueous phase products, disposal of the solid phase products through burying (denoted as “carbon sequestration”), and production of chemicals and fertilisers from the organic and inorganic fractions of the aqueous phase:

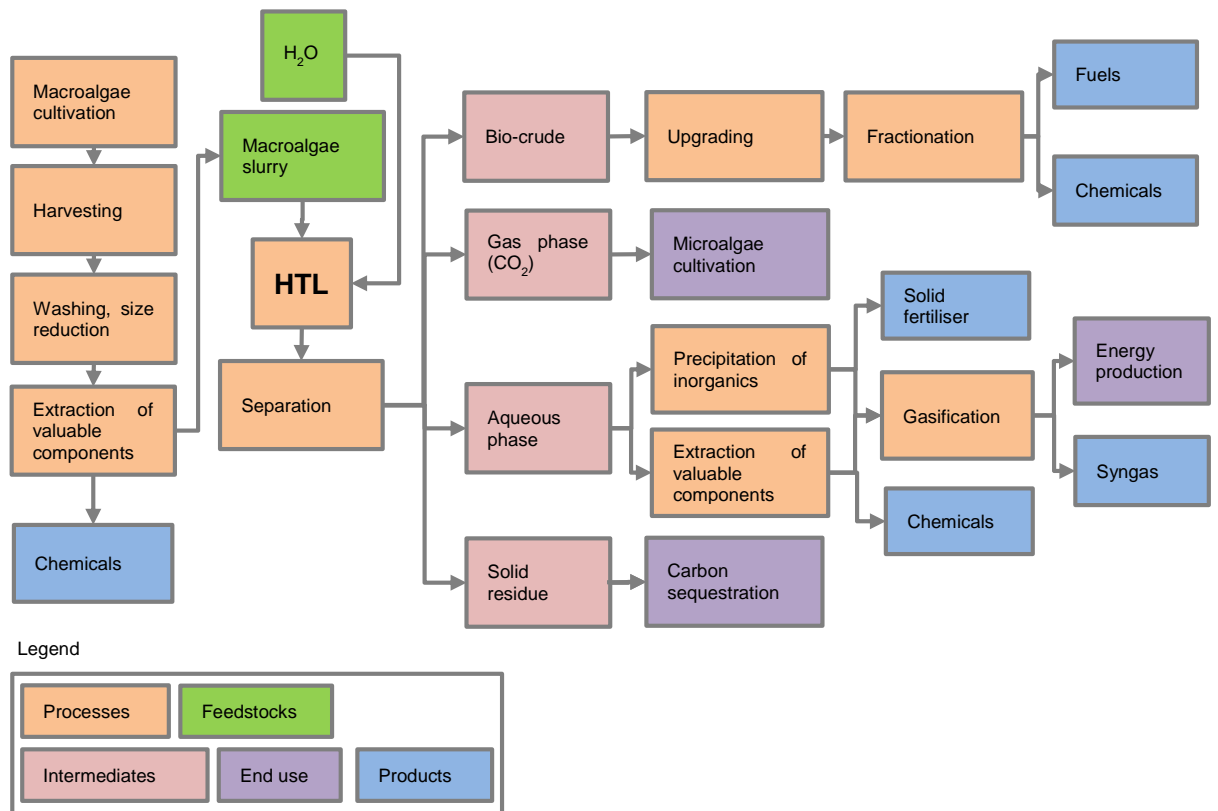


**Figure 1.6-3** – Cradle-to-grave model of hypothetical biorefinery centred around macroalgal HTL

This biorefinery could be located onshore, or alternatively, offshore, near to the cultivation site. A conceptual design of a kelp farm centred around a floating biorefinery is presented below:



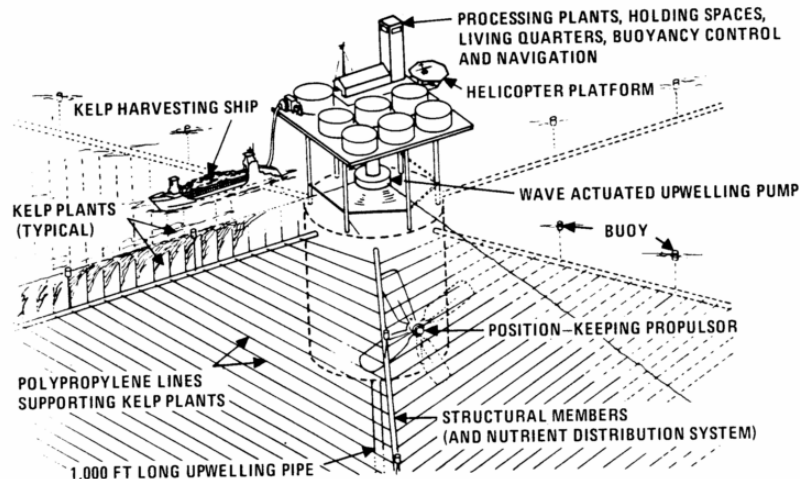


**Figure 1.6-4** – Conceptual design of a floating biorefinery, incorporating cultivation, harvesting and processing [156]

The ability to process material onsite could minimise carbon emissions from transporting wet biomass between the farm and onshore processing site, although the logistics of such an offshore construction would need considerable further research.

#### 1.6.4 Technoeconomics and life cycle assessment

A range of different LCA studies aiming to assess the viability of macroalgal fuel production systems have been conducted to date. A comparison of open-pond on-land macroalgal cultivation compared to conventional fuel crops has called into question the environmental advantages of algae over terrestrial plants in terms of GHG emissions and overall energy use, although the incorporation of wastewater treatment within the system (replacing fertilisers) significantly reduced total system energy consumption and GHG emissions [157]. The results of other studies into biogas and ethanol production from macroalgae have been more favourable [158], although information is sparse as the majority of LCA studies to date have focused on micro-, as opposed to macro-, algae. Aresta *et al.* published a report comparing fuel production from macroalgae, finding that HTL was more efficient at producing long chain fatty acid-rich oils than extraction using supercritical CO<sub>2</sub> [38]. Subsequently, preliminary results of an LCA study comparing a range of cultivation options and biochemical and thermochemical means of fuel production were presented, although the focus fell predominantly on a comparison of the cultivation methods and CO<sub>2</sub> supply, and no definitive preference for thermochemical vs. biochemical conversion was indicated [159].

Neveux *et al.* [66] examined macroalgae cultivated in outdoor tanks (rather than collected from the wild) to give a more holistic assessment of the process life cycle

viability. An overall productivity value in terms of bio-crude production was assigned to each feedstock, with units of grams biocrude per m<sup>2</sup> per day. The highest overall productivity was obtained for *Derbesia tenuissima* at 2.4 g biocrude m<sup>-2</sup> day<sup>-1</sup>: 46 % higher than that of *Oedogonium* sp., despite having a lower bio-crude yield per unit mass. These results highlight the crucial importance of taking a whole-system approach to determining optimal conditions for biorefinery operation, examining all stages of biofuel production, encompassing biomass cultivation as well as production. A range of product valorisation options were also discussed, with nutrient recovery from the aqueous phase forming a key process. In a separate paper, the group also compared the results to potential yields from macroalgal lipid biodiesel production from the same feedstocks. A sensitivity analysis determined that biomass productivity was the most influential parameter, with the potential to double or even triple the value of a feedstock when produced at scale, as well as HTL technology optimisation [160]. In the best-case scenario, marine macroalga *Derbesia* was projected to have a value of \$23,600 ha<sup>-1</sup> a<sup>-1</sup>, with bio-crude production highlighted as a more profitable route to fuel production than biodiesel. The valorisation of the solid, gaseous and aqueous phases from whole-algae liquefaction was discussed, with nutrient recycling from both the aqueous and solid phases. The sequential extraction of high-value coproducts such as algal proteins, sulphated polysaccharides, sterols and pigments was alternatively proposed to add significant value within a biorefinery paradigm.

## 1.7 Concluding remarks

Hydrothermal liquefaction of macroalgae has been shown to be a promising route to the production of bio-crudes and multiple co-products within a biorefinery paradigm, and can provide a route to sustainable biofuel production in a marine environment without placing constraints on scarce terrestrial resources. A variety of species show promise as feedstocks, and a wide range of HTL conditions have been examined by different researchers across the globe.

Bio-crudes produced from macroalgae are as diverse in composition as the feedstocks they originate from, but have potential to be upgraded using existing refinery infrastructure to create blendable biofuels. Nutrient- and carbon-rich aqueous products present ample opportunities for energy recovery and have potential to be used as a fertiliser or growth medium for algae or higher plants.

## 1.8 Aims and objectives

A substantial number of studies on hydrothermal liquefaction of microalgae have been published, and although macroalgae offers a potentially cheaper feedstock, this has been researched less extensively. Whilst a range of macroalgae species has been examined by researchers, most teams tends to examine a single species from a single geographical location, making comparisons difficult. To this end, there is no systematic evaluation of multiple macroalgal species spanning all three classes from one location at the same harvesting point to determine an 'ideal' species for a set locality. In addition, a number of models attempting to rationalise or predict macroalgal reactivity and bio-crude production have been proposed based on model compounds. However, macroalgae contain a number of compounds unique to aquatic biomass, hence, there is scope for an examination of the relationship between composition and reactivity based on real feedstocks from the same location, processed using identical protocols.

It is well known that macroalgae growth and composition is influenced by growing location and localised environmental conditions, however, no studies to date have examined the effect of location on one macroalgae species in terms of its HTL feedstock suitability. An understanding this is essential for the design and implementation of HTL macroalgal biorefineries worldwide, and for species selection.

Finally, within a macroalgal biorefinery, the presence of marine plastics is unavoidable, and likely to become increasingly prevalent in the decades to come. It is of vital importance to understand how plastics will affect macroalgal HTL processing.

The overarching aim of this thesis is, therefore, to explore the effect of species, location and possible contamination on the hydrothermal liquefaction of macroalgae with a view to developing a model marine biorefinery.

To achieve the above aim, the core objectives of the project were defined as follows:

1. Use a wide range of UK macroalgae species from one growing location, spanning all three major classes, as feedstocks for HTL and explore the effect of biochemical composition on bio-crude yield and composition, as well as aqueous phase nutrient recovery, with a view to finding the most suitable species for a South West UK biorefinery.

2. Taking a single macroalgal species harvested at the same time of year, examine the effect of geographical variation on HTL outcomes, and determine whether a single species could serve as a suitable feedstock across a wide range of locations.
  
3. Examine the effect of co-liquefaction of macroalgae with common marine plastic pollutants to determine the products formed and optimise processing conditions in order to gain a better understanding of the challenges faced in a future marine macroalgae biorefinery.

## 1.9 References

- [1] Y. Guo, T. Yeh, W. Song, D. Xu, S. Wang, A review of bio-oil production from hydrothermal liquefaction of algae, *Renew. Sustain. Energy Rev.* 48 (2015) 776–790. doi:10.1016/j.rser.2015.04.049.
- [2] D.F. Wass, New catalysts for the conversion of ethanol to advanced biofuels, in: *Renew. Feed. A Fantasy Or Reality? (CSCT Symp., 2015)*.
- [3] BP Statistical Review of World Energy (63rd edition), 2014. [bp.com/statisticalreview](http://bp.com/statisticalreview).
- [4] IEA, Renewable Energy in Transport, (2013). [http://www.iea.org/media/training/presentations/Day\\_2\\_Renewables\\_5\\_Transport.pdf](http://www.iea.org/media/training/presentations/Day_2_Renewables_5_Transport.pdf) (accessed March 8, 2015).
- [5] I. Billege, 700 Refineries supply oil products to the world, *NAFTA*. 60 (2009) 404–406.
- [6] OICA, Number of Passenger Cars and Commercial Vehicles in Use Worldwide from 2006 to 2014 in (1,000 Units), *Stat. - Stat. Portal.* (2014). <http://www.statista.com/statistics/281134/number-of-vehicles-in-use-worldwide/> (accessed August 8, 2016).
- [7] V. Daioglou, B. Wicke, A.P.C. Faaij, D.P. van Vuren, Competing uses of biomass for energy and chemicals: implications for long-term global CO<sub>2</sub> mitigation potential, *GCB Bioenergy*. 7 (2014) 1321–1334. doi:10.1111/gcbb.12228.
- [8] NREL, Can “drop-in” biofuels solve integration issues?, *Contin. Mag.* 5 (2013) 8–13. <https://www.nrel.gov/docs/fy13osti/58775.pdf> (accessed April 13, 2018).
- [9] K. Sudhakar, R. Mamat, M. Samykano, W.H. Azmi, W.F.W. Ishak, T. Yusaf, An overview of marine macroalgae as bioresource, *Renew. Sustain. Energy Rev.* 91 (2018) 165–179. doi:10.1016/j.rser.2018.03.100.
- [10] EIA, International Energy Statistics: Biofuels production, (2014). <http://www.eia.gov/cfapps/ipdbproject/iedindex3.cfm?tid=79&pid=79&aid=1&cid=regions&syid=2000&eyid=2012&unit=TBDP> (accessed March 14, 2015).
- [11] M. von Lampe, OECD Directorate for Food Agriculture and Fisheries, Agricultural

- Market Impacts of Future Growth in the Production of Biofuels. Working Policy on Agricultural Policies and Markets, (2005) 1–27. <http://www.oecd.org/trade/agricultural-trade/36074135.pdf> (accessed April 3, 2015).
- [12] M.B. Charles, R. Ryan, N. Ryan, R. Oloruntoba, Public policy and biofuels: The way forward?, *Energy Policy*. 35 (2007) 5737–5746. doi:10.1016/j.enpol.2007.06.008.
- [13] A.J. Liska, H. Yang, M. Milner, S. Goddard, H. Blanco-canqui, M.P. Pelton, X.X. Fang, H. Zhu, A.E. Suyker, Biofuels from crop residue can reduce soil carbon and increase CO<sub>2</sub> emissions, *Nat. Clim. Chang.* 4 (2014) 398–401. doi:10.1038/nclimate2187.
- [14] R. Slade, R. Saunders, R. Gross, A. Bauen, *Energy from biomass: the size of the global resource*, London, 2011. [https://spiral.imperial.ac.uk/bitstream/10044/1/12650/4/GlobalBiomassReport\\_LOLO.pdf](https://spiral.imperial.ac.uk/bitstream/10044/1/12650/4/GlobalBiomassReport_LOLO.pdf).
- [15] R. Sims, M. Taylor, J. Saddler, W. Mabee, From 1st- to 2nd-Generation Biofuel Technologies: an overview of current industry and RD&D activities, (2008) 1–124. <http://www.ieabioenergy.com/wp-content/uploads/2013/10/Task-IEAHQ-2nd-generation-Biofuels-Executive-Summary.pdf>.
- [16] S. Raikova, H. Smith-Baedorf, R. Bransgrove, O. Barlow, F. Santomauro, J.L. Wagner, M.J. Allen, C.G. Bryan, D. Sapsford, C.J. Chuck, Assessing hydrothermal liquefaction for the production of bio-oil and enhanced metal recovery from microalgae cultivated on acid mine drainage, *Fuel Process. Technol.* 142 (2016) 219–227. doi:10.1016/j.fuproc.2015.10.017.
- [17] M. Lockwood, The political sustainability of climate policy: The case of the UK Climate Change Act, *Glob. Environ. Chang.* 23 (2013) 1339–1348. doi:10.1016/j.gloenvcha.2013.07.001.
- [18] A.A. Acquaye, T. Sherwen, A. Genovese, J. Kuylenstierna, S. Lenny Koh, S. McQueen-Mason, Biofuels and their potential to aid the UK towards achieving emissions reduction policy targets, *Renew. Sustain. Energy Rev.* 16 (2012) 5414–5422. doi:10.1016/j.rser.2012.04.046.
- [19] HM Government, *The Carbon Plan: Delivering our low carbon future* (Presented

to Parliament pursuant to Sections 12 and 14 of the Climate Change Act 2008), 2011.

[https://www.gov.uk/government/uploads/system/uploads/attachment\\_data/file/47613/3702-the-carbon-plan-delivering-our-low-carbon-future.pdf](https://www.gov.uk/government/uploads/system/uploads/attachment_data/file/47613/3702-the-carbon-plan-delivering-our-low-carbon-future.pdf).

- [20] DfT, RTFO Quarterly Report 12: 15 April 2010–14 April 2011, 2011.
- [21] P. Boucher, The role of controversy, regulation and engineering in UK biofuel development, *Energy Policy*. 42 (2012) 148–154. doi:10.1016/j.enpol.2011.11.058.
- [22] DfT, Renewable Transport Fuel Obligation statistics: period 8 2015/16, report 4 (4 August 2016), 2016. [https://www.gov.uk/government/uploads/system/uploads/attachment\\_data/file/543693/rtfo-year\\_8-report-4.pdf](https://www.gov.uk/government/uploads/system/uploads/attachment_data/file/543693/rtfo-year_8-report-4.pdf).
- [23] Department for Environment Food and Rural Affairs, Department of Agriculture and Rural Development (Northern Ireland), Welsh Assembly - The Department for Rural Affairs and Heritage, The Scottish Government - Rural and Environment Research and Analysis Directorate, *Agriculture in the United Kingdom*, 2014. [https://www.gov.uk/government/uploads/system/uploads/attachment\\_data/file/430411/aug-2014-28may15a.pdf](https://www.gov.uk/government/uploads/system/uploads/attachment_data/file/430411/aug-2014-28may15a.pdf).
- [24] J.P. McCalmont, A. Hastings, N.P. McNamara, G.M. Richter, P. Robson, I.S. Donnison, J. Clifton-Brown, Environmental costs and benefits of growing *Miscanthus* for bioenergy in the UK, *GCB Bioenergy*. 9 (2015) 489–507. doi:10.1111/gcbb.12294.
- [25] B. Jin, P. Duan, Y. Xu, F. Wang, Y. Fan, Co-liquefaction of micro- and macroalgae in subcritical water., *Bioresour. Technol.* 149 (2013) 103–110. doi:10.1016/j.biortech.2013.09.045.
- [26] J. Milledge, B. Smith, P. Dyer, P. Harvey, Macroalgae-Derived Biofuel: A Review of Methods of Energy Extraction from Seaweed Biomass, *Energies*. 7 (2014) 7194–7222. doi:10.3390/en7117194.
- [27] M.D. Guiry, How many species of algae are there?, *J. Phycol.* 48 (2012) 1057–1063.
- [28] J. Rowbotham, P. Dyer, H. Greenwell, M. Theodorou, Thermochemical

processing of macroalgae: a late bloomer in the development of third-generation biofuels?, *Biofuels*. 3 (2012) 441–461. doi:10.4155/bfs.12.29.

- [29] Food and Agriculture Organization of the United Nations, World aquaculture production of aquatic plants by producers in 2013, 2013. <ftp://ftp.fao.org/FI/STAT/summary/a-5.pdf> (accessed December 1, 2015).
- [30] G. Roesijadi, S.B. Jones, Y. Zhu, Macroalgae as a Biomass Feedstock: A Preliminary Analysis, Pacific Northwest National Laboratory. Report no.: PNNL-19944. Sponsored by the US Department of Energy; September 2010, Richland, Washington, 2010.
- [31] T. Bruton, H. Lyons, Y. Lerat, M. Stanley, M.B. Rasmussen, A Review of the Potential of Marine Algae as a Source of Biofuel in Ireland (report prepared for Sustainable Energy Ireland), (2009) 1–88. [http://www.seai.ie/Publications/Renewables\\_Publications\\_/Bioenergy/Algaereport.pdf](http://www.seai.ie/Publications/Renewables_Publications_/Bioenergy/Algaereport.pdf) (accessed January 1, 2016).
- [32] K. Anastasakis, A.B. Ross, Hydrothermal liquefaction of the brown macro-alga *Laminaria saccharina*: effect of reaction conditions on product distribution and composition., *Bioresour. Technol.* 102 (2011) 4876–83. doi:10.1016/j.biortech.2011.01.031.
- [33] L. Gouveia, *Microalgae as a Feedstock for Biofuels*, Springer, Heidelberg, 2011. doi:10.1007/978-3-642-17997-6.
- [34] L. Rodolfi, G.C. Zittelli, N. Bassi, G. Padovani, N. Biondi, G. Bonini, M.R. Tredici, Microalgae for oil: Strain selection, induction of lipid synthesis and outdoor mass cultivation in a low-cost photobioreactor, *Biotechnol. Bioeng.* 102 (2009) 100–112. doi:10.1002/bit.22033.
- [35] J. Pirt, The thermodynamic efficiency (quantum demand) and dynamics of photosynthetic growth, *New Phytol.* 102 (1986) 3–37.
- [36] A. Dave, Y. Huang, S. Rezvani, D. McIlveen-Wright, M. Novaes, N. Hewitt, Techno-economic assessment of biofuel development by anaerobic digestion of European marine cold-water seaweeds, *Bioresour. Technol.* 135 (2013) 120–127. doi:10.1016/j.biortech.2013.01.005.
- [37] M. Daroch, S. Geng, G. Wang, Recent advances in liquid biofuel production from



- algal feedstocks, *Appl. Energy.* 102 (2013) 1371–1381. doi:10.1016/j.apenergy.2012.07.031.
- [38] M. Aresta, A. Dibenedetto, M. Carone, T. Colonna, C. Fragale, Production of biodiesel from macroalgae by supercritical CO<sub>2</sub> extraction and thermochemical liquefaction, *Environ. Chem. Lett.* 3 (2005) 136–139. doi:10.1007/s10311-005-0020-3.
- [39] Y. Chisti, Biodiesel from microalgae., *Biotechnol. Adv.* 25 (2007) 294–306. doi:10.1016/j.biotechadv.2007.02.001.
- [40] D.C. Elliott, Review of recent reports on process technology for thermochemical conversion of whole algae to liquid fuels, *Algal Res.* 13 (2016) 255–263. doi:10.1016/j.algal.2015.12.002.
- [41] D. López Barreiro, W. Prins, F. Ronsse, W. Brilman, Hydrothermal liquefaction (HTL) of microalgae for biofuel production: State of the art review and future prospects, *Biomass and Bioenergy.* 53 (2013) 113–127. doi:10.1016/j.biombioe.2012.12.029.
- [42] S. Raikova, C.D. Le, J.L. Wagner, V.P. Ting, C.J. Chuck, Chapter 9 – Towards an Aviation Fuel Through the Hydrothermal Liquefaction of Algae, in: C.J. Chuck (Ed.), *Biofuels Aviat.*, Elsevier, London, 2016: pp. 217–239. doi:10.1016/B978-0-12-804568-8.00009-3.
- [43] C. Tian, B. Li, Z. Liu, Y. Zhang, H. Lu, Hydrothermal liquefaction for algal biorefinery: A critical review, *Renew. Sustain. Energy Rev.* 38 (2014) 933–950. doi:10.1016/j.rser.2014.07.030.
- [44] H.P. Ruyter, J.H.J. Annee, Process for producing hydrocarbon-containing liquids from biomass, US 4670613 A, 1987.
- [45] M. Ghadiryanfar, K.A. Rosentrater, A. Keyhani, M. Omid, A review of macroalgae production, with potential applications in biofuels and bioenergy, *Renew. Sustain. Energy Rev.* 54 (2016) 473–481. doi:10.1016/j.rser.2015.10.022.
- [46] L. Xu, D.W.F. Wim Brilman, J. a M. Withag, G. Brem, S. Kersten, Assessment of a dry and a wet route for the production of biofuels from microalgae: Energy balance analysis, *Bioresour. Technol.* 102 (2011) 5113–5122. doi:10.1016/j.biortech.2011.01.066.

- [47] D.L. Sills, V. Paramita, M.J. Franke, M.C. Johnson, T.M. Akabas, C.H. Greene, J.W. Tester, Quantitative uncertainty analysis of Life Cycle Assessment for algal biofuel production., *Environ. Sci. Technol.* 47 (2013) 687–94. doi:10.1021/es3029236.
- [48] P. Duan, X. Bai, Y. Xu, A. Zhang, F. Wang, L. Zhang, J. Miao, Catalytic upgrading of crude algal oil using platinum/gamma alumina in supercritical water, *Fuel*. 109 (2013) 225–233. doi:10.1016/j.fuel.2012.12.074.
- [49] P. Biller, A.B. Ross, 17 - Production of biofuels via hydrothermal conversion, in: R. Luque, C. Lin, K. Wilson, J. Clark (Eds.), *Handb. Biofuels Prod.* 2e, 2nd ed., Elsevier, 2016: pp. 509–547. doi:10.1016/B978-0-08-100455-5.00017-5.
- [50] Y. Zhang, Hydrothermal Liquefaction to Convert Biomass into Crude Oil, in: H.P. Blaschek, T.C. Ezeji, J. Scheffran (Eds.), *Biofuels from Agric. Wastes Byprod.*, Blackwell Publishing, 2010: pp. 201–232.
- [51] Y. Zhu, K.O. Albrecht, D.C. Elliott, R.T. Hallen, S.B. Jones, Development of hydrothermal liquefaction and upgrading technologies for lipid-extracted algae conversion to liquid fuels, *Algal Res.* 2 (2013) 455–464. doi:10.1016/j.algal.2013.07.003.
- [52] C. Torri, D. Fabbri, L. Garcia-Alba, D.W.F. Brilman, Upgrading of oils derived from hydrothermal treatment of microalgae by catalytic cracking over H-ZSM-5: A comparative Py–GC–MS study, *J. Anal. Appl. Pyrolysis*. 101 (2013) 28–34. doi:10.1016/j.jaap.2013.03.001.
- [53] Z. Li, P.E. Savage, Feedstocks for fuels and chemicals from algae: Treatment of crude bio-oil over HZSM-5, *Algal Res.* 2 (2013) 154–163. doi:10.1016/j.algal.2013.01.003.
- [54] A.A. Peterson, F. Vogel, R.P. Lachance, M. Fröling, M.J. Antal, Jr., J.W. Tester, Thermochemical biofuel production in hydrothermal media: A review of sub- and supercritical water technologies, *Energy Environ. Sci.* 1 (2008) 32–65. doi:10.1039/b810100k.
- [55] S.S. Toor, L. Rosendahl, A. Rudolf, Hydrothermal liquefaction of biomass: A review of subcritical water technologies, *Energy*. 36 (2011) 2328–2342. doi:10.1016/j.energy.2011.03.013.

- [56] K. Tekin, S. Karagöz, S. Bektaş, A review of hydrothermal biomass processing, *Renew. Sustain. Energy Rev.* 40 (2014) 673–687. doi:10.1016/j.rser.2014.07.216.
- [57] W. Yang, X. Li, Z. Li, C. Tong, L. Feng, Understanding low-lipid algae hydrothermal liquefaction characteristics and pathways through hydrothermal liquefaction of algal major components : Crude polysaccharides , crude proteins and their binary mixtures, *Bioresour. Technol.* 196 (2015) 99–108. doi:10.1016/j.biortech.2015.07.020.
- [58] L. Garcia Alba, C. Torri, C. Samori, J. Van Der Spek, D. Fabbri, S.R.A. Kersten, D.W.F. Brilman, Hydrothermal treatment (HTT) of microalgae: Evaluation of the process as conversion method in an algae biorefinery concept, *Energy and Fuels.* 26 (2012) 642–657. doi:10.1021/ef201415s.
- [59] N. Akiya, P.E. Savage, Roles of water for chemical reactions in high-temperature water, *Chem. Rev.* 102 (2002) 2725–2750. doi:10.1021/cr000668w.
- [60] D. López Barreiro, M. Beck, U. Hornung, F. Ronsse, A. Kruse, W. Prins, Suitability of hydrothermal liquefaction as a conversion route to produce biofuels from macroalgae, *Algal Res.* 11 (2015) 234–241. doi:10.1016/j.algal.2015.06.023.
- [61] K. Anastasakis, A.B. Ross, Hydrothermal liquefaction of four brown macro-algae commonly found on the UK coasts: An energetic analysis of the process and comparison with bio-chemical conversion methods, *Fuel.* 139 (2015) 546–553. doi:10.1016/j.fuel.2014.09.006.
- [62] D. Zhou, L. Zhang, S. Zhang, H. Fu, J. Chen, Hydrothermal Liquefaction of Macroalgae *Enteromorpha prolifera* to Bio-oil, *Energy & Fuels.* 24 (2010) 4054–4061. doi:10.1021/ef100151h.
- [63] D.C. Elliott, L.J. Sealock Jr., S.R. Butner, Product Analysis from Direct Liquefaction of Several High-Moisture Biomass Feedstocks, in: E.J. Soltes, T.A. Milne (Eds.), *Pyrolysis Oils From Biomass Prod. Anal. Upgrad. - ACS Symp. Ser.*, American Chemical Society, Washington, D. C., 1988: pp. 179–188. doi:doi:10.1021/bk-1988-0376.ch017.
- [64] D. Li, L. Chen, D. Xu, X. Zhang, N. Ye, F. Chen, S. Chen, Preparation and characteristics of bio-oil from the marine brown alga *Sargassum patens* C. Agardh, *Bioresour. Technol.* 104 (2012) 737–742.

doi:10.1016/j.biortech.2011.11.011.

- [65] W. Yang, X. Li, S. Liu, L. Feng, Direct hydrothermal liquefaction of undried macroalgae *Enteromorpha prolifera* using acid catalysts, *Energy Convers. Manag.* 87 (2014) 938–945. doi:10.1016/j.enconman.2014.08.004.
- [66] N. Neveux, A.K.L. Yuen, C. Jazrawi, M. Magnusson, B.S. Haynes, A.F. Masters, A. Montoya, N.A. Paul, T. Maschmeyer, R. de Nys, Biocrude yield and productivity from the hydrothermal liquefaction of marine and freshwater green macroalgae, *Bioresour. Technol.* 155 (2014) 334–341.
- [67] D.C. Elliott, T.R. Hart, G.G. Neuenschwander, L.J. Rotness, G. Roesijadi, A.H. Zacher, J.K. Magnuson, Hydrothermal Processing of Macroalgal Feedstocks in Continuous-Flow Reactors, *ACS Sustain. Chem. Eng.* 2 (2014) 201–215. doi:10.1021/sc400251p.
- [68] Y. He, X. Liang, C. Jazrawi, A. Montoya, A. Yuen, A.J. Cole, N. Neveux, N.A. Paul, R. de Nys, T. Maschmeyer, B.S. Haynes, Continuous hydrothermal liquefaction of macroalgae in the presence of organic co-solvents, *Algal Res.* 17 (2016) 185–195. doi:10.1016/j.algal.2016.05.010.
- [69] M. Parsa, H. Jalilzadeh, M. Pazoki, R. Ghasemzadeh, M.A. Abduli, Hydrothermal liquefaction of *Gracilaria gracilis* and *Cladophora glomerata* macro-algae for biocrude production, *Bioresour. Technol.* 250 (2018) 26–34. doi:10.1016/j.biortech.2017.10.059.
- [70] B. Biswas, A.C. Fernandes, J. Kumar, U.D. Muraleedharan, T. Bhaskar, Valorization of *Sargassum tenerrimum*: Value addition using hydrothermal liquefaction, *Fuel*. 222 (2018) 394–401. doi:10.1016/j.fuel.2018.02.153.
- [71] D. Zhou, S. Zhang, H. Fu, J. Chen, Liquefaction of Macroalgae *Enteromorpha prolifera* in Sub-/Supercritical Alcohols: Direct Production of Ester Compounds, *Energy & Fuels*. 26 (2012) 2342–2351. doi:10.1021/ef201966w.
- [72] Y.-P. Xu, P.-G. Duan, F. Wang, Hydrothermal processing of macroalgae for producing crude bio-oil, *Fuel Process. Technol.* 130 (2015) 268–274. doi:10.1016/j.fuproc.2014.10.028.
- [73] R. Singh, T. Bhaskar, B. Balagurumurthy, Effect of solvent on the hydrothermal liquefaction of macro algae *Ulva fasciata*, *Process Saf. Environ. Prot.* 93 (2015)

154–160. doi:10.1016/j.psep.2014.03.002.

- [74] R. Singh, B. Balagurumurthy, T. Bhaskar, Hydrothermal liquefaction of macro algae: Effect of feedstock composition, *Fuel*. 146 (2015) 69–74. doi:10.1016/j.fuel.2015.01.018.
- [75] P. Biller, A.B. Ross, Potential yields and properties of oil from the hydrothermal liquefaction of microalgae with different biochemical content, *Bioresour. Technol.* 102 (2011) 215–25. doi:10.1016/j.biortech.2010.06.028.
- [76] G. Yu, Y. Zhang, L. Schideman, T.L. Funk, Z. Wang, Hydrothermal liquefaction of low lipid content microalgae into bio-crude oil, *Am. Soc. Agric. Biol. Eng.* 54 (2011) 239–246.
- [77] G. Teri, L. Luo, P.E. Savage, Hydrothermal Treatment of Protein, Polysaccharide, and Lipids Alone and in Mixtures, *Energy Fuels*. 28 (2014) 7501–7509. doi:10.1021/ef501760d.
- [78] P. Biller, R. Riley, A.B. Ross, Catalytic hydrothermal processing of microalgae: decomposition and upgrading of lipids, *Bioresour. Technol.* 102 (2011) 4841–8. doi:10.1016/j.biortech.2010.12.113.
- [79] S. Zou, Y. Wu, M. Yang, C. Li, J. Tong, Bio-oil production from sub- and supercritical water liquefaction of microalgae *Dunaliella tertiolecta* and related properties, *Energy Environ. Sci.* 3 (2010) 1073. doi:10.1039/c002550j.
- [80] B. Zhang, M. von Keitz, K. Valentas, Thermochemical liquefaction of high-diversity grassland perennials, *J. Anal. Appl. Pyrolysis*. 84 (2009) 18–24. doi:10.1016/j.jaap.2008.09.005.
- [81] J. Akhtar, N.A.S. Amin, A review on process conditions for optimum bio-oil yield in hydrothermal liquefaction of biomass, *Renew. Sustain. Energy Rev.* 15 (2011) 1615–1624. doi:10.1016/j.rser.2010.11.054.
- [82] K.-Q. Tran, Fast hydrothermal liquefaction for production of chemicals and biofuels from wet biomass: The need to develop a plug-flow reactor, (2016). doi:10.1016/j.biortech.2016.04.002.
- [83] S.S. Toor, H. Reddy, S. Deng, J. Hoffmann, D. Spangsmark, L.B. Madsen, J.B. Holm-Nielsen, L.A. Rosendahl, Hydrothermal liquefaction of *Spirulina* and

- Nannochloropsis salina under subcritical and supercritical water conditions, *Bioresour. Technol.* 131 (2013) 413–419. doi:10.1016/j.biortech.2012.12.144.
- [84] W.T. Chen, Y. Zhang, J. Zhang, G. Yu, L.C. Schideman, P. Zhang, M. Minarick, Hydrothermal liquefaction of mixed-culture algal biomass from wastewater treatment system into bio-crude oil, *Bioresour. Technol.* 152 (2014) 130–139. doi:10.1016/j.biortech.2013.10.111.
- [85] T. Matsui, A. Nishihara, C. Ueda, M. Ohtsuki, N. Ikenaga, T. Suzuki, Liquefaction of micro-algae with iron catalyst, *Fuel*. 76 (1997) 1043–1048. doi:10.1016/S0016-2361(97)00120-8.
- [86] D. Xu, P.E. Savage, Characterization of biocrudes recovered with and without solvent after hydrothermal liquefaction of algae M1-A, *Algal Res.* 6 (2014) 1–7. doi:10.1016/j.algal.2014.08.007.
- [87] S.N. Xiu, A. Shahbazi, J. Croonenberghs, L.J. Wang, Oil Production from Duckweed by Thermochemical Liquefaction, *Energy Sources, Energy Sources, Part A*. 32 (2010) 1293–1300. doi:10.1080/15567030903060408.
- [88] H.M. Khairy, S.M. El-Shafay, Seasonal variations in the biochemical composition of some common seaweed species from the coast of Abu Qir Bay, Alexandria, Egypt, *Oceanologia*. 55 (2013) 435–452. doi:10.5697/oc.55-2.435.
- [89] E. Marinho-Soriano, P.C. Fonseca, M.A.A. Carneiro, W.S.C. Moreira, Seasonal variation in the chemical composition of two tropical seaweeds, *Bioresour. Technol.* 97 (2006) 2402–2406. doi:10.1016/j.biortech.2005.10.014.
- [90] J.M.M. Adams, A.B. Ross, K. Anastasakis, E.M. Hodgson, J.A. Gallagher, J.M. Jones, I.S. Donnison, Seasonal variation in the chemical composition of the bioenergy feedstock *Laminaria digitata* for thermochemical conversion, *Bioresour. Technol.* 102 (2011) 226–234. doi:10.1016/j.biortech.2010.06.152.
- [91] B. Zhang, M. von Keitz, K. Valentas, Thermal Effects on Hydrothermal Biomass Liquefaction, *Appl. Biochem. Biotechnol.* 147 (2008) 143–150.
- [92] J.L. Faeth, P.J. Valdez, P.E. Savage, Fast Hydrothermal Liquefaction of *Nannochloropsis* sp. To Produce Biocrude, *Energy & Fuels*. 27 (2013) 1391–1398. doi:10.1021/ef301925d.

- [93] K. Anastasakis, The Potential of the Production of Fuels and Chemicals From Marine Biomass, University of Leeds (Energy Resources and Research Institute), 2011. doi:<http://etheses.whiterose.ac.uk/id/eprint/4167>.
- [94] P. Duan, P.E. Savage, Hydrothermal liquefaction of a microalga with heterogeneous catalysts, *Ind. Eng. Chem. Res.* 50 (2011) 52–61. doi:10.1021/ie100758s.
- [95] Y. Chen, Q. Wei, X. Ren, The effect of hydrophilic amines on hydrothermal liquefaction of macroalgae residue, *Bioresour. Technol.* 243 (2017) 409–416. doi:10.1016/j.biortech.2017.06.148.
- [96] B. Biswas, A. Arun Kumar, Y. Bisht, R. Singh, J. Kumar, T. Bhaskar, A.A. Kumar, Y. Bisht, R. Singh, J. Kumar, T. Bhaskar, Effects of temperature and solvent on hydrothermal liquefaction of *Sargassum tenerrimum* algae, *Bioresour. Technol.* 242 (2017) 344–350. doi:10.1016/j.biortech.2017.03.045.
- [97] D.C. Elliott, P. Biller, A.B. Ross, A.J. Schmidt, S.B. Jones, Hydrothermal liquefaction of biomass: Developments from batch to continuous process, *Bioresour. Technol.* 178 (2015) 147–156. doi:10.1016/j.biortech.2014.09.132.
- [98] D.C. Elliott, T.R. Hart, A.J. Schmidt, G.G. Neuenschwander, L.J. Rotness, M. V. Olarte, A.H. Zacher, K.O. Albrecht, R.T. Hallen, J.E. Holladay, Process development for hydrothermal liquefaction of algae feedstocks in a continuous-flow reactor, *Algal Res.* 2 (2013) 445–454. doi:10.1016/j.algal.2013.08.005.
- [99] C. Jazrawi, P. Biller, A.B. Ross, A. Montoya, T. Maschmeyer, B.S. Haynes, Pilot plant testing of continuous hydrothermal liquefaction of microalgae, *Algal Res.* 2 (2013) 268–277. doi:10.1016/j.algal.2013.04.006.
- [100] E.J. Berglin, C.W. Enderlin, A.J. Schmidt, Review and Assessment of Commercial Vendors/Options for Feeding and Pumping Biomass Slurries for Hydrothermal Liquefaction (Report PNNL-21981), n.d. [http://www.pnnl.gov/main/publications/external/technical\\_reports/PNNL-21981.pdf](http://www.pnnl.gov/main/publications/external/technical_reports/PNNL-21981.pdf).
- [101] H. Li, Z. Liu, Y. Zhang, B. Li, H. Lu, N. Duan, M. Liu, Z. Zhu, B. Si, Conversion efficiency and oil quality of low-lipid high-protein and high-lipid low-protein microalgae via hydrothermal liquefaction, *Bioresour. Technol.* 154 (2014) 322–329. doi:10.1016/j.biortech.2013.12.074.

- [102] G.W. Huber, S. Iborra, A. Corma, Synthesis of transportation fuels from biomass: Chemistry, catalysts, and engineering, *Chem. Rev.* 106 (2006) 4044–4098.
- [103] M. Fatih Demirbas, Biorefineries for biofuel upgrading: A critical review, *Appl. Energy*. 86 (2009) S151–S161. doi:10.1016/j.apenergy.2009.04.043.
- [104] J.G. Speight, *Handbook of Petroleum Analysis*, 1st ed., Wiley Interscience, New York, 2001.
- [105] S. Bjelić, J. Yu, B. Brummerstedt Iversen, M. Glasius, P. Biller, Detailed Investigation into the Asphaltene Fraction of Hydrothermal Liquefaction Derived Bio-Crude and Hydrotreated Bio-Crudes, *Energy & Fuels*. 32 (2018) 3579–3587. doi:10.1021/acs.energyfuels.7b04119.
- [106] D.R. Vardon, B.K. Sharma, J. Scott, G. Yu, Z. Wang, L. Schideman, Y. Zhang, T.J. Strathmann, Chemical properties of biocrude oil from the hydrothermal liquefaction of *Spirulina* algae, swine manure, and digested anaerobic sludge, *Bioresour. Technol.* 102 (2011) 8295–8303. doi:10.1016/j.biortech.2011.06.041.
- [107] P. Duan, P.E. Savage, Catalytic hydrotreatment of crude algal bio-oil in supercritical water, *Appl. Catal. B Environ.* 104 (2011) 136–143. doi:10.1016/j.apcatb.2011.02.020.
- [108] P. Duan, P.E. Savage, Catalytic treatment of crude algal bio-oil in supercritical water: optimization studies, *Energy Environ. Sci.* 4 (2011) 1447. doi:10.1039/c0ee00343c.
- [109] X. Bai, P. Duan, Y. Xu, A. Zhang, P.E. Savage, Hydrothermal catalytic processing of pretreated algal oil: A catalyst screening study, *Fuel*. 120 (2014) 141–149. doi:10.1016/j.fuel.2013.12.012.
- [110] D. López Barreiro, B. Ríos Gómez, F. Ronsse, U. Hornung, A. Kruse, W. Prins, Heterogeneous catalytic upgrading of biocrude oil produced by hydrothermal liquefaction of microalgae: State of the art and own experiments, *Fuel Process. Technol.* 148 (2016) 117–127. doi:10.1016/j.fuproc.2016.02.034.
- [111] J. Hoffmann, C. Uhrenholt Jensen, L.A. Rosendahl, Co-processing potential of HTL bio-crude at petroleum refineries – Part 1: Fractional distillation and characterization, *Fuel*. 165 (2016) 526–535. doi:10.1016/j.fuel.2015.10.094.



- [112] C. Uhrenholt Jensen, J. Hoffmann, L.A. Rosendahl, C. Uhrenholt Jensen, J. Hoffmann, L.A. Rosendahl, Co-processing potential of HTL bio-crude at petroleum refineries. Part 2: A parametric hydrotreating study, *Fuel*. 165 (2016) 536–543. doi:10.1016/j.fuel.2015.08.047.
- [113] A. Cole, Y. Dinburg, B.S. Haynes, Y. He, M. Herskowitz, C. Jazrawi, M. Landau, X. Liang, M. Magnusson, T. Maschmeyer, A.F. Masters, N. Meiri, N. Neveux, R. de Nys, N. Paul, M. Rabaev, R. Vidruk-Nehemya, A.K.L. Yuen, From macroalgae to liquid fuel via waste-water remediation, hydrothermal upgrading, carbon dioxide hydrogenation and hydrotreating, *Energy Environ. Sci.* 9 (2016) 1828–1840. doi:10.1039/c6ee00414h.
- [114] M. Lavanya, A. Meenakshisundaram, S. Renganathan, S. Chinnasamy, D.M. Lewis, J. Nallasivam, S. Bhaskar, Hydrothermal liquefaction of freshwater and marine algal biomass: A novel approach to produce distillate fuel fractions through blending and co-processing of biocrude with petrocrude, *Bioresour. Technol.* 203 (2016) 228–235. doi:10.1016/j.biortech.2015.12.013.
- [115] F.A. Agblevor, O. Mante, R. McClung, S.T. Oyama, Co-processing of standard gas oil and biocrude oil to hydrocarbon fuels, *Biomass and Bioenergy*. 45 (2012) 130–137. doi:10.1016/j.biombioe.2012.05.024.
- [116] C. Uhrenholt Jensen, J. Hoffmann, L.A. Rosendahl, Co-processing potential of HTL bio-crude at petroleum refineries. Part 2: A parametric hydrotreating study, (2016). doi:10.1016/j.fuel.2015.08.047.
- [117] P. Biller, A.B. Ross, S.C. Skill, A. Lea-Langton, B. Balasundaram, C. Hall, R. Riley, C.A. Llewellyn, Nutrient recycling of aqueous phase for microalgae cultivation from the hydrothermal liquefaction process, *Algal Res.* 1 (2012) 70–76. doi:10.1016/j.algal.2012.02.002.
- [118] U. Jena, N. Vaidyanathan, S. Chinnasamy, K.C. Das, Evaluation of microalgae cultivation using recovered aqueous co-product from thermochemical liquefaction of algal biomass, *Bioresour. Technol.* 102 (2011) 3380–3387. doi:10.1016/j.biortech.2010.09.111.
- [119] P.J. Valdez, M.C. Nelson, H.Y. Wang, X.N. Lin, P.E. Savage, Hydrothermal liquefaction of *Nannochloropsis* sp.: Systematic study of process variables and analysis of the product fractions, *Biomass and Bioenergy*. 46 (2012) 317–331.

doi:10.1016/j.biombioe.2012.08.009.

- [120] S.R. Shanmugam, S. Adhikari, R. Shakya, Nutrient removal and energy production from aqueous phase of bio-oil generated via hydrothermal liquefaction of algae, *Bioresour. Technol.* 230 (2017) 43–48. doi:10.1016/j.biortech.2017.01.031.
- [121] Y. Hu, S. Feng, Z. Yuan, C. (Charles) Xu, A. Bassi, Investigation of aqueous phase recycling for improving bio-crude oil yield in hydrothermal liquefaction of algae, *Bioresour. Technol.* 239 (2017) 151–159. doi:10.1016/j.biortech.2017.05.033.
- [122] S. Papadokonstantakis, A. Gambardella, J. Askmar, Y. Ding, Superstructure investigation for P-recovery technologies integration with macroalgae based hydrothermal liquefaction, Elsevier Masson SAS, 2018. doi:10.1016/B978-0-444-64241-7.50287-1.
- [123] P.G. Duan, S.K. Yang, Y.P. Xu, F. Wang, D. Zhao, Y.J. Weng, X.L. Shi, Integration of hydrothermal liquefaction and supercritical water gasification for improvement of energy recovery from algal biomass, *Energy*. 155 (2018) 734–745. doi:10.1016/j.energy.2018.05.044.
- [124] P. Biller, R.B. Madsen, M. Klemmer, J. Becker, B.B. Iversen, M. Glasius, Effect of hydrothermal liquefaction aqueous phase recycling on bio- crude yields and composition, *Bioresour. Technol.* 220 (2016) 190–199. doi:10.1016/j.biortech.2016.08.053.
- [125] M. Nelson, L. Zhu, A. Thiel, Y. Wu, M. Guan, J. Minty, H.Y. Wang, X.N. Lin, Microbial utilization of aqueous co-products from hydrothermal liquefaction of microalgae *Nannochloropsis oculata.*, *Bioresour. Technol.* 136 (2013) 522–8. doi:10.1016/j.biortech.2013.03.074.
- [126] M. Pham, L. Schideman, J. Scott, N. Rajagopalan, M.J. Plewa, Chemical and Biological Characterization of Wastewater generated from Hydrothermal Liquefaction of *Spirulina*, *Environ. Sci. Technol.* 47 (2013) 2131–2138. doi:10.1021/es304532c.
- [127] Y. Zhou, L. Schideman, Y. Zhang, G. Yu, Z. Wang, M. Pham, Resolving Bottlenecks in Current Algal Wastewater Treatment Paradigms: A Synergistic Combination of Low-Lipid Algal Wastewater Treatment and Hydrothermal

Liquefaction for Large-Scale Biofuel Production, *Energy and Water*. 15 (2011) 347–361.

- [128] L. Leng, J. Li, Z. Wen, W. Zhou, Use of microalgae to recycle nutrients in aqueous phase derived from hydrothermal liquefaction process, *Bioresour. Technol.* 256 (2018) 529–542. doi:10.1016/j.biortech.2018.01.121.
- [129] P. Biller, A.B. Ross, Hydrothermal processing of algal biomass for the production of biofuels and chemicals, *Biofuels*. 3 (2012) 603–623. doi:10.4155/bfs.12.42.
- [130] D. Matovic, Biochar as a viable carbon sequestration option: Global and Canadian perspective, *Energy*. 36 (2011) 2011–2016. doi:10.1016/j.energy.2010.09.031.
- [131] T. Berntsson, B. Sandén, L. Olsson, A. Åsblad, What is a biorefinery?, in: B. Sandén, K. Pettersson (Eds.), *Syst. Perspect. Biorefineries*, 3.1, Chalmers University of Technology, Göteborg, 2014: pp. 18–30. <http://circa.europa.eu/Public/irc/rtd/susbioref/library?l=/> (accessed December 11, 2018).
- [132] Y. Zhou, L. Schideman, G. Yu, Y. Zhang, A synergistic combination of algal wastewater treatment and hydrothermal biofuel production maximized by nutrient and carbon recycling, *Energy Environ. Sci.* 6 (2013) 3765. doi:10.1039/c3ee24241b.
- [133] Y. Zhou, L. Schideman, Y. Zhang, G. Yu, Environment-Enhancing Energy: A Novel Wastewater Treatment System that Maximizes Algal Biofuel Production and Minimizes Greenhouse Gas Emissions, in: *Proc. Water Environ. Fed.*, 2011: p. 7268–7282(15).
- [134] B.H. Buck, C.M. Buchholz, The offshore-ring: A new system design for the open ocean aquaculture of macroalgae, *J. Appl. Phycol.* 16 (2004) 355–368. doi:10.1023/B:JAPH.0000047947.96231.ea.
- [135] D.P. Chynoweth, Review of biomethane from marine biomass (report prepared for Tokyo Gas Company), (2002). [http://abe.ufl.edu/chyn/download/Publications\\_DC/Reports/marinefinal\\_FT.pdf](http://abe.ufl.edu/chyn/download/Publications_DC/Reports/marinefinal_FT.pdf) (accessed January 7, 2016).
- [136] T. Roberts, P. Upham, Prospects for the use of macro-algae for fuel in Ireland and the UK: An overview of marine management issues, *Mar. Policy*. 36 (2012) 1047–

1053. doi:10.1016/j.marpol.2012.03.001.

- [137] Ordnance Survey, Geography and maps, UK Ordnance Surv. (2016). <https://www.ordnancesurvey.co.uk/support/geography-map-facts.html> (accessed August 9, 2016).
- [138] J.H. Reith, E.P. Deurwaarder, K. Hemmes, A.P.W.M. Curvers, P. Kamermans, W. Brandenburg, G. Zeeman, Bio-Offshore: Grootschalige teelt van zeeieren in combinatie met offshore windparken in de Noordzee, ECN Energy Research Centre of the Netherlands, 2005.
- [139] S. van den Burg, M. Stuiver, F. Veenstra, P. Bikker, A.L. Contreras, A. Palstra, J. Broeze, H. Jansen, R. Jak, A. Gerritsen, P. Harmsen, J. Kals, A. Blanco, W. Brandenburg, M. van Krimpen, A.P. van Duijn, W. Mulder, L. van Raamsdonk, A Triple P review of the feasibility of sustainable offshore seaweed production in the North Sea - LEI Report 13-077, Wageningen UR (University & Research centre), Wageningen, 2012.
- [140] ECOFYS, Ecofys launches test module for seaweed cultivation in offshore wind farms, Press Release. (2012). <http://www.ecofys.com/en/press/ecofys-launches-trial-module-for-seaweed-cultivation-in-offshore-wind-farm/> (accessed October 17, 2016).
- [141] G. Roesijadi, A.E. Copping, M.H. Huesemann, J. Forster, R.M. Thom, A. Ventures, Techno-Economic Feasibility Analysis of Offshore Seaweed Farming for Bioenergy and Biobased Products Independent Research and Development Report IR Number: PNWD-3931, 2008. [https://arpa.e.energy.gov/sites/default/files/Techno-Economic Feasibility Analysis of Offshore Seaweed Farming for Bioenergy and Biobased Products-2008.pdf](https://arpa.e.energy.gov/sites/default/files/Techno-Economic%20Feasibility%20Analysis%20of%20Offshore%20Seaweed%20Farming%20for%20Bioenergy%20and%20Biobased%20Products-2008.pdf) (accessed July 25, 2017).
- [142] L. Van Khoi, R. Fotedar, Integration of western king prawn (*Penaeus latisulcatus* Kishinouye, 1896) and green seaweed (*Ulva lactuca* Linnaeus, 1753) in a closed recirculating aquaculture system, *Aquaculture*. 322–323 (2011) 201–209. doi:10.1016/j.aquaculture.2011.09.030.
- [143] E. Marinho-Soriano, S.O. Nunes, M.A.A. Carneiro, D.C. Pereira, Nutrients' removal from aquaculture wastewater using the macroalgae *Gracilaria birdiae*, *Biomass and Bioenergy*. 33 (2009) 327–331.

doi:10.1016/j.biombioe.2008.07.002.

- [144] S.G. Nelson, E.P. Glenn, J. Conn, D. Moore, T. Walsh, M. Akutagawa, Cultivation of *Gracilaria parvispora* (Rhodophyta) in shrimp-farm effluent ditches and floating cages in Hawaii: a two-phase polyculture system, *Aquaculture*. 193 (2001) 239–248. doi:doi:10.1016/S0044-8486(00)00491-9.
- [145] H. Mai, R. Fotedar, J. Fewtrell, Evaluation of *Sargassum* sp. as a nutrient-sink in an integrated seaweed-prawn (ISP) culture system, *Aquaculture*. 310 (2010) 91–98. doi:10.1016/j.aquaculture.2010.09.010.
- [146] E. van Sebille, C. Spathi, A. Gilbert, The ocean plastic pollution challenge: towards solutions in the UK (Briefing paper No 19), London, 2016. [www.imperial.ac.uk/grantham/publications](http://www.imperial.ac.uk/grantham/publications) (accessed August 31, 2018).
- [147] G. Suaria, S. Aliani, Floating debris in the Mediterranean Sea, *Mar. Pollut. Bull.* 86 (2014) 494–504. doi:10.1016/j.marpolbul.2014.06.025.
- [148] UNEP, Valuing Plastics: The Business Case for Measuring, Managing and Disclosing Plastic Use in the Consumer Goods Industry, 2014. [www.unep.org/pdf/ValuingPlastic/](http://www.unep.org/pdf/ValuingPlastic/).
- [149] L. Gutow, A. Eckerlebe, L. Gimeez, R. Saborowski, Experimental Evaluation of Seaweeds as a Vector for Microplastics into Marine Food Webs, *Environ. Sci. Technol.* 50 (2016) 915–923. doi:10.1021/acs.est.5b02431.
- [150] B.B. Uzoejinwa, X. He, S. Wang, A. El-Fatah Abomohra, Y. Hu, Q. Wang, Co-pyrolysis of biomass and waste plastics as a thermochemical conversion technology for high-grade biofuel production: Recent progress and future directions elsewhere worldwide, *Energy Convers. Manag.* 163 (2018) 468–492. doi:10.1016/j.enconman.2018.02.004.
- [151] X. Yuan, H. Cao, H. Li, G. Zeng, J. Tong, L. Wang, Quantitative and qualitative analysis of products formed during co-liquefaction of biomass and synthetic polymer mixtures in sub- and supercritical water, *Fuel Process. Technol.* 90 (2009) 428–434. doi:10.1016/j.fuproc.2008.11.005.
- [152] B. Wang, Y. Huang, J. Zhang, Hydrothermal liquefaction of lignite, wheat straw and plastic waste in sub-critical water for oil: Product distribution, *J. Anal. Appl. Pyrolysis*. 110 (2014) 382–389. doi:10.1016/j.jaap.2014.10.004.

- [153] X. Pei, X. Yuan, G. Zeng, H. Huang, J. Wang, H. Li, H. Zhu, Co-liquefaction of microalgae and synthetic polymer mixture in sub- and supercritical ethanol, *Fuel Process. Technol.* 93 (2012) 35–44. doi:10.1016/j.fuproc.2011.09.010.
- [154] X. Wu, J. Liang, Y. Wu, H. Hu, S. Huang De, K. Wu, Co-liquefaction of microalgae and polypropylene in sub-/super-critical water, *RSC Adv.* 7 (2017) 13768. doi:10.1039/c7ra01030c.
- [155] J. Lu, Z. Liu, Y. Zhang, B. Li, Q. Lu, Y. Ma, R. Shen, Z. Zhu, Improved production and quality of biocrude oil from low-lipid high-ash macroalgae *Enteromorpha prolifera* via addition of crude glycerol, *J. Clean. Prod.* 142 (2017) 749–757. doi:10.1016/j.jclepro.2016.08.048.
- [156] T.M. Leese, The conversion of ocean farm kelp to methane and other products, in: *Clean Fuels from Biomass, Sewage, Urban Refus. Agric. Wastes*, Institute of Gas Technology, Orlando, FL, FL, 1976: pp. 253–266.
- [157] A.F. Clarens, E.P. Resurreccion, M.A. White, L.M. Colosi, Environmental Life Cycle Comparison of Algae to Other Bioenergy Feedstocks, *Environ. Sci. Technol.* 44 (2010) 1813–1819. doi:10.1021/es902838n.
- [158] D. Aitken, C. Bulboa, A. Godoy-Faundez, J.L. Turrion-Gomez, B. Antizar-Ladislao, Life cycle assessment of macroalgae cultivation and processing for biofuel production, *J. Clean. Prod.* 75 (2014) 45–56. doi:10.1016/j.jclepro.2014.03.080.
- [159] M. Aresta, A. Dibenedetto, G. Barberio, Utilization of macro-algae for enhanced CO<sub>2</sub> fixation and biofuels production: Development of a computing software for an LCA study, *Fuel Process. Technol.* 86 (2005) 1679–1693. doi:10.1016/j.fuproc.2005.01.016.
- [160] N. Neveux, M. Magnusson, T. Maschmeyer, Comparing the potential production and value of high-energy liquid fuels and protein from marine and freshwater macroalgae, *Glob. Chang. Biol. - Bioenergy.* 7 (2015) 673–689. doi:10.1111/gcbb.12171.

## Chapter 2

---

# Towards a marine biorefinery through the hydrothermal liquefaction of macroalgae native to the United Kingdom

This work was published in *Biomass and Bioenergy* (Elsevier) in October 2017. This work was completed in collaboration with Plymouth Marine Laboratory (PML).

**Raikova, S.**, Le, C.D., Beacham, T.A., Jenkins, R.W., Allen, M.J., Chuck, C.J., 2017. Towards a marine biorefinery through the hydrothermal liquefaction of macroalgae native to the United Kingdom. *Biomass and Bioenergy*, **107**, 244–253.  
doi:10.1016/j.biombioe.2017.10.010

## 2.1 Context

A recent meta-analysis of HTL literature has demonstrated that biomass type and composition are the most significant parameters controlling bio-crude production [1]. However, the bulk of research on macroalgal HTL has thus far focused on exploring a small number of individual macroalgae species for bio-crude production, largely limited to brown and green macroalgae (Heterokontophyceae and Chlorophyceae, respectively), with no mention of red macroalgae (Rhodophyceae).

Although the mechanisms broadly underlying HTL of biomass in general have been characterised, little has been done to understand the reactivity of macroalgae specifically, which contains many biochemical components not observed in terrestrial plants. The field is still largely in its infancy, with little cohesion between different researchers with respect to optimal experimental conditions and equipment, leading to difficulties in drawing comparisons between past studies.

Multivariate analysis has demonstrated that, in addition to biomass type, heating velocity is one of the main factors governing biomass conversion [1], while reaction temperature is widely acknowledged as another of the most important factors affecting HTL reactivity [2]. Temperature and heating rate would significantly affect the energy balance within a biorefinery. Size reduction can be energy-intensive, and could potentially constitute a significant contribution to the overall energy balance of a biorefinery.

Additionally, although recycling and nutrient recovery from HTL aqueous products has attracted some attention for microalgae [3–5], the nutrient-rich aqueous phase products of macroalgal HTL have thus far been overlooked.

The aim of this study was to rationalise HTL reactivity across a wider range of macroalgae species than explored in previous literature, incorporating a representative from the Rhodophyta family, and spanning a wider range of biochemical compositions. The study aimed to map these compositions against product mass and elemental distributions to gain an understanding of the effect of groups of biochemicals (specifically, proteins, lipids and carbohydrates) on bio-crude production and quality. This understanding could then be used to select biochemical specifications for an “ideal” macroalgae feedstock for the UK on the basis of maximising bio-crude production (to be co-refined with mineral crude or upgraded to biofuels) and nutrient recovery in the aqueous phase (for potential utilisation as a fertiliser). The biochemical compositions of many macroalgae species are already largely known, and establishing patterns in reactivity could help to predict the reactivity of a wide variety of feedstocks without carrying out HTL, potentially identifying a huge range of novel biorefinery options.



This chapter is submitted in an alternative format in line with Appendix 6A of the “Specifications for Higher Degree Theses and Portfolios” as required by the University of Bath.

The work completed in this paper was conducted by the author with the exception of the following:

HTL reactions at varying heating rates were carried out by Chien Dinh Le, one of the paper’s co-authors.

Lipid and polysaccharide quantification were conducted by Tracey Beacham (PML), one of the paper’s co-authors.

Elemental analysis was carried out by analytical department personnel at London Metropolitan University.

## 2.2 Biomass and Bioenergy paper

### Towards a marine biorefinery through the hydrothermal liquefaction of macroalgae native to the United Kingdom

S. Raikova<sup>a</sup>, C. D. Le<sup>b</sup>, T. A. Beacham<sup>c</sup>, R. W. Jenkins<sup>d</sup>, M. J. Allen<sup>c</sup>, C. J. Chuck<sup>d\*</sup>

<sup>a</sup> Centre for Doctoral Training in Sustainable Chemical Technologies, , Department of Chemical Engineering, University of Bath, Claverton Down, Bath BA2 7AY, United Kingdom

<sup>b</sup> Department of Oil Refining and Petrochemistry, Hanoi University of Mining and Geology, Hanoi, Vietnam

<sup>c</sup> Plymouth Marine Laboratory, Prospect Place, The Hoe, Plymouth PL1 3DH, United Kingdom

<sup>d</sup> Department of Chemical Engineering, University of Bath, Claverton Down, Bath BA2 7AY, United Kingdom

#### 2.2.1 Keywords

Macroalgae

Hydrothermal liquefaction

Biorefinery

Bio-crude

#### 2.2.2 Abbreviations

AP – Aqueous phase

ER – energy recovery

HHV – higher heating value

HTG – hydrothermal gasification

HTL – hydrothermal liquefaction

### 2.2.3 Highlights

- Hydrothermal liquefaction conditions were optimised for bio-crude and nutrient recovery using *Ascophyllum nodosum*
- Liquefaction (345 °C; 30 K min<sup>-1</sup>) of 13 UK macroalgae species were carried out
- Bio-crude yields of up to 29.9 % were obtained for HTL of *Ulva lactuca*
- Phosphate (max. 236 mg kg<sup>-1</sup> aqueous phase) was detected in the aqueous phase products for HTL of *Solieria chordalis*
- Biochemical compositions were not a clear predictor of product distribution
- Varying biomass particle size (between < 125 µm - 1.4 mm) did not affect bio-crude production

### 2.2.4 Abstract

Hydrothermal liquefaction (HTL) is a promising biomass conversion method that can be incorporated into a biorefinery paradigm for simultaneous production of fuels, aqueous fertilisers and potential remediation of municipal or mariculture effluents. HTL of aquatic crops, such as marine macro- or microalgae, has significant potential for the UK owing to its extensive coastline. As such, macroalgae present a particularly promising feedstock for future UK biofuel production. This study aimed to bridge the gaps between previous accounts of macroalgal HTL by carrying out a more comprehensive screen of a number of species from all three major macroalgae classes, and examining the correlations between biomass biochemical composition and HTL reactivity. HTL was subsequently used to process thirteen South West UK macroalgae species from all three major classes (Chlorophyceae, Heterokontophyceae and Rhodophyceae) to produce bio-crude oil, a bio-char, gas and aqueous phase products. Chlorophyceae of the genus *Ulva* generated the highest bio-crude yields (up to 29.9 % for *U. lactuca*). Aqueous phase phosphate concentrations of up to 236 mg L<sup>-1</sup> were observed, obtained from the Rhodophyta, *S. chordalis*. Across the 13 samples, a correlation between increasing biomass lipids and increasing bio-crude yield was observed, as well as an increase in biomass nitrogen generally contributing to bio-crude nitrogen content. A broader range of macroalgae species has been examined than in any study previously and, by processing using identical conditions across all feedstocks, has enabled a more cohesive assessment of the effects of biochemical composition.

### 2.2.5 Introduction

The increasing unreliability of crude oil supplies, coupled with the causal link between fossil fuel use, CO<sub>2</sub> emissions and climate change, has led to extensive research into alternative liquid fuel sources compatible with the existing transport infrastructure. The production of first- and second-generation biofuels has been fraught with concerns over effective and ethical utilisation of arable land and fresh water [6], leading to a shift in focus from terrestrial to marine biomass feedstocks. Marine biomass, such as micro- and macroalgae, typically have higher biomass yields [7,8], owing to their higher photosynthetic efficiencies with respect to terrestrial crops (approx. 6–8 %, *c.f.* approx. 1.8–2.2 %) [2]. Although cultivation and harvesting of biomass constitutes a roadblock to widespread commercialisation of fuel production technologies [8], micro- and macroalgal fuel production systems also have the potential to be integrated with industrial and municipal waste remediation [9], aquaculture [10–13] or biomining of metals [14] to create an added-value biorefinery.

Investigations into micro- and macroalgae utilisation for biofuel production have spanned anaerobic digestion [15], fermentation [16] and conversion to biodiesel [17,18], with thermochemical processing techniques, such as hydrothermal gasification (HTG), pyrolysis and hydrothermal liquefaction (HTL) attracting attention in more recent years [19]. HTL in particular is ideally suited to wet feedstocks such as micro- and macroalgae, significantly lowering the prohibitive energy requirements associated with feedstock drying [20], and boosting the HHV of the resulting bio-crudes [21] with respect to pyrolysis bio-oils.

HTL utilises water at sub-/near-critical conditions (200–380 °C) as both a solvent and a reactant for a complex cascade of reactions, converting algal biomass into a bio-crude oil, alongside a nutrient-rich aqueous phase, a solid char and gaseous products. HTL of microalgae has been explored in great detail in recent years [22,23] but energy-intensive cultivation and harvesting on an industrial scale remains a major setback to obtaining good energy returns on investment (EROI) [20]. Macroalgal biomass has comparatively lower associated production costs [24] and, as such, has been the subject of a range of recent HTL investigations.

Since the first documented liquefaction of *Macrocystis* sp. [25], a number of different macroalgae species have been examined across all three major classes (Heterokontophyceae, Rhodophyceae and Chlorophyceae – brown, red and green seaweeds) [2,17,26–34]. A comprehensive mechanistic study of microalgae conversion using HTL by Biller and Ross [35] found that biochemical components contributed to

bio-crude formation in the order lipids > proteins > carbohydrates proposing a simple additive model for predicting bio-crude yield from biochemical composition. In a similar study examining specifically low-lipid algae, Yang *et al.* [36] confirmed that proteins made a greater contribution to bio-crude oil yields than polysaccharides, albeit at the expense of inflated nitrogen content. While this serves as a useful proxy for macroalgae, which tend to contain low lipid and high carbohydrate levels, no macroalgae-specific verification of this relationship has been published to date. Conversely, Elliott *et al.* have suggested that the oil generated from liquefaction of *Saccharina spp.* is more similar in composition and properties to lignocellulosic HTL bio-crude than the microalgal equivalent [37], despite the almost complete absence of any lignin in the macroalgal feedstock.

A number of investigations [35,38,39] have looked into rationalising HTL reactivity through the use of individual and multiple model compounds, Neveux *et al.* [32] attempted to use the model proposed by Biller and Ross [35] to predict the bio-crude yields of marine and freshwater Chlorophyceae, but experimentally obtained bio-crude yields did not fit the proposed additive conversion framework. The group speculate that Biller and Ross's model was not an accurate descriptor of the process due to its failure to account for bio-crude generated through secondary reactions between biochemical compounds, in addition to individual additive conversion yields from each biochemical fraction. The occurrence of secondary reactions was confirmed by Jin *et al.* [40]. In addition to bio-crude oil, hydrothermal liquefaction of marine biomass also generates a range of aqueous products, including water-soluble light organics, ammonia and phosphates. The composition of the aqueous products is dependent on the composition of the feedstock and exact conditions used. The aqueous phase products from HTL of microalgae have been demonstrated to be as effective in promoting growth in microalgal cultures as the industry standard growth media 3N-BBM +V [41]. The recovery of nutrients could prove to be a crucial step in the development of a viable biorefinery, particularly if finite resources, such as phosphorus, are able to be recycled. To date, there has been no assessment of phosphate recovery in the aqueous phase products of macroalgal HTL.

In light of these findings, this investigation aimed to identify optimal conditions for both bio-crude production and nutrient partitioning into the aqueous phase from hydrothermal liquefaction of UK macroalgae species. A comprehensive screening of a range of seaweed species prevalent on the South West coast of the UK was subsequently carried out, and biomass biochemical compositions linked to product yields and properties in order to rationalise reactivity. Based on this, specifications for an ideal biomass

feedstock were sought, with the ultimate aim of developing a theoretical model of a South-West UK-based biorefinery for the production of bio-crude oil and fertilisers for terrestrial or microalgal crops.

## 2.2.6 Methods

### 2.2.6.1 Materials and apparatus

Fresh macroalgal biomass samples were collected from Paignton, Devon (specifically, Broadsands Beach 50°24'24.9"N 3°33'16.2"W, Oyster Cove 50°25'04.1"N 3°33'20.9"W and Saltern Cove 50°24'57.9"N 3°33'24.4"W). Prior to analysis, all samples were freeze-dried and milled to <1.4 mm diameter. Samples were stored in sealed vials at -18 °C. Macroalgal species used were *Ascophyllum nodosum* (AN), *Chondrus crispus* (CC), *Fucus ceranoides* (FC), *Fucus vesiculosus* (FV), *Himanthalia elongata* (HE), *Laminaria digitata* (LD), *Laminaria hyperborea* (LH), *Pelvetia canaliculata* (PC), *Rhizoclonium riparium* (RR), *Sargassum muticum* (SM), *Solieria chordalis* (SC), *Ulva intestinalis* (UI) and *Ulva lactuca* (UL). A more detailed description of the collection and preparation of the biomass samples is included in the Supplementary Information.

Batch reactors were fabricated according to literature precedent using stainless steel Swagelok® tube fittings [35,42,43]. The reactor body consisted of a length of tubing capped at one end, and connected at the other to a pressure gauge, thermocouple, needle valve, and relief valve. The total internal volume of the reactors was *ca.* 50 cm<sup>3</sup>.

### 2.2.6.2 Procedure

Reaction procedures have been reported previously [43]. In a typical reaction, the reactor was loaded with 4 g biomass and 20 cm<sup>3</sup> freshly deionized water, and heated within a vertical tubular furnace set to 400 °C, 550 °C, 700 °C or 850 °C until the specified reaction temperature was reached (300–350 °C, 5–47 min), then removed from the furnace and allowed to cool to room temperature.

After cooling, gaseous products were released *via* the needle valve into an inverted, water-filled measuring cylinder to measure gaseous fraction volume. The gas phase is typically composed of 96–98 % CO<sub>2</sub>, observed experimentally for liquefaction of *A. nodosum* at 345 °C, and confirmed by Raikova *et al.* [43,44]. Hence, gas phase yields were calculated using the ideal gas law,<sup>c</sup> approximating the gas phase as 100 % CO<sub>2</sub>, assuming an approximate molecular weight of 44 g mol<sup>-1</sup> and a volume of 22.465 dm<sup>3</sup>

---

<sup>c</sup> Please refer to Appendix 2A

mol<sup>-1</sup> gas phase at 25 °C. The yield of gaseous product was determined using the following equation:

$$\text{yield}_{\text{gas}} = (V_{\text{gas}} \times 1.789 \times 10^{-3}) / (m_{\text{dry biomass}}) \times 100 \% \quad (1)$$

Following this, the aqueous phase was decanted from the reactor contents and filtered through a Fisher qualitative filter paper pre-dried overnight at 60 °C. The product yield in the water phase was determined by leaving a 2.5 g aliquot to dry in a 60 °C oven overnight, and scaling the residue yield to the total aqueous phase mass. Aqueous phase residue yield was determined using the following equation:

$$\text{yield}_{\text{AP residue}} = m_{\text{residue}} / m_{\text{dry biomass}} \times 100 \% \quad (2)$$

To separate the remaining bio-crude oil and char phase, the reactor was washed repeatedly using chloroform until the solvent ran clear, and filtered through the same filter paper used to separate the aqueous phase (after drying for a minimum of 1 h). The filter paper and collected char were washed thoroughly with chloroform to remove all remaining bio-crude. The filtrate was collected, and solvent removed *in vacuo* (40 °C, 72 mbar) until no further solvent evaporation was observed visually, and bio-crude samples were left to stand in septum-sealed vials venting to the atmosphere *via* a needle for a further 12 h to remove residual solvent. Bio-crude yield was determined using the following equation:

$$\text{yield}_{\text{bio-crude}} = m_{\text{bio-crude}} / m_{\text{dry biomass}} \times 100 \% \quad (3)$$

The char yield was calculated from the mass of the retentate collected on the filter paper after drying overnight in an oven at 60 °C.

Solid yield was determined using the following equation:

$$\text{yield}_{\text{solid}} = m_{\text{solid}} / m_{\text{dry biomass}} \times 100 \% \quad (4)$$

Inevitable material losses occurred during work-up, predominantly through evaporation of light organics from the aqueous and bio-crude phases during filtration and solvent removal.

### **2.2.6.3 Biomass and product characterisation**

For the macroalgal biomass, lipid quantification was carried out as described previously [42]. Polysaccharide quantification was carried out using the DuBois method [45] as described by Taylor *et al.* [46], incorporating an upfront two-step hydrolysis protocol adapted from Kostas *et al.* [47], with polysaccharides quantified on the basis of glucose equivalents.

Elemental analysis was carried out externally at London Metropolitan University on a Carlo Erba Flash 2000 Elemental Analyser to determine CHN content. (Elemental analyses were carried out at least in duplicate for each sample, and average values are reported.) From this, higher heating value (HHV) was calculated using the equation set out by Channiwala & Parikh [48] from elemental composition. Biomass ash was quantified using thermogravimetric analysis (TGA). Approximately 15 mg finely ground biomass was analysed on a Setaram TG-92 Thermogravimetric Analyzer. The sample was heated in air between room temperature and 110 °C at a ramp rate of 10 K min<sup>-1</sup>, and held for 3–10 min at 110 °C. The mass loss between room temperature and 110 °C was used to determine the sample moisture content. From 110 °C, the temperature was ramped to 1000 °C at a rate of 10–20 K min<sup>-1</sup> and held for 3–120 min, until TG stabilised. The mass remaining at the end of the experiment was taken to be the ash.<sup>D</sup>

For bio-crude and char, elemental analysis and HHV calculations were carried out as described above for the biomass. HHV values calculated using the Channiwala & Parikh equation [48] were found to be in line with values determined experimentally using an IKA C1 bomb calorimeter (within ± 5 %).

A 25 mL sample of the gas phase from liquefaction of *A. nodosum* at 345 °C was analysed using a gas chromatograph (Agilent 7890A) containing an HP-Plot-Q capillary column and fitted with an Agilent 5975C MSD detector. Samples were loaded at 35 °C, held for 7 min at 35 °C, ramped to 150 °C at 20 K min<sup>-1</sup>, then ramped to 250 °C at 15 K min<sup>-1</sup>, with a final hold time of 16 min. Helium (1.3 cm<sup>3</sup> min<sup>-1</sup>) was used as the carrier gas.

The concentration of ammonium ions in the aqueous phase was determined using a Randox® urea test kit. The sample was diluted with distilled water to a concentration of 1 % prior to analysis. Urea concentration was calculated relative to a standard solution. From this, ammonium ion concentration was calculated. Aqueous phase total nitrogen was determined by difference, subtracting the total N in the bio-crude and char from the total N in the biomass feedstock (assuming that the N content of the gas phase was negligible). Phosphate concentration in the aqueous phase was determined using a Spectroquant® test kit and photometer system. Prior to analysis, each sample was diluted with deionised water. The total phosphate concentration was determined using a pre-calibrated Spectroquant® photometer.

---

<sup>D</sup> Please refer to Appendix 2B



In order to determine experimental error and test the repeatability of experimental results, three repeat HTL runs of *A. nodosum* were carried out at a range of temperatures between 300–350 °C to determine the standard deviation in mass balances at different reaction temperatures. For ammonia and phosphate quantification, the products of *A. nodosum* liquefaction at 345 °C were analysed in triplicate in all cases to determine standard deviation, and errors assumed to be consistent across different biomass species. All elemental analyses (CHN) were carried out at least in duplicate, and average values used.

## **2.2.7 Results and Discussion**

### ***2.2.7.1 Optimisation of heating rate and temperature***

The effect of heating rate on bio-crude production from HTL of the macroalga *A. nodosum* at 350 °C was examined (Fig. 2.2-1a). Variation of heating rates were achieved by changing the furnace temperature: 400 °C, 550 °C, 700 °C and 850 °C set points gave heating rates of 6.7 K min<sup>-1</sup>, 15.8 K min<sup>-1</sup>, 34.2 K min<sup>-1</sup> and 56.3 K min<sup>-1</sup>, respectively. Oil yields increased from 18.5 to 20.9 % oil yield on increasing heating rate from 6.7 K min<sup>-1</sup> to 15.8 K min<sup>-1</sup>, slowing progressively on increasing the heating rate to 34.2 K min<sup>-1</sup> to give a yield of 21.6 %, increasing modestly to 21.9 % yield on increasing heating rates to 56.3 K min<sup>-1</sup>.

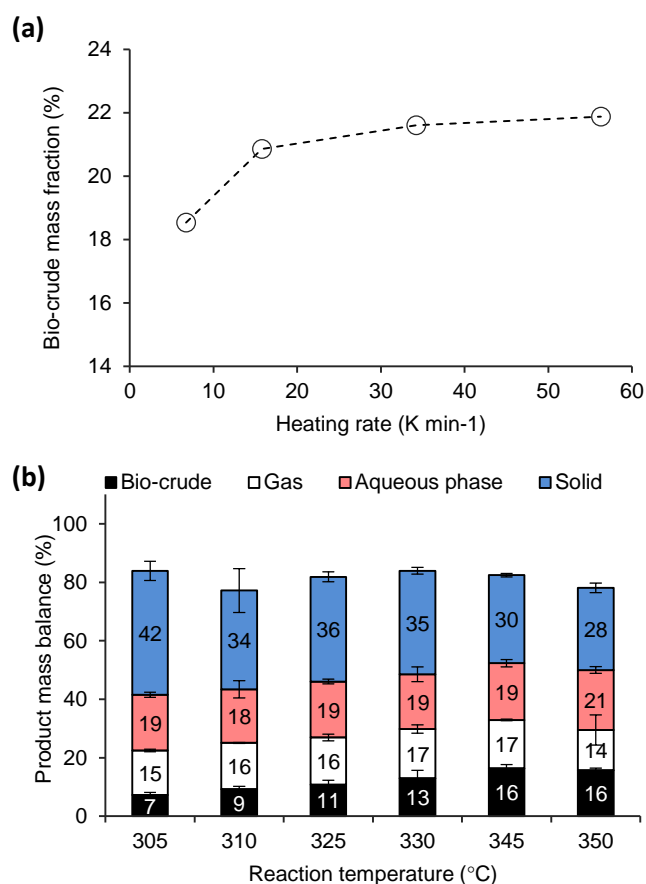


**Figure 2.2-1** – Effect of a) the heating rate on the bio-crude yield from *A. nodosum* and b) reaction temperature on product distribution from the HTL of *A. nodosum* (mass fractions on dry basis). Non-closure of the mass balance is predominantly due to loss of some volatiles from the aqueous and bio-crude fractions on work up.

Although the results confirm the previously identified positive correlation between heating rate and oil production efficiency observed for other biomass types [49,50], the effect was found to become progressively less pronounced at higher heating rates. Furthermore, repeated exposure to furnace temperatures of 850 °C was found to cause damage to reactor fittings. A lower furnace temperature of 700 °C was deemed sufficient to give optimal bio-crude production without compromising reactor integrity. This set point (giving a heating rate of ~30 K min<sup>-1</sup>) was subsequently used for all HTL experiments.

The effect of HTL reaction temperature on product mass balance was assessed (Fig. 2.2-1a). Bio-crude oil yields increased with reaction temperature, up to a maximum of 16.3 % (19.5 % on a dry, ash-free basis) at 345 °C. Previously examined macroalgae have given similar results: Anastasakis and Ross [2] obtained the highest yields of bio-crude from *L. saccharina* (19.3 %) at 350 °C, whilst Zhou *et al.* found that bio-crude yields (23 %) from HTL of *E. prolifera* were highest at 300 °C [29].

The highest overall mass fraction of the product was distributed in the solid phase, predominantly accounted for by the biomass ash (16.2 %). With increasing bio-crude yields, a concomitant decrease in solid products was observed, although a small amount of organic matter from the solid phase also partitioned to the aqueous phase products, which made up the largest product mass fraction on an ash-free basis at temperatures above 310 °C. Material recovery in the gas phase remained relatively stable across the temperature range.

In this investigation, mass balances were determined by measuring the yields of all four product phases, rather than calculating the recovery of one phase by difference. Overall mass closures ranged from 77.2 to 83.9 %. The loss of material is due in part to light organics lost on work-up of the bio-crude phase and thermal drying of the aqueous phase to determine residue content. It has also been suggested that some loss could also be attributed to partitioning of oxygen to the aqueous phase in the form of water [33]. Overall, these mass closures are similar to those observed by Anastasakis and Ross [2] in the hydrothermal processing of *L. digitata*.<sup>E</sup>

Despite the variation in yields, bio-crude elemental compositions (and, consequently, calculated HHV) were unaffected by reaction temperature. All bio-crude HHV values fell between 29.7–32.6 MJ kg<sup>-1</sup> (see supporting information). Anastasakis and Ross [2] observed that bio-crude HHV increased slightly on increasing temperatures from 300 °C to 350 °C during the liquefaction of *L. saccharina*, although the degree of experimental error was not specified.

The potential for utilisation of the nutrient-rich aqueous phase from HTL has been explored for microalgae process water [26,41,51]. However, macroalgal HTL process water has yet to be examined. To this end, the concentrations of phosphate and dissolved ammonia in the aqueous phase was analysed with respect to reaction temperature (Fig. 2.2-2).

---

<sup>E</sup> Please refer to Appendix 2C

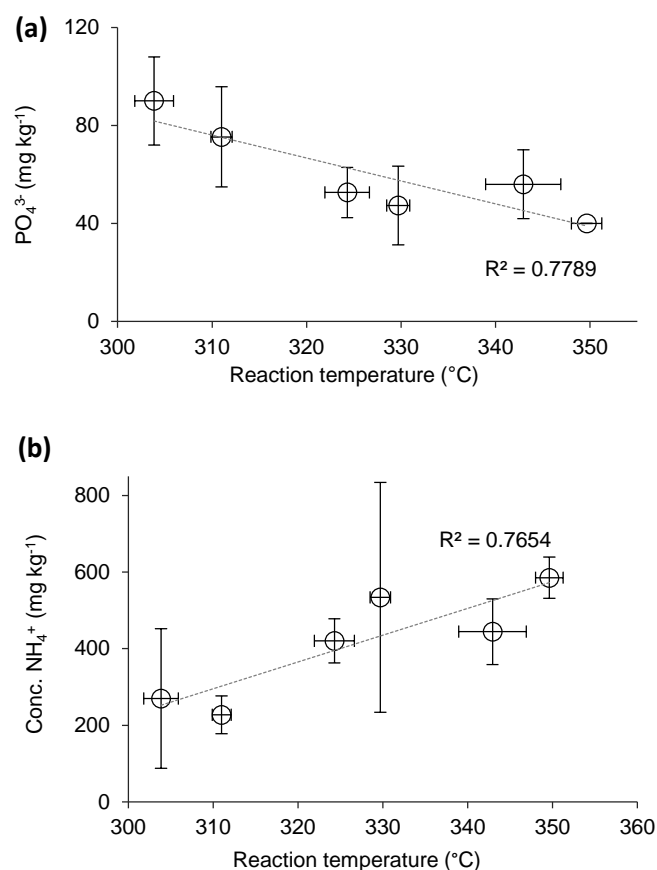


**Figure 2.2-2** – Effect of reaction temperature on a) phosphate and b) ammonia concentration of aqueous phase from HTL of *A. nodosum*

The increase in reaction temperature from 300–350 °C caused phosphate partitioning to the aqueous phase to drop slightly (Fig. 2.2-2a), with a simultaneous increase in ammonia concentrations observed (Fig. 2.2-2b). Although nutrient levels are still relatively high, they are not as substantial as produced in the aqueous phases from the HTL of most microalgae [43]. Hence, although the aqueous phase products may be of use within a biorefinery paradigm incorporating macroalgal HTL with microalgal cultivation (e.g. for fuels or chemicals), it probably does not represent a higher-value platform than fuel production from bio-crude. Hence, the optimal reaction temperature was selected on the basis of optimising bio-crude oil production, with nutrient recovery presenting a secondary route for product valorisation.

The effect of particle size on the biocrude yield was also examined (Fig. 2.2-3). It was found that varying particle size of between 125 μm >  $n \geq 1.4$  mm did not have a notable effect on bio-crude yield. Given the energy-intensive nature of milling material to a fine particle size on an industrial scale, using the maximum possible particle size is likely to result in significant cost and energy savings. Although additional issues of feedstock processability would need to be addressed for a continuous system at scale, particle

sizes of <1.4 mm were deemed appropriate for this investigation. The final conditions taken forward to examine the effect of varying macroalgae feedstock species were a particle size of <1.4 mm, and a reaction temperature of 345 °C, with heating rates of ~30 K min<sup>-1</sup>.

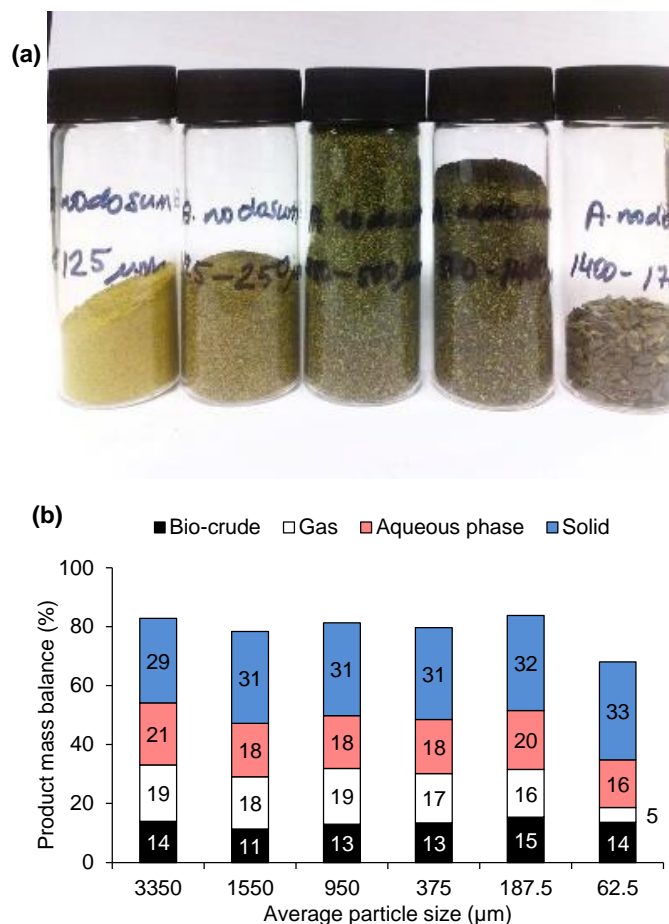


**Figure 2.2-3** – a) *A. nodosum* ground particles with from left to right with an average particle size of 62.5, 187.5, 375, 950, 1550 μm. b) Product mass balance from the HTL conversion of *A. nodosum* over variable particle size, at 345 °C (dry basis). The remaining fraction of the mass is assigned to volatile losses from the aqueous and bio-crude fractions on work up.

### 2.2.7.2 Properties of South West UK marine macroalgae

Thirteen macroalgae species were selected for analysis, belonging to all three major divisions: Rhodophyceae (red macroalgae), Chlorophyceae (green macroalgae) and Heterokontophyceae (brown macroalgae).

The proximate, biochemical and ultimate analyses of the seaweed species are presented in Table 2.2-1. The compositions of many macroalgae generally exhibit pronounced seasonal variation, as well as being strongly affected by growing temperature, geographical location [52], water salinity, and aqueous nutrient content [53], so can differ substantially from samples of the same species grown in alternative climates.

**Table 2.2-1** – Biomass proximate, biochemical and ultimate analysis, and higher heating value (HHV)

Properties		Proximate (%)		Biochemical (%)				Ultimate (%) <sup>a</sup>				(MJ kg <sup>-1</sup> )
Type <sup>b</sup>		Moisture <sup>c</sup>	Ash <sup>d</sup>	Protein <sup>e</sup>	Lipid <sup>f</sup>	Carb. <sup>f</sup>	Carb. <sup>g</sup>	C	H	N	O <sup>h</sup>	HHV <sup>i</sup>
UL	C	3.7	17.3	20.0	6.9	48.7	55.8	34.9	5.3	4.1	38.4	14.1
UI	C	7.7	24.5	20.9	5.9	48.9	48.8	35.2	5.8	4.2	30.4	15.4
RR	C	11.3	44.5	13.2	1.9	28.1	40.4	26.8	5.1	2.6	21.0	12.2
AN	H	3.6	16.2	8.9	6.7	25.5	68.2	38.7	5.8	1.8	37.5	15.4
FC	H	14.0	12.6	11.6	3.3	14.8	72.5	28.4	3.9	2.3	52.8	8.7
FV	H	14.3	12.6	10.5	3.8	15.9	73.1	38.8	5.1	2.1	41.4	15.0
HE	H	10.5	14.3	9.1	2.6	23.1	74.0	34.3	5.0	1.8	44.6	12.9
LD	H	2.1	11.6	11.6	1.1	38.3	75.7	38.2	5.6	2.3	42.3	15.3
LH	H	10.2	10.8	13.2	2.6	17.4	73.4	30.7	5.0	2.6	50.9	11.1
PC	H	12.2	19.0	9.9	5.0	19.1	66.1	39.0	5.7	2.0	34.3	16.4
SM	H	10.5	11.8	9.9	1.5	11.3	76.9	26.4	3.6	2.0	56.2	7.4
SC	R	6.0	17.1	13.4	1.2	39.5	68.3	25.3	3.5	2.7	51.4	7.3
CC	R	3.5	15.6	21.1	3.0	46.7	60.4	37.5	5.6	4.2	37.1	15.4

<sup>a</sup> Average of two replicates; elemental mass fraction quoted on dry basis. <sup>b</sup> C – Chlorophyta (green); H – Heterokontophyta (brown), R – Rhodophyta (red). <sup>c</sup> Moisture mass fraction quoted on total biomass basis. <sup>d</sup> Ash mass fraction quoted on dry basis. <sup>e</sup> Protein calculated from biomass N; mass fraction quoted on dry basis. <sup>f</sup> Analytical; mass fraction quoted on dry basis. <sup>g</sup> Calculated by difference; mass fraction quoted on dry basis. <sup>h</sup> Calculated by difference according to Jin *et al.* [40]; mass fraction quoted on dry basis. <sup>i</sup> Calculated from elemental composition using Channiwala and Parikh equation [48]

The elemental composition of the macroalgae analysed varied widely, with Chlorophyceae and Rhodophyceae typically containing higher nitrogen and calculated protein than Heterokontophyceae (3–4 % *c.f.* 1–2 % N). Ash was also highly variable, ranging from 10.8 % for *L. hyperborea* to a maximum of 44.5 % for *R. riparium*. *R. riparium*, and *U. intestinalis* had particularly high ash, 20 % on a dry weight basis. Biomass HHV, calculated using the method set out by Channiwala and Parikh [48], ranged between 8.6 MJ kg<sup>-1</sup> and 18.2 MJ kg<sup>-1</sup>, with no obvious dependence on macroalgae division.

Chlorophyceae of the genus *Ulva* and the Heterokontophyceae *A. nodosum* and *P. canaliculata* had the highest lipid (>5 %), which was expected to be beneficial for bio-crude yields. *U. intestinalis*, *U. lactuca* and the Rhodophyta *C. crispus* had notably high protein contents *ca.* 20 %. This was anticipated to have a positive effect on bio-crude yields, simultaneously increasing ammonia concentrations in the aqueous phase, but possibly having a detrimental effect on bio-crude quality by inflating bio-crude N. High nitrogen levels in crude oil are undesirable: nitrogen-rich fuels generate substantially elevated NO<sub>x</sub> emissions on combustion, and nitrogen must therefore be removed through hydrotreatment during the refining process. This can prove somewhat of a setback within a biorefinery context, increasing the energy demand for refining, consuming large quantities of H<sub>2</sub>, and posing an increased risk of refinery catalyst poisoning, [32] which must be taken into account for any high-protein feedstocks such as *C. crispus*.

Carbohydrate quantification was carried out using the DuBois method [45]. This method is widely used to quantify carbohydrates in macroalgae, but has the significant drawback of quantifying carbohydrates on the basis of glucose equivalents. Whilst this is highly accurate for simple glucose-based carbohydrates, the method is significantly less sensitive to other monosaccharide units, such as galactose in the common macroalgal carbohydrate carrageenan, or monosaccharides unique to seaweeds, such as mannuronic and guluronic acids present in alginates [47]. Additionally, the method's sensitivity is strongly affected by carbohydrate charge [54]. In this work, analytically determined soluble carbohydrate is presented alongside estimated total carbohydrate, determined by difference:

$$X_{\text{carbohydrate (tot.)}} = 100 \% - (X_{\text{protein}} + X_{\text{lipid}} + X_{\text{ash}}) \quad (5)$$

Where  $X_{\text{component}}$  is the mass fraction (%) of each biochemical component.

*U. lactuca*, *S. chordalis* and *C. crispus* had the highest analysed carbohydrate, suggesting the presence of high levels of glucose-based polysaccharides. In contrast,

the highest total carbohydrate yields as determined by difference were found for the Heterokontophyceae *F. vesiculosus*, *H. elongata*, *L. digitata* and *L. hyperborea*, with all four containing >70 % total carbohydrate.

Differences between analysed and calculated carbohydrate were significant for some seaweed species. For example, 71.8 % total carbohydrate was expected for *L. hyperborea*, but only 17.4 % detected. *L. hyperborea* has previously been found to contain significantly higher levels of mannitol (34 %) than the glucose-based polysaccharide laminarin (0.86 %) [55], which may have led to false low readings for total carbohydrate using colourimetric methods based on a glucose standard. In general, a significant difference (38–55 %) between analysed and calculated carbohydrate was observed for all Heterokontophyceae analysed, suggesting the presence of high levels of non-glucose monosaccharides. Carbohydrate compositions can fluctuate substantially in brown macroalgae, with mannitol alone seen to contribute anywhere between 5 % and 45 % of the dry weight of *L. saccharina* [53] in response to fluctuations in aqueous salinity [56]. The analysed and calculated carbohydrate differed to a smaller degree for the Rhodophyceae and Chlorophyceae.

### ***2.2.7.3 Liquefaction results***

Liquefaction of 13 UK macroalgae species was carried out using the optimised conditions described previously (345 °C; 30 K min<sup>-1</sup>). Mass balances are summarised in Fig. 2.2-4, and bio-crude yields are quoted on a dry basis. The highest overall bio-crude yields were obtained for the two macroalgae of the genus *Ulva* (28.8 % and 29.9 % for *U. intestinalis* and *U. lactuca*, respectively), although the third Chlorophyta *R. riparium* performed significantly worse, yielding a modest 15.0 % bio-crude product. *L. digitata* yielded 16.4 % bio-crude – similar to the 17.6 % obtained by Anastasakis and Ross [33], although *L. hyperborea* was found to give 9.8 % bio-crude product in the same study, whereas the macroalgae used in this investigation yielded 12.3 % bio-crude. This can likely be explained by regional and seasonal variations in biomass composition [52,57,58].



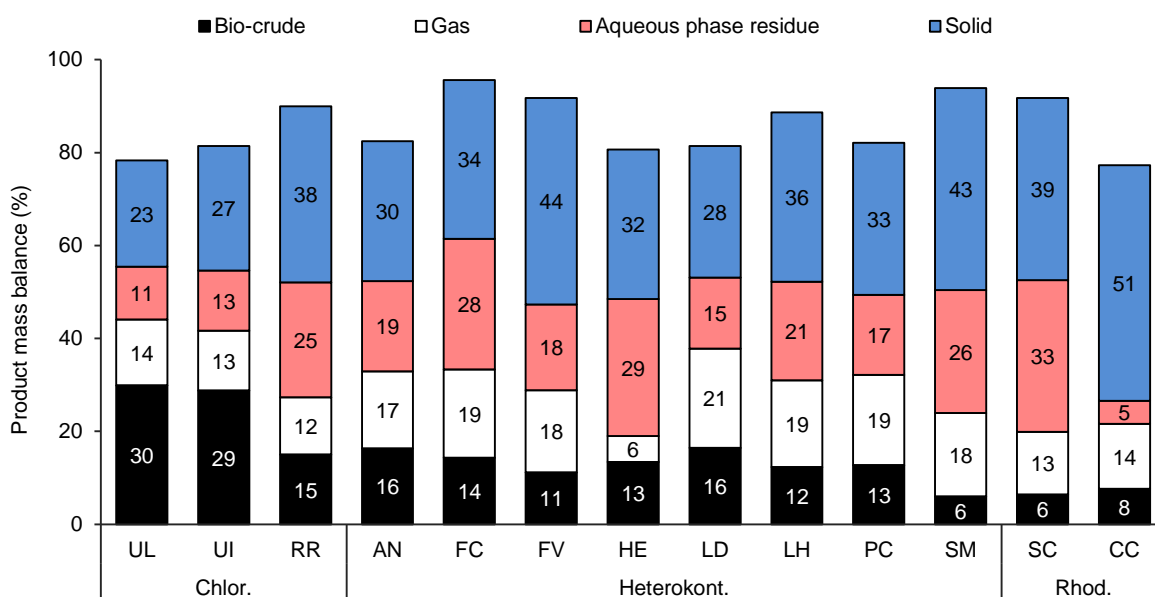


**Figure 2.2-4** – Product distribution from HTL of 13 macroalgae species (345 °C; ca. 30 K min<sup>-1</sup>). The remaining fraction of the mass is assigned to volatile losses from the aqueous and bio-crude fractions on work up.

Rhodyphyceae gave the highest recoveries of solid products (>45 %), whilst measured gas yields varied substantially (from 5.6 % for *H. elongata* to a maximum of 21.4 % for *L. digitata*). Up to 32.7 % of the feedstock was recovered in the aqueous phase residue (*S. chordalis*), whilst only 5.0 % water-soluble organic product was generated from *C. crispus*. It has been suggested previously [35] that the presence of high volumes of carbohydrate results in the formation of higher levels of water-soluble polar organics (such as formic, lactic, acetic and acrylic acids formed from the hydrothermal liquefaction of glucose), but aqueous phase residue yields do not appear to reflect this: despite having high analysed and calculated carbohydrate, *U. lactuca*, *U. intestinalis* and *C. crispus* yielded relatively low yields of aqueous phase products (11.4 %, 13.0 % and 5.0 %, respectively), whilst 29.5 % of the feedstock was recovered in the aqueous phase for *H. elongata*, with a comparatively low carbohydrate content of 23.1 %.

Although it was anticipated that higher organic carbon content in the starting biomass would be conducive to obtaining higher bio-crude yields as previously noted [32], there appeared to be no statistically significant correlation between the two parameters. In each case, losses of 4–23 % were encountered. As previously, these are attributed to the loss of volatiles on work-up, and partitioning of oxygen to the aqueous phase in the form of water.

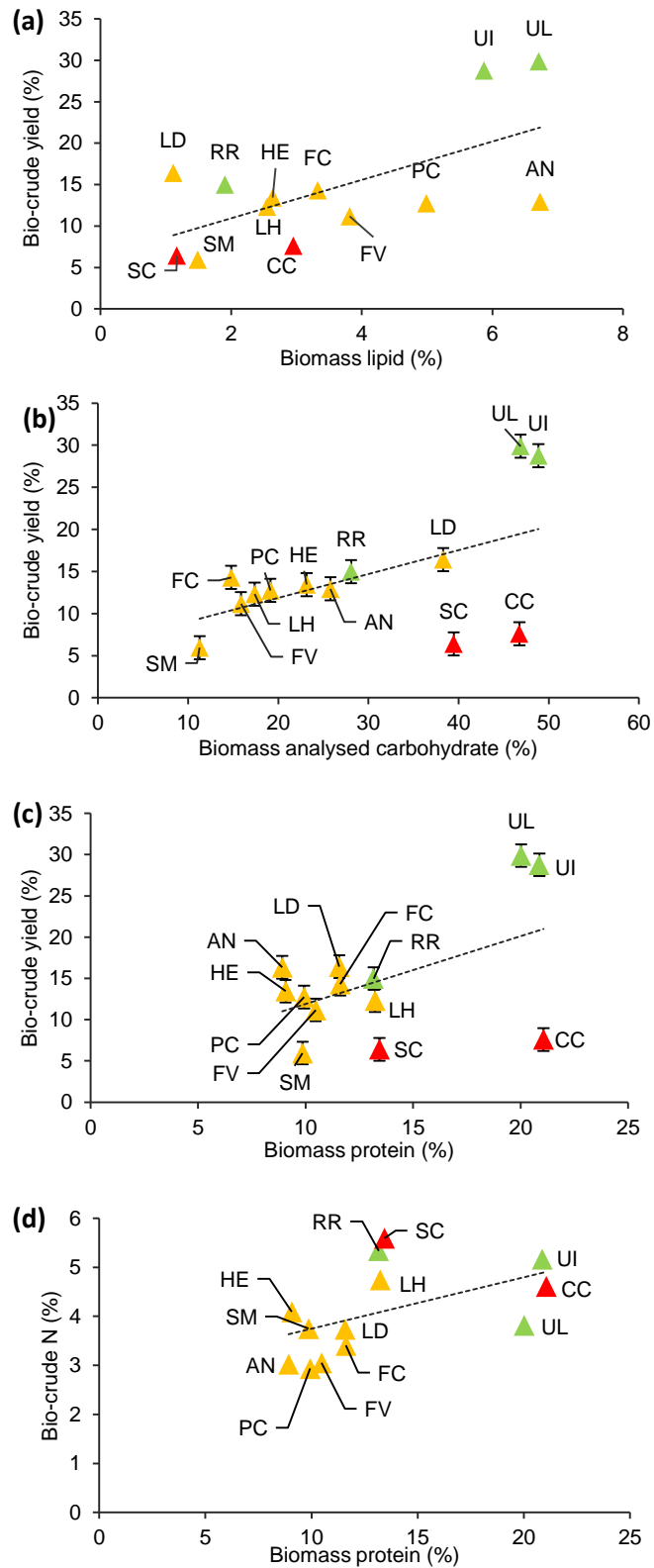


**Figure 2.2-5** – Correlation between biomass biochemical composition and bio-crude yields and bio-crude nitrogen from HTL of 13 macroalgae species: a) biomass lipid vs. yield; b) biomass analysed carbohydrate vs. yield; c) biomass protein vs. yield; and d) biomass protein vs. bio-crude nitrogen.

Increasing lipid yields appeared to encourage bio-crude production (Fig. 2.2-5a). The correlation between carbohydrate (Fig. 2.2-5b) and protein (Fig. 2.2-5c) and bio-crude production appeared to be weaker, in line with the observation that lipids are more readily converted to bio-crude than other biochemical components in model studies [35]. To verify these observations, a multiple regression was carried out to quantify the effect of biomass protein, lipid, carbohydrate and ash on bio-crude production. A statistically significant correlation (>95 % confidence) was observed only for lipids. A further regression was carried out for the effect of lipid alone. It was found that variation in biomass lipid accounted for 49 % of the total variation in bio-crude production. The bio-crude yield could be predicted from lipid mass fraction by the following formula:

$$\text{yield}_{\text{bio-crude}} = 5.71 + 2.6(X_{\text{lipid}}) \quad (6)$$

Where  $X_{\text{lipid}}$  represents the mass fraction (%) of lipid in the macroalgal biomass.

However, despite the broad correlation, notable exceptions exist in each case: although *U. lactuca* has the highest lipid of the macroalgae analysed (6.9 %), it appears to give a disproportionately high bio-crude yield (29.9 %), significantly higher than *A. nodosum*, which gives a yield of 16.0 % with a similar lipid of 6.7 %. As *U. lactuca* has significantly higher protein and measured carbohydrate relative to *A. nodosum*, this may imply that bio-crude yield is positively correlated to overall organic biomolecule content (and hence, negatively correlated to ash), however, no such correlation is observed in practice. The lowest ash was observed for *L. hyperborea* (10.8 %), but a modest bio-crude yield of 12.3 % was obtained. Conversely, a similar yield of 12.9 % bio-crude is obtained from *R. riparium*, despite an ash content of 44.5 %. In certain cases, ash may play a catalytic role in bio-crude formation, but this is also likely to be due to differences in reactivity between individual lipid, protein and carbohydrate types. Biomass protein was found also to be weakly correlated to bio-crude nitrogen, with the notable exception of *U. lactuca*, which yielded a bio-crude with only 3.8 % N despite containing 24.3 % biomass protein.

An attempt was made to calculate theoretical bio-crude yields using the additive model for bio-crude yield prediction proposed by Biller and Ross [35]:

$$\text{total theoretical yield bio-crude} = (\text{conv.}_{\text{lipid}} \times X_{\text{lipid}}) + (\text{conv.}_{\text{protein}} \times X_{\text{protein}}) + (\text{conv.}_{\text{carbohydrate}} \times X_{\text{carbohydrate}}) \quad (7)$$

where  $\text{conv.}_{\text{component}}$  represents the theoretical conversion (%) to bio-crude of a given biomass component (lipid, protein and carbohydrate) and  $X_{\text{lipid}}$ ,  $X_{\text{protein}}$  and  $X_{\text{carbohydrate}}$  represent the lipid, protein or carbohydrate mass fraction (%) of the feedstock, respectively. The values for theoretical maximum and minimum conversion to bio-crude

from individual model lipid, protein and carbohydrate fractions were reported by Neveux *et al.* [32], who utilised similar feedstocks and processing conditions. Carbohydrate content as determined by difference was used for the calculation of theoretical yields.

Similarly to Neveux *et al.*, this investigation found that predicted maximum yields did not fit well to the model (Fig. 2.2-6), with yields under-predicted by a wide margin (50–82 %) for the three Chlorophyceae, and over-predicted for the remaining feedstocks (by 8–59 %), although the predicted yield was accurate (> 5 % difference) for *F. vesiculosus* and the two Rhodophyceae.

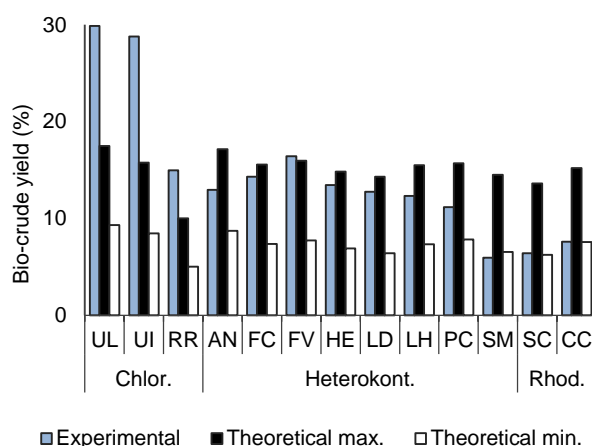


**Figure 2.2-6** – Comparison of experimentally obtained bio-crude yields and yields calculated using the additive model proposed by Biller and Ross for HTL of 13 UK macroalgae species

This confirms that the reactivity of a given feedstock under HTL conditions cannot necessarily be inferred from the total levels of lipid, protein and carbohydrate alone. A more complete biochemical breakdown would be necessary to examine mechanistic aspects of bio-crude production, but given the vast number of individual biomolecules within each feedstock, and the variability of biochemical compositions between species, this is likely to be an extremely complex system to analyse. With the large number of potential secondary reactions between primary decomposition products, in practise, when assessing prospective HTL feedstocks for a biorefinery, it will be significantly simpler to determine feedstock suitability experimentally on a case-by-case basis.

All species yielded bio-crudes containing 65–71 % carbon, 7–9 % hydrogen and 3–5 % nitrogen, with the remainder attributed to oxygen, and the HHV of the bio-crudes showed little variation across species, ranging from 28.4–33.0 MJ kg<sup>-1</sup> (see supporting information), despite the significant variation in biomass biochemical composition, biomass HHV, and bio-crude yields. These crude oils have approximately 75 % of the

energy density of a typical crude oil, and comparable to those obtained for microalgal bio-crude at similar HTL conditions [59]. This effect has been previously observed by Neveux *et al.* [32] for a range of Chlorophyceae.

The elemental deposition to the bio-oil is presented in Fig. 2.2-7a. For *U. intestinalis* and *U. lactuca*, carbon recovery in the bio-crude was reasonably high, at 53 % and 57 % respectively. For *C. crispus*, on the other hand the majority of biomass carbon was recovered in the solid phase (see supporting information), with only 13 % in the bio-crude. Although this is unfavourable from a liquid fuel production perspective, energy recovery from bio-char has also been discussed in literature [33]. In this study, while approximately 60 % of the energy from the initial feedstock was retained in the biocrude for *U. lactuca* and *U. intestinalis*, this was reduced substantially to just 14 % for *C. crispus* with the majority being found in the solid residue product for this seaweed species (Fig. 2.2-7b).

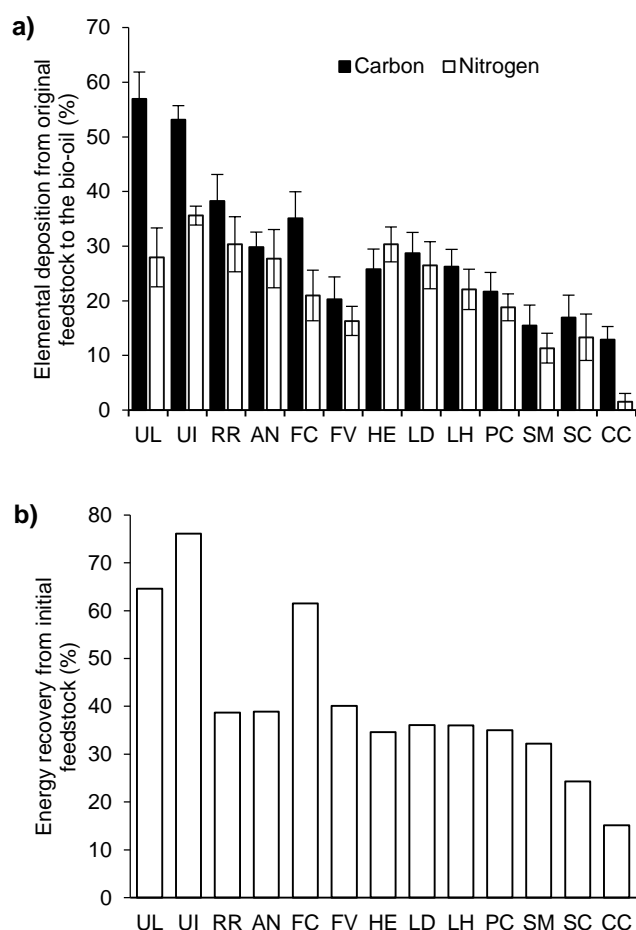


**Figure 2.2-7** – a) Deposition of carbon and nitrogen from the initial feedstock into the bio-crude for the 13 species of macroalgae b) energy recovery of the bio-crude as a proportion of the biomass HHV.

Nitrogen distribution between the products was notably different to that seen for carbon, with the bulk of feedstock N recovered in the aqueous phase, present mainly as  $\text{NH}_4^+$ . Although the protein content of *U. intestinalis* and *C. crispus* biomass was almost identical (20.8 % and 20.2 %, respectively), 36 % of the total nitrogen was recovered in the bio-crude for *U. intestinalis*, compared to only 9 % for *C. crispus*. High protein in the feedstock led to partitioning of nitrogen to the bio-crude phase (as well as the aqueous and solid phases), leading to bio-crude nitrogen contents of 3–5 % (see supporting information). The presence of high nitrogen levels in bio-crude is a setback for co-refining operations, increasing the energy demand for refining and posing an increased risk of catalyst poisoning [32], however, the bio-crude nitrogen contents for all feedstocks screened are notably lower than those encountered for bio-crudes obtained from other macroalgae species. Neveux *et al.* [32] reported bio-crude nitrogen levels from 5.8 % for the marine macroalga *Ulva ohnoi* to 7.1 % for *Cladophora coelothrix*. Both species of *Ulva* analysed in this study gave bio-crudes with lower nitrogen – 3.8 % for *U. intestinalis* and 5.2 % for *U. lactuca* – with the lowest nitrogen content observed for bio-crude from *P. canaliculata* (2.9 %).

Total process energy calculations based on the HHV of the feedstocks and total energy recovery from the bio-crude and char found that in some species a significant amount of energy was being lost to the gaseous and aqueous phase. The energy recovery in the aqueous phase has not been considered at this point, although it is acknowledged that this is theoretically possible if additional processing steps (e.g. hydrothermal gasification) were incorporated [37].

The levels of soluble inorganic nutrients in HTL process water varied significantly with macroalgae species examined (Fig. 2.2-8). Ammonia concentrations exceeding  $1 \text{ g kg}^{-1}$  were observed for *U. intestinalis*, *L. digitata*, *L. hyperborea*, *S. chordalis* and *C. crispus*. *L. digitata* and *C. crispus* exhibited particularly high aqueous phase ammonia concentrations, at  $2\,235 \text{ mg kg}^{-1}$  and  $2\,415 \text{ mg kg}^{-1}$ , respectively. Aqueous phase phosphate concentrations observed were reasonably high, although not as high as those observed for microalgal HTL process water in previous studies [43]. The highest phosphate concentrations ( $> 100 \text{ mg kg}^{-1}$ ) were observed for the *F. ceranoides* and *P. canaliculata*. These concentrations are comparable to those found in the standard microalgae growth media 3N-BBM +V. Process waters with high ammonia and phosphate could be considered for use as a growth supplement for microalgal or macroalgal cultivation, or terrestrial crops, although the effect of the elevated non-

ammonia nitrogen (likely to be due to the presence of heterocycles [39]) on plant or algae growth are unclear.

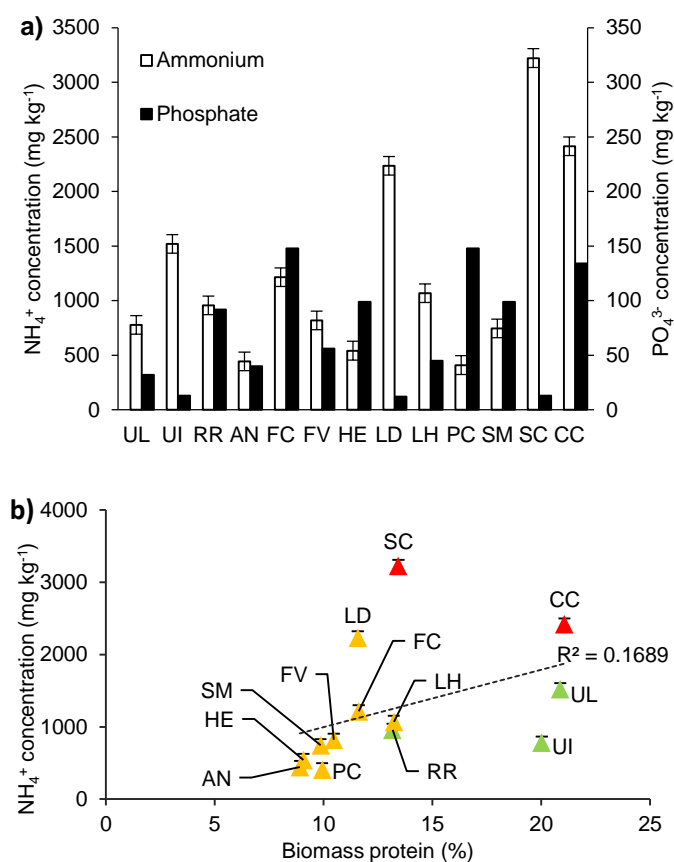


**Figure 2.2-8** – a) Ammonia and phosphate deposition in the aqueous phase for each strain of macroalgae. b) Correlation between biomass protein and ammonia concentration in the aqueous phase from HTL of 13 macroalgae species.

A weak correlation was observed between increasing protein in the biomass feedstock and increasing ammonia concentrations detected in the aqueous phase (Fig. 2.2-8b), though again this was not enough to be able to predict the concentration of  $\text{NH}_4^+$  in the aqueous phase.

## 2.2.8 Conclusions

Hydrothermal liquefaction has been demonstrated as an effective technique for the conversion of thirteen UK macroalgae species, nine unexplored in previous literature. Macroalgae of the genus *Ulva* gave the highest bio-crude yields up to 29.9 %, containing up to 60 % of total biomass energy content. Due in part to low nitrogen in the initial feedstocks, less nitrogen and phosphate were obtained in the aqueous phase compared with microalgal species. As such, with macroalgae, nutrient partitioning into the aqueous

phase presents only a minor secondary route for product valorisation, after the reaction conditions have been optimised for bio-crude production. Despite significant variation in biomass elemental and biochemical composition, all bio-crudes produced were similar in elemental composition and HHV. Lipid content was found to account for a substantial proportion of the variation in bio-crude yield. However, feedstock performance could not be predicted from the biochemical breakdown alone. More extensive system modelling, incorporating feedstock-specific components and incorporation of secondary reactions, would be required to identify prospective new feedstock specifications, but in practice, experimentation will be the sole reliable route to assessing feedstock suitability. From the selection of seaweeds assessed, *Ulva lactuca*, and other members of the family Chlorophyceae, were found to give the best performance for a future biorefinery in the South West region of the UK.

### **2.2.9 Acknowledgements**

The project has been partially supported by the EPSRC through the Centre for Doctoral Training in Sustainable Chemical Technologies (EP/L016354/1), and the RAEng Newton Research Collaboration Programme (NRCP/1415/176). The authors extend a special thank you to our collaborative partners Rosie and Archie Allen for their invaluable assistance in sourcing the macroalgae species used in this investigation.



## 2.2.10 References

- [1] K.R. Arturi, S. Kucheryavskiy, E.G. Søgaaard, Performance of hydrothermal liquefaction (HTL) of biomass by multivariate data analysis, *Fuel Process. Technol.* 150 (2016) 94–103. doi:10.1016/j.fuproc.2016.05.007.
- [2] K. Anastasakis, A.B. Ross, Hydrothermal liquefaction of the brown macro-alga *Laminaria saccharina*: effect of reaction conditions on product distribution and composition., *Bioresour. Technol.* 102 (2011) 4876–83. doi:10.1016/j.biortech.2011.01.031.
- [3] P. Biller, R.B. Madsen, M. Klemmer, J. Becker, B.B. Iversen, M. Glasius, Effect of hydrothermal liquefaction aqueous phase recycling on bio- crude yields and composition, *Bioresour. Technol.* 220 (2016) 190–199. doi:10.1016/j.biortech.2016.08.053.
- [4] L. Garcia Alba, C. Torri, D. Fabbri, S.R. a Kersten, D.W.F. Wim Brilman, Microalgae growth on the aqueous phase from Hydrothermal Liquefaction of the same microalgae, *Chem. Eng. J.* 228 (2013) 214–223. doi:10.1016/j.cej.2013.04.097.
- [5] M. Nelson, L. Zhu, A. Thiel, Y. Wu, M. Guan, J. Minty, H.Y. Wang, X.N. Lin, Microbial utilization of aqueous co-products from hydrothermal liquefaction of microalgae *Nannochloropsis oculata*., *Bioresour. Technol.* 136 (2013) 522–8. doi:10.1016/j.biortech.2013.03.074.
- [6] K.G. Cassman, A.J. Liska, Food and fuel for all: Realistic or foolish?, *Biofuels, Bioprod. Biorefining.* 1 (2007) 18–23.
- [7] L. Gouveia, Microalgae and Biofuels Production, in: *Microalgae as a Feed. Biofuels*, Springer, Heidelberg, 2011: pp. 2–20. doi:10.1007/978-3-642-17997-6.
- [8] J.J. Milledge, P.J. Harvey, Potential process 'hurdles' in the use of macroalgae as feedstock for biofuel production in the British Isles, *J. Chem. Technol. Biotechnol.* 91 (2016) 2221–2234. doi:10.1002/jctb.5003.
- [9] W.T. Chen, Y. Zhang, J. Zhang, G. Yu, L.C. Schideman, P. Zhang, M. Minarick, Hydrothermal liquefaction of mixed-culture algal biomass from wastewater treatment system into bio-crude oil, *Bioresour. Technol.* 152 (2014) 130–139. doi:10.1016/j.biortech.2013.10.111.
- [10] L. Van Khoi, R. Fotedar, Integration of western king prawn (*Penaeus latisulcatus* Kishinouye, 1896) and green seaweed (*Ulva lactuca* Linnaeus, 1753) in a closed

- recirculating aquaculture system, *Aquaculture*. 322–323 (2011) 201–209. doi:10.1016/j.aquaculture.2011.09.030.
- [11] E. Marinho-Soriano, S.O. Nunes, M.A.A. Carneiro, D.C. Pereira, Nutrients' removal from aquaculture wastewater using the macroalgae *Gracilaria birdiae*, *Biomass and Bioenergy*. 33 (2009) 327–331. doi:10.1016/j.biombioe.2008.07.002.
- [12] S.G. Nelson, E.P. Glenn, J. Conn, D. Moore, T. Walsh, M. Akutagawa, Cultivation of *Gracilaria parvispora* (Rhodophyta) in shrimp-farm effluent ditches and floating cages in Hawaii: a two-phase polyculture system, *Aquaculture*. 193 (2001) 239–248. doi:10.1016/S0044-8486(00)00491-9.
- [13] H. Mai, R. Fotedar, J. Fewtrell, Evaluation of *Sargassum* sp. as a nutrient-sink in an integrated seaweed-prawn (ISP) culture system, *Aquaculture*. 310 (2010) 91–98. doi:10.1016/j.aquaculture.2010.09.010.
- [14] S. Raikova, C.D. Le, J.L. Wagner, V.P. Ting, C.J. Chuck, Chapter 9 – Towards an Aviation Fuel Through the Hydrothermal Liquefaction of Algae, in: C.J. Chuck (Ed.), *Biofuels Aviat.*, Elsevier, London, 2016: pp. 217–239. doi:10.1016/B978-0-12-804568-8.00009-3.
- [15] A. Dave, Y. Huang, S. Rezvani, D. McIlveen-Wright, M. Novaes, N. Hewitt, Techno-economic assessment of biofuel development by anaerobic digestion of European marine cold-water seaweeds, *Bioresour. Technol.* 135 (2013) 120–127. doi:10.1016/j.biortech.2013.01.005.
- [16] M. Daroch, S. Geng, G. Wang, Recent advances in liquid biofuel production from algal feedstocks, *Appl. Energy*. 102 (2013) 1371–1381. doi:10.1016/j.apenergy.2012.07.031.
- [17] M. Aresta, A. Dibenedetto, M. Carone, T. Colonna, C. Fragale, Production of biodiesel from macroalgae by supercritical CO<sub>2</sub> extraction and thermochemical liquefaction, *Environ. Chem. Lett.* 3 (2005) 136–139. doi:10.1007/s10311-005-0020-3.
- [18] Y. Chisti, Biodiesel from microalgae., *Biotechnol. Adv.* 25 (2007) 294–306. doi:10.1016/j.biotechadv.2007.02.001.
- [19] D.C. Elliott, Review of recent reports on process technology for thermochemical conversion of whole algae to liquid fuels, *Algal Res.* 13 (2016) 255–263. doi:10.1016/j.algal.2015.12.002.

- [20] D.L. Sills, V. Paramita, M.J. Franke, M.C. Johnson, T.M. Akabas, C.H. Greene, J.W. Tester, Quantitative uncertainty analysis of Life Cycle Assessment for algal biofuel production., *Environ. Sci. Technol.* 47 (2013) 687–94. doi:10.1021/es3029236.
- [21] J. Rowbotham, P. Dyer, H. Greenwell, M. Theodorou, Thermochemical processing of macroalgae: a late bloomer in the development of third-generation biofuels?, *Biofuels*. 3 (2012) 441–461. doi:10.4155/bfs.12.29.
- [22] D. López Barreiro, W. Prins, F. Ronsse, W. Brilman, Hydrothermal liquefaction (HTL) of microalgae for biofuel production: State of the art review and future prospects, *Biomass and Bioenergy*. 53 (2013) 113–127. doi:10.1016/j.biombioe.2012.12.029.
- [23] Y. Guo, T. Yeh, W. Song, D. Xu, S. Wang, A review of bio-oil production from hydrothermal liquefaction of algae, *Renew. Sustain. Energy Rev.* 48 (2015) 776–790. doi:10.1016/j.rser.2015.04.049.
- [24] R. Maceiras, M. Rodríguez, A. Cancela, S. Urréjola, A. Sánchez, Macroalgae: Raw material for biodiesel production, *Appl. Energy*. 88 (2011) 3318–3323. doi:10.1016/j.apenergy.2010.11.027.
- [25] D.C. Elliott, L.J. Sealock Jr., S.R. Butner, Product Analysis from Direct Liquefaction of Several High-Moisture Biomass Feedstocks, in: E.J. Soltes, T.A. Milne (Eds.), *Pyrolysis Oils From Biomass Prod. Anal. Upgrad. - ACS Symp. Ser.*, American Chemical Society, Washington, D. C., 1988: pp. 179–188. doi:doi:10.1021/bk-1988-0376.ch017.
- [26] D. López Barreiro, M. Bauer, U. Hornung, C. Posten, A. Kruse, W. Prins, Cultivation of microalgae with recovered nutrients after hydrothermal liquefaction, *Algal Res.* 9 (2015) 99–106. doi:10.1016/j.algal.2015.03.007.
- [27] J. Wang, G. Wang, M. Zhang, M. Chen, D. Li, F. Min, M. Chen, S. Zhang, Z. Ren, Y. Yan, A comparative study of thermolysis characteristics and kinetics of seaweeds and fir wood, *Process Biochem.* 41 (2006) 1883–1886. doi:10.1016/j.procbio.2006.03.018.
- [28] A. Ross, J. Jones, M. Kubacki, T. Bridgeman, Classification of macroalgae as fuel and its thermochemical behaviour, *Bioresour. Technol.* 99 (2008) 6494–6504. doi:10.1016/j.biortech.2007.11.036.
- [29] D. Zhou, L. Zhang, S. Zhang, H. Fu, J. Chen, Hydrothermal Liquefaction of

- Macroalgae *Enteromorpha prolifera* to Bio-oil, *Energy & Fuels*. 24 (2010) 4054–4061. doi:10.1021/ef100151h.
- [30] D. Li, L. Chen, D. Xu, X. Zhang, N. Ye, F. Chen, S. Chen, Preparation and characteristics of bio-oil from the marine brown alga *Sargassum patens* C. Agardh, *Bioresour. Technol.* 104 (2012) 737–742. doi:10.1016/j.biortech.2011.11.011.
- [31] H. Li, Z. Liu, Y. Zhang, B. Li, H. Lu, N. Duan, M. Liu, Z. Zhu, B. Si, Conversion efficiency and oil quality of low-lipid high-protein and high-lipid low-protein microalgae via hydrothermal liquefaction, *Bioresour. Technol.* 154 (2014) 322–329. doi:10.1016/j.biortech.2013.12.074.
- [32] N. Neveux, A.K.L. Yuen, C. Jazrawi, M. Magnusson, B.S. Haynes, A.F. Masters, A. Montoya, N.A. Paul, T. Maschmeyer, R. de Nys, Biocrude yield and productivity from the hydrothermal liquefaction of marine and freshwater green macroalgae, *Bioresour. Technol.* 155 (2014) 334–341.
- [33] K. Anastasakis, A.B. Ross, Hydrothermal liquefaction of four brown macro-algae commonly found on the UK coasts: An energetic analysis of the process and comparison with bio-chemical conversion methods, *Fuel*. 139 (2015) 546–553. doi:10.1016/j.fuel.2014.09.006.
- [34] D. López Barreiro, M. Beck, U. Hornung, F. Ronsse, A. Kruse, W. Prins, Suitability of hydrothermal liquefaction as a conversion route to produce biofuels from macroalgae, *Algal Res.* 11 (2015) 234–241. doi:10.1016/j.algal.2015.06.023.
- [35] P. Biller, A.B. Ross, Potential yields and properties of oil from the hydrothermal liquefaction of microalgae with different biochemical content., *Bioresour. Technol.* 102 (2011) 215–25. doi:10.1016/j.biortech.2010.06.028.
- [36] W. Yang, X. Li, Z. Li, C. Tong, L. Feng, Understanding low-lipid algae hydrothermal liquefaction characteristics and pathways through hydrothermal liquefaction of algal major components : Crude polysaccharides , crude proteins and their binary mixtures, *Bioresour. Technol.* 196 (2015) 99–108. doi:10.1016/j.biortech.2015.07.020.
- [37] D.C. Elliott, T.R. Hart, G.G. Neuenschwander, L.J. Rotness, G. Roesijadi, A.H. Zacher, J.K. Magnuson, Hydrothermal Processing of Macroalgal Feedstocks in Continuous-Flow Reactors, *ACS Sustain. Chem. Eng.* 2 (2014) 201–215. doi:10.1021/sc400251p.

- [38] G. Teri, L. Luo, P.E. Savage, Hydrothermal Treatment of Protein, Polysaccharide, and Lipids Alone and in Mixtures, *Energy Fuels*. 28 (2014) 7501–7509. doi:10.1021/ef501760d.
- [39] P. Biller, R. Riley, A.B. Ross, Catalytic hydrothermal processing of microalgae: decomposition and upgrading of lipids, *Bioresour. Technol.* 102 (2011) 4841–8. doi:10.1016/j.biortech.2010.12.113.
- [40] B. Jin, P. Duan, Y. Xu, F. Wang, Y. Fan, Co-liquefaction of micro- and macroalgae in subcritical water., *Bioresour. Technol.* 149 (2013) 103–10. doi:10.1016/j.biortech.2013.09.045.
- [41] P. Biller, A.B. Ross, S.C. Skill, A. Lea-Langton, B. Balasundaram, C. Hall, R. Riley, C. a. Llewellyn, Nutrient recycling of aqueous phase for microalgae cultivation from the hydrothermal liquefaction process, *Algal Res.* 1 (2012) 70–76. doi:10.1016/j.algal.2012.02.002.
- [42] J. Wagner, R. Bransgrove, T.A. Beacham, M.J. Allen, K. Meixner, B. Drosig, V.P. Ting, C.J. Chuck, Co-production of bio-oil and propylene through the hydrothermal liquefaction of polyhydroxybutyrate producing cyanobacteria, *Bioresour. Technol.* 207 (2016) 166–174. doi:10.1016/j.biortech.2016.01.114.
- [43] S. Raikova, H. Smith-Baedorf, R. Bransgrove, O. Barlow, F. Santomauro, J.L. Wagner, M.J. Allen, C.G. Bryan, D. Sapsford, C.J. Chuck, Assessing hydrothermal liquefaction for the production of bio-oil and enhanced metal recovery from microalgae cultivated on acid mine drainage, *Fuel Process. Technol.* 142 (2016) 219–227. doi:10.1016/j.fuproc.2015.10.017.
- [44] Y.-P. Xu, P.-G. Duan, F. Wang, Hydrothermal processing of macroalgae for producing crude bio-oil, *Fuel Process. Technol.* 130 (2015) 268–274. doi:10.1016/j.fuproc.2014.10.028.
- [45] M. DuBois, K. Gilles, J. Hamilton, P. Rebers, F. Smith, Colorimetric method for determination of sugars and related substances, *Anal. Chem.* 28 (1956) 350–356.
- [46] K.A.C.C. Taylor, A modification of the phenol/sulfuric acid assay for total carbohydrates giving more comparable absorbances, *Appl. Biochem. Biotechnol.* 53 (1995) 207–214. doi:10.1007/BF02783496.
- [47] E.T. Kostas, S.J. Wilkinson, D.A. White, D.J. Cook, Optimization of a total acid hydrolysis based protocol for the quantification of carbohydrate in macroalgae, *J. Algal Biomass Util.* 7 (2016) 21–36.

- [48] S.A.A. Channiwala, P.P.P. Parikh, A unified correlation for estimating HHV of solid, liquid and gaseous fuels, *Fuel*. 81 (2002) 1051–1063. doi:10.1016/S0016-2361(01)00131-4.
- [49] J.L. Faeth, P.J. Valdez, P.E. Savage, Fast Hydrothermal Liquefaction of *Nannochloropsis* sp. To Produce Biocrude, *Energy & Fuels*. 27 (2013) 1391–1398. doi:10.1021/ef301925d.
- [50] B. Zhang, M. von Keitz, K. Valentas, Thermal Effects on Hydrothermal Biomass Liquefaction, *Appl. Biochem. Biotechnol.* 147 (2008) 143–150.
- [51] U. Jena, N. Vaidyanathan, S. Chinnasamy, K.C. Das, Evaluation of microalgae cultivation using recovered aqueous co-product from thermochemical liquefaction of algal biomass, *Bioresour. Technol.* 102 (2011) 3380–3387. doi:10.1016/j.biortech.2010.09.111.
- [52] H.M. Khairy, S.M. El-Shafay, Seasonal variations in the biochemical composition of some common seaweed species from the coast of Abu Qir Bay, Alexandria, Egypt, *Oceanologia*. 55 (2013) 435–452. doi:10.5697/oc.55-2.435.
- [53] P.D. Kerrison, M.S. Stanley, M.D. Edwards, K.D. Black, A.D. Hughes, The cultivation of European kelp for bioenergy: Site and species selection, *Biomass and Bioenergy*. 80 (2015) 229–242. doi:10.1016/j.biombioe.2015.04.035.
- [54] A.A. Albalasmeh, A.A. Berhe, T.A. Ghezzehei, A new method for rapid determination of carbohydrate and total carbon concentrations using UV spectrophotometry, *Carbohydr. Polym.* 97 (2013) 253–261. doi:10.1016/j.carbpol.2013.04.072.
- [55] A. Graiff, W. Ruth, U. Kragl, U. Karsten, Chemical characterization and quantification of the brown algal storage compound laminarin — A new methodological approach, *J. Appl. Phycol.* 28 (2016) 533–543. doi:10.1007/s10811-015-0563-z.
- [56] R.H. Reed, I.R. Davison, J.A. Chudek, R. Foster, The osmotic role of mannitol in the Phaeophyta: an appraisal, *Phycologia*. 24 (1985) 35–47.
- [57] E. Marinho-Soriano, P.C. Fonseca, M. a a Carneiro, W.S.C. Moreira, Seasonal variation in the chemical composition of two tropical seaweeds, *Bioresour. Technol.* 97 (2006) 2402–2406. doi:10.1016/j.biortech.2005.10.014.
- [58] J.M.M. Adams, A.B. Ross, K. Anastasakis, E.M. Hodgson, J.A. Gallagher, J.M.

Jones, I.S. Donnison, Seasonal variation in the chemical composition of the bioenergy feedstock *Laminaria digitata* for thermochemical conversion, *Bioresour. Technol.* 102 (2011) 226–234. doi:10.1016/j.biortech.2010.06.152.

- [59] D. López Barreiro, C. Zamalloa, N. Boon, W. Vyverman, F. Ronsse, W. Brilman, W. Prins, Influence of strain-specific parameters on hydrothermal liquefaction of microalgae., *Bioresour. Technol.* 146 (2013) 463–71. doi:10.1016/j.biortech.2013.07.123.

## 2.3 Supplementary information

### 2.3.1 Collection and preparation of macroalgal biomass

Fresh macroalgal biomass samples were collected from Paignton, Devon (specifically, Broadsands Beach, Oyster Cove and Saltern Cove) between March 2015 and March 2016 (Table 2.3-1). Healthy macroalgae displaying no signs of obvious significant grazing, erosion, disease or biofouling were sampled in their entirety and the whole biomass processed (inclusive of fronds, stems and blades). Following harvesting, samples were washed in 1.2 µm filtered seawater, to remove any residual sediment, plant and animal material, within 24 hours of harvesting, rinsed in deionised water, and immediately snap frozen in liquid nitrogen. Samples were then freeze dried for up to 72 hours at -55 °C (Coolsafe, Scanvac).

Prior to analysis, all samples were milled to <1700 µm diameter. Samples were stored in sealed vials at -18 °C. Macroalgal species used were *Ascophyllum nodosum* (AN), *Chondrus crispus* (CC), *Fucus ceranoides* (FC), *Fucus vesiculosus* (FV), *Himanthalia elongata* (HE), *Laminaria digitata* (LD), *Laminaria hyperborea* (LH), *Pelvetia canaliculata* (PC), *Rhizoclonium riparium* (RR), *Sargassum muticum* (SM), *Solieria chordalis* (SC), *Ulva intestinalis* (UI) and *Ulva lactuca* (UL).



**Table 2.3-1 – Location and description of macroalgal samples**

<b>Species</b>	<b>Location</b>	<b>Date</b>	<b>Physical description of sample</b>
<i>Ascophyllum nodosum</i>	50.4168 -3.5558	29/3/15	Approximately 1m long fronds, cut at base above holdfast.
<i>Chondrus crispus</i>	50.4168 -3.5558	29/3/15	Approximately 0.15m flat fronds, removed at base.
<i>Fucus ceranoides</i>	50.4168 -3.5558	29/3/15	Approximately 0.6m long fronds, cut at base above holdfast.
<i>Fucus vesiculosus</i>	50.4168 -3.5558	29/3/15	Approximately 0.6m long fronds, cut at base above holdfast.
<i>Himanthalia elongata</i>	50.4168 -3.5558	29/3/15	Approximately 1.5m long cords, broken away from disc holdfast.
<i>Laminaria digitata</i>	50.4168 -3.5558	29/3/15	Approximately 1m long including stem, cut at base above holdfast.
<i>Laminaria hyperborea</i>	50.4168 -3.5558	29/3/15	Approximately 1m long including stem, cut at base above holdfast.
<i>Pelvetia canaliculata</i>	50.4168 -3.5558	4/1/16	Approximately 0.15m fronds, removed at base.
<i>Rhizoclonium riparium</i>	50.41416 -3.5564	6/3/16	Approximately 0.15m fronds, removed at base.
<i>Sargassum muticum</i>	50.4067 -3.5553	20/11/15	Approximately 0.75m fronds, cut at base.
<i>Solieria chordalis</i>	50.4067 -3.5553	20/11/15	0.3m long clumps, free floating.
<i>Ulva intestinalis</i>	50.4168 -3.5558	29/3/15	Approximately 0.15m tubular fronds, removed at base.
<i>Ulva lactuca</i>	50.4168 -3.5558	29/3/15	Approximately 0.2m fronds, removed at base.

## 2.4 Appendices

### 2.4.1 Appendix 2A

The ideal gas law has been used as an approximation to calculate gas phase yields based on CO<sub>2</sub> in this case. Alternatively, the Van der Waals equation, which accounts for non-ideal behaviour, could have been used to calculate yields:

$$\left(P + \frac{an^2}{V^2}\right) \times (V - nb) = nRT \quad (1)$$

where  $P$  = pressure,  $V$  = gas phase volume,  $a = 3.640 \text{ L}^2 \text{ bar mol}^{-2}$  for CO<sub>2</sub>,  $b = 0.04267 \text{ L}^2 \text{ mol}^{-1}$  for CO<sub>2</sub>,  $n$  = no. moles CO<sub>2</sub>,  $R$  = universal gas constant, and  $T$  = temperature.

For 460 cm<sup>3</sup> gas phase obtained after processing 4.006 g *A. nodosum*, the gas phase yield (based on CO<sub>2</sub>) was determined to be 21.62 % using the ideal gas law, and 21.65 % using the Van der Waals equation. This constitutes a difference of <0.05 % between the two values; therefore, it can be confirmed that the ideal gas equation serves as a suitable approximation to calculate gas phase yields.

### 2.4.2 Appendix 2B

Ash content was evaluated using TGA as previously described by Anastasakis and Ross [2]. Temperatures of 900 °C were used to assess HTL solid phase products; 1000 °C was used in this case.

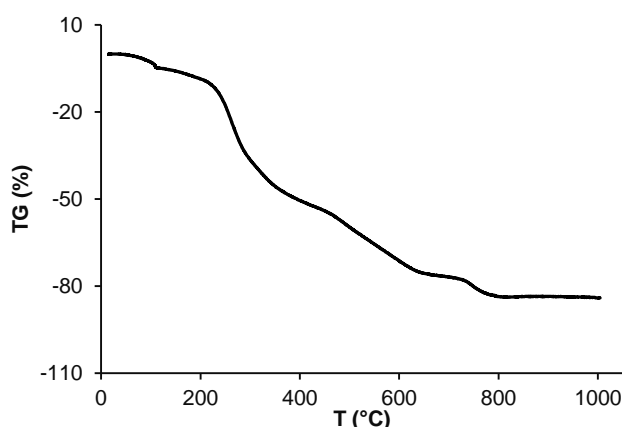


**Figure 2.4-1** – TGA of *A. nodosum*, used to assess ash and moisture content

There is no notable decomposition between 900–1000 °C, therefore, the methods can be deemed to be comparable to those used in prior literature. However, it is acknowledged that there may have been a degree of volatilisation of the inorganic

portion of the ash beyond 600 °C. Temperatures of 550 °C were used in subsequent studies for ash determination.

### **2.4.3 Appendix 2C**

Non-closures of the mass balance have been assigned to the loss of volatiles from the bio-crude and aqueous phases during work-up. It is also possible that some of the losses may be attributable to the formation of water through condensation and dehydration reactions, which would also be lost during work-up of the aqueous phase.

## 2.5 Context and appendix references

- [1] K.R. Arturi, S. Kucheryavskiy, E.G. Søgaard, Performance of hydrothermal liquefaction (HTL) of biomass by multivariate data analysis, *Fuel Process. Technol.* 150 (2016) 94–103. doi:10.1016/j.fuproc.2016.05.007.
- [2] K. Anastasakis, A.B. Ross, Hydrothermal liquefaction of the brown macro-alga *Laminaria saccharina*: effect of reaction conditions on product distribution and composition., *Bioresour. Technol.* 102 (2011) 4876–83. doi:10.1016/j.biortech.2011.01.031.
- [3] P. Biller, R.B. Madsen, M. Klemmer, J. Becker, B.B. Iversen, M. Glasius, Effect of hydrothermal liquefaction aqueous phase recycling on bio- crude yields and composition, *Bioresour. Technol.* 220 (2016) 190–199. doi:10.1016/j.biortech.2016.08.053.
- [4] L. Garcia Alba, C. Torri, D. Fabbri, S.R.A. Kersten, D.W.F. Brilman, Microalgae growth on the aqueous phase from Hydrothermal Liquefaction of the same microalgae, *Chem. Eng. J.* 228 (2013) 214–223. doi:10.1016/j.cej.2013.04.097.
- [5] M. Nelson, L. Zhu, A. Thiel, Y. Wu, M. Guan, J. Minty, H.Y. Wang, X.N. Lin, Microbial utilization of aqueous co-products from hydrothermal liquefaction of microalgae *Nannochloropsis oculata*., *Bioresour. Technol.* 136 (2013) 522–8. doi:10.1016/j.biortech.2013.03.074.

## Chapter 3

---

# Effect of geographical location on the variation in products formed from the hydrothermal liquefaction of *Ulva intestinalis*

This work has been accepted for publication in the special edition of Energy and Fuels (ACS) titled “Best of ACS from Energy and Fuels Division at the 255th ACS National Meeting” in August 2018.

This work was completed in collaboration with Chalmers University of Technology.

**Raikova, S.**, Olsson, J., Mayers, J., Nylund, G., Albers, E., Chuck, C.J., 2018. Effect of geographical location on the variation in products formed from the hydrothermal liquefaction of *Ulva intestinalis*. Energy & Fuels Accepted manuscript.  
doi:10.1021/acs.energyfuels.8b02374

### 3.1 Context

The previous chapter of this thesis examined the variation in HTL outcomes for a range of macroalgal species within a single location. Although the relationships between biomass composition and HTL outcomes are complex, optimal bio-crude yields for biomass within the South West of the UK were obtained for the green macroalgae *Ulva lactuca* and *Ulva intestinalis*. These would therefore be preferred as the basis for a South West UK biorefinery.

However, it is unclear whether this would hold universally and, whether the same species would be ideal in an entirely separate locality. It is well known that macroalgal growth rate and composition varies across different geographical locations [1], influenced by aqueous nutrient composition, salinity, temperature, and even water turbulence [2–6]. These factors may have knock-on effects on the suitability of a macroalgae for use as an HTL feedstock in different countries and regions.

To this end, the study described in this chapter aimed to examine the influence of geographical factors on the hydrothermal conversion of a single macroalgae species. *U. intestinalis*, a successful biorefinery feedstock candidate within the UK, was sampled in eight distinct locations along a 1,200 km stretch of coastline in Sweden, and processed using identical HTL conditions. Three samples were taken at each site, allowing an assessment of localised environmental effects, as well as differences between more distant sites.

This chapter focuses primarily on HTL outcomes; a more in-depth examination of geographical effects on the biochemical composition of *U. intestinalis* is the subject of a separate upcoming publication led by collaborators at Chalmers University of Technology, who coauthored the publication presented in this chapter.

This chapter is submitted in an alternative format in line with Appendix 6A of the “Specifications for Higher Degree Theses and Portfolios” as required by the University of Bath.

The work completed in this paper was conducted by the author with the exception of the following:

Lipid and polysaccharide quantification were conducted by Joakim Olsson and Göran Nylund, two of the paper’s co-authors.

Elemental analysis was carried out by analytical department personnel at London Metropolitan University.

ICP-OES analysis was carried out by analytical department personnel at Yara International (acid digestion and sample preparation was carried out by the lead author).

## 3.2 Energy and Fuels paper

### Effect of geographical location on the variation in products formed from the hydrothermal liquefaction of *Ulva intestinalis*

Sofia Raikova<sup>1</sup>, Joakim Olsson<sup>2</sup>, Joshua J. Mayers<sup>2</sup>, Göran M. Nylund<sup>3</sup>, Eva Albers<sup>2</sup>,  
Christopher J. Chuck<sup>4\*</sup>

<sup>1</sup> Centre for Doctoral Training in Sustainable Chemical Technologies, Department of Chemical Engineering, University of Bath, Claverton Down, Bath BA2 7AY, United Kingdom

<sup>2</sup> Department of Biology and Biological Engineering - Industrial Biotechnology, Chalmers University of Technology, SE-412 96 Göteborg, Sweden

<sup>3</sup> Department of Marine Sciences - Tjärnö, University of Gothenburg, SE-452 96 Strömstad, Sweden

<sup>4</sup> Department of Chemical Engineering, University of Bath, Claverton Down, Bath BA2 7AY, United Kingdom

\*Corresponding author

Keywords: Macroalgae; HTL; biofuel; seaweed

#### 3.2.1 Abstract

Hydrothermal liquefaction of macroalgae offers a promising route to advanced biofuel production, though the distinct biochemical compositions of different macroalgae species can lead to widely different product yields and compositions. Based on this, there is an implicit assumption that there exists a universal optimal feedstock species for a bioenergy-based biorefinery, which could be exploited across a wide region. However, no studies to date have examined the effect of this large geographical variation on a single macroalgae species for biofuel production. In this study, 24 samples of *Ulva intestinalis* were collected along 1200 km of Swedish coastline and assessed as a feedstock for HTL. Significant variation in composition was observed between samples from Baltic and Atlantic regions, but substantial variation also existed between sites



within close proximity. This was reflected in the HTL bio-crude yields, which varied from between 9–20 % (14–28 % dry ash free) across the sample set. In a number of cases, greater variation was seen for adjacent sites than for sites at opposite ends of the sampling spectrum. Bio-crude yields in this study also differed substantially from those published previously obtained for *U. intestinalis* from the United Kingdom and Viet Nam. Localised environmental conditions affected the HTL product composition significantly, in particular, the elemental distribution within the sample set. The variability observed in this study suggests that no single species will be dominant within a macroalgal biorefinery concept, but rather a species would need to be selected to match the needs of the exact local environment.

### 3.2.2 Introduction

In order to limit global temperature increases to 2 °C, the vast majority of the energy sector must be decarbonised by 2075 [1]. However, liquid fuels are likely to continue to play a major role in the transport sector long into the future [2] and “drop-in” biofuels or crude oil alternatives compatible with current transport and refinery infrastructure are a crucial step in the transition to cleaner energy sources [3]. The use of terrestrial crops as feedstocks for biofuel production has been explored extensively, but concerns about utilisation of arable land [4], as well as general availability, have spurred a search for alternative marine feedstocks [5].

Macroalgae are a fast-growing and important global resource. With production of aquatic plants reaching 30.5 million tonnes in 2015 harvested for commercial use [6] and cultivation increasing on average 8 % per year [7], it constitutes a promising source of biomass for food, pharmaceuticals and agriculture. As production volumes continue to grow, macroalgae has the potential to be used as an alternative to terrestrial biofuel feedstocks [8].

A number of processing techniques have been examined for the conversion of macroalgae to liquid fuels, including biodiesel production [9–11], fermentation to bioethanol and biobutanol [12–14] and anaerobic digestion [15]. In recent years, thermochemical processing techniques, such as pyrolysis [16] and hydrothermal liquefaction (HTL) [17], have been examined as a route to producing high energy content oils as precursors for biofuel production. Of these, HTL has a number of advantages over pyrolysis: it is a low-temperature technique, utilising water at subcritical conditions (280–370 °C), and is ideally suited to inherently high-moisture feedstocks, thereby avoiding the substantial energetic penalty of feedstock drying. HTL also generates bio-

crude oils with lower oxygen contents, higher energy content [18], and higher thermal stability [19] compared to pyrolysis oils. HTL bio-crude oils can be upgraded directly to biofuels through hydrotreating [20], although oils have the potential to be co-refined with fossil crudes in existing refineries in the future [19,21,22]. Upgrading options and refining protocols are dependent on bio-crude composition.

The exact composition and properties of bio-crude oils are influenced by HTL reaction conditions, but are most strongly influenced by the composition of the feedstock [23]. The earliest studies on the hydrothermal liquefaction of macroalgal biomass focused on individual feedstock species [24–27], but recent reports have demonstrated the vast difference in products obtainable from different species growing in one place [28]. However, even within a single species, compositions can be influenced substantially by localised environmental conditions such as salinity, temperature, and nutrient availability, and there is some evidence that certain biochemical components can vary widely between different geographical locations [29–33]. For example, brown macroalgae grown in more turbulent conditions typically have elevated levels of alginate [34], and salinity has been shown to increase fatty acid levels in the green alga *Ulva pertusa* and the brown *Sargassum piluliferum* [35]. Cultivation of macroalgae downstream from aquaculture, such as salmon farms, has been shown to induce accumulation of higher levels of nitrogen [30] and phosphorus [36], whilst biomasses grown in contaminated waters also exhibit bioaccumulation of heavy metals [37], which could potentially be exploited as a route to environmental remediation of marine environments. Aside from direct increases in contaminant levels as a result of biosorption, the presence of metals has also been shown to affect the expression of polyunsaturated fatty acids (PUFA) [38]. All of these fluctuations have the potential to affect biomass reactivity and suitability as a feedstock for HTL.

Large-scale cultivation of macroalgae for fuel and food production in Sweden has recently been explored [39,40]. The waters of the Swedish coastline are divided into two distinct regions: high-salinity and nutrient-rich in the North Sea on the western coast, and shallower, more brackish waters in the Baltic Sea in the east [40]. Within these regions there are also variations in both biotic and abiotic factors that give rise to eutrophication, although the Helsinki Convention has led to overall improvements in water quality in recent decades [41,42]. These variations give rise to potential differences in macroalgal productivity and composition, which in turn could significantly affect the efficiency of the HTL process. In this investigation, the suitability of a single species, *U. intestinalis*, was

assessed as a feedstock for a macroalgal HTL biorefinery through the conversion of biomass harvested from a range of locations around the coast of Sweden.

### 3.2.3 Methods

#### 3.2.3.1 Materials and apparatus

Fresh macroalgal biomass samples were collected in late summer over 22 days at eight sites along the Swedish coast. Three samples were collected at each site, 50–7000 metres apart (several hundred metres for the majority of sites). The samples were dewatered using a salad spinner and frozen in a portable freezer shortly after collection. Prior to analysis, all samples were freeze-dried and milled to a homogenous powder. Freeze-dried samples were stored at -80 °C prior to compositional analysis, and subsequently stored at ambient conditions prior to being processed by HTL.

Sampling locations in graphs and tables are referred to using abbreviations: Tjärnö (TJÖ), Tjörn outside Göteborg (GBG), Helsingborg (HBG), Trelleborg (TBG), Åhus (ÅHS), Karlskrona (KKR), Västervik (VSV) and Stockholm (STH). Locations are summarised in Fig. 3.2-1.



**Figure 3.2-1** – Map of sampling sites; Atlantic sites are represented by yellow markers, Baltic sites represented by blue markers. Three samples were obtained at each site, with sampling locations located approx. 50–7000 m apart.

Batch reactors were fabricated according to literature precedent using stainless steel Swagelok® tube fittings [43–45]. The reactor body consisted of a length of stainless steel tubing capped at one end, and connected at the other to a pressure gauge,

thermocouple, needle valve, and relief valve. The total internal volume of the reactors was *ca.* 50 cm<sup>3</sup>.

### 3.2.3.2 Procedure

Reaction procedures have been reported previously [45]. In a typical reaction, the reactor was loaded with 3 g biomass and 15 cm<sup>3</sup> freshly deionized water, and heated within a vertical tubular furnace set to 700 °C until the specified reaction temperature was reached (345 °C, approx. 11 min), then removed from the furnace and allowed to cool to room temperature.

After cooling, gaseous products were released *via* the needle valve into an inverted, water-filled measuring cylinder to measure gaseous fraction volume. The gas phase is typically composed of 96–98 % CO<sub>2</sub> [45,46]. Hence, gas phase yields were calculated using the ideal gas law, approximating the gas phase as 100 % CO<sub>2</sub>, assuming an approximate molecular weight of 44 g mol<sup>-1</sup> and a volume of 22.465 dm<sup>3</sup> mol<sup>-1</sup> gas phase at 25 °C. The yield of gaseous product was determined using the following equation:

$$\text{yield}_{\text{gas}} = (V_{\text{gas}} \times 1.789 \times 10^{-3}) / (m_{\text{dry biomass}}) \times 100 \% \quad (1)$$

Following this, the aqueous phase was decanted from the reactor contents and filtered through a Fisher qualitative filter paper pre-dried overnight at 60 °C. The product yield in the water phase was determined by leaving a 2.5 g aliquot to dry in a 60 °C oven overnight, and scaling the residue yield to the total aqueous phase mass. Aqueous phase residue yield was determined using the following equation:

$$\text{yield}_{\text{AP residue}} = m_{\text{residue}} / m_{\text{dry biomass}} \times 100 \% \quad (2)$$

To separate the remaining bio-crude oil and char phase, the reactor was washed repeatedly using chloroform until the solvent ran clear, and filtered through the same filter paper used to separate the aqueous phase (after drying for a minimum of 1 h). The filter paper and collected char were washed thoroughly with chloroform to remove all remaining bio-crude. The filtrate was collected, and solvent removed *in vacuo* (40 °C, 72 mbar) until no further solvent evaporation was observed visually, and bio-crude samples were left to stand in septum-sealed vials venting to the atmosphere *via* a needle for a further 12 h to remove residual solvent. Bio-crude yield was determined using the following equation:

$$\text{yield}_{\text{bio-crude}} = m_{\text{bio-crude}} / m_{\text{dry biomass}} \times 100 \% \quad (3)$$

The char yield was calculated from the mass of the retentate collected on the filter paper after drying overnight in an oven at 60 °C.

Solid yield was determined using the following equation:

$$\text{yield}_{\text{solid}} = m_{\text{solid}}/m_{\text{dry biomass}} \times 100 \% \quad (4)$$

Inevitable material losses occurred during work-up, predominantly through evaporation of light organics from the aqueous and bio-crude phases during filtration and solvent removal. The shortfall in the mass balance has thus been designated “volatiles”.

### ***3.2.3.3 Biomass and product characterisation***

For the macroalgal biomass, lipid quantification was carried out on freeze-dried biomass using *in situ* transesterification with GC-FID detection as described previously [47]. Analysis was carried out in triplicate. Monosaccharide quantification was carried out using acid hydrolysis as described by Bikker *et al.* [48], without neutralization. Samples were diluted and kept at 4 °C, and analysis performed in triplicate within approximately 48 hours. DHPAEC-PAD was utilized for detection as described previously [47], with minor modifications, incorporating a gradient of increasing sodium acetate content to separate sugar acids [49]. Total carbohydrate content was calculated as the sum of all monosaccharides and sugar acids with correction for addition of water during hydrolysis of polysaccharides. Crude protein content was calculated from biomass nitrogen content using a conversion factor of 5 as established previously [50].

Biomass ash was quantified by heating a 500 mg sample of biomass in a Carbolite muffle furnace at 550 °C for 5 hours. The mass remaining at the end of the experiment was taken to be the ash.

For macroalgal biomass, bio-crude and char, elemental (CHN) analysis was carried out externally at London Metropolitan University on a Carlo Erba Flash 2000 Elemental Analyser to determine CHN content (Elemental analyses were carried out at least in duplicate for each sample, and average values are reported.). From this, higher heating value (HHV) was calculated using the equation set out by Channiwala & Parikh (2002) from elemental composition. HHV values calculated using the Channiwala & Parikh equation [51] were found to be in line with values determined experimentally using an IKA C1 bomb calorimeter (within ± 5 %) [28].

The aqueous phase products were analysed for total carbon (TC) and total nitrogen content (TN) using a Shimadzu TOC-L TOC analyser fitted with a TNM-L total nitrogen analyser unit and an ASI-L autosampler.

Further elemental analysis was carried out using ICP-OES. Samples were digested in 4 mL *aqua regia* at 95 °C for 1 hour, then left to digest at ambient temperature for 24 hours before being made up to 20 mL with 10 % NaOH solution in deionised water to a pH of approx. 3. The resulting solution was filtered through a 0.45 µm filter membrane prior to analysis. ICP-OES was carried out externally by Yara U.K. Ltd. using an Agilent 700 series inductively coupled plasma optical emission spectrometer.

In order to determine experimental error and test the repeatability of experimental results, three repeat HTL runs of *U. intestinalis* collected in Göteborg were carried out to determine the standard deviation in mass balances at different reaction temperatures. All elemental analyses (CHN) were carried out in duplicate, and average values used.

#### ***3.2.3.4 Statistical analysis***

Statistical analysis (two-tailed T-test; regression) was conducted using Microsoft Excel's built-in data analysis module, as well as the XLSTAT add-in for non-parametric testing (Mann-Whitney's U-test).

### **3.2.4 Results and discussion**

#### ***3.2.4.1 Geographical variation in biomass biochemical composition***

Three seaweed samples, sampled no less than 50 m apart, were collected at each of the eight locations around the coast of Sweden. The biochemical composition of the macroalgae tested displayed some geographical variation (Fig. 3.2-2). The Atlantic region (Tjärnö and Göteborg) has higher salinity compared to the more brackish waters of the Baltic (the remaining six sampling locations, with Helsingborg at the border of the two regions), which is one factor that may influence composition. Indeed, samples from Atlantic sites had elevated lipid, protein and ash levels and reduced carbohydrate content, compared to the Baltic sites. Protein and lipid content have previously been found to increase in more saline environments [29,35] and a negative correlation between total carbohydrate content and water salinity has also been reported [29].

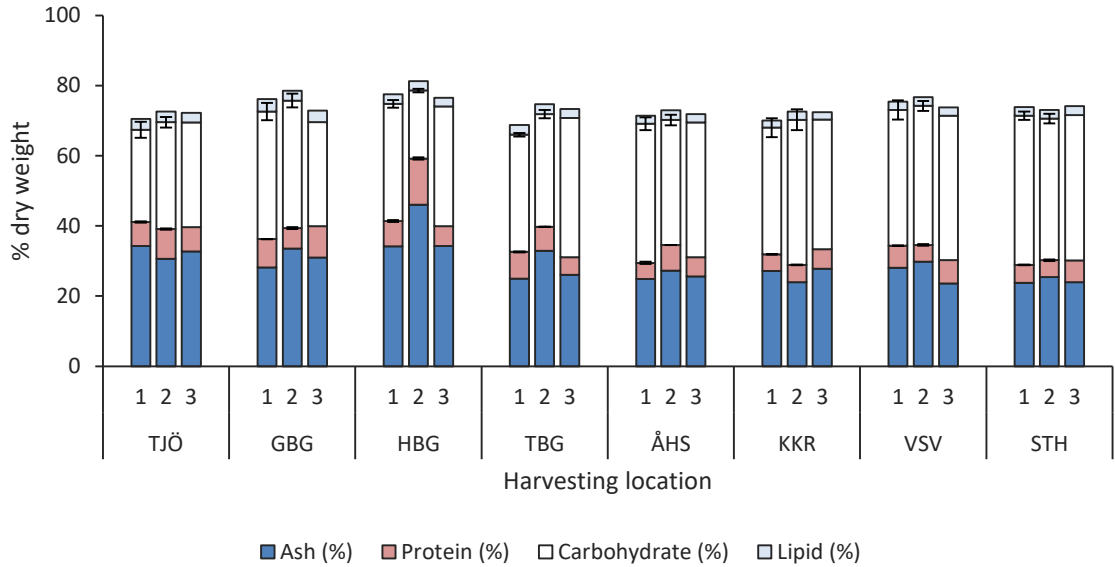


**Figure 3.2-2** – Total biochemical mass balance for *U. intestinalis* collected from three sampling sites across eight locations around the coast of Sweden. Error bars are derived from duplicate analysis of protein content, and triplicate analysis of total carbohydrate.

The overall biochemical composition differed substantially from that observed for *U. intestinalis* harvested in the UK, and other regions [28]. Most notably, protein and lipid levels were significantly lower (4.6–13.2 % protein, *c.f.* 20.9 % for UK *U. intestinalis*, and, similarly 2.0–3.6 % lipid, *c.f.* 5.9 % in the UK). The UK macroalgae was harvested during spring, when protein and lipid levels are at their highest for many species [52], so these differences could also be attributable to seasonal, as well as other geographical and environmental factors. A further evaluation of environmental condition at collection sites correlated to biomass composition will be presented separately [49].

The elemental compositions of the samples displayed some variation, with total carbon contents ranging from 22.2 % in HBG to a maximum of 29.4 % observed for Västervik and Stockholm (Fig. 3.2-3). The largest standard deviation for carbon content within any one sampling location was 2.2 % for Göteborg. Sulfur content increased towards the northernmost sampling points in the Baltic region (Västervik and Stockholm), with statistically significant differences between the Atlantic and Baltic ( $P=0.010$ ), and the highest sulfur content observed to be 8.3 %. A significant difference between Atlantic and Baltic sites was also found for nitrogen content ( $P=0.022$ ) – an elevated nitrogen content was observed for Atlantic sites, although the difference was modest.

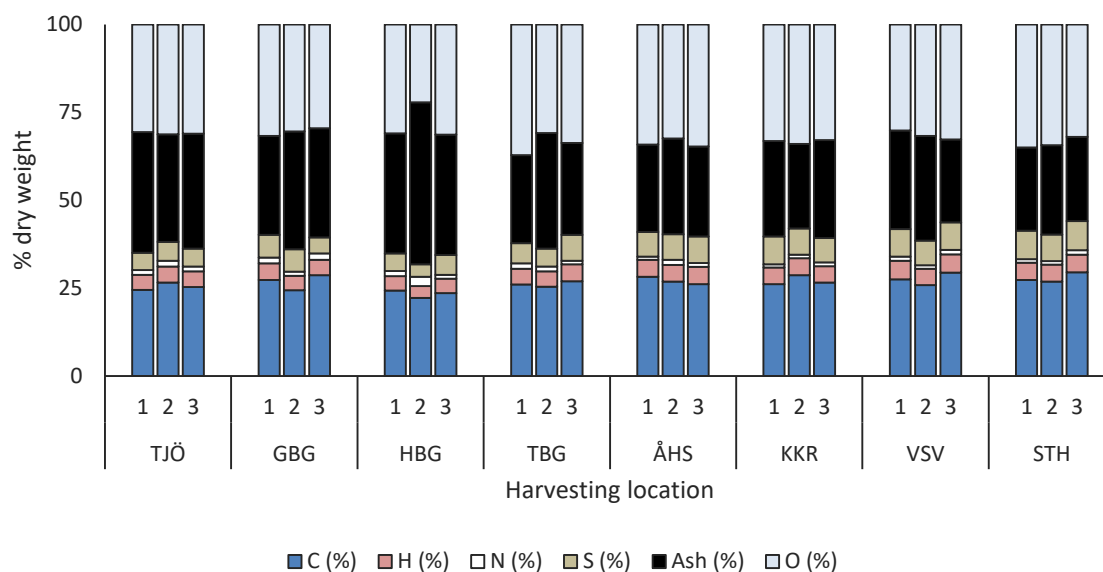


**Figure 3.2-3** – Elemental composition of *U. intestinalis* collected from three sampling sites across eight locations around the coast of Sweden. Carbon, hydrogen and nitrogen analysis was carried out in duplicate; error was negligible.

### 3.2.4.2 Variation in bio-crude oil production and quality

Hydrothermal liquefaction was carried out on all 24 collected samples across the eight locations. The reaction conditions were selected based on previous work [28] to give optimal bio-crude production. Mass closures of 70–85 % were observed, in line with those previously seen for similar feedstocks [53], with losses attributed to the evaporation of light volatiles from the aqueous fraction during water removal to calculate yields, and during solvent evaporation from the bio-crude products.



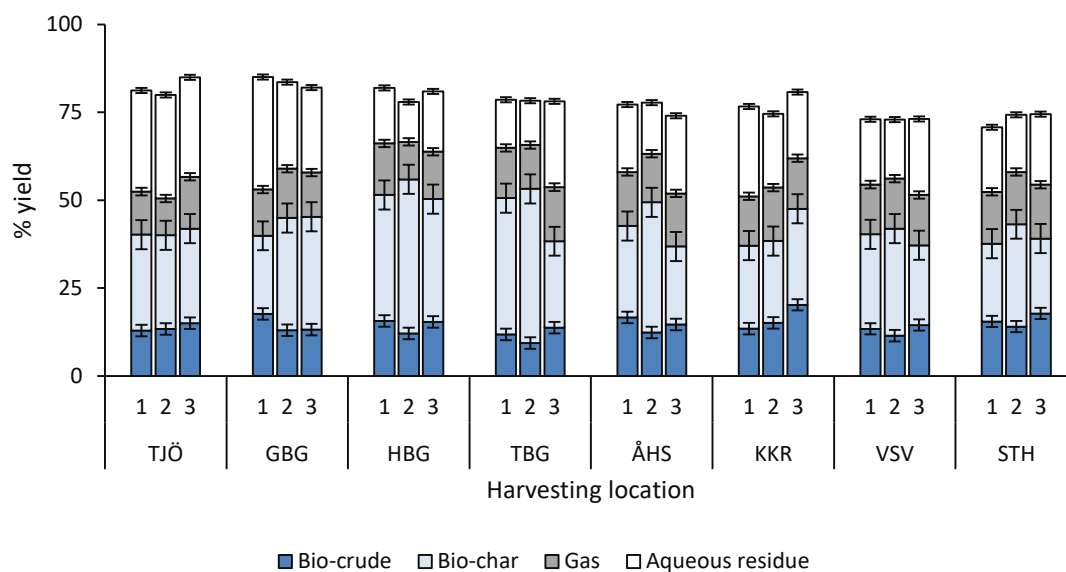


**Figure 3.2-4** – Mass balance of product fractions obtained from the hydrothermal liquefaction of 24 samples of *U. intestinalis* from three sampling sites across eight locations around the coast of Sweden. The remaining fraction of the mass is assigned to volatile losses from the aqueous and bio-crude fractions on work up. Mass yields quoted on a dry basis. Error bars represent the standard deviation of the product mass fractions obtained from three repeat runs of HTL using the GBG3 feedstock.

Bio-crude ranged from 9 % for a sample from Trelleborg to a maximum of 20 % observed for one of the biomasses from Karlskrona, still somewhat more modest than yields obtained from the same species, *U. intestinalis*, collected in the UK [28]. The majority of the bio-crude yields were similar, falling between 13 % and 17 %, with a small number of outliers. The bio-crude yields on a DAF basis are given in Table 3.2-1.

**Table 3.2-1** – Bio-crude yields from Swedish *U. intestinalis*, reported on a dry, ash-free basis (DAF %)

Location	Yield (DAF %)		
	1	2	3
Tjärnö	19.6	19.3	22.3
Göteborg	24.5	19.5	19.1
Helsingborg	23.8	22.4	23.4
Trelleborg	15.7	13.9	18.6
Åhus	22.2	17.0	19.7
Karlskrona	18.4	19.9	28.0
Västervik	18.6	16.3	19.0
Stockholm	20.3	18.8	23.4

It is well-established that lipids and proteins are preferentially converted to bio-crude [43], and the depleted lipid and protein contents of the autumn-harvested Swedish biomass compared to the lipid-rich spring *Ulva* crop in the UK would also make a difference. Despite significant differences observed between the biomass compositions of Atlantic and Baltic samples, no statistically significant differences between bio-crude yields obtained from Atlantic vs. Baltic macroalgae were identified ( $P > 0.05$ ). The variation in bio-crude yields generated from samples within each location was, in some cases, greater than the variation between samples collected from geographically remote sites. Yields ranging from 13 % to 20 % were obtained for the three Karlskrona samples, whilst identical bio-crude yields of 13 % were observed for multiple feedstocks sampled across both the Atlantic and Baltic regions (Tjärnö, Göteborg, Karlskrona and Västervik).

Total material recoveries in the aqueous phase products ranged from 11.4–32.0 %, with substantial variation within sampling sites: for the three biomasses collected in Trelleborg, aqueous phase yields ranged from 12.6 % to 24.5 %, with a similar level of variation observed for Åhus (14.6–22.1 % aqueous product yield). Previous studies have suggested that biomass carbohydrates are preferentially converted to aqueous phase products [54] such as a range of water-soluble polar organics [26]. However, a direct correlation between carbohydrate levels and aqueous phase yields was not observed in this case.

In recent years, there has been some focus on attempting to rationalise the reactivity of different macroalgal feedstocks across species [18,28,55] to supplement the investigations of biomass reactivity using model compounds [43,56,57]. Due to substantial species-related differences between individual protein, lipid and carbohydrate types within each broad compound class, simple and clear-cut correlations enabling the prediction of bio-crude yields based on biochemical composition have thus far been elusive [28,55]. It was hypothesised that for a single species, fluctuations in environmental conditions would induce changes in the relative quantities of biochemical components, but the individual protein, lipid and carbohydrate types would remain constant. This could potentially enable the derivation of a more strongly predictive model for bio-crude production based on biomass biochemical breakdown. Lipids have been previously found to be linked to bio-crude yields [28], however, regression analysis could not confirm any statistically significant correlations between the levels of lipid, protein, carbohydrate or total ash and bio-crude production ( $P > 0.05$ ). Alkali and alkaline earth metals in biomass ash have been variously attributed as having a catalytic or inhibitive effect on bio-crude formation, although mechanisms are still poorly understood [58]. The fluctuating content of alkali and alkaline earth metals, such as Ca, Mg and K, as well as other metallic species, across the locations sampled could play a role in directing bio-crude production, and counteract the effect of increasing lipid content.

Bio-crude nitrogen and sulfur contents were found to be strongly correlated with biomass nitrogen and sulfur levels. The levels of both elements appeared to follow a similar pattern, peaking at Helsingborg (the first sampling location in the Baltic region), and decreasing steadily as the sampling location moved north towards Stockholm, albeit with a small increase at Västervik. The Sound (Öresund), with Helsingborg at its narrowest point, attracts some of the highest marine traffic intensity in the Baltic region [59], with emissions of  $\text{SO}_x$  and  $\text{NO}_x$  potentially leading to elevated sulfur and nitrogen levels in seawater, and concomitant N and S increases in biomass. The lowest nitrogen and sulfur levels were observed for bio-crude produced from biomass obtained in Stockholm – lower than the Atlantic bio-crudes (somewhat surprisingly, given the high level of industrial and shipping activity in the Baltic region compared to the Atlantic). Sulfur levels in the bio-crudes (ranging from 0.9 % for Stockholm to 4.4 % for Helsingborg) fall in line with those observed for many fossil crudes (0.05–5 %), although sulfur levels of over 0.5 % are undesirable, and oils with sulfur levels exceeding this require hydrodesulfurisation prior to refining and use. Both the sulfur and nitrogen content of the bio-crudes derived from biomass harvested in Helsingborg exhibited the highest level of variability, with a factor of two difference between the highest and lowest N values (3 *c.f.* 6 %). These

exceed the nitrogen contents typically observed in fossil crudes (0.5–2.1 %) [60], although values under 1 % are more typical [61]). Nitrogen in crude oils is highly unfavourable in terms of fuel properties, as they can denature petroleum cracking catalysts, inhibit hydrodesulfurisation, and contribute to NO<sub>x</sub> emissions on combustion [60], and hydrotreatment would be necessary before bio-crudes could be co-processed with crude oils or used as fuel. In terms of nitrogen and sulfur content, bio-crudes derived from biomass harvested in Stockholm would be optimal for co-refining and fuel use, closely followed by Karlskrona and Västervik.

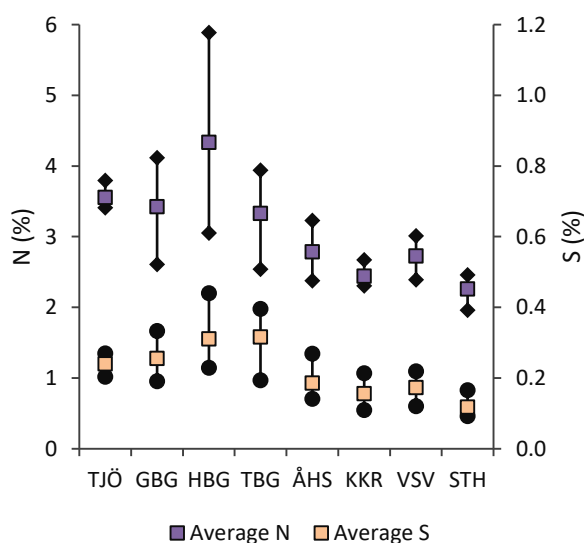


**Figure 3.2-5** – Bio-crude nitrogen and sulfur levels. The markers represent average values for each sampling location; the bars represent the highest and lowest values for bio-crude N and S obtained for each location.

Contrastingly, the bio-crudes with the lowest nitrogen and sulfur content exhibited the lowest energy density. Bio-crudes energy contents fell within the range 24.4–33.2 MJ kg<sup>-1</sup>, corresponding to approximately 55–75 % of the energy density of a typical crude oil (ca. 42–44 MJ kg<sup>-1</sup>). Most of the bio-crudes analysed had energy contents exceeding 30 MJ kg<sup>-1</sup>, although three of the Baltic bio-crudes, two derived from biomass originating in Stockholm, and one from Karlskrona, had markedly depleted HHV values, more similar to those obtained for pyrolysis bio-oils [62]. Between 29.1 % and 55.5 % of the total energy content of the biomasses was recovered in the bio-crude oil fraction.

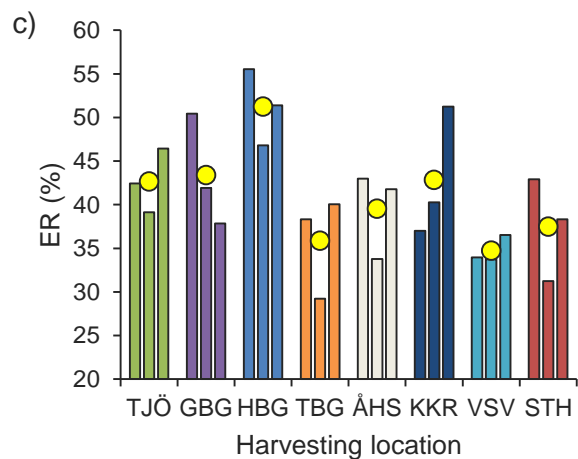
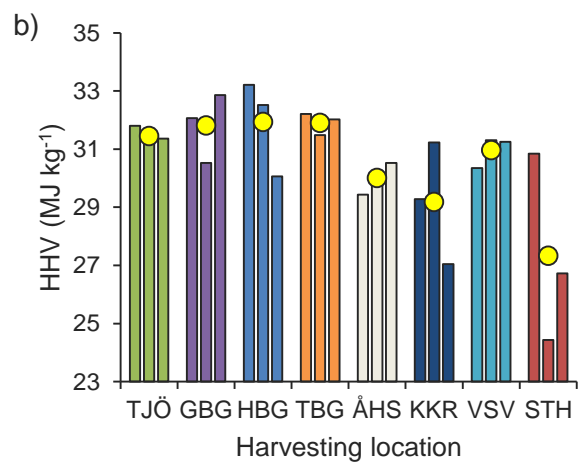
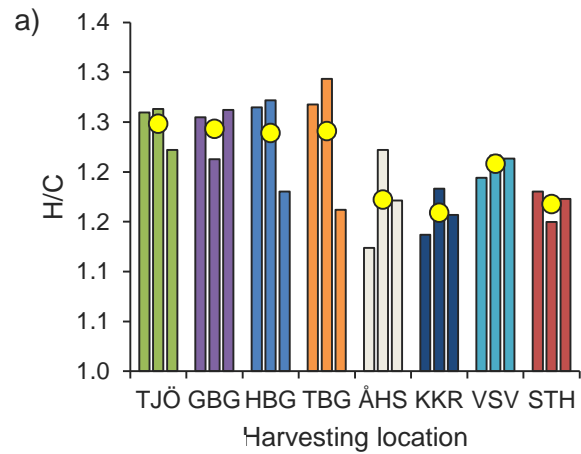


**Figure 3.2-6** – Characteristics of the bio-crude produced through HTL processing of *U. intestinalis* from three sampling sites across eight locations around the coast of Sweden; a) bio-crude H/C ratios, b) higher heating values (HHV), and c) the energy recovery (ER) in the bio-crude products. Bars represent the values obtained for individual bio-crudes; yellow markers denote averages for each location.

Analysis of the bio-crude compositions by GC/MS revealed broad similarities between the samples across all locations. Phenols made up a substantial proportion of compounds identified, with phenol, m-cresol, p-cresol, 4-aminophenol and 2,6-dimethylphenol present in all samples, alongside isomers of methyl- and dimethylcyclopenten-1-one. All samples also contained a substantial contribution from (Z)-9-octadecenamide. 5-Methylfurfural was observed in several of the samples, appearing more frequently in the bio-crudes derived from the Baltic macroalgae, whilst 1-tetradecanol was more prevalent in Atlantic bio-crudes. Notably, limonene was observed one of the Helsingborg bio-crudes, and two of the bio-crudes from macroalgae harvested in Trelleborg, suggesting some terpene production. A full summary of the bio-crude compositions and GC/MS chromatograms are provided in the Supplementary Information.

Ultimately, there are high levels of variability in both the yields and properties of the bio-crude oils. There is as much variation over a small, localised environment as over a large geographic range, and even for a single species, differences in marine environments can lead to significant fluctuations in HTL outcomes and bio-crude properties.

#### ***3.2.4.3 Elemental distribution***

Overall, carbon was recovered predominantly in the bio-crude and solid char product phases, with a maximum of 18.4 % recovered in the aqueous phase, and 17.2 % as CO<sub>2</sub> in the gas phase (Fig. 3.2-7). The most substantial variation was seen for Trelleborg, with between 19 and 41 % of carbon recovered in the bio-crude, and 27–65 % in the solid char for the three samples. As the total carbon content of the bio-crudes was generally relatively consistent, this variation was attributable predominantly to the variation in the bio-crude yields obtained.

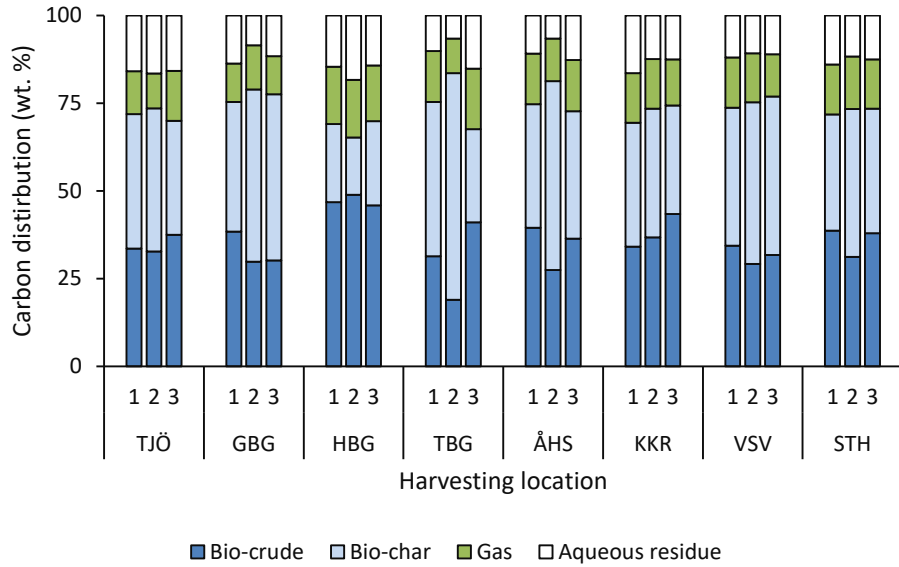


**Figure 3.2-7** – Carbon distribution (weight %) between the product phases of HTL of *U. intestinalis* from three sampling sites across eight locations around the coast of Sweden

The distribution of biomass metals between different product phases was assessed using ICP-OES. In all cases, the metals partitioned predominantly between the solid and aqueous phases (Fig. 3.2-8), with bio-crude metals constituting only a small fraction of overall recovery.

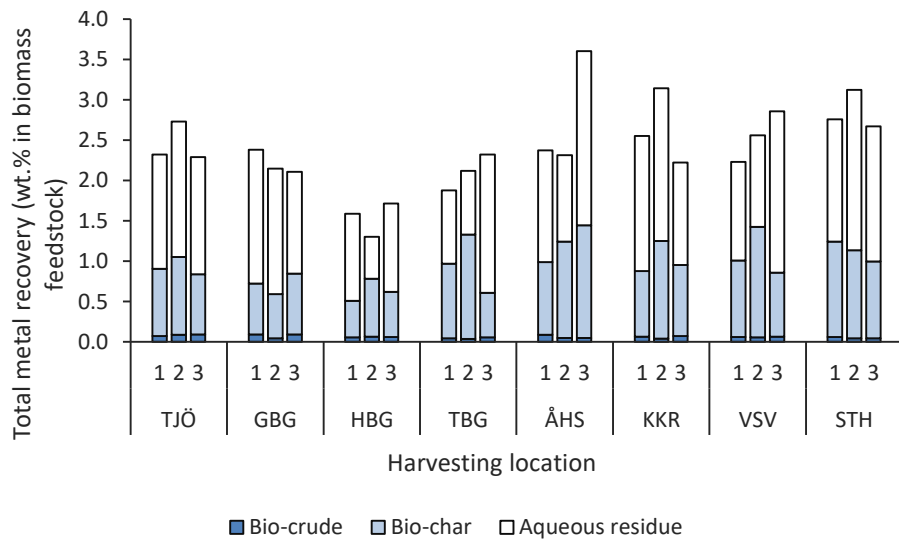


**Figure 3.2-8** – Partitioning of biomass metals between HTL product phases, presented as a proportion of the total metal content of the macroalgae feedstock

Although the proportion of total metals recovered in the bio-crude was small, bio-crude metal levels nonetheless significantly exceeded those found in fossil crudes. The balance of metal distributions between the bio-crude and aqueous phase products is affected by HTL reaction parameters, with more severe reaction conditions (increasing temperatures and holding times) driving the partitioning of metals into the bio-crude [63].

Bio-crude metal levels were highly variable, both within and between sampling sites, whilst the most abundant elements, alongside S and N, measured in the bio-crude were Al, Ca, Fe, K, Mg and Si. Although common crude oil metal contaminants, such as cadmium and vanadium, are present at lower levels than those observed in fossil crude, Ca levels are comparable to super-heavy crudes [64], which could impact upgrading procedures, and limit the blend levels that can be used in co-refining. High iron levels of up to 415 ppm were observed, which have been shown to cause rapid plugging of catalyst beds and catalyst degradation by highly stable iron porphyrin structures during hydrotreatment of microalgal bio-crudes [65]. Magnesium content was highly variable, falling between 30 ppm and 733 ppm for the three Göteborg bio-crudes. Metal levels are comparable to those observed for microalgal bio-crude [63], although Si and Al levels are notably higher. A summary of all the metals detected in the bio-crude can be found in Table S3.3-1 in the Supplementary Information.

The aqueous product is also rich in dissolved minerals and micronutrients, such as Na, K, Ca and Mg, as well as nitrogen and phosphorus, which are essential for plant/algae growth. A number of studies have addressed the possibility of nutrient recovery through the utilisation of diluted HTL aqueous phases as a growth media for microalgal cultures [66–71]. HTL aqueous phase growth media has given rise to biomass productivity comparable to, or even exceeding [66,68,70] that observed in standard growth media, although growth has been found to be limited by toxic organic compounds such as phenol [71].



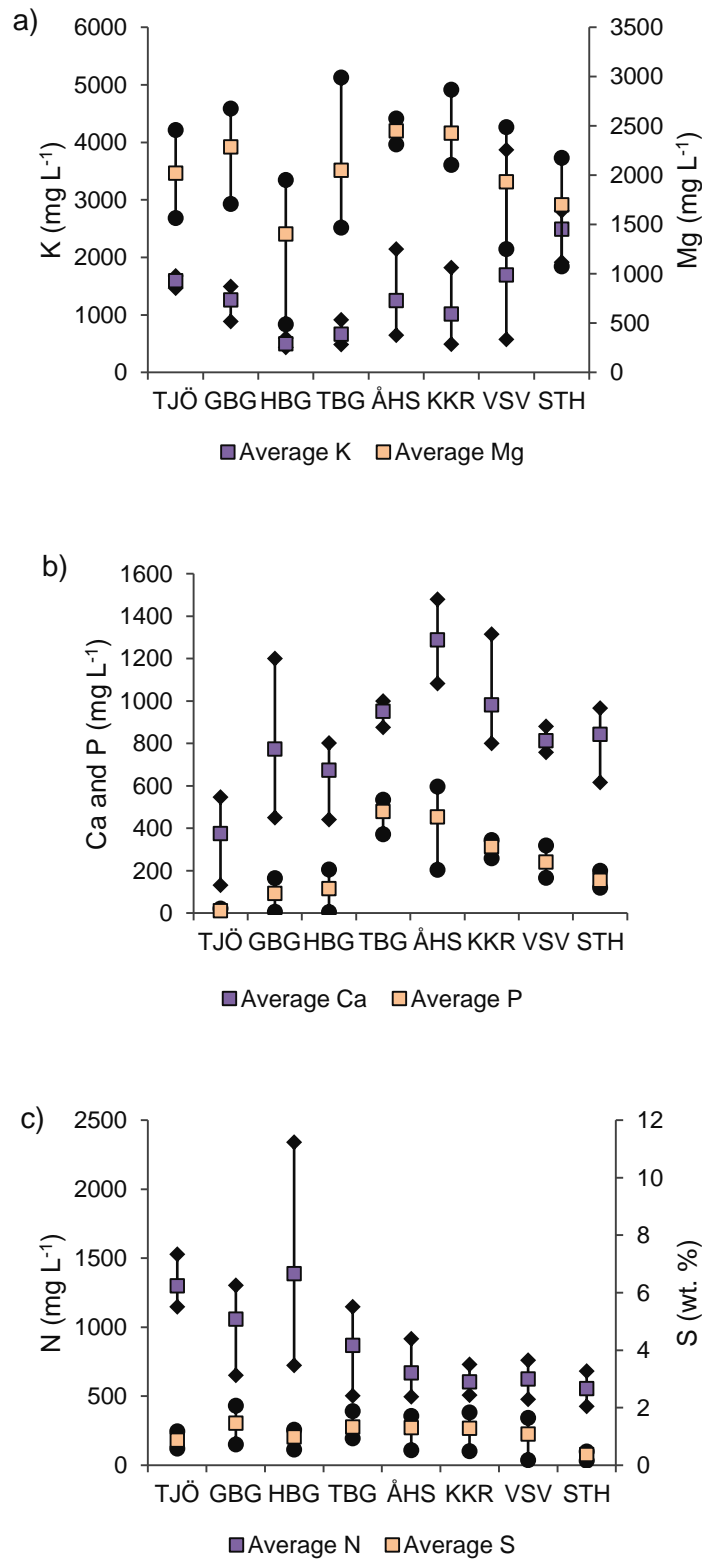


**Figure 3.2-9** – Partitioning of key elements suitable for plant growth in the aqueous phase: a) K and Mg; b) Ca and P; c) N and S

Essential elements for plant growth are presented in Fig. 3.2-9. A full breakdown of the metal concentrations in the aqueous products is presented in Table S3.3-2 in the Supplementary Information. Dissolved micronutrient concentrations are high, and aqueous phases would require dilutions of around  $\times 100$ – $300$  to obtain concentrations suitable for cultivation of microalgae, although, notably, the aqueous phase sulfur levels obtained are up to  $700\times$  higher than those used in a typical microalgal growth medium [68]. Certain species of microalgae express higher levels of triacylglycerol under conditions of sulfur starvation [72], so the high-sulfur aqueous phases may not be optimal for production of microalgae for biodiesel. A recent study found that a growth medium derived from HTL products performed better with the addition of trace metals, such as Co and Mo, resulting in higher biomass yields and an increase in maximum specific growth rates for *Chlorella sorokiniana* [68].

Substantial variation in aqueous nutrient levels was observed both within and between locations: calcium levels between 131 and 546 ppm were observed for the Tjärnö aqueous phases, while potassium levels fluctuated between 575 and 3872 ppm for the Västervik sample set. Crucially, the concentrations of nutrients beneficial to plant growth (K, Mg, Ca) are high, whereas levels of toxic metals, such as arsenic and lead, are limited (0–14 ppm As; a maximum of 1 ppm for Pb) across all locations, and will be further diminished at the dilutions necessary for aqueous phase utilisation as a growth medium. The variation and unpredictability of metal and nutrient recoveries within some locations could create problems in streamlining the utilisation of the aqueous phase as a growth medium within a biorefinery.

Total nitrogen content of up to  $2340 \text{ mg L}^{-1}$  were seen in the aqueous phase. Nitrogen in HTL aqueous phases tends to be in the form of ammonium, rather than nitrate. This may be beneficial in terms of utilisation for microalgae cultivation, as ammonium may be more efficient source of nitrogen for aquatic plants than nitrate, especially under light-limited conditions [73]. Aqueous phase nitrogen content was variable ( $427$ – $2340 \text{ mg L}^{-1}$ ), and somewhat elevated for aqueous phases derived from Atlantic macroalgae with respect to Baltic samples, although the highest N content observed was for a feedstock from Helsingborg.

Phosphorus is an important and increasingly expensive worldwide resource, and could constitute a significant source of value within an HTL biorefinery. Although the aqueous phase products contain up to 596 ppm phosphorus that could be utilised for microalgal or higher plant cultivation, at the conditions examined, biomass phosphorus is recovered

predominantly in the solid phase products. Precipitation of metal phosphates (e.g.  $\text{CaPO}_3$ ) is a key route of metal partitioning to the solid products [74]. Phosphate recovery from solid phase products may be possible, as previously demonstrated for pyrolysis char [75], and utilised for fertiliser production. Aqueous phase phosphorus content was highly variable, with higher levels, on average, for Baltic macroalgae. Notably, the aqueous phase phosphorus content of the Tjärnö biomasses was substantially lower than the remaining samples (a maximum of 22 ppm observed across the three samples), whilst the biomasses in Trelleborg and Åhus yielded aqueous phases with the highest dissolved phosphorus (204–596 ppm). Trelleborg and Åhus are situated in one of the main agricultural areas of Sweden, and it is expected that leaching of nutrients from fertiliser use may reach coastal areas and be available for seaweeds, translating to higher nutrient levels in aqueous phase HTL products.

A substantial proportion of biomass phosphorus is also recovered in the solid char products (Fig. 3.2-10), with phosphorus contents of up to 8504 ppm (Trelleborg). Phosphorus recovery is feasible for HTL char (having previously been demonstrated for pyrolysis char [75]), and could constitute a highly lucrative process within an HTL biorefinery. Although biomass phosphorus levels are approximately similar for Tjärnö and Stockholm, the distribution of phosphorus between the aqueous and solid phases differs: phosphorus is recovered predominantly in the solid phase for Tjärnö, and the aqueous products for Stockholm. This may be linked to the fluctuating levels of other dissolved inorganic species, which can form phosphate salts with varying water solubility.

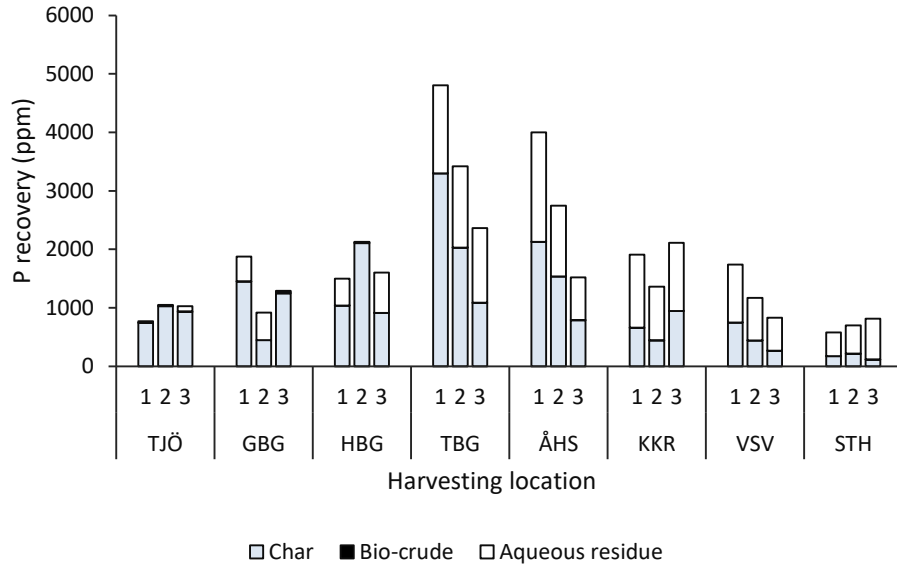


**Figure 3.2-10** – Partitioning of P between the product phases for the HTL of *U. intestinalis* from three sampling sites across eight locations around the coast of Sweden

### 3.2.5 Conclusions

Recent studies have demonstrated a large variation in the yields and composition of products formed from the HTL of different species of macroalgae. In this study, the effect of geographic location on a single species of macroalgae harvested across a large area was examined. Whilst *U. intestinalis* has previously been demonstrated as one of the most suitable macroalgae species for bio-crude production in the United Kingdom, this does not necessarily translate worldwide, with reduced bio-crude production observed for the same species sampled across Sweden. All samples of the Swedish *U. intestinalis* produced broadly similar yields of bio-crude oil, however, environmental variations led to large fluctuations in the elemental composition and metal content, with knock-on effects for the uniformity of HTL mass distributions, even within a highly localised area. A significant difference in the composition of the aqueous and solids phases was also observed. Geographic variability plays a huge role in the yields and composition of the HTL products and it is probable that there will not be one suitable species for a macroalgal biorefinery; rather, feedstock suitability will need to be assessed and optimised individually for each growing location.

### **3.2.6 Acknowledgements**

The project has been partially supported by the Engineering and Physical Sciences Research Council (EPSRC) through the Centre for Doctoral Training in Sustainable Chemical Technologies (EP/L016354/1). The Swedish collaborators acknowledge funding from the cooperation program “Preem and Chalmers Towards a Sustainable Refinery” between Preem and Area of Advance Energy at Chalmers.

### **3.2.7 Dedication**

The authors thank their dear friend and colleague Viktor Andersson, previously at Chalmers University of Technology, for discussions within their joint project. May he rest in peace. This paper is dedicated to Viktor Andersson, and the authors believe he would have been proud of the outcome of the project.

### 3.2.8 References

- [1] IPCC, Climate Change 2007 Synthesis Report Contribution of Working Groups I, II and III to the Fourth Assessment Report of the Intergovernmental Panel on Climate Change, IPCC, Geneva, Switzerland, 2007.
- [2] L.M. Fulton, L.R. Lynd, A. Körner, N. Greene, L.R. Tonachel, The need for biofuels as part of a low carbon energy future, *Biofuels, Bioprod. Biorefining.* 9 (2015) 476–483. doi:10.1002/bbb.1559.
- [3] NREL, Can “drop-in” biofuels solve integration issues?, *Contin. Mag.* 5 (2013) 8–13. <https://www.nrel.gov/docs/fy13osti/58775.pdf> (accessed April 13, 2018).
- [4] K.G. Cassman, A.J. Liska, Food and fuel for all: Realistic or foolish?, *Biofuels, Bioprod. Biorefining.* 1 (2007) 18–23.
- [5] K.A. Jung, S.-R. Lim, Y. Kim, J.M. Park, Potentials of macroalgae as feedstocks for biorefinery., *Bioresour. Technol.* 135 (2013) 182–90. doi:10.1016/j.biortech.2012.10.025.
- [6] FAO, FAO Yearbook: Fishery and Aquaculture Statistics. 2015, FAO Annu. Yearb. (2017) 1–230. doi:10.5860/CHOICE.50-5350.
- [7] FAO, The State of World Fisheries and Aquaculture 2016. Contributing to food security and nutrition for all., Rome, 2016. <http://www.fao.org/3/a-i5555e.pdf>.
- [8] H. Chen, D. Zhou, G. Luo, S. Zhang, J. Chen, Macroalgae for biofuels production: Progress and perspectives, *Renew. Sustain. Energy Rev.* 47 (2015) 427–437. doi:10.1016/j.rser.2015.03.086.
- [9] M. Aresta, A. Dibenedetto, M. Carone, T. Colonna, C. Fragale, Production of biodiesel from macroalgae by supercritical CO<sub>2</sub> extraction and thermochemical liquefaction, *Environ. Chem. Lett.* 3 (2005) 136–139. doi:10.1007/s10311-005-0020-3.
- [10] T. Suganya, S. Renganathan, Optimization and kinetic studies on algal oil extraction from marine macroalgae *Ulva lactuca*, *Bioresour. Technol.* 107 (2012) 319–326.
- [11] T. Suganya, N. Nagendra Gandhi, S. Renganathan, Production of algal biodiesel from marine macroalgae *Enteromorpha compressa* by two step process:

- Optimization and kinetic study., *Bioresour. Technol.* 128 (2013) 392–400.
- [12] M.H. Huesemann, L.J. Kuo, L. Urquhart, G.A. Gill, G. Roesijadi, Acetone-butanol fermentation of marine macroalgae, *Bioresour. Technol.* 108 (2012) 305–309.
- [13] A.J. Wargacki, E. Leonard, M.N. Win, D.D. Regitsky, C.N.S. Santos, P.B. Kim, S.R. Cooper, R.M. Raisner, A. Herman, A.B. Sivitz, An engineered microbial platform for direct biofuel production from brown macroalgae, *Science* (80-. ). 335 (2012) 308–313.
- [14] H. Van der Wal, B.L.H.M. Sperber, B. Houweling-Tan, R.R.C. Bakker, W. Brandenburg, A.M. López-Contreras, Production of acetone, butanol, and ethanol from biomass of the green seaweed *Ulva lactuca*, *Bioresour. Technol.* 128 (2013) 431–437.
- [15] A. Sutherland, J. Varela, Comparison of various microbial inocula for the efficient anaerobic digestion of *Laminaria hyperborea*, *BMC Biotechnol.* (2014) 14.
- [16] L. Song, M. Hu, D. Liu, D. Zhang, C. Jiang, Thermal cracking of *Enteromorpha prolifera* with solvents to bio-oil, *Energy Convers. Manag.* 77 (2014) 7–12.
- [17] D.C. Elliott, T.R. Hart, G.G. Neuenschwander, L.J. Rotness, G. Roesijadi, A.H. Zacher, J.K. Magnuson, Hydrothermal Processing of Macroalgal Feedstocks in Continuous-Flow Reactors, *ACS Sustain. Chem. Eng.* 2 (2014) 201–215. doi:10.1021/sc400251p.
- [18] R. Singh, B. Balagurumurthy, T. Bhaskar, Hydrothermal liquefaction of macro algae: Effect of feedstock composition, *Fuel.* 146 (2015) 69–74. doi:10.1016/j.fuel.2015.01.018.
- [19] J. Hoffmann, C. Uhrenholt Jensen, L.A. Rosendahl, Co-processing potential of HTL bio-crude at petroleum refineries – Part 1: Fractional distillation and characterization, *Fuel.* 165 (2016) 526–535. doi:10.1016/j.fuel.2015.10.094.
- [20] I.J. Tews, Y. Zhu, C.V. Drennan, D.C. Elliott, L.J. Snowden-Swan, K. Onarheim, Y. Solantausta, D. Beckman, Biomass direct liquefaction options: techno-economic and life cycle assessment, *Pacific Northwest Natl. Lab.* (2014). doi:10.2172/1184983.
- [21] D. López Barreiro, W. Prins, F. Ronsse, W. Brillman, Hydrothermal liquefaction

- (HTL) of microalgae for biofuel production: State of the art review and future prospects, *Biomass and Bioenergy*. 53 (2013) 113–127. doi:10.1016/j.biombioe.2012.12.029.
- [22] C. Uhrenholt Jensen, J. Hoffmann, L.A. Rosendahl, C. Uhrenholt Jensen, J. Hoffmann, L.A. Rosendahl, Co-processing potential of HTL bio-crude at petroleum refineries. Part 2: A parametric hydrotreating study, *Fuel*. 165 (2016) 536–543. doi:10.1016/j.fuel.2015.08.047.
- [23] J. Akhtar, N.A.S. Amin, A review on process conditions for optimum bio-oil yield in hydrothermal liquefaction of biomass, *Renew. Sustain. Energy Rev.* 15 (2011) 1615–1624. doi:10.1016/j.rser.2010.11.054.
- [24] D.C. Elliott, L.J. Sealock Jr., S.R. Butner, Product Analysis from Direct Liquefaction of Several High-Moisture Biomass Feedstocks, in: E.J. Soltes, T.A. Milne (Eds.), *Pyrolysis Oils From Biomass Prod. Anal. Upgrad. - ACS Symp. Ser.*, American Chemical Society, Washington, D. C., 1988: pp. 179–188. doi:doi:10.1021/bk-1988-0376.ch017.
- [25] K. Anastasakis, A.B. Ross, Hydrothermal liquefaction of the brown macro-alga *Laminaria saccharina*: effect of reaction conditions on product distribution and composition., *Bioresour. Technol.* 102 (2011) 4876–83. doi:10.1016/j.biortech.2011.01.031.
- [26] D. Zhou, L. Zhang, S. Zhang, H. Fu, J. Chen, Hydrothermal Liquefaction of Macroalgae *Enteromorpha prolifera* to Bio-oil, *Energy & Fuels*. 24 (2010) 4054–4061. doi:10.1021/ef100151h.
- [27] D. Li, L. Chen, D. Xu, X. Zhang, N. Ye, F. Chen, S. Chen, Preparation and characteristics of bio-oil from the marine brown alga *Sargassum patens* C. Agardh, *Bioresour. Technol.* 104 (2012) 737–742. doi:10.1016/j.biortech.2011.11.011.
- [28] S. Raikova, C.D. Le, T.A. Beacham, R.W. Jenkins, M.J. Allen, C.J. Chuck, Towards a marine biorefinery through the hydrothermal liquefaction of macroalgae native to the United Kingdom, *Biomass and Bioenergy*. 107 (2017) 244–253. doi:10.1016/j.biombioe.2017.10.010.
- [29] M.M. Nielsen, D. Manns, M. D'este, D. Krause-Jensen, M.B. Rasmussen, M.M.



- Larsen, M. Alvarado-Morales, I. Angelidaki, A. Bruhn, Variation in biochemical composition of *Saccharina latissima* and *Laminaria digitata* along an estuarine salinity gradient in inner Danish waters, *Algal Res.* 13 (2016) 235–245. doi:10.1016/j.algal.2015.12.003.
- [30] J.C. Sanderson, M.J. Dring, K. Davidson, M.S. Kelly, Culture, yield and bioremediation potential of *Palmaria palmata* (Linnaeus) Weber, Mohr and *Saccharina latissima* (Linnaeus) C.E. Lane, C. Mayes, Druehl, G.W. Saunders adjacent to fish farm cages in northwest Scotland, *Aquaculture.* 354–355 (2012) 128–135. doi:10.1016/j.aquaculture.2012.03.019.
- [31] G.S. Marinho, S.L. Holdt, M.J. Birkeland, I. Angelidaki, Commercial cultivation and bioremediation potential of sugar kelp, *Saccharina latissima*, in Danish waters, *J. Appl. Phycol.* 27 (2015) 1963–1973. doi:10.1007/s10811-014-0519-8.
- [32] A. Handå, S. Forbord, X. Wang, O.J. Broch, S.W. Dahle, T.R. Størseth, K.I. Reitan, Y. Olsen, J. Skjeremo, Seasonal- and depth-dependent growth of cultivated kelp (*Saccharina latissima*) in close proximity to salmon (*Salmo salar*) aquaculture in Norway, *Aquaculture.* 414–415 (2013) 191–201. doi:10.1016/j.aquaculture.2013.08.006.
- [33] Ole Jacob Broch, Ingrid Helene Ellingsen, Silje Forbord, Xinxin Wang, Zsolt Volent, Morten Omholt Alver, Aleksander Handå, Kjersti Andresen<sup>3</sup>, Dag Slagstad, Kjell Inge Reitan, Yngvar Olsen, Jorunn Skjeremo, Modelling the cultivation and bioremediation potential of the kelp *Saccharina latissima* in close proximity to an exposed salmon farm in Norway, *Aquac. Environ. Interact.* 4 (2013) 187–206. doi:10.3354/aei00080.
- [34] D.J. McHugh, A guide to the seaweed industry: fisheries technical paper 441, Rome, 2003. <http://www.fao.org/3/a-y4765e.pdf> (accessed April 19, 2018).
- [35] E.A.T. Floreto, S. Teshima, The fatty acid composition of seaweeds exposed to different levels of light intensity and salinity, *Bot. Mar.* 41 (1998) 467–481. doi:https://doi.org/10.1515/botm.1998.41.1-6.467.
- [36] T. Chopin, C. Yarish, R. Wilkes, E. Belyea, S. Lu, A.-T. Mathieson, Developing *Porphyra*/salmon integrated aquaculture for bioremediation and diversification of the aquaculture industry, *J. Appl. Phycol.* 11 (1999) 463–472. <https://link.springer.com/content/pdf/10.1023%2FA%3A1008114112852.pdf>

(accessed April 19, 2018).

- [37] P.O. Souza, L.R. Ferreira, N.R.X. Pires, P.J.S. Filho, F. a. Duarte, C.M.P. Pereira, M.F. Mesko, Algae of economic importance that accumulate cadmium and lead: A review, *Brazilian J. Pharmacogn.* 22 (2012) 825–837. doi:10.1590/S0102-695X2012005000076.
- [38] J. Collen, R. Pinto, M. Pedersen, P. Colepicolo, Induction of oxidative stress in the red macroalga *Gracilaria tenuistipitata* by pollutant metals, *Arch. Environ. Contam. Toxicol.* 45 (2003) 337–342.
- [39] J.-B.E. Thomas, J. Nordström, E. Risén, M.E. Malmström, F. Gröndahl, The perception of aquaculture on the Swedish West Coast, *Ambio.* 47 (2018) 398–409. doi:10.1007/s13280-017-0945-3.
- [40] J.S. Pechsiri, J.-B.E. Thomas, E. Risén, M.S. Ribeiro, M.E. Malmström, G.M. Nylund, A. Jansson, U. Welander, H. Pavia, F. Gröndahl, Energy performance and greenhouse gas emissions of kelp cultivation for biogas and fertilizer recovery in Sweden, *Sci. Total Environ.* 573 (2016) 347–355. doi:10.1016/j.scitotenv.2016.07.220.
- [41] HELCOM, Baltic Marine Environment Protection Commission - Helsinki Commission, (2018). <http://www.helcom.fi/about-us/convention> (accessed May 3, 2018).
- [42] R. Rosenberg, R. Elmgren, S. Fleischer, P. Jonsson, G. Persson, H. Dahlin, Marine Eutrophication Case Studies in Sweden, *Ambio.* 19 (1990) 102–108. <http://www.jstor.org/stable/4313674> (accessed April 20, 2018).
- [43] P. Biller, A.B. Ross, Potential yields and properties of oil from the hydrothermal liquefaction of microalgae with different biochemical content., *Bioresour. Technol.* 102 (2011) 215–25. doi:10.1016/j.biortech.2010.06.028.
- [44] J. Wagner, R. Bransgrove, T.A. Beacham, M.J. Allen, K. Meixner, B. Drosig, V.P. Ting, C.J. Chuck, Co-production of bio-oil and propylene through the hydrothermal liquefaction of polyhydroxybutyrate producing cyanobacteria, *Bioresour. Technol.* 207 (2016) 166–174. doi:10.1016/j.biortech.2016.01.114.
- [45] S. Raikova, H. Smith-Baedorf, R. Bransgrove, O. Barlow, F. Santomauro, J.L. Wagner, M.J. Allen, C.G. Bryan, D. Sapsford, C.J. Chuck, Assessing

- hydrothermal liquefaction for the production of bio-oil and enhanced metal recovery from microalgae cultivated on acid mine drainage, *Fuel Process. Technol.* 142 (2016) 219–227. doi:10.1016/j.fuproc.2015.10.017.
- [46] Y.-P. Xu, P.-G. Duan, F. Wang, Hydrothermal processing of macroalgae for producing crude bio-oil, *Fuel Process. Technol.* 130 (2015) 268–274. doi:10.1016/j.fuproc.2014.10.028.
- [47] J.J. Mayers, S. Vaiciulyte, E. Malmhäll-Bah, J. Alcaide-Sancho, S. Ewald, A. Godhe, S. Ekendahl, E. Albers, Identifying a marine microalgae with high carbohydrate productivities under stress and potential for efficient flocculation, *Algal Res.* 31 (2018) 430–442. doi:10.1016/j.algal.2018.02.034.
- [48] P. Bikker, M.M. Van Krimpen, P. van Wikselaar, B. Houweling-Tan, N. Scaccia, J.W. Van Hal, W.J.J. Huijgen, J.W. Cone, A.M. López-Contreras, J.W. Van, H.V. Ni Wouter, J.J. Huijgen, J.C. Ni, Biorefinery of the green seaweed *Ulva lactuca* to produce animal feed, chemicals and biofuels, *J. Appl. Phycol.* 28 (2016) 1–15. doi:10.1007/s10811-016-0842-3.
- [49] J. Olsson, S. Raikova, J.J. Mayers, C. Chuck, G. Nylund, E. Albers, Environmental effects on potentially valuable components of *Ulva intestinalis* along the Swedish coast, (2018) Manuscript in preparation.
- [50] A.R. Angell, L. Mata, R. de Nys, N.A. Paul, The protein content of seaweeds: a universal nitrogen-to-protein conversion factor of five, *J. Appl. Phycol.* 28 (2016) 511–524. doi:10.1007/s10811-015-0650-1.
- [51] S.A.A. Channiwala, P.P.P. Parikh, A unified correlation for estimating HHV of solid, liquid and gaseous fuels, *Fuel.* 81 (2002) 1051–1063. doi:10.1016/S0016-2361(01)00131-4.
- [52] H.M. Khairy, S.M. El-Shafay, Seasonal variations in the biochemical composition of some common seaweed species from the coast of Abu Qir Bay, Alexandria, Egypt, *Oceanologia.* 55 (2013) 435–452. doi:10.5697/oc.55-2.435.
- [53] K. Anastasakis, A.B. Ross, Hydrothermal liquefaction of four brown macro-algae commonly found on the UK coasts: An energetic analysis of the process and comparison with bio-chemical conversion methods, *Fuel.* 139 (2015) 546–553. doi:10.1016/j.fuel.2014.09.006.

- [54] D. López Barreiro, M. Beck, U. Hornung, F. Ronsse, A. Kruse, W. Prins, Suitability of hydrothermal liquefaction as a conversion route to produce biofuels from macroalgae, *Algal Res.* 11 (2015) 234–241. doi:10.1016/j.algal.2015.06.023.
- [55] M.C. Chow, W.R. Jackson, A.L. Chaffee, M. Marshall, Thermal Treatment of Algae for Production of Biofuel, *Energy & Fuels.* 27 (2013) 1926–1950. doi:10.1021/ef3020298.
- [56] G. Teri, L. Luo, P.E. Savage, Hydrothermal Treatment of Protein, Polysaccharide, and Lipids Alone and in Mixtures, *Energy Fuels.* 28 (2014) 7501–7509. doi:10.1021/ef501760d.
- [57] P. Biller, R. Riley, A.B. Ross, Catalytic hydrothermal processing of microalgae: decomposition and upgrading of lipids, *Bioresour. Technol.* 102 (2011) 4841–8. doi:10.1016/j.biortech.2010.12.113.
- [58] L.M. Díaz-Vázquez, A. Rojas-Pérez, M. Fuentes-Caraballo, I. V Robles, U. Jena, Demineralization of *Sargassum* spp . macroalgae biomass: selective hydrothermal liquefaction process for bio-oil production, *Front. Energy Resarch.* 3 (2015) 1–11. doi:10.3389/fenrg.2015.00006.
- [59] SIME, Mapping shipping intensity and routes in the Baltic Sea, Göteborg, 2014. [http://havsmiljoinstitutet.se/digitalAssets/1506/1506887\\_sime\\_ais\\_report\\_2014\\_5.pdf](http://havsmiljoinstitutet.se/digitalAssets/1506/1506887_sime_ais_report_2014_5.pdf) (accessed May 9, 2018).
- [60] O.P. Ward, A. Singh, J.D. Van Hamme, G. Voordouw, Petroleum Microbiology, in: *Encycl. Microbiol.*, Elsevier, 2009: pp. 443–456. doi:10.1016/B978-012373944-5.00171-1.
- [61] J.S. Ball, M.L. Whisman, W.J. Wenger, Nitrogen Content of Crude Petroleums, *Ind. Eng. Chem.* (1951) 2577–2581. <https://pubs.acs.org/doi/pdf/10.1021/ie50503a047> (accessed May 8, 2018).
- [62] T.N. Trinh, P. Arendt Jensen, K. Dam-Johansen, N.O. Knudsen, H.R. Sørensen, S. Hvilsted, Comparison of Lignin, Macroalgae, Wood, and Straw Fast Pyrolysis, *Energy & Fuels.* 27 (2013) 1399–1409. doi:10.1021/ef301927y.
- [63] J. Jiang, P.E. Savage, Metals and Other Elements in Biocrude from Fast and Isothermal Hydrothermal Liquefaction of Microalgae, *Energy & Fuels.* 32 (2018) 4118–4126. doi:10.1021/acs.energyfuels.7b03144.

- [64] W. Bencheng, Z. Jianhua, L. Xiaohui, Distribution of calcium, nickel, iron, and manganese in super-heavy oil from Liaohe Oilfield, China, *Pet. Sci.* 11 (2014) 590–595. doi:10.1007/s12182-014-0376-8.
- [65] J.M. Jarvis, N.M. Sudasinghe, K.O. Albrecht, A.J. Schmidt, R.T. Hallen, D.B. Anderson, J.M. Billing, T.M. Schaub, Impact of iron porphyrin complexes when hydroprocessing algal HTL biocrude, *Fuel*. 182 (2016) 411–418. doi:10.1016/j.fuel.2016.05.107.
- [66] P. Biller, A.B. Ross, S.C. Skill, A. Lea-Langton, B. Balasundaram, C. Hall, R. Riley, C. a. Llewellyn, Nutrient recycling of aqueous phase for microalgae cultivation from the hydrothermal liquefaction process, *Algal Res.* 1 (2012) 70–76. doi:10.1016/j.algal.2012.02.002.
- [67] U. Jena, N. Vaidyanathan, S. Chinnasamy, K.C. Das, Evaluation of microalgae cultivation using recovered aqueous co-product from thermochemical liquefaction of algal biomass, *Bioresour. Technol.* 102 (2011) 3380–3387. doi:10.1016/j.biortech.2010.09.111.
- [68] S. Edmundson, M. Huesemann, R. Kruk, T. Lemmon, J. Billing, A. Schmidt, D. Anderson, Phosphorus and nitrogen recycle following algal bio-crude production via continuous hydrothermal liquefaction, *Algal Res.* 26 (2017) 415–421. doi:10.1016/j.algal.2017.07.016.
- [69] L. Garcia Alba, C. Torri, D. Fabbri, S.R. a Kersten, D.W.F. Wim Brillman, Microalgae growth on the aqueous phase from Hydrothermal Liquefaction of the same microalgae, *Chem. Eng. J.* 228 (2013) 214–223. doi:10.1016/j.cej.2013.04.097.
- [70] T. Selvaratnam, H. Reddy, T. Muppaneni, F.O. Holguin, N. Nirmalakhandan, P.J. Lammers, S. Deng, Optimizing energy yields from nutrient recycling using sequential hydrothermal liquefaction with *Galdieria sulphuraria*, *Algal Res.* 12 (2015) 74–79. doi:10.1016/j.algal.2015.07.007.
- [71] D. López Barreiro, M. Bauer, U. Hornung, C. Posten, A. Kruse, W. Prins, Cultivation of microalgae with recovered nutrients after hydrothermal liquefaction, *Algal Res.* 9 (2015) 99–106. doi:10.1016/j.algal.2015.03.007.
- [72] T. Cakmak, P. Angun, Y.E. Demiray, A.D. Ozkan, Z. Elibol, T. Tekinay, Differential

Effects of Nitrogen and Sulfur Deprivation on Growth and Biodiesel Feedstock Production of *Chlamydomonas reinhardtii*, *Biotechnol. Bioeng.* 109 (2012) 1947–1957.

<https://pdfs.semanticscholar.org/0bd0/3277a7edd1e6452c4fadab6287c1832c5d0d.pdf> (accessed May 29, 2018).

- [73] P.J. Harrison, C.L. Hurd, Nutrient physiology of seaweeds: Application of concepts to aquaculture, *Cah. Biol. Mar.* 42 (2001) 71–82.
- [74] D.C. Elliott, T.R. Hart, A.J. Schmidt, G.G. Neuenschwander, L.J. Rotness, M. V. Olarte, A.H. Zacher, K.O. Albrecht, R.T. Hallen, J.E. Holladay, Process development for hydrothermal liquefaction of algae feedstocks in a continuous-flow reactor, *Algal Res.* 2 (2013) 445–454. doi:10.1016/j.algal.2013.08.005.
- [75] M. Atienza-Martínez, G. Gea, J. Arauzo, S.R.A. Kersten, A.M.J. Kootstra, Phosphorus recovery from sewage sludge char ash, *Biomass and Bioenergy.* 65 (2014) 42–50. doi:10.1016/j.biombioe.2014.03.058.

### 3.3 Supporting information

Table S3.3-1 – Elemental composition of bio-crudes from HTL of *U. intestinalis*

	Ag	Al	As	Au	B	Ba	Bi	Ca	Cr	Cu	Fe	Hg	K	La	Mg	Mn	Mo	Ni	P	Pb	Pd	S	Sb	Se	Si	Sn	Sr	Ti	Tl	V	W	Zn	Zr	
		(ppm)																																
<b>TJÖ</b>	1	67	189	10	3	1366	24	3	479	10	3	7	0	4572	3	293	10	0	0	40	0	3	2697	0	0	7037	0	13	0	0	0	0	7	0
	2	686	177	8	4	1355	21	8	677	8	12	4	4	4430	4	599	12	0	0	53	0	4	2463	0	0	6926	0	16	0	0	0	0	37	0
	3	322	208	16	0	1270	20	4	664	8	4	12	0	4523	12	330	12	0	0	85	0	4	2035	0	0	6574	0	16	0	0	0	0	8	0
<b>GBG</b>	1	144	236	48	4	1474	20	8	356	12	12	100	12	4233	4	60	4	8	8	32	12	4	2403	0	32	6700	12	8	4	8	4	0	16	4
	2	31	191	38	8	1086	15	19	294	8	4	31	8	2673	0	31	4	0	4	0	4	0	1912	27	8	4612	11	4	0	4	0	4	8	0
	3	138	225	17	0	1146	25	0	821	13	13	146	4	4702	25	734	21	4	4	163	0	0	3335	0	0	5194	0	29	0	0	4	0	21	4
<b>HBG</b>	1	154	206	45	7	1067	15	7	303	15	4	116	7	2722	0	67	4	4	26	15	4	4	2621	4	26	4415	4	4	0	4	4	4	15	0
	2	253	205	48	0	1057	15	15	793	11	7	415	4	3182	0	239	11	0	4	77	11	4	4404	15	0	4528	7	11	4	0	4	4	18	4
	3	84	324	61	0	1564	15	0	431	11	4	160	11	2842	0	38	4	4	15	8	8	0	2289	0	15	4998	11	4	4	8	0	8	23	4
<b>TBG</b>	1	94	175	22	4	1094	13	18	309	9	13	18	4	2972	0	49	0	0	4	18	0	0	3587	13	4	5187	13	9	0	9	0	13	9	0
	2	141	220	48	4	1080	13	0	343	18	4	92	4	2820	0	105	4	4	13	22	13	4	3953	18	0	5077	4	4	0	4	0	13	9	0
	3	111	237	34	10	1334	15	15	411	10	5	29	15	3090	0	135	5	5	5	19	15	0	1934	5	58	5178	10	5	0	24	0	10	19	0
<b>ÅHS</b>	1	231	179	57	5	1432	19	28	358	9	5	5	14	4231	0	80	5	0	9	5	19	0	1414	33	28	6484	5	9	0	14	0	14	9	0
	2	135	242	46	0	1238	15	0	365	15	27	154	8	2679	0	108	19	4	15	12	12	4	2691	0	15	4682	15	4	4	12	0	4	19	4
	3	155	97	39	10	276	5	0	436	10	19	121	10	2206	0	92	10	5	53	39	19	5	1454	29	10	228	19	5	0	19	0	24	24	5
<b>KKR</b>	1	164	249	32	0	1280	18	14	420	21	4	71	4	3350	0	345	21	0	4	28	0	0	2134	0	0	4848	0	7	0	4	4	0	14	0
	2	53	82	53	5	327	5	0	322	10	10	72	5	1975	0	91	5	5	24	34	14	5	1442	0	0	384	10	5	0	19	0	0	19	0
	3	157	172	33	7	1040	15	0	245	7	4	18	7	2866	0	80	4	0	0	7	0	4	1095	22	22	4582	18	4	0	4	0	11	7	0

	1	278	296	62	0	1499	15	15	453	11	4	51	0	2968	0	252	4	0	4	11	15	0	2193	29	37	4818	22	7	4	15	0	15	11	4
<b>VSV</b>	2	152	213	32	4	1457	20	4	341	12	8	4	4	4205	0	68	4	0	4	8	0	0	1204	0	0	6404	0	8	0	0	0	0	20	0
	3	57	217	36	0	1277	18	4	309	14	4	28	11	3828	0	39	4	0	18	18	0	4	1779	11	0	5884	11	7	0	0	0	4	11	0
	1	29	257	46	17	1418	17	4	390	8	4	29	12	3097	0	50	4	4	4	12	12	0	1658	0	29	5211	21	4	0	21	0	0	12	4
<b>STH</b>	2	226	71	52	9	287	5	0	377	33	9	104	5	1998	0	52	5	0	33	42	5	0	942	9	33	339	9	5	0	24	0	5	113	0
	3	79	79	42	5	328	5	9	277	14	14	79	9	1831	0	51	5	0	28	28	0	5	925	14	37	338	9	0	0	5	0	9	23	0



**Table S3.3-2** – Elemental composition of aqueous phase products from HTL of *U. intestinalis*

	Al	As	Au	B	Ba	Ca	Cu	Fe	K	La	Mg	Mn	P	Pb	Rb	S	Si	Sr	Tl	W	Zn	
	(ppm)																					
	1	505	133	0	332	0	1742	0	13	19476	0	27133	13	80	0	106	111671	891	66	27	13	0
TJÖ	2	554	132	0	445	12	6573	36	24	19769	12	29605	12	48	0	72	142064	1132	96	36	24	36
	3	505	109	0	491	14	6073	55	41	22915	14	21359	27	300	14	96	79157	1488	82	27	14	41
	1	362	125	0	387	12	8336	50	650	11060	12	30956	37	1312	12	87	197456	1362	87	37	12	37
GBG	2	350	152	0	385	12	14003	47	618	16230	23	31201	105	1912	0	82	241351	2495	140	47	12	35
	3	476	168	0	448	0	6300	56	28	20888	14	23940	14	84	0	112	100800	1288	112	14	28	42
	1	846	239	0	976	22	17400	108	651	10110	22	38422	130	2907	0	152	249495	4100	152	22	43	87
HBG	2	1113	257	0	913	0	12588	114	29	16955	29	13901	29	114	29	200	154133	3711	114	0	57	86
	3	491	196	0	471	20	15294	59	550	8540	20	38343	216	4025	0	137	241486	3809	118	20	20	39
	1	555	164	0	637	21	18010	82	82	12130	21	34664	206	10979	21	144	238492	2796	144	41	21	41
TBG	2	475	289	0	434	21	20239	83	248	10026	41	30327	372	10998	0	124	192256	3225	145	83	41	62
	3	436	169	0	576	14	14055	56	42	12861	28	42067	169	5214	0	84	264238	2586	112	28	28	28
	1	608	214	0	920	16	17792	66	246	10580	33	42304	181	9791	16	82	280929	2744	131	16	33	33
ÅHS	2	610	208	0	1086	15	19347	59	342	14217	30	36538	1680	8313	0	104	249832	2602	134	45	15	30
	3	355	16	0	2116	16	23894	16	323	34605	16	37368	501	3296	0	32	84009	2456	323	0	0	16
	1	539	146	0	787	15	11679	58	29	10673	15	41804	219	4885	0	102	268292	2362	102	87	29	44

KKR	2	373	68	17	2474	17	22285	17	51	30877	17	35673	576	4372	0	17	83040	4474	339	0	0	17
	3	647	144	0	989	18	14910	54	90	8849	18	41420	809	6187	18	126	273375	2896	126	108	36	36
VSV	1	401	167	0	602	17	13348	50	33	9618	17	41633	134	5336	0	117	275990	2141	117	17	33	33
	2	593	241	0	908	19	16302	74	37	11616	19	38051	185	4335	0	130	259358	2983	148	37	37	93
STH	3	109	0	0	750	0	11845	0	16	60507	0	19549	156	2610	0	78	28128	766	172	0	0	0
	1	92	0	0	831	18	11373	0	37	50477	0	19884	535	2197	0	92	27694	868	129	0	0	18
STH	2	163	0	20	1383	20	19654	0	163	57191	20	44272	203	2950	0	61	97658	4842	285	0	20	0
	3	122	0	17	1337	17	16424	0	295	33265	17	31980	833	3472	0	69	81599	5886	243	0	0	0

**Table S3.3-3** – Identities of notable compounds in bio-crude products from the liquefaction of *U. intestinalis* from multiple locations

Compound	TJÖ			GBG			HBG			TBG			ÅHS			KKR			VSV			STH		
	1	2	3	1	2	3	1	2	3	1	2	3	1	2	3	1	2	3	1	2	3	1	2	3
2-Cyclopenten-1-one, 2-methyl-	■	■	■	■	■	■	■	■	■	■	■	■	■	■	■	■	■	■	■	■	■	■	■	■
Ethanone, 1-(2-furanyl)-	■	■	■	■	■	■	■	■	■	■	■	■	■	■	■	■	■	■	■	■	■	■	■	■
5-Methylfurfural	■	■	■	■	■	■	■	■	■	■	■	■	■	■	■	■	■	■	■	■	■	■	■	■
2-Cyclopenten-1-one, 3-methyl-	■	■	■	■	■	■	■	■	■	■	■	■	■	■	■	■	■	■	■	■	■	■	■	■
Phenol	■	■	■	■	■	■	■	■	■	■	■	■	■	■	■	■	■	■	■	■	■	■	■	■
<i>D</i> -Limonene	■	■	■	■	■	■	■	■	■	■	■	■	■	■	■	■	■	■	■	■	■	■	■	■
2-Acetyl-5-methylfuran	■	■	■	■	■	■	■	■	■	■	■	■	■	■	■	■	■	■	■	■	■	■	■	■
2-Cyclopenten-1-one, 2,3-dimethyl-	■	■	■	■	■	■	■	■	■	■	■	■	■	■	■	■	■	■	■	■	■	■	■	■
<i>m</i> -Cresol	■	■	■	■	■	■	■	■	■	■	■	■	■	■	■	■	■	■	■	■	■	■	■	■
Phenol, 2-methoxy-	■	■	■	■	■	■	■	■	■	■	■	■	■	■	■	■	■	■	■	■	■	■	■	■
<i>p</i> -Cresol	■	■	■	■	■	■	■	■	■	■	■	■	■	■	■	■	■	■	■	■	■	■	■	■

---

4-Pyridinol

2-Propenal, 3-phenyl-

Benzofuran, 2-methyl-

Cycloheptene, 1,2-dimethyl-

Phenol, 4-amino-

Phenol, 4-ethyl-

Phenol, 2,6-dimethyl-

1-Tetradecanol

Pentadecane

8-Heptadecene

Hexadecanoic acid, ethyl ester

9-Octadecenamide, (Z)-

---

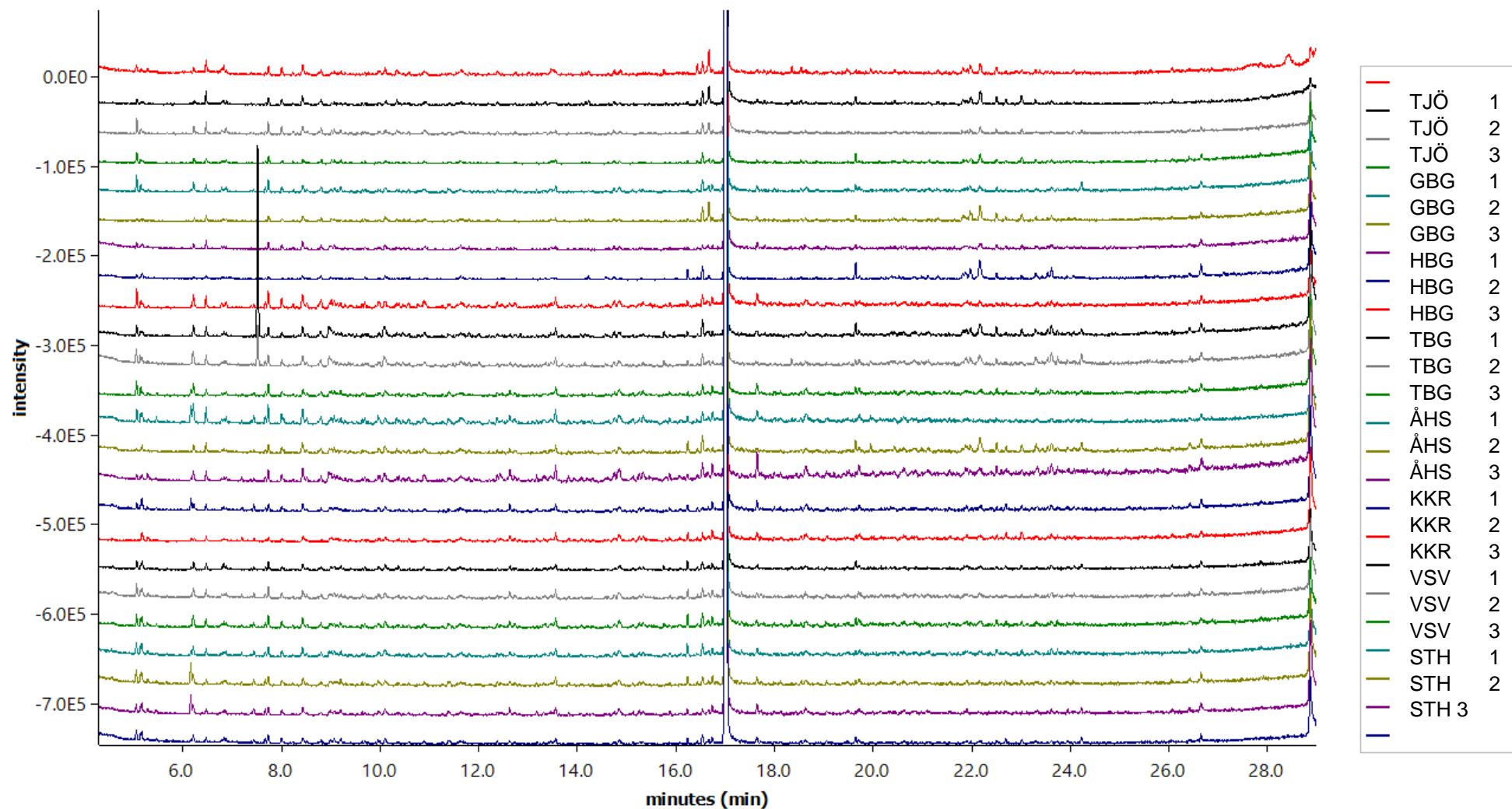
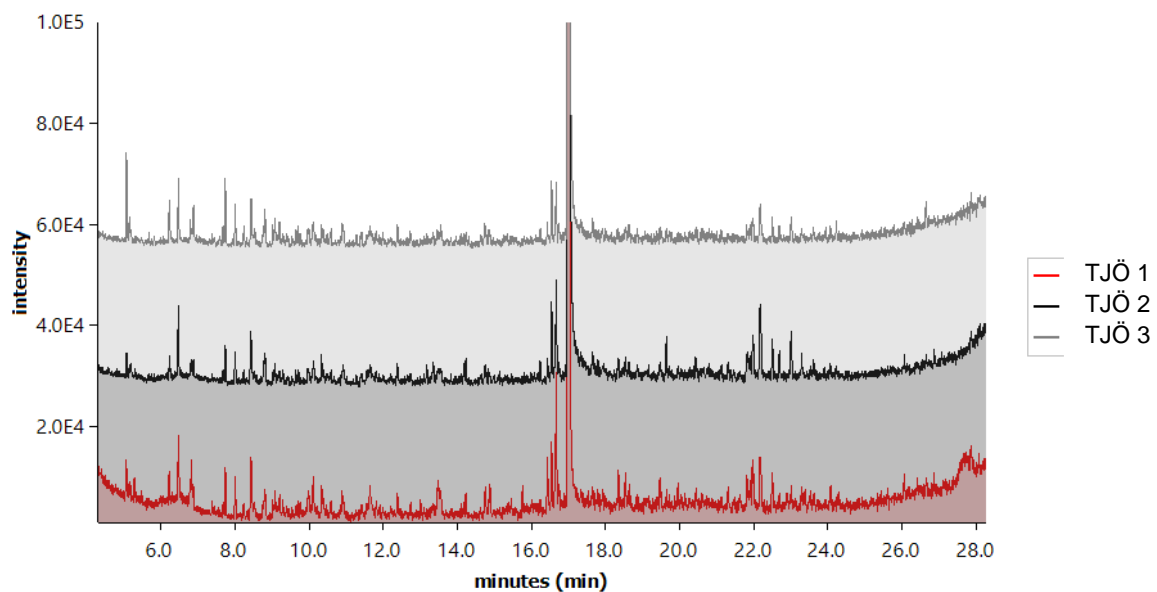
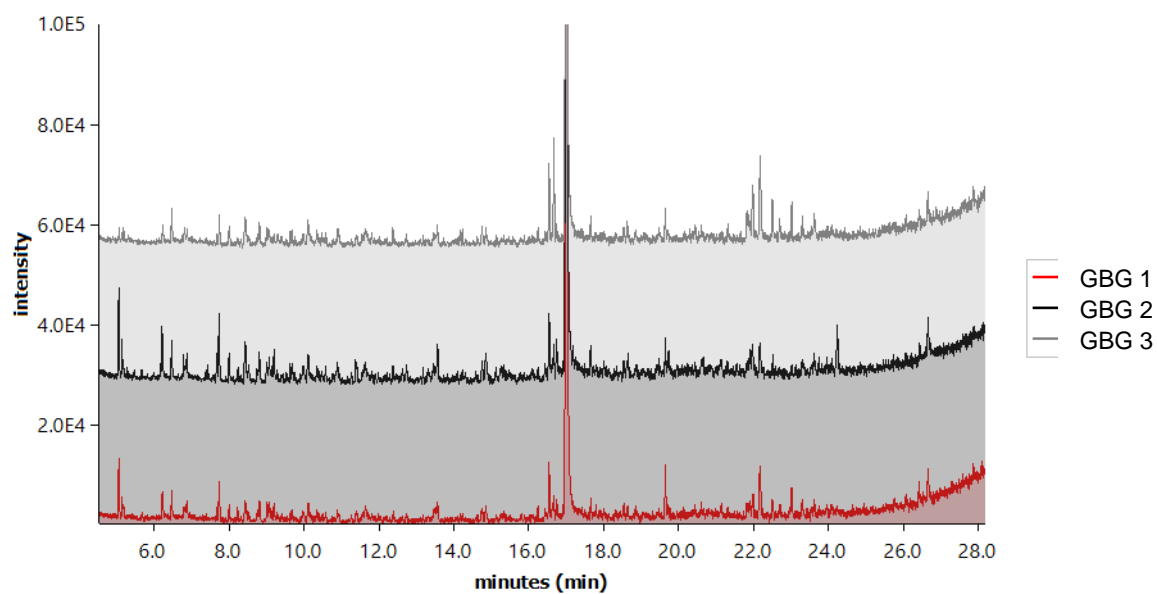


Figure S3.3-1 - Overlaid GC/MS chromatograms for 24 bio-crudes derived from macroalgae harvested across eight locations around the coast of Sweden



**Figure S3.3-2** - Overlaid GC/MS chromatograms for TJO bio-crudes



**Figure S3.3-3** - Overlaid GC/MS chromatograms for GBG bio-crudes

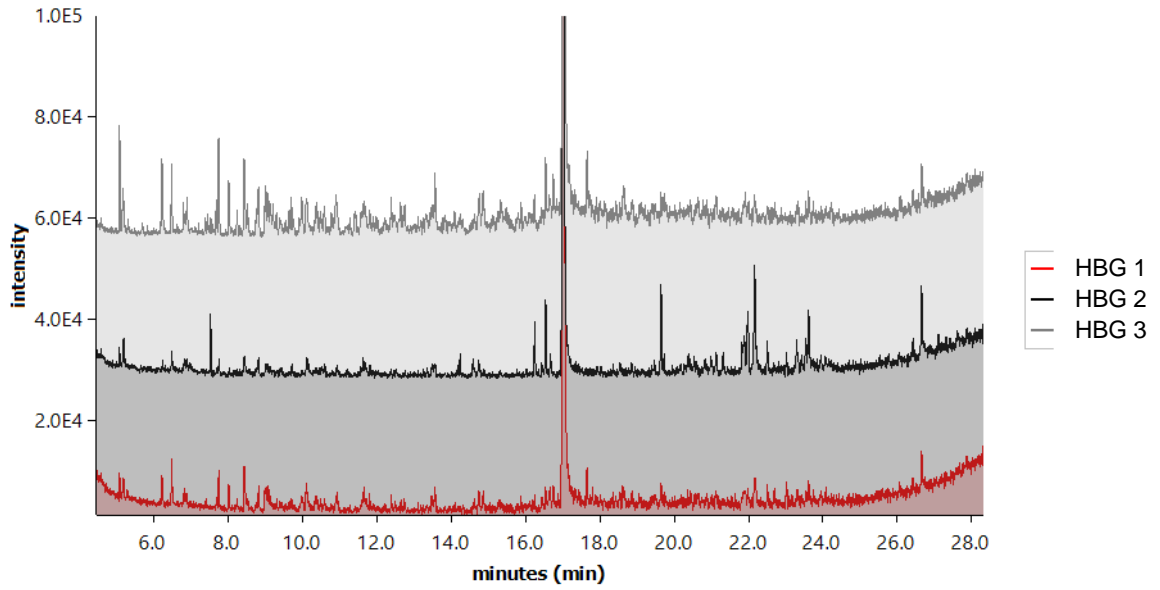


*Figure S3.3-4 - Overlaid GC/MS chromatograms for HBG bio-crudes*

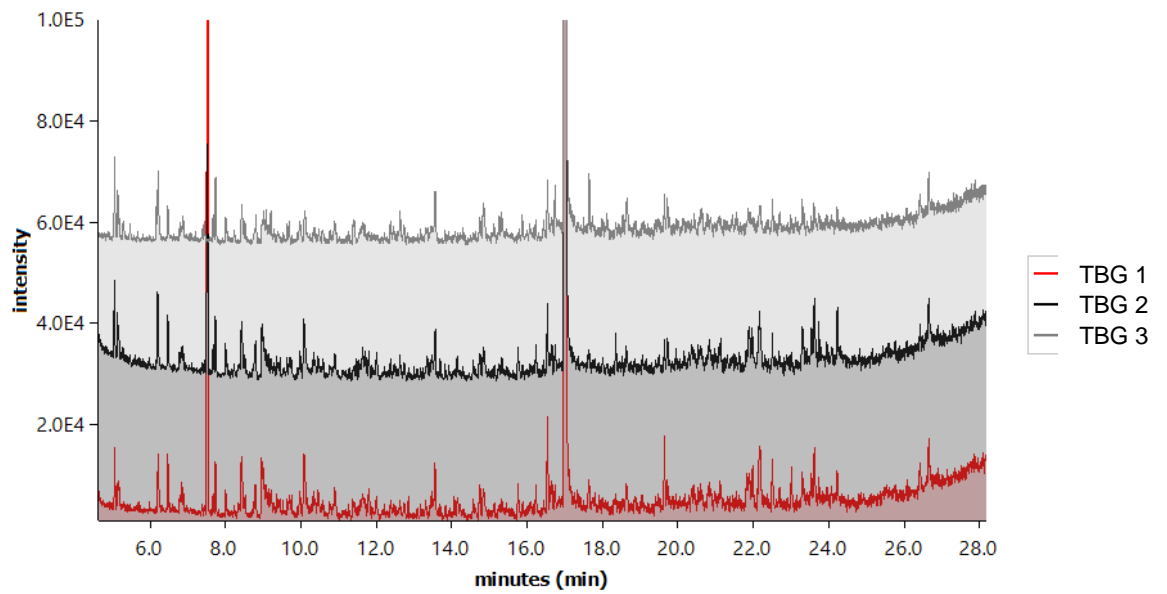


*Figure S3.3-5 - Overlaid GC/MS chromatograms for TBG bio-crudes*

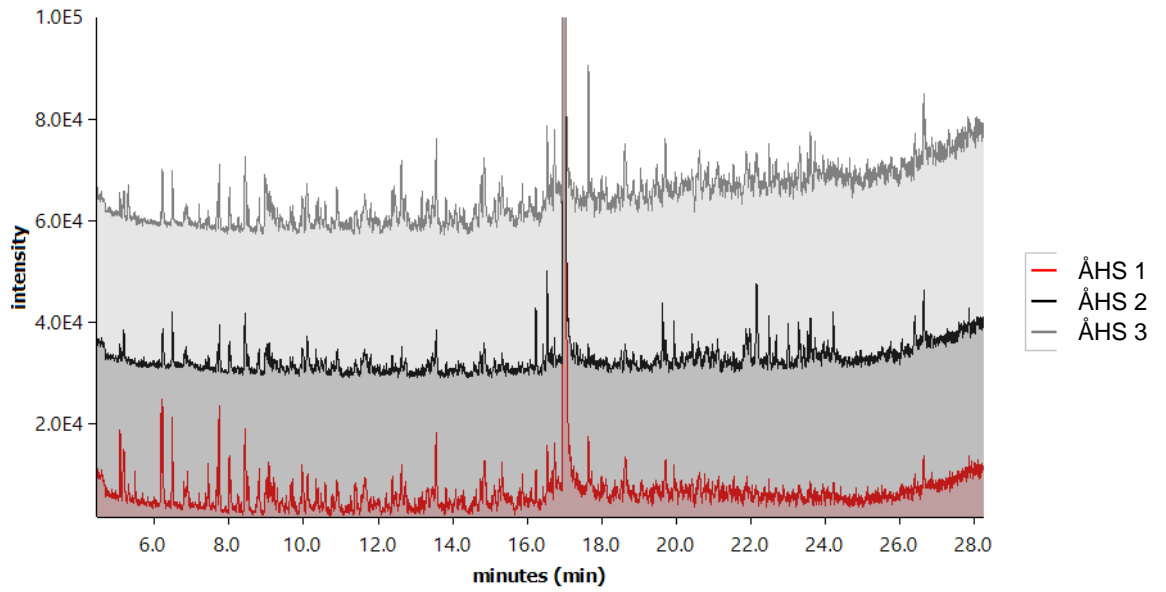


Figure S3.3-6 – Overlaid GC/MS chromatograms for ÅHS bio-crudes

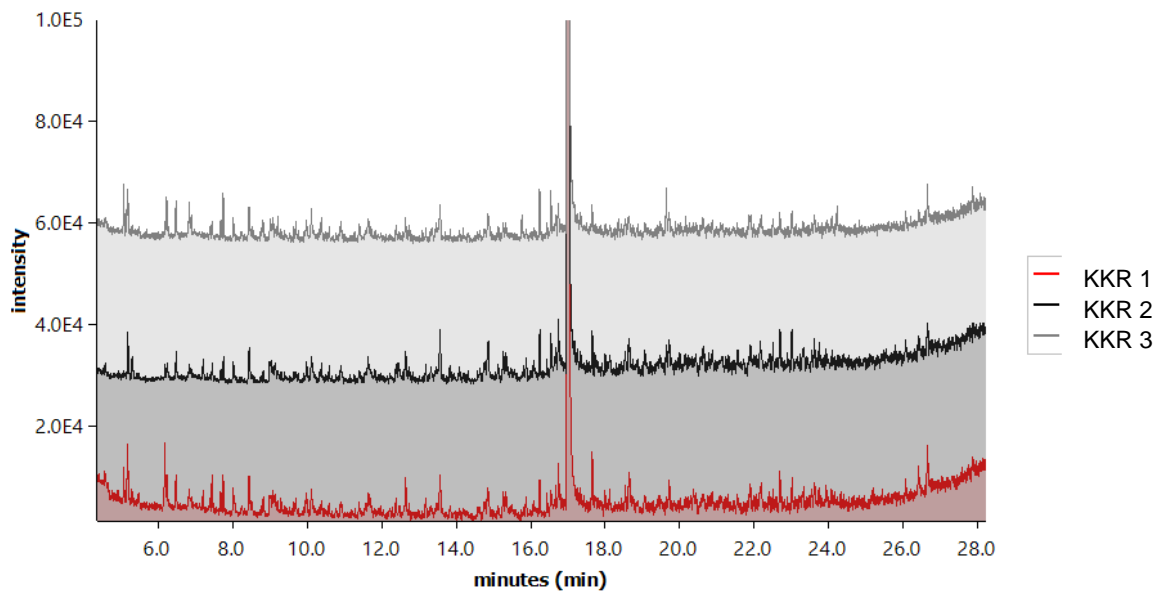
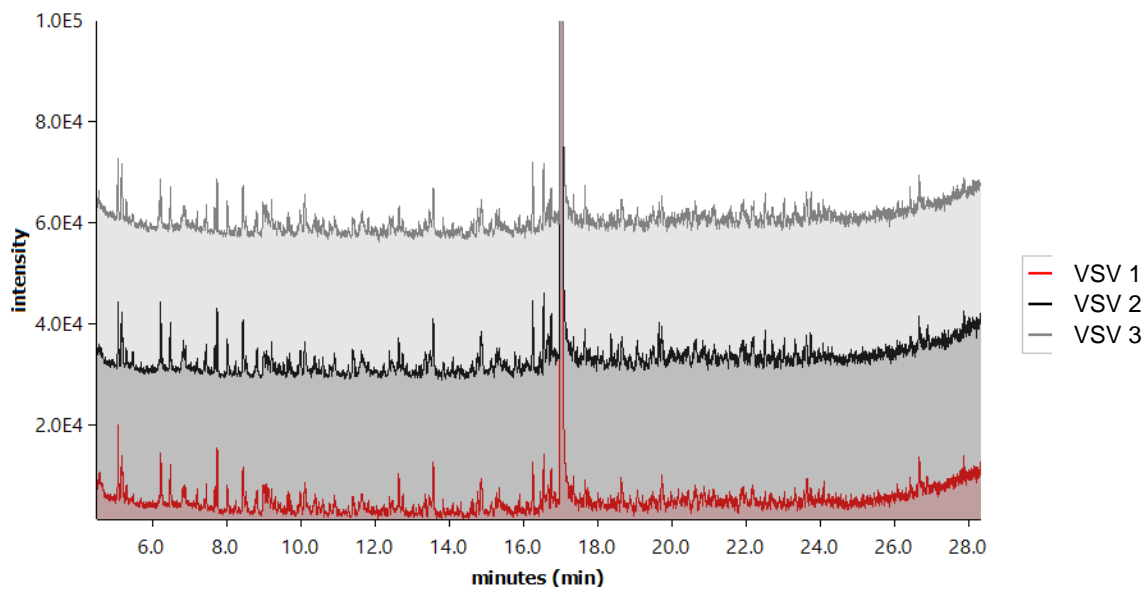
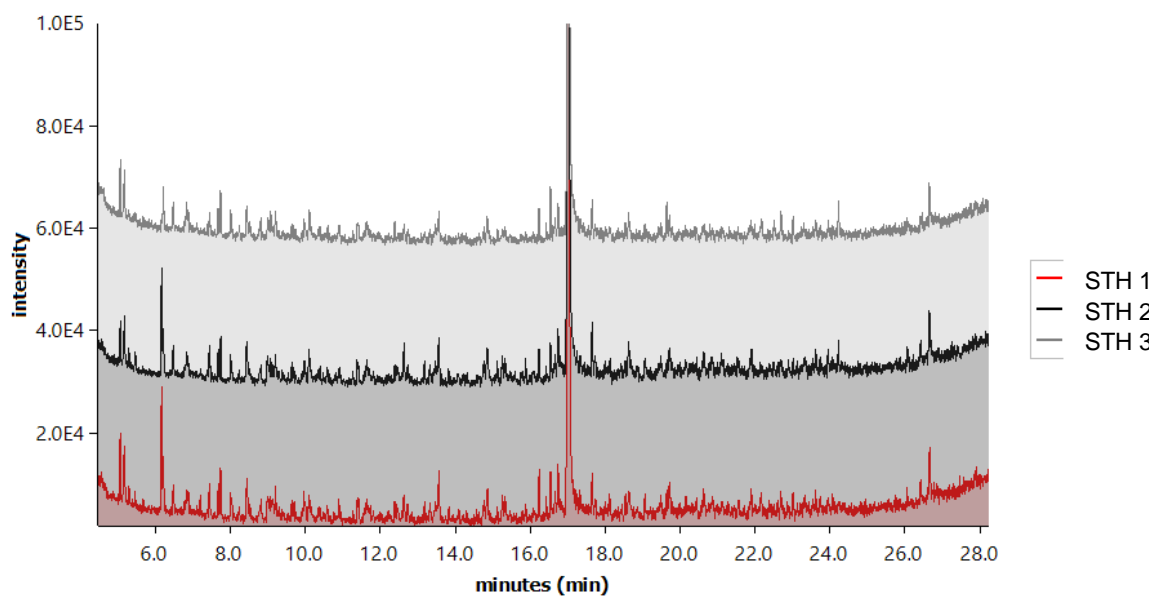


Figure S3.3-7 – Overlaid GC/MS chromatograms for KKR bio-crudes





**Figure S3.3-8** - Overlaid GC/MS chromatograms for VSV bio-crudes



**Figure S3.3-9** - Overlaid GC/MS chromatograms for STH bio-crudes

### 3.4 Context references

- [1] P. Bikker, M.M. van Krimpen, P. van Wikselaar, B. Houweling-Tan, N. Scaccia, J.W. van Hal, W.J.J. Huijgen, J.W. Cone, A.M. López-Contreras, Biorefinery of the green seaweed *Ulva lactuca* to produce animal feed, chemicals and biofuels, *J. Appl. Phycol.* (2016) 1–15. doi:10.1007/s10811-016-0842-3.
- [2] M.M. Nielsen, D. Manns, M. D 'este, D. Krause-Jensen, M.B. Rasmussen, M.M. Larsen, M. Alvarado-Morales, I. Angelidaki, A. Bruhn, Variation in biochemical composition of *Saccharina latissima* and *Laminaria digitata* along an estuarine salinity gradient in inner Danish waters, *Algal Res.* 13 (2016) 235–245. doi:10.1016/j.algal.2015.12.003.
- [3] J.C. Sanderson, M.J. Dring, K. Davidson, M.S. Kelly, Culture, yield and bioremediation potential of *Palmaria palmata* (Linnaeus) Weber & Mohr and *Saccharina latissima* (Linnaeus) C.E. Lane, C. Mayes, Druehl & G.W. Saunders adjacent to fish farm cages in northwest Scotland, *Aquaculture.* 354–355 (2012) 128–135. doi:10.1016/j.aquaculture.2012.03.019.
- [4] G.S. Marinho, S.L. Holdt, M.J. Birkeland, I. Angelidaki, Commercial cultivation and bioremediation potential of sugar kelp, *Saccharina latissima*, in Danish waters, *J. Appl. Phycol.* 27 (2015) 1963–1973. doi:10.1007/s10811-014-0519-8.
- [5] A. Handå, S. Forbord, X. Wang, O.J. Broch, S.W. Dahle, T.R. Størseth, K.I. Reitan, Y. Olsen, J. Skjermo, Seasonal- and depth-dependent growth of cultivated kelp (*Saccharina latissima*) in close proximity to salmon (*Salmo salar*) aquaculture in Norway, *Aquaculture.* 414–415 (2013) 191–201. doi:10.1016/j.aquaculture.2013.08.006.
- [6] Ole Jacob Broch, Ingrid Helene Ellingsen, Silje Forbord, Xinxin Wang, Zsolt Volent, Morten Omholt Alver, Aleksander Handå, Kjersti Andresen, Dag Slagstad, Kjell Inge Reitan, Yngvar Olsen, Jorunn Skjermo, Modelling the cultivation and bioremediation potential of the kelp *Saccharina latissima* in close proximity to an exposed salmon farm in Norway, *Aquac. Environ. Interact.* 4 (2013) 187–206. doi:10.3354/aei00080.

# Chapter 4

---

## Co-liquefaction of UK macroalgae with common marine plastic pollutants

This work has been submitted for publication to Sustainable Chemistry and Engineering (ACS) in November 2018.

The article was published as Raikova, S, Allen, M & Chuck, C 2019, 'Co-liquefaction of Macroalgae with Common Marine Plastic Pollutants', ACS Sustainable Chemistry and Engineering, vol. 7, no. 7, pp. 6769-6781 available online via: <https://doi.org/10.1021/acssuschemeng.8b06031>

## 4.1 Context

The utilisation of macroalgae as a feedstock for HTL has been discussed at length in the preceding chapters. However, seaweeds are rarely found in isolation in the marine environment. The ubiquitous presence of marine plastic pollution has been attracting increasing scientific research and public attention in recent years: at present, there is estimated to be between 7,000 and 236,000 tonnes of marine plastic floating on the ocean surface, with the total amount of plastic entering the ocean several orders of magnitude higher [1]. A conservative 2014 estimate by UNEP has valued the environmental damage to marine ecosystems at around \$13 billion annually [2,3]. In particular, microplastics (particles with diameters < 5 mm), which originate from industries, personal care products and the gradual degradation of larger plastic litter, are persistent in marine environments, can adsorb other organic pollutants, and bioaccumulate in food chains with unknown effects on animal and human health.

Thus, the simultaneous conversion of macroalgal biomass with marine plastic pollutants was explored in this chapter. Conversion of algal biomass and marine plastics presents both opportunities and challenges. Processes typically used for the disposal of energy-rich plastic waste, such as direct combustion or pyrolysis, are not suitable for high-moisture marine biomass, which would require substantial energy expenditure for drying prior to processing. However, plastics are unsuitable feedstocks for technologies typically used for wet biomass, such as fermentation or anaerobic digestion. Hydrothermal liquefaction (HTL) is capable of processing a range of organic material types [4], and, as such, presents an interesting alternative for application with mixed feedstocks.

Although the bulk of HTL literature has focused predominantly with a view to processing fresh biomass, HTL of coal and plastics has also been reported [5]. Moreover, co-liquefaction of fossil and fossil-derived feedstocks with biomass has been demonstrated to have beneficial effects on bio-crude production [6,7]. Studies of plastic co-liquefaction are limited, with the HTL of plastics with lignocellulosic biomass [5,6], coal [8], and residual oil [9] having been previously investigated, and just one published study focusing on marine biomass [10]. In this case, ethanol was used as the solvent. However, in order for HTL to be carried out sustainably, water would constitute the natural solvent of choice within a functioning marine biorefinery.

This piece of work aimed to explore the co-liquefaction of UK macroalgal species with common marine pollutants. The brown seaweed *Laminaria digitata*, a well-established candidate for widespread cultivation, was used, as well as the *Fucus serratus*,

*Sargassum muticum* (both brown) and *Ulva lactuca* (green). Polyethylene, polypropylene and nylon 6 are known to be common marine pollutants [11], and were therefore selected as model polymers.

This chapter is submitted in an alternative format in line with Appendix 6A of the “Specifications for Higher Degree Theses and Portfolios” as required by the University of Bath.

The work completed in this paper was conducted by the author with the exception of the following:

Elemental analysis was carried out by analytical department personnel at London Metropolitan University.

<sup>14</sup>C analysis was carried out by Timothy Knowles at the University of Bristol, one of the paper’s co-authors.

## 4.2 Sustainable Chemistry and Engineering paper

### Co-liquefaction of macroalgae with common marine plastic pollutants

Sofia Raikova,<sup>a</sup> Timothy D. J. Knowles,<sup>b</sup> Michael J. Allen<sup>c,d\*</sup> and Christopher J. Chuck<sup>e\*</sup>

<sup>a</sup>. Centre for Doctoral Training in Sustainable Chemical Technologies, Department of Chemical Engineering, University of Bath, Claverton Down, Bath BA2 7AY, United Kingdom.

<sup>b</sup>. Bristol Radiocarbon Accelerator Mass Spectrometer, University of Bristol, 43 Woodland Road, Bristol BS8 1UU, United Kingdom.

<sup>c</sup>. Plymouth Marine Laboratory (PML), Prospect Place, The Hoe, Plymouth PL1 3DH, United Kingdom.

<sup>d</sup>. College of Life and Environmental Sciences, University of Exeter, Stocker Road, Exeter, EX4 4QD, UK.

<sup>e</sup>. Department of Chemical Engineering, University of Bath, Claverton Down, Bath BA2 7AY, United Kingdom.

\*Corresponding authors: [mija@pml.ac.uk](mailto:mija@pml.ac.uk), [c.chuck@bath.ac.uk](mailto:c.chuck@bath.ac.uk)

#### 4.2.1 Abstract

Macroalgal blooms are environmentally problematic and costly to remediate, but also represent a vast untapped resource for the production of renewable chemicals and fuels. The responsible exploitation of such marine resources will become increasingly prominent in the transition away from the crude oil economy that currently dominates global productivity. However, crude oil-derived plastic pollution is now a ubiquitous presence in the marine environment, which hampers the effective conversion of marine feedstocks. If the full potential of macroalgae is to be realised, any large-scale industrial process will need to accommodate the presence of this plastic. This study aimed to assess the effect of several common marine plastic pollutants on the hydrothermal liquefaction (HTL) of four UK macroalgae species, and determine the impact on the major HTL products and bio-crude oil quality. Co-liquefaction of polyethylene and

polypropylene with *L. digitata*, *U. lactuca*, *F. serratus* and *S. muticum* led to modest synergistic effects for plastic conversion. Under hydrothermal conditions, polyethylene underwent fragmentation to olefinic species, as well as oxidative depolymerisation to form ketones. Modest synergistic effects on bio-crude production were also observed for polypropylene, which depolymerised more readily in the presence of biomass to form gaseous propylene as well as oil-phase products. In both cases, the presence of plastics increased total bio-crude carbon content, decreased nitrogen, and boosted higher heating value (HHV), constituting an overall improvement in bio-crude fuel properties. Nylon 6, typically originating from fisheries debris, depolymerised under HTL conditions to form caprolactam, which partitioned between the bio-crude and aqueous phases, increasing bio-crude nitrogen. Whilst this is not favourable for bio-crude production, the reclamation of marine nylon debris for hydrothermal processing to monomers may present a promising revenue stream in future biorefineries. The results demonstrate that plastic contaminants may well represent an opportunity, rather than a threat, to the successful development of an HTL macroalgal biorefinery.

#### **4.2.2 Introduction**

There is a pressing need to decarbonise global energy production systems, and biofuels compatible with current refinery and transportation infrastructure are a vital component of the transition. Macroalgae represent a particularly promising and under-exploited feedstock for advanced biofuel production, with substantially higher growth rates and photosynthetic efficiencies than terrestrial crops [1], and, unlike microalgae, mature cultivation and harvesting technologies. Hydrothermal liquefaction (HTL) is a low-energy thermochemical processing method, ideally suited to high-moisture marine biomass, and macroalgal HTL has attracted increasing attention in recent years [2,3].

A key advantage of macroalgae over microalgae as a large-scale biofuel feedstock is the ability to cultivate and harvest *in-situ*, in marine environments. Macroalgae take up dissolved nutrients directly from seawater, thus do not require additional fertiliser input or artificial illumination (as is the case for microalgal cultivation). Cultivation of macroalgae is well-developed in parts of Asia [4], but cultivation projects are also being established across Europe [5–7] and East Africa [8].

Macroalgal cultivation is also utilised to great effect for remediation of waters contaminated by terrestrial agricultural run-off or wastewater from fish aquaculture [9–14]. However, one of the most concerning forms of water pollution at the present moment

are marine plastics, which have attracted a significant amount of research interest [15], as well as increasing media attention, in recent years. The meticulous removal of 'contaminating' macroplastics following harvesting is a standard feature of macroalgae pre-processing procedures [16,17]. However, to develop a practical and effective industrial process based on macroalgae (whether cultivated, or from harvested natural stocks), any biorefinery based process will need to accommodate both the natural variation in biomass composition and variations in plastic abundance and composition.

Marine plastics originate primarily from single-use packaging [15], such as plastic drink bottles and polyethylene bags, as well as a smaller contribution from maritime debris, such as nylon from fishery activities [18]. Recent studies estimate that a minimum of 5.25 trillion plastic particles are afloat in the ocean, weighing almost 300,000 tonnes [19] – although this figure excludes debris on the seafloor, as well as litter washed up on beaches. Marine litter is degraded by physical and chemical means to microplastics [20], which are ingested by marine biota, making their way up the food chain to human consumption [18,21], and both micro- and macroplastics have now become ubiquitous at all strata of the ocean, including the deep ocean floor [22]. As a result, harvested crops of marine macroalgae are likely to be associated with both plastic litter and microplastics, which adsorb onto macroalgal surfaces [21], in increasing quantities. Larger debris could potentially be removed manually during biomass preparation for processing, but residual microplastics can remain even after washing [21], meaning that macroalgal fuel feedstocks are always likely to contain some level of plastic. However, this can potentially be used to an advantage, coupling fuel production with simultaneous marine plastic remediation.

Co-processing of lignocellulose and microalgae with plastic wastes, including co-pyrolysis [23,24] and co-liquefaction [25–27] has been investigated previously. Synergistic effects between plastic and microalgae on yields of bio-crude from liquefaction have been observed. The presence of highly reactive biomass decomposition products have been shown to lower the thermal stability of polyethylene, and accelerate its thermal degradation at lower temperatures; polyethylene, in turn, can act as a hydrogen source in biomass liquefaction [27,28]. Co-liquefaction of polyethylene with *Spirulina* was found to decrease the oxygen content of the bio-crude products [27], whilst we have previously demonstrated that co-liquefaction of Vietnamese *Ulva intestinalis* with polyethylene gave bio-crudes with decreased nitrogen levels and increased HHV [28] – an overall improvement in fuel properties. The presence of plastics was also found to promote the conversion of biomass to bio-crude.



The aim of this investigation was to assess co-hydrothermal liquefaction of a wider range of UK macroalgae species with a range of plastics commonly found in marine environments (polyethylene, polypropylene, and nylon 6) in order to model the effect of plastic contaminants on macroalgal bio-crude production within a marine biorefinery context. Biomass feedstock species were selected with the overarching aim of developing a future biorefinery for the simultaneous production of biofuels and remediation of marine plastic pollution: *Laminaria digitata*, cultivated at large scales worldwide, with mature and well-developed cultivation and harvesting technologies, was therefore of particular interest, amongst other common UK species. The effect of plastics on the yields and compositions of the product phases was examined, and potential valorisation routes for each product phase were assessed.

### **4.2.3 Methods**

#### ***4.2.3.1 Materials and apparatus***

Fresh macroalgal biomass samples were collected from Saltern Cove, Paignton, Devon. Contaminating macroplastics were removed manually prior to snap freezing in liquid nitrogen and storage at -80 °C. Prior to analysis, all samples were freeze-dried and milled to ca. 500 µm diameter. Freeze-dried samples were stored at ambient conditions.

Granulated (approx. 500 µm) polyethylene and polypropylene were obtained from Sigma Aldrich. Pelletised nylon 6 was obtained from Alfa Aesar; particle size was reduced to <500 µm using a commercial food processor. Plastics were stored at ambient conditions prior to use.

Batch reactors were fabricated according to literature precedent using stainless steel Swagelok® tube fittings [29–31]. The reactor body consisted of a length of stainless steel tubing capped at one end, and connected at the other to a pressure gauge, thermocouple, needle valve, and relief valve. The total internal volume of the reactors was ca. 50 cm<sup>3</sup>.

#### ***4.2.3.2 Procedure***

Reaction procedures have been reported previously [31]. In a typical reaction, the reactor was loaded with 3 g total material (biomass and plastic) and 15 cm<sup>3</sup> freshly deionized water, and heated within a vertical tubular furnace until the specified reaction

temperature was reached, then removed from the furnace and allowed to cool to room temperature.

After cooling, gaseous products were released *via* the needle valve into an inverted, water-filled measuring cylinder to measure gaseous fraction volume. Gas phase yields were calculated using the ideal gas law, approximating the gas phase as 100 % CO<sub>2</sub>, assuming an approximate molecular weight of 44 g mol<sup>-1</sup> and a volume of 22.465 dm<sup>3</sup> mol<sup>-1</sup> gas phase at 25 °C. The yield of gaseous product was determined using the following equation:

$$\text{yield}_{\text{gas}} = (V_{\text{gas}} \times 1.789 \times 10^{-3}) / (m_{\text{dry biomass}} + m_{\text{plastic}}) \times 100 \% \quad (1)$$

Following this, the aqueous phase was decanted from the reactor contents and filtered through a Fisher qualitative filter paper pre-dried overnight at 60 °C. The product yield in the water phase was determined by leaving a 2.5 g aliquot to dry in a 60 °C oven overnight, and scaling the residue yield to the total aqueous phase mass. Aqueous phase residue yield was determined using the following equation:

$$\text{yield}_{\text{AP residue}} = m_{\text{residue}} / (m_{\text{dry biomass}} + m_{\text{plastic}}) \times 100 \% \quad (2)$$

To separate the remaining bio-crude oil and char phase, the reactor was washed repeatedly using chloroform until the solvent ran clear, and filtered through the same filter paper used to separate the aqueous phase (after drying for a minimum of 1 h). The filter paper and collected char were washed thoroughly with chloroform to remove all remaining bio-crude. The filtrate was collected, and solvent removed *in vacuo* (40 °C, 72 mbar) until no further solvent evaporation was observed visually, and bio-crude samples were left to stand in septum-sealed vials venting to the atmosphere *via* a needle for a further 12 h to remove residual solvent. Bio-crude yield was determined using the following equation:

$$\text{yield}_{\text{bio-crude}} = m_{\text{bio-crude}} / (m_{\text{dry biomass}} + m_{\text{plastic}}) \times 100 \% \quad (3)$$

The char yield was calculated from the mass of the retentate collected on the filter paper after drying overnight in an oven at 60 °C. Solid yield was determined using the following equation:

$$\text{yield}_{\text{solid}} = m_{\text{solid}} / (m_{\text{dry biomass}} + m_{\text{plastic}}) \times 100 \% \quad (4)$$

Inevitable material losses occurred during work-up, predominantly through evaporation of light organics from the aqueous and bio-crude phases during filtration and solvent removal. The shortfall in the mass balance has thus been designated “volatiles”.

#### *4.2.3.3 Characterisation*

Biomass ash was quantified by heating a 500 mg sample of biomass in a Carbolite CWF 11 muffle furnace at 550 °C for 5 hours. The mass remaining at the end of the experiment was taken to be the ash.

For macroalgal biomass, bio-crude and char, elemental (CHN) analysis was carried out externally at London Metropolitan University on a Carlo Erba Flash 2000 Elemental Analyser to determine CHN content. Elemental analyses were carried out at least in duplicate for each sample, and average values are reported. Higher heating value (HHV) was calculated from elemental composition according to literature precedent [32].

The aqueous phase products were analysed for total carbon (TC) and total nitrogen content (TN) using a Shimadzu TOC-L TOC analyser fitted with a TNM-L total nitrogen analyser unit and an ASI-L autosampler.

Thermogravimetric analyses were conducted using a Setaram TG-92. Samples were heated from ambient temperature to 1000 °C at a rate of 20 °C min<sup>-1</sup> under an air atmosphere.

FTIR spectra were obtained on a Thermo Scientific Nicolet iS5 FTIR spectrometer. All samples were analysed in the wavenumber range 4000–500 cm<sup>-1</sup>.

GC-MS of bio-crudes was carried out using an Agilent 7890A gas chromatograph fitted with an Agilent HP5-MS capillary column (30 m x 250 µm x 0.25 µm), and an Agilent 5975C MS detector. Helium (1.2 mL min<sup>-1</sup>) was used as the carrier gas. Samples were injected (10:1 split injection) at 50 °C, held for 1 min, ramped to 290 °C at a rate of 7.5 °C min<sup>-1</sup>, and held for 3 min at 290 °C. Identification of compounds was performed using the NIST mass spectral database.

Gas phases were analysed using an Agilent 7890A gas chromatograph fitted with an Agilent HP5-MS capillary column (30 m x 250 µm x 0.25 µm), an FID detector, and an Agilent 5975C MSD detector. Helium (1.2 mL min<sup>-1</sup>) was used as the carrier gas. Gas samples were injected directly onto the column at 40 °C, held for 7 min, then ramped to

150 °C at 20 °C min<sup>-1</sup>, ramped to 250 °C at 15 °C min<sup>-1</sup>, and held for 6 min at 250 °C. Identification of compounds was performed using the NIST mass spectral database.

For radiocarbon analyses by accelerator mass spectrometry (AMS), samples were combusted and graphitised with an Elementar Vario Isotope Select elemental analyser interfaced to an IonPlus AGE3 graphitization system [33] and radiocarbon determinations performed using the BRIS-MICADAS AMS. Data reduction was performed using the software package BATS [34].

In order to determine experimental error and test the repeatability of experimental results, three repeat HTL runs of *L. digitata* were carried out to determine the standard deviation in mass balances. All elemental analyses (CHN) were carried out in duplicate, and average values used.

## 4.2.4 Results and discussion

### 4.2.4.1 HTL conversion of common marine plastic contaminants

Polyethylene and polypropylene are highly thermally stable polymers. Thermal decomposition of polyethylene in supercritical water has been reported previously [35,36], but the behaviour of polyethylene at the subcritical conditions which constitute HTL remains largely unexplored, save for co-liquefaction with residual oil [37]. Under the given HTL processing conditions, reactions containing solely polyethylene or polypropylene as a feedstock did not react to give typical HTL products: upon cooling the reactor, the plastics were found to have partially melted and fused into a solid plug, separate from the water layer, with no measurable gas production, and no extractable bio-crude.

In contrast, liquefaction of nylon 6 at HTL temperatures (340 °C) led to the conversion of 6.6 % of the polymeric material to chloroform-soluble “bio-crude” product, and 10.9 % to water-soluble material. Polycondensation polymers such as nylon 6 are susceptible to thermal degradation, and nylon 6 has been shown to depolymerise by hydrolysis at subcritical conditions to form monomeric  $\epsilon$ -caprolactam *via* an  $\epsilon$ -aminocaproic acid intermediate [38].

Caprolactam is soluble in both aqueous media and chloroform [39]: correspondingly, analysis by GC/MS revealed substantial levels of caprolactam partitioned between the bio-crude and aqueous phases. The presence of 2,4-di-*tert*-butylphenol in the bio-crude phase was also detected. 2,4-Di-*tert*-butylphenol is present in plastics as a UV stabiliser and antioxidant, but is, alongside other similar phenolics, also widely used as an

antioxidant [40], which may prove advantageous for fuel production from bio-crude derived from nylon-containing feeds.

#### ***4.2.4.2 Conversion of plastic-enriched Laminaria digitata***

*L. digitata* blended with common marine pollutants polyethylene, polypropylene and nylon 6 was processed using HTL conditions previously reported [41,42]. Product yields were calculated on the basis of total feedstock input; product mass balances are presented in Figure 4.2-1.

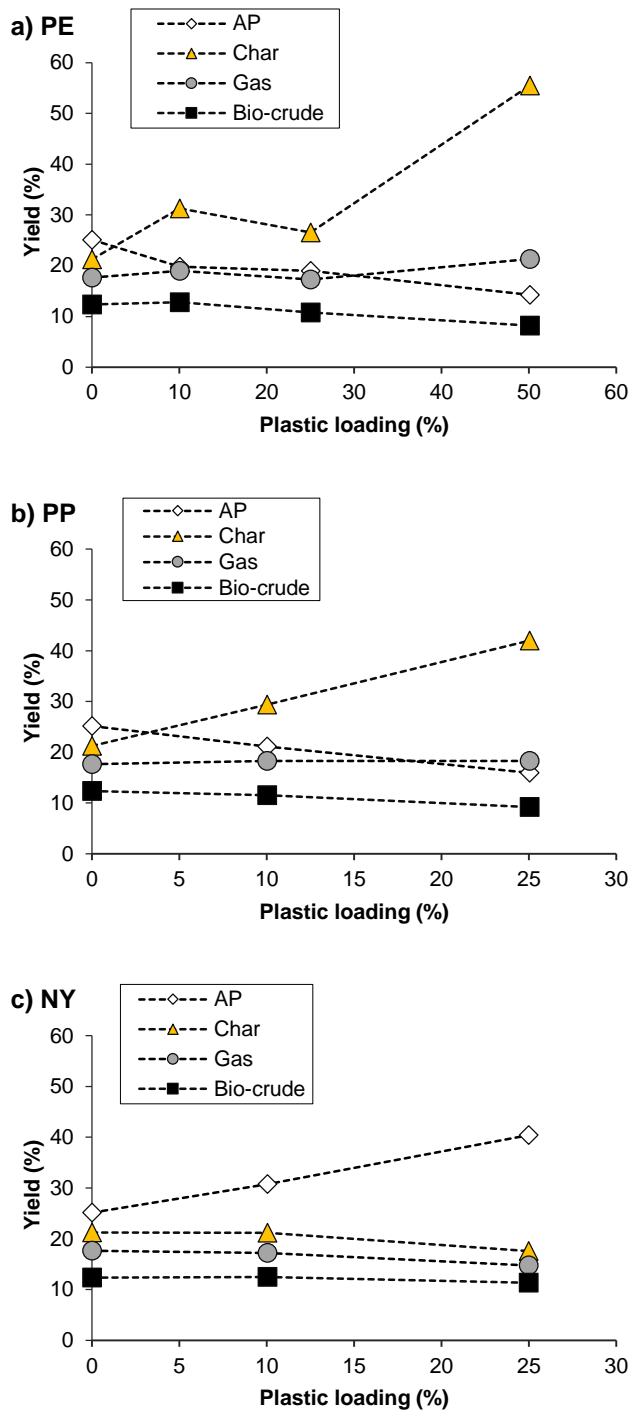


Figure 4.2-1 – Mass balances of HTL products from liquefaction of *L. digitata* blended with a) polyethylene, b) polypropylene and c) nylon 6.

For liquefaction of biomass alone, the bulk of the organic material in the feedstocks (25.1 %) was recovered in the aqueous phase products. On the addition of PE, a modest increase in bio-crude yield was observed for a 10 % blend of PE with *L. digitata*, whilst slight decreases in overall bio-crude production were seen for 25 % and 50 % blends (bio-crude yields of 10.8 and 8.2 %, respectively). The majority of the PE was recovered in the solid phase products, with char yields increasing concomitantly with bio-crude

depletion, up to a maximum solid yield of 55.5 % for a 50 % PE blend level, although a notable dip in solid phase recovery (26.5 % solid at a 25 % PE blend level, down from 31.5 % at a 10 % PE blend) was observed. Aqueous phase product recovery declined steadily (25.1 % for pure biomass, down to 14.3 % for a 50 % PE blend), whilst increasing PE blend levels also caused a modest increase in the yield of gas phase products at 10 % and 50 % blend levels.

A similar pattern of results was observed for PP: aqueous phase products and bio-crude yields declined with increasing PP blend level (down to 9.2 % bio-crude for a 25 % PP blend level), whilst gas phase product yield stayed approximately constant. The majority of the plastic-enriched feed was, once again, recovered in the solid phase products (up to a maximum of 42.0 % solid yield for a 25 % PP blend).

For co-liquefaction with nylon 6, however, increasing polymer blends, bio-crude production remained constant at 12.4 % on increasing to a 10 % nylon 6 blend, and decreased slightly to 11.3 % for the 25 % blend. Gas and solid phase yields declined steadily, whilst a substantial increase in the aqueous phase product recovery was seen: 40.4 % of the total feed partitioned to the aqueous phase for a 25 % nylon 6 blend level.

For the liquefaction of plastics in the presence of biomass, modest synergistic effects were observed. The extent of synergistic effects between the biomass and plastic reactants was calculated using the equation proposed by Wu *et al.* [26]:

$$\text{Synergistic effect} = Y_{BC} - (X_{macroalgae} \times Y_{macroalgae} + (1 - X_{plastic}) \times Y_{plastic}) \quad (5)$$

where  $Y_{BC}$  represents the yield of bio-crude in a given experiment,  $Y_{\text{component}}$  represents the yield of bio-crude from an individual component when processed in isolation, and  $X_{\text{component}}$  represents the mass fraction of each component in the reaction mixture. A positive value of SE indicates that a greater yield of bio-crude was obtained from the blended feedstock than the linear sum of the yields expected from each the individual feedstocks, and vice versa.

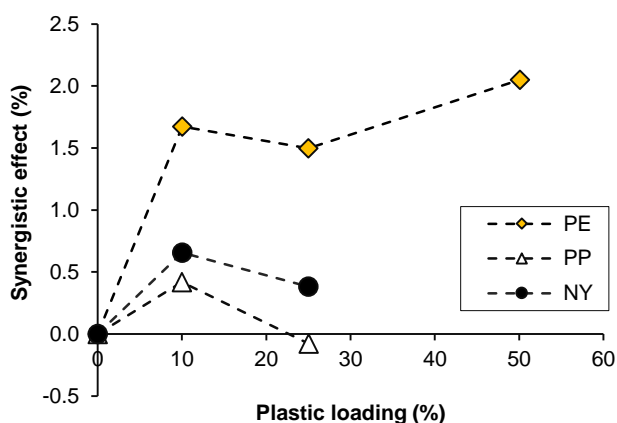


Figure 4.2-2 – Synergistic effects on bio-crude yields from liquefaction of *L. digitata*, blended with plastics (PE = polyethylene, PP = polypropylene, NY = nylon 6).

The degree of synergistic effects for co-liquefaction of *L. digitata* with PE and PP was relatively modest, but positive in all cases, with the exception of a 3:1 blend of *L. digitata* with polypropylene.

The presence of any non-polymeric species, such as residual polymerisation catalysts or additives, can affect the resistance of a plastic to thermal degradation. Transition metals including manganese can be activated at elevated temperatures and act as a pro-oxidant for polyethylene, generating radicals on the polymer chain, which can then undergo oxidation or chain scission [43]. Ash present in macroalgal biomass can potentially supply metals, which act as pro-oxidants for PE and PP, although it has also been suggested that the presence of organic biomass fragments and radicals can also promote polymer chain scission [25]. Hydrogen transfer from polyolefinic chains can, in turn, stabilise radicals generated by biomass thermal degradation and prevent re-condensation to solid char, generating higher oil yields [25]. It is noted that these effects may be temperature-dependent, and, beyond a certain temperature threshold, synergistic effects may diminish [25].

#### 4.2.4.2.1 Effect of heating rate

The heating rate plays a significant role in determining HTL outcomes [41,44,45]. Processing of pure biomass and biomass blended with polyethylene at a 10 % level was, therefore, investigated. The reaction temperature remained constant at 340 °C, but heating rates were varied from 11 °C min<sup>-1</sup> to 25 °C min<sup>-1</sup>.



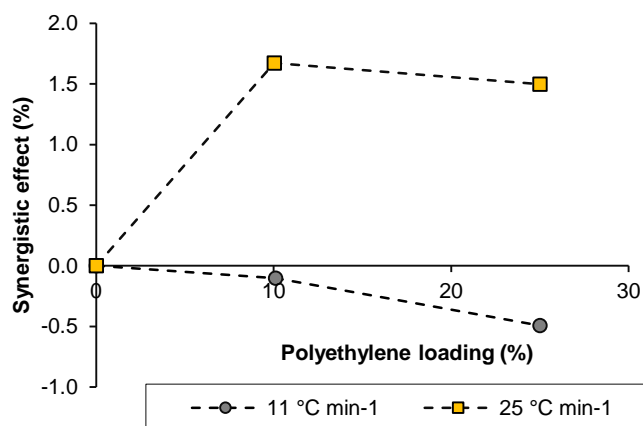


Figure 4.2-3 – Synergistic effects on bio-crude production for co-liquefaction of *L. digitata* with polyethylene (10 % blend) at a range of heating rates

The degree of synergistic effects seen for bio-crude production was not the same for the two heating rates, with a positive synergistic effect observed for HTL carried out at a heating rate of 25 °C min<sup>-1</sup>, but negative effects observed for 11 °C min<sup>-1</sup>. This suggests that for optimal polyethylene conversion under HTL conditions, elevated heating rates are preferred. This is advantageous, as short reaction times and high heating rates are also preferred for the production of bio-crude from macroalgal biomass [41], and it will therefore not be necessary to compromise on heating rates to obtain optimal conversion of both biomass and plastics.

#### 4.2.4.2.2 Bio-crude composition

Plastic co-liquefaction had a significant impact on bio-crude elemental composition. Co-liquefaction of *L. digitata* with increasing blends of PE led to an increase in both carbon and hydrogen, thereby increasing bio-crude HHV (an initial modest increase from 33.5 to 34.2 MJ kg<sup>-1</sup> on moving from pure *L. digitata* to a 25 % PE blend, and a more substantial jump to 39.3 MJ kg<sup>-1</sup> for 50 % PE). A corresponding decrease in bio-crude nitrogen was also observed. These changes equate to an overall improvement in bio-crude fuel properties. Under pyrolytic conditions (i.e. in the absence of H<sub>2</sub>O), it has been proposed that polyolefins can readily donate hydrogen to biomass radicals [46]. For hydrothermal conditions, D<sub>2</sub>O studies have demonstrated that H<sub>2</sub> can be liberated from water and migrate to the bio-crude phase products [35], but polymers may also act as a hydrogen source in hydrothermal co-processing [25], potentially contributing to the increase in bio-crude hydrogen.

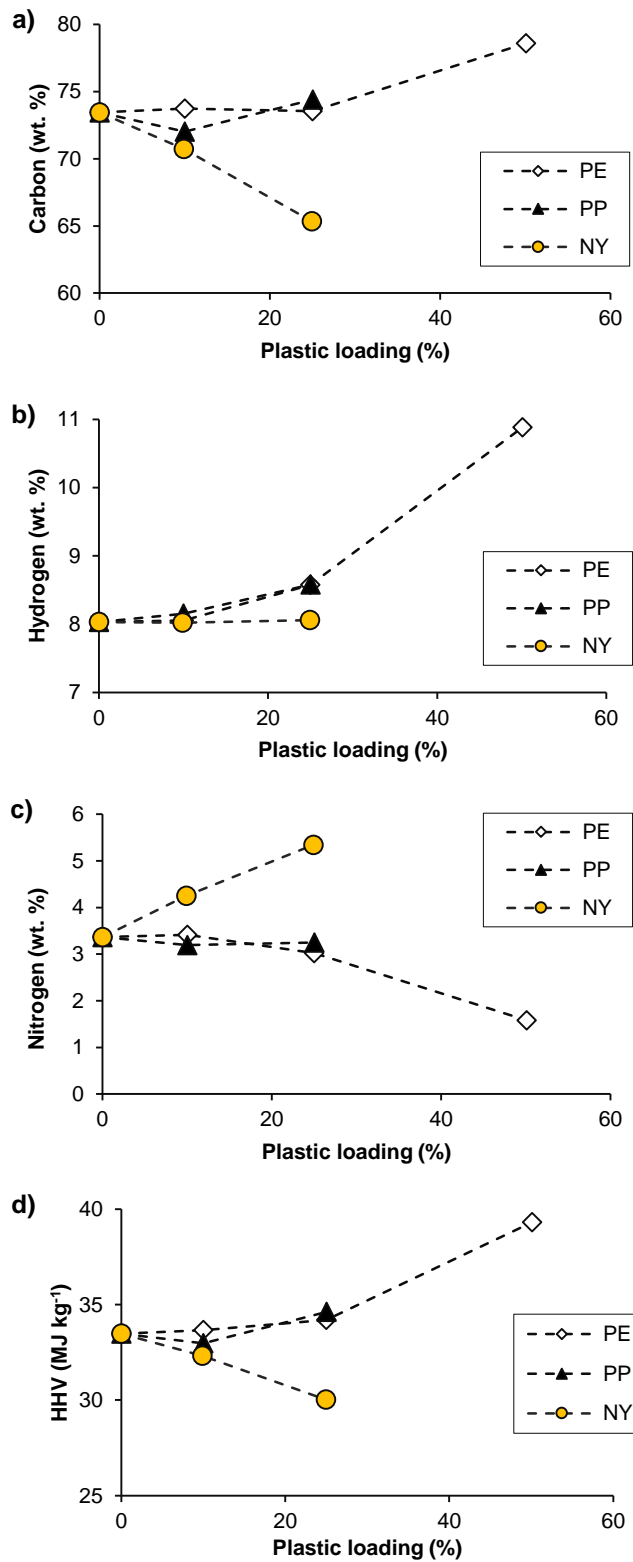


Figure 4.2-4 – Bio-crude compositions produced from the co-liquefaction of *L. digitata* with PE, PP and nylon 6, where a) is carbon wt. %, b) hydrogen wt. % c) nitrogen wt. % and d) is HHV of the bio-crudes

For co-liquefaction with PP, the overall impact on bio-crude elemental composition was similar to that observed for PE, although the reduction in nitrogen content was somewhat more modest. For co-liquefaction with nylon, hydrogen levels stayed approximately constant, but a significant depletion in total carbon was observed (from 73.7 % for pure *L. digitata* to 65.4 % for a 25 % nylon 6 blend), alongside a corresponding depletion in HHV (33.5 MJ kg<sup>-1</sup> to 30.3 MJ kg<sup>-1</sup>). A substantial increase in total nitrogen to 5.4 % for the 25 % nylon 6 blend from 3.4 % for a pure *L. digitata* feedstock was also seen. The presence of elevated nitrogen in crude can poison refinery catalysts and lead to elevated NO<sub>x</sub> emissions on combustion, and high-nitrogen crudes require extensive hydrotreatment prior to use, so the presence of nylon 6 in feedstocks may have detrimental effects on bio-crude fuel properties.

FT-IR spectra of bio-crudes obtained from liquefaction of pure *L. digitata* and *L. digitata* blends with polyethylene, polypropylene and nylon 6 are presented in Figure 4.2-5.

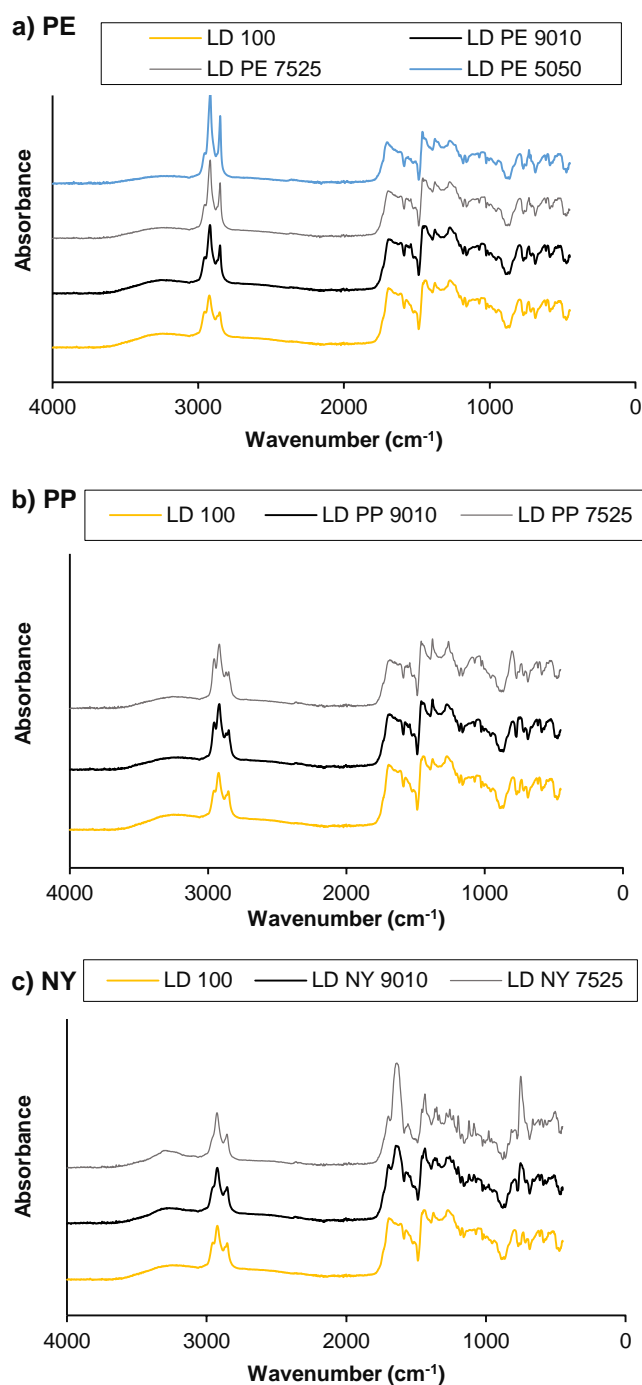


Figure 4.2-5 – FT-IR spectra of bio-crudes obtained from liquefaction of pure *L. digitata* and *L. digitata* blends with polyethylene, polypropylene and nylon 6

Co-liquefaction of *L. digitata* with increasing blends of PE gave rise to increasing intensity in absorbance at  $2916\text{ cm}^{-1}$ , attributable to C–H stretching, with an attendant decrease in the broad peak at  $3650\text{--}3100\text{ cm}^{-1}$ , arising from N–H and O–H stretching in alcohols and amines. A sharpening of the C=O ketone stretch at  $1700\text{ cm}^{-1}$  was also observed, although overall absorbance decreased. These observations are supported by GC/MS analysis. Similar changes in IR absorbance were observed for bio-crudes produced from

co-liquefaction with PP, although the differences were somewhat less pronounced. For co-liquefaction with nylon 6, increasing blend levels gave rise to an amide C=O stretch at 1629 cm<sup>-1</sup> not observed in bio-crude obtained from pure *L. digitata*, as well as a N–H stretch at 3300 cm<sup>-1</sup>.

Analysis of the bio-crudes by GC/MS allowed a more in-depth assessment of bio-crude composition. Bio-crude derived from *L. digitata* alone contained primarily phenolic species, with a contribution from organic acids formed via the depolymerisation of lipids. A full compositional breakdown of the volatile fraction of the bio-crudes can be found in the Supplementary Information. Under HTL conditions, PE was expected to show random bond scission along the chain, resulting in producing a distribution of aliphatic hydrocarbons of varying length [27], including a substantial contribution from alkenes [47]. Indeed, for co-liquefaction of *L. digitata* with PE, at 10 % and 25 % blend levels, the emergence of low levels of long-chain aliphatic hydrocarbons ( $\geq C_{13}$ ) was observed. Additionally, the common plasticiser bis(2-ethylhexyl) phthalate was present in bio-crudes, as well as a substantial contribution from long-chain ketones ( $\geq C_{12}$ ). These were formed in substantially higher quantities when *L. digitata* was processed at a 50 % blend level with PE. It is noteworthy that PE processed under analogous HTL conditions in isolation (i.e. without macroalgal co-feedstock) did not produce bio-crude oil. An overlay of the GC-MS chromatograms for the bio-crudes is presented in Figure 4.2-6, with key compounds identified in Table 4.2-1.

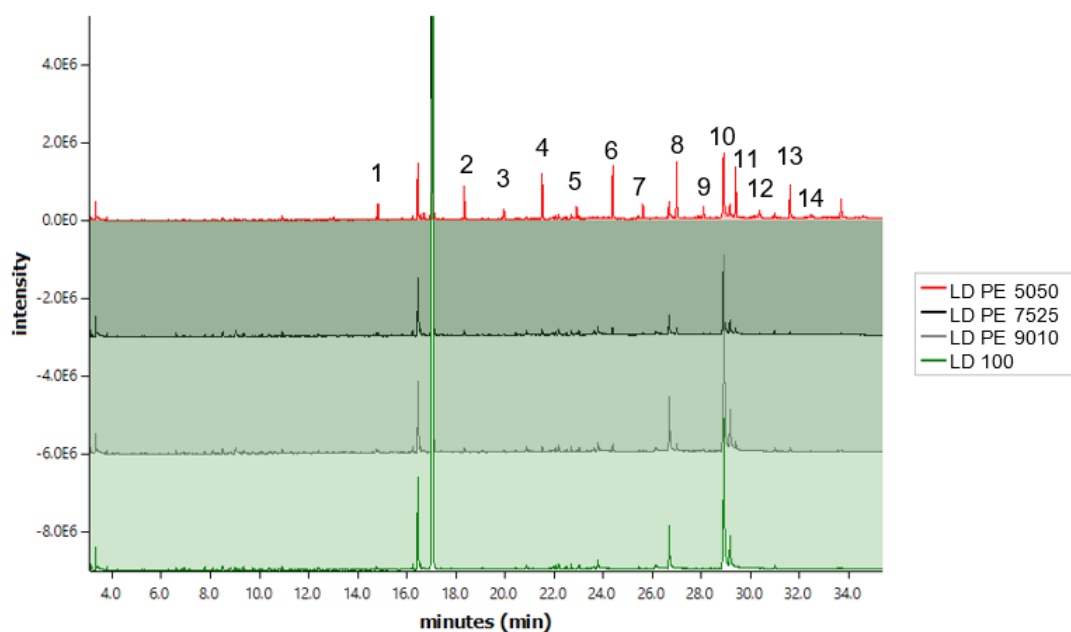


Figure 4.2-6– Overlay of GC chromatograms of bio-crudes created from *L. digitata*/PE feedstocks at PE blend levels of 0, 10, 25 and 50 %. The high-intensity peak at 17.09 min is of solvent origin.

Table 4.2-1 – Identities of notable compounds in bio-crude products from co-liquefaction of *L. digitata* with polyethylene

Peak	RT	Compound
1	14.82	2-Dodecanone
2	18.35	2-Tetradecanone
3	19.96	Heptadecane
4	21.52	2-Hexadecanone
5	22.92	Nonadecane
6	24.39	2-Octadecanone
7	25.63	Hexadecane
8	27.01	2-Nonadecanone
9	28.10	Octadecane
10	28.90	Octadecenamide
11	29.41	2-Docosanone
12	30.37	Octadecane
13	30.99	Bis(2-ethylhexyl) phthalate
14	31.62	2-Pentacosanone

A significant proportion of the peaks formed only in the presence of PE are long chain ketones. An increase in ketone levels has also been observed by Wu *et al.* for the co-liquefaction of microalgae and PP [26]. HTL reaction mechanisms are complex and not fully understood, due to the occurrence of hundreds of simultaneous reactions. Under hydrothermal conditions, radical species are formed *via* C–C scission [48]: the emergence of long-chain ketones in the bio-crude is, therefore, speculated to originate from polyethylene *via* a radical oxidation mechanism. Moriya *et al.* have suggested that alcoholic intermediates are formed initially, and subsequently converted to their corresponding ketones [35],<sup>F</sup> but the conspicuous absence of long-chain alcohols in the final products suggests that the reaction may instead proceed *via* an unstable hydroperoxide intermediate [49]. Long-chain alcohols are stable and slower to oxidise, and their presence has been found to inhibit the oxidation of long-chain paraffins [49]. The mechanism is initiated *via* the abstraction of a proton from a CH<sub>2</sub> adjacent to a terminal methyl group by an alkyl radical. This is followed by the reaction of the resulting polyethylene radical with dissolved O<sub>2</sub>, reaction with a hydrogen radical to generate an —OOH group, and finally dehydration to generate a ketone end group. A summary of the proposed mechanism is presented in Figure S4.3-1 in Supplementary Information.

The presence of metals in the biomass ash may also play a catalytic role in ketone formation. Hydroperoxide conversion to ketones has also been shown to be catalysed by copper and iron stearates [49]: these species could feasibly arise *in situ* from degradation biomass lipids to fatty acids in the presence of cuprous and ferric species in biomass ash.

---

<sup>F</sup> Please refer to Appendix 4A

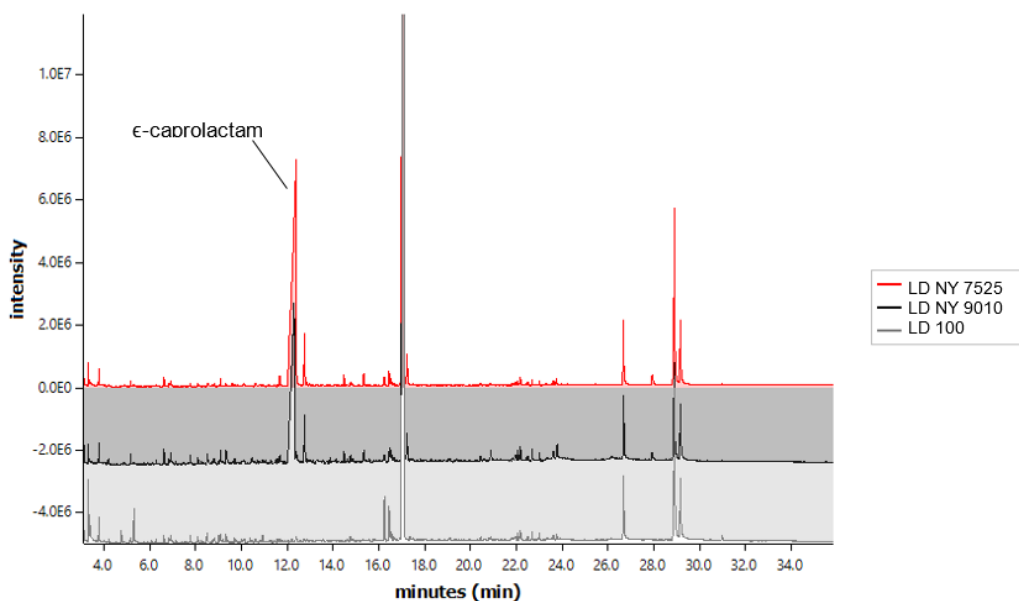


Figure 4.2-7 – Overlay of GC chromatograms of bio-crudes created from *L. digitata*/nylon 6 feedstocks at nylon blend levels of 0, 10 and 25 %. The high-intensity peak at 17.09 min is of solvent origin.

Co-liquefaction of biomass with nylon 6 resulted in the emergence of a large peak attributable to caprolactam. Nylon 6 depolymerises in water at temperatures as low as 100 °C to generate  $\epsilon$ -aminocaproic acid, and subsequently undergoes cyclodehydration to  $\epsilon$ -caprolactam (as well as further degradation to smaller molecules) [38,50]. The presence of caprolactam in the HTL products may also arise, in part, from residual monomer present in the nylon 6. Correspondingly, total detectable nitrogen in the aqueous phase products were found to increase. Other nitrogen-containing species formed in the presence of nylon 6 include tropinone and 2-piperidinemethanol at low levels. The presence of substantial levels of caprolactam in bio-crudes and aqueous phase products may present an opportunity for value-addition within the biorefinery.

#### 4.2.4.3 Aqueous phase products

Co-liquefaction of *L. digitata* with PE and PP led to an overall reduction in aqueous phase carbon content. Although the majority of the PE and PP decomposition products were not expected to be water-soluble, the presence of plastics also appears to drive partitioning of biogenic material away from the aqueous phase. In contrast, co-liquefaction with nylon 6 increases both the carbon and nitrogen recovered in the aqueous phase materials, predominantly due to the formation of water-soluble caprolactam, which is also present in the oil phase products.



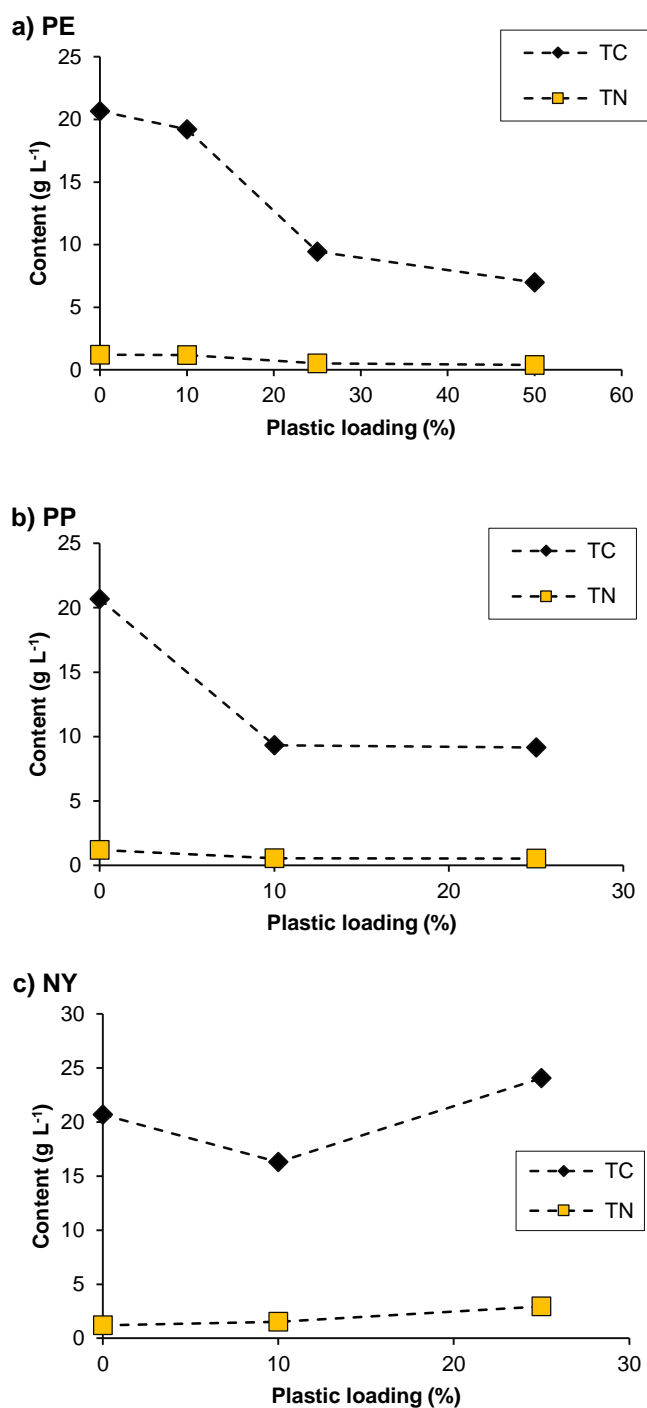


Figure 4.2-8 – Elemental composition of aqueous phases produced from liquefaction of *L. digitata* blended with a) PE, b) PP and c) nylon 6

#### 4.2.4.4 Gas phase products

The effect of incorporating plastics into the HTL feedstock on the gas phase products was assessed using GC-MS. The total volumes of the gas phase were only modestly affected in most cases. For the liquefaction of 75:25 blends of *L. digitata* with polyethylene, polypropylene and nylon 6, the gas phase was composed of 96 wt.% CO<sub>2</sub>.

Polyethylene is a highly thermally stable polymer, and thermal degradation tends to result in fragmentation into shorter olefinic fragments *via* a random scission mechanism, and, although monomer production tends to be low, [43], co-liquefaction with polyethylene led to a modest increase in the production of ethene, as well as ethane, propene, propane and 1,2-dimethylcyclopropane. For co-liquefaction with polypropylene, a notable increase in the production of propane was observed. In addition to undergoing scission to olefinic fragments of varying sizes [51], polypropylene can be thermally depolymerised to its monomeric form *via* a radical mechanism [43], giving rise to propylene fragments. This radical depolymerisation may be accelerated by the presence of biomass ash. An increase in the production of acetaldehyde and acetone was also observed. Somewhat surprisingly, co-liquefaction of *L. digitata* with nylon 6 did not appear to contribute to an increase in volatile nitrogenous species. A table of gas phase product compositions may be found in the Supplementary Information.

#### ***4.2.4.5 Conversion of marine plastics***

Synergistic effects on bio-crude production were evident, but it was unclear to what extent the plastic reacted, and how it was partitioned between the product phases. To determine the amount of plastic-derived (<sup>14</sup>C-free, radiocarbon 'dead') carbon in the bio-crude, the <sup>14</sup>C content was determined by accelerator mass spectrometry (Figure 4.2-9). A simple two-phase mixing model was employed based on plastic-derived C containing no <sup>14</sup>C and using 100% LD bio-crude as the biomass C endmember. With increasing plastic blends, an increasing level of fossil carbon (originating from plastics) partitioned to the bio-crude products. For polyethylene, approximately 7 % of the total carbon in the plastic feedstock was converted to bio-crude products at each blend level, constituting up to 41 % of the total bio-crude carbon content for a 50 % blend. For polypropylene, 7 % of the plastic carbon was converted to bio-crude products at a 10 % blend level, although this decreased to only 4 % conversion at a 25 % blend. In each case, the presence of biomass facilitated the conversion of plastic to bio-crude products, but the presence of plastic caused a modest decrease in the conversion of biomass.

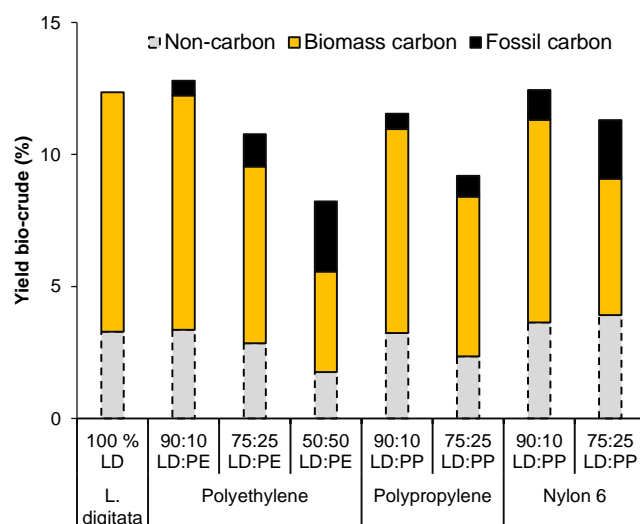


Figure 4.2-9 – Distribution of biogenic carbon, fossil (plastic) carbon, and other elements in bio-crude oils produced from co-liquefaction of *L. digitata* with plastics

For both PP and PE, low levels of volatiles were observed in the gas phase products, whilst aqueous phase carbon levels were depleted with decreasing biomass in the feedstock. It therefore seems likely that any reacted plastics either partitioned to the bio-crude, or were converted to solid char, while the remaining unreacted plastics also partitioning to the solid phase (Table 4.2-2).

Table 4.2-2 – Distribution of carbon from the initial plastic into the bio-crude phase

Plastic	Initial plastic loading (wt %)	Plastic C partitioning to bio-crude (%)
PE	10	7.7
PE	25	6.7
PE	50	7.3
PP	10	6.8
PP	25	3.7
NY	10	18.0
NY	25	14.2

Whilst it is difficult to quantify exactly what proportion of the alkane polymers reacted under HTL conditions, TGA of the solid phase is indicative.

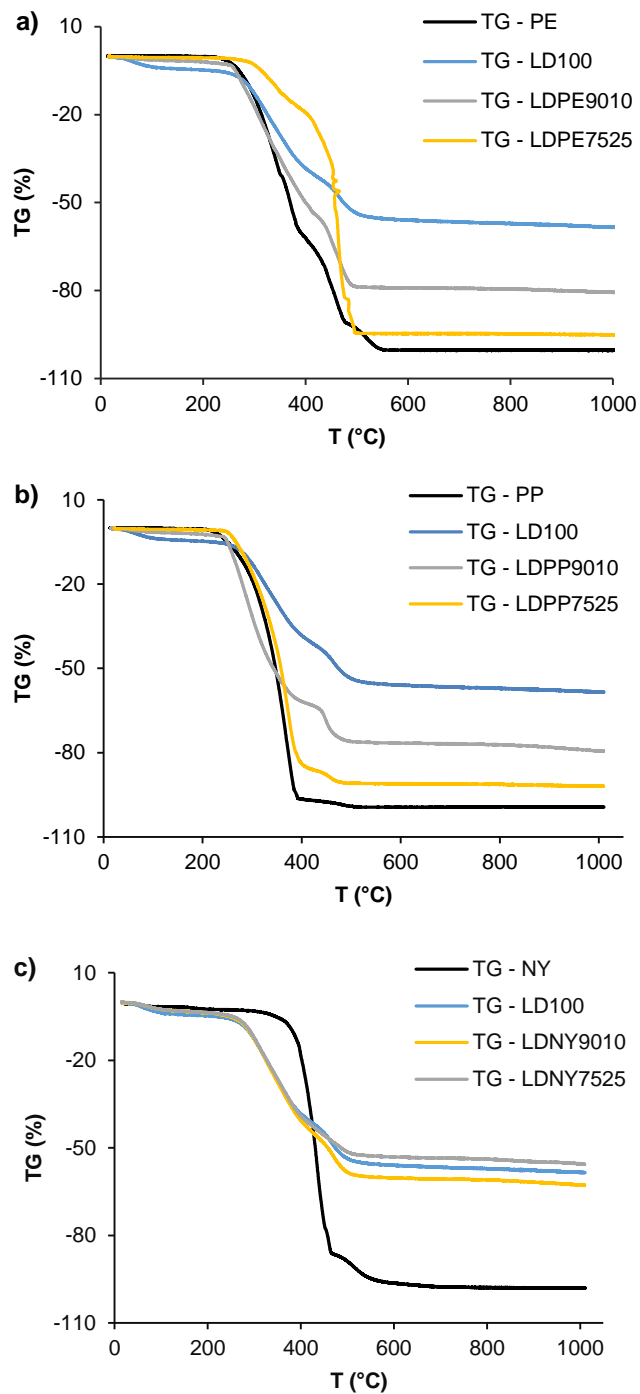


Figure 4.2-10 – TGA of pure plastics and solid phase products from co-liquefaction of *L. digitata* with plastics<sup>G</sup>

A degradation peak observed at around 400 °C is present for the solid phase from HTL of pure *L. digitata*, but the rate of degradation for pure polyethylene is substantially higher (Figure 4.2-10). For the solid phase samples from the macroalgae/plastic blended feeds, the rate of degradation increases progressively with increasing plastic blend, suggesting

<sup>G</sup> Please refer to Appendix 4B

that there is a substantial quantity of unreacted polyethylene in the solids. For polypropylene, almost no degradation is seen within the 400–500 °C range, unlike for the solid phase from HTL of *L. digitata*. With increasing polypropylene blend levels, degradation between 400 and 500 °C becomes less pronounced, suggesting that unreacted polypropylene is present. This suggests that while more of the polymers break down under HTL conditions with macroalgae present, a significant proportion of the plastic retains some of its macrostructure and remains in the solid phase.

However, for nylon 6, the TGA profiles of the solid phases from liquefaction of *L. digitata* alone and with 10 % and 25 % blends are almost identical, and markedly different to the TGA curve for pure nylon 6. This indicates that, although some carbon of fossil origin does indeed partition to the solid phase products for nylon 6 co-liquefaction, it is highly unlikely to be in the form of unreacted polymeric or oligomeric species, but has instead been incorporated into the solid phase products in the form of new molecules.

The caprolactam depolymerisation product is soluble in both aqueous and bio-crude phases, and a large increase in TOC in the aqueous phase is observed on increasing nylon content in the feed. At both 10 % and 25 % blend levels, approximately 14 % of the total fossil carbon was found to have partitioned to the solid phase, whereas 18 % of the fossil carbon partitioned to the bio-crude phase at the 10 % blend level, decreasing slightly to 14 % at a 25 % blend level. In both cases, 13–14 % of the plastic carbon partitioned to the solid phase, with 68 % and 73 % remaining dissolved in the aqueous phase products (Figure 4.2-11).

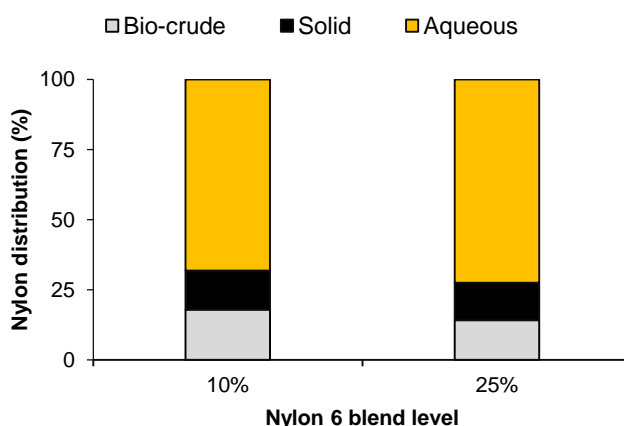


Figure 4.2-11 – Distribution of nylon 6 between HTL product phases

Alkane contaminants in found in harvested marine biomass will likely partition into the solid phase on HTL processing, with minimal conversion into bio-crude, but waste biomass rich in nylon 6 (commonly originating from fishing line and nets) presents a promising source of value through the recovery of caprolactam from the aqueous phase.

#### 4.2.4.6 Co-liquefaction of alternative macroalgae species with plastics

Having examined the effect of co-processing of *L. digitata* with plastics in detail, co-liquefaction of PE, PP and nylon 6 was also carried out with the brown macroalgae *Fucus serratus* and *Sargassum muticum* and the green macroalga *Ulva lactuca*.

In general, on the addition of PE overall mass yields of bio-crude tended to decrease, or stay approximately constant. A modest increase in yield was observed for a 10 % blend of PE with *S. muticum*, whilst decreases in overall bio-crude production were observed for 25 % blends of PE with all three feedstocks. The majority of the PE was recovered in the solid phase products, with char yields increasing concomitantly with bio-crude depletion. Aqueous phase product recovery declined for *F. serratus* and *U. lactuca*, although a modest increase in aqueous phase products was observed for both 10 % and 25 % blends of PE with *S. muticum*. For all three macroalgae, increasing PE blend levels also caused a modest increase in the yield of gas phase products.

A similar pattern of results was observed for PP: bio-crude yields stayed constant for 10 % blends of PP with *F. serratus* and *U. lactuca*, and were depleted relative to liquefaction of pure biomass in all other cases. Total bio-crude yields were also depleted for 25 % blends of PP.

For co-liquefaction with nylon 6, however, both 10 % and 25 % blend levels led to an increase in bio-crude production relative to pure biomass, although the increase in bio-crude yield was not linear: an initial increase from 7.8 % to 10.3 % bio-crude for a 10 % blend of *F. serratus* with nylon 6 was only boosted to 10.9 % at the 25 % blend level. Similar effects were observed for *U. lactuca* (an initial increase from 16.0 % to 19.9 %, followed by a modest bio-crude yield increase to 20.1 %), whereas for *S. muticum*, yields of 4.9, 7.5 and 7.3 % were observed for pure biomass, and 10 % and 25 % blend levels, respectively.

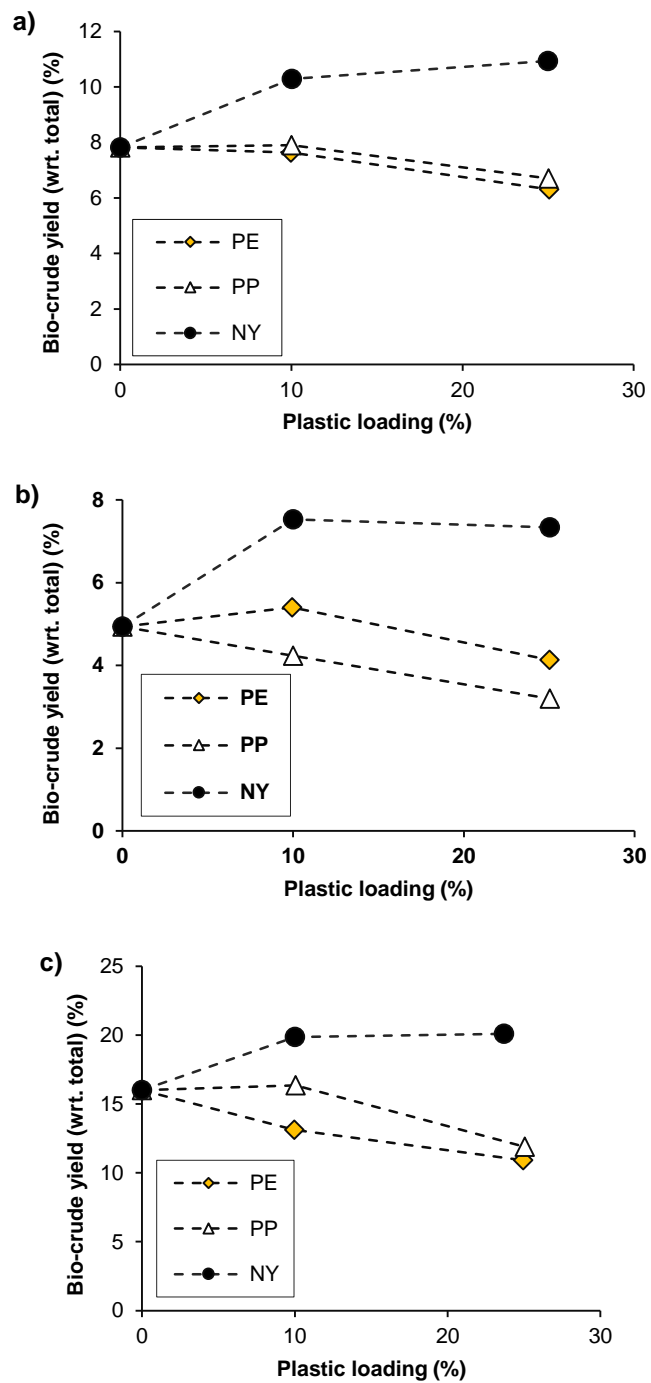


Figure 4.2-12 – Bio-crude yields from liquefaction of blended macroalgae/plastic feedstocks; a) *F. serratus*, b) *S. muticum*, c) *U. lactuca*. (PE = polyethylene, PP = polypropylene, NY = nylon 6).

The synergistic effects of co-processing are presented in Figure 4.2-13; full product mass balances are presented in the Supplementary Information.

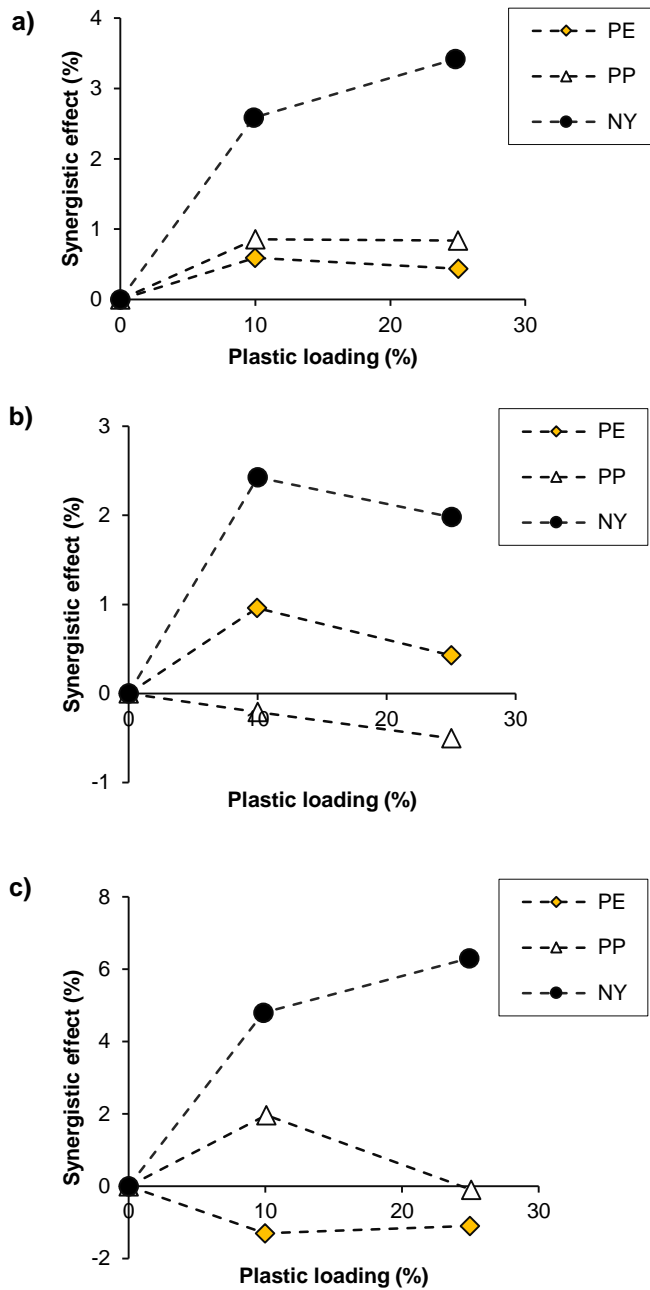


Figure 4.2-13 – Synergistic effects on bio-crude yields from liquefaction of blended macroalgae/plastic feedstocks; a) *F. serratus*, b) *S. muticum*, c) *U. lactuca*. (PE = polyethylene, PP = polypropylene, NY = nylon 6).

The degree of synergistic effects for co-liquefaction of each of the three macroalgae species with PE and PP was variable, but for the most part, relatively modest, limited to  $\pm 1$  %. Positive synergistic effects were observed for the co-liquefaction of PE with *F. serratus* and *S. muticum*, whilst a detrimental effect was observed for *U. lactuca*. For PP, positive synergistic effects on bio-crude production were observed for *F. serratus* and *U. lactuca*, but not for *S. muticum*. However, for nylon 6, synergistic effects were strongly



positive in all instances, with a maximum synergistic effect of 7.9 % for a 1:3 blend of *U. lactuca* with nylon.

#### **4.2.5 Conclusions**

Plastic pollution is ubiquitous throughout the marine environment. Any large-scale industrial biorefinery process exploiting marine biomasses will therefore be exposed to fluctuating quantities of plastic of diverse composition. In this study, the effect of common marine plastic pollutants on hydrothermal liquefaction of four UK macroalgae species was assessed. Polyethylene, polypropylene and nylon 6 were found to interact with biomass under HTL conditions: plastic reactivity in subcritical water was enhanced by the presence of reactive biomass fragments, and, rather than inhibiting the process, synergistic effects were observed. The presence of plastics in macroalgal HTL feedstocks led to compositional changes in the resulting bio-crudes, giving an overall improvement in bio-crude fuel properties for polyethylene and polypropylene, but a decrease in total energy content and an increase in nitrogen for nylon 6. Polyethylene, unreactive under HTL conditions in isolation, was found to partially fragment into long-chain hydrocarbons and undergo oxidative depolymerisation to contribute long-chain ketones to the bio-crude products when processed alongside biomass, though less than 10 % of the polymer deposited into this phase. Alternatively, nylon 6 almost entirely depolymerised to monomeric caprolactam. Co-processing of plastics alongside marine biomass can serve the purpose of improving bio-crude energy content, but the presence of heteroatoms, such as nitrogen in nylon, may necessitate additional steps in bio-crude pre-processing prior to utilisation as a fuel. Considering the simplicity of nylon depolymerisation, separation of nylon-based marine litter for regeneration of caprolactam may present an additional lucrative revenue stream. Rather than being regarded as problematic contaminants of marine-derived biomasses to be tolerated reluctantly in a biorefinery setting, plastics represent an interesting opportunity to further improve on the process economics. Indeed, the controlled addition of waste plastics to farmed or opportunistically harvested macroalgal biomasses prior to their conversion via HTL may ultimately prove a useful tool in dealing with the plastic problem blighting the 21<sup>st</sup> century.

#### **4.2.6 Conflicts of interest**

There are no conflicts to declare.

#### **4.2.7 Acknowledgments**

The project has been partially supported by the EPSRC through the Centre for Doctoral Training in Sustainable Chemical Technologies (EP/L016354/1) and by the Roddenberry Foundation Catalyst Fund grant 'SeaClean' awarded to the corresponding authors.

#### 4.2.8 References

- [1] A. Ross, J. Jones, M. Kubacki, T. Bridgeman, Classification of macroalgae as fuel and its thermochemical behaviour, *Bioresour. Technol.* 99 (2008) 6494–6504. doi:10.1016/j.biortech.2007.11.036.
- [2] K. Kumar, S. Ghosh, I. Angelidaki, S.L. Holdt, B. Karakashev, M.A. Morales, D. Das, D.B. Karakashev, M.A. Morales, D. Das, Recent developments on biofuels production from microalgae and macroalgae, *Renew. Sustain. Energy Rev.* 65 (2016) 235–249. doi:10.1016/j.rser.2016.06.055.
- [3] P. Biller, A.B. Ross, Hydrothermal processing of algal biomass for the production of biofuels and chemicals, *Biofuels*. 3 (2012) 603–623. doi:10.4155/bfs.12.42.
- [4] Y. Lehahn, K.N. Ingle, A. Golberg, Global potential of offshore and shallow waters macroalgal biorefineries to provide for food, chemicals and energy: feasibility and sustainability, *Algal Res.* 17 (2016) 150–160. doi:10.1016/j.algal.2016.03.031.
- [5] P. Stévant, C. Rebours, A. Chapman, Seaweed aquaculture in Norway: recent industrial developments and future perspectives, *Aquac. Int.* 25 (2017) 1373–1390. doi:10.1007/s10499-017-0120-7.
- [6] L. Watson<sup>1</sup>, F. O 'mahony, M. Edwards, M.L. Dring, A. Werner, The Economics of Seaweed Aquaculture in Ireland *Laminaria digitata* and *Palmaria palmata*, (n.d.). [https://www.was.org/documents/MeetingPresentations/AQUA2012/AQUA2012\\_0540.pdf](https://www.was.org/documents/MeetingPresentations/AQUA2012/AQUA2012_0540.pdf) (accessed August 16, 2017).
- [7] J.-B.E. Thomas, J. Nordström, E. Risén, M.E. Malmström, F. Gröndahl, The perception of aquaculture on the Swedish West Coast, *Ambio*. 47 (2018) 398–409. doi:10.1007/s13280-017-0945-3.
- [8] C. Rebours, E. Marinho- Soriano, J.A. Zertuche- González, L. Hayashi, J.A. Vásquez, P. Kradolfer, G. Soriano, R. Ugarte, M.H. Abreu, I. Bay- Larsen, Seaweeds: an opportunity for wealth and sustainable livelihood for coastal communities, *J. Appl. Phycol.* 26 (2014) 1939–1951.
- [9] M. Troell, C. Halling, A. Nilsson, A.H. Buschmann, N. Kautsky, L. Kautsky, Integrated marine cultivation of *Gracilaria chilensis* (Gracilariales, Rhodophyta) and salmon cages for reduced environmental impact and increased economic output, *Aquaculture*. 156 (1997) 45–61. doi:doi:10.1016/S0044-8486(97)00080-X.
- [10] S.G. Nelson, E.P. Glenn, J. Conn, D. Moore, T. Walsh, M. Akutagawa, Cultivation of *Gracilaria parvispora* (Rhodophyta) in shrimp-farm effluent ditches and floating

- cages in Hawaii: a two-phase polyculture system, *Aquaculture*. 193 (2001) 239–248. doi:doi:10.1016/S0044-8486(00)00491-9.
- [11] Ole Jacob Broch, Ingrid Helene Ellingsen, Silje Forbord, Xinxin Wang, Zsolt Volent, Morten Omholt Alver, Aleksander Handå, Kjersti Andresen<sup>3</sup>, Dag Slagstad, Kjell Inge Reitan, Yngvar Olsen, Jorunn Skjermo, Modelling the cultivation and bioremediation potential of the kelp *Saccharina latissima* in close proximity to an exposed salmon farm in Norway, *Aquac. Environ. Interact.* 4 (2013) 187–206. doi:10.3354/aei00080.
- [12] T. Chopin, C. Yarish, R. Wilkes, E. Belyea, S. Lu, A.-T. Mathieson, Developing *Porphyra*/salmon integrated aquaculture for bioremediation and diversification of the aquaculture industry, *J. Appl. Phycol.* 11 (1999) 463–472. <https://link.springer.com/content/pdf/10.1023%2FA%3A1008114112852.pdf> (accessed April 19, 2018).
- [13] J.C. Sanderson, M.J. Dring, K. Davidson, M.S. Kelly, Culture, yield and bioremediation potential of *Palmaria palmata* (Linnaeus) Weber & Mohr and *Saccharina latissima* (Linnaeus) C.E. Lane, C. Mayes, Druehl & G.W. Saunders adjacent to fish farm cages in northwest Scotland, *Aquaculture*. 354–355 (2012) 128–135. doi:10.1016/j.aquaculture.2012.03.019.
- [14] A.H. Buschmann, D.A. Varela, M.C. Hernández-González, P. Huovinen, Opportunities and challenges for the development of an integrated seaweed-based aquaculture activity in Chile: determining the physiological capabilities of *Macrocystis* and *Gracilaria* as biofilters, (2008). doi:10.1007/s10811-007-9297-x.
- [15] A.A. Koelmans, T. Gouin, R. Thompson, N. Wallace, C. Arthur, Plastics in the marine environment, *Environ. Toxicol. Chem.* 33 (2014) 5–10. doi:10.1002/etc.2426.
- [16] T. Bruton, H. Lyons, Y. Lerat, M. Stanley, M.B. Rasmussen, A Review of the Potential of Marine Algae as a Source of Biofuel in Ireland (report prepared for Sustainable Energy Ireland), (2009) 1–88. [http://www.seai.ie/Publications/Renewables\\_Publications\\_/Bioenergy/Algaereport.pdf](http://www.seai.ie/Publications/Renewables_Publications_/Bioenergy/Algaereport.pdf) (accessed January 1, 2016).
- [17] M. Ghadiryanfar, K.A. Rosentrater, A. Keyhani, M. Omid, A review of macroalgae production, with potential applications in biofuels and bioenergy, *Renew. Sustain. Energy Rev.* 54 (2016) 473–481. doi:10.1016/j.rser.2015.10.022.
- [18] F.E. Possatto, M. Barletta, M.F. Costa, J.A. Ivar Do Sul, D. V Dantas, Plastic

- debris ingestion by marine catfish: An unexpected fisheries impact, *Mar. Pollut. Bull.* 62 (2011) 1098–1102. doi:10.1016/j.marpolbul.2011.01.036.
- [19] M. Eriksen, L.C.M. Lebreton, H.S. Carson, M. Thiel, C.J. Moore, J.C. Borerro, F. Galgani, P.G. Ryan, J. Reisser, Plastic Pollution in the World's Oceans: More than 5 Trillion Plastic Pieces Weighing over 250,000 Tons Afloat at Sea, *PLoS One.* 9 (2014) 1–15. doi:10.1371/journal.pone.0111913.
- [20] M. Claessens, S. De Meester, L. Van Landuyt, K. De Clerck, C.R. Janssen, Occurrence and distribution of microplastics in marine sediments along the Belgian coast, *Mar. Pollut. Bull.* 62 (2011) 2199–2204. doi:10.1016/j.marpolbul.2011.06.030.
- [21] L. Gutow, A. Eckerlebe, L. Gimeez, R. Saborowski, Experimental Evaluation of Seaweeds as a Vector for Microplastics into Marine Food Webs, *Environ. Sci. Technol.* 50 (2016) 915–923. doi:10.1021/acs.est.5b02431.
- [22] M. Bergmann, L. Gutow, M. Klages, *Marine Anthropogenic Litter*, Springer International Publishing, 2015. doi:10.1007/978-3-319-16510-3.
- [23] K. Kositkanawuth, A. Bhatt, M. Sattler, B. Dennis, Renewable Energy from Waste: Investigation of Co-pyrolysis between Sargassum Macroalgae and Polystyrene, *Energy & Fuels.* 31 (2017) 5088–5096. doi:10.1021/acs.energyfuels.6b03397.
- [24] X. Wu, Y. Wu, K. Wu, Y. Chen, H. Hu, M. Yang, Study on pyrolytic kinetics and behavior: The co-pyrolysis of microalgae and polypropylene, *Bioresour. Technol.* 192 (2015) 522–528. doi:10.1016/j.biortech.2015.06.029.
- [25] X. Yuan, H. Cao, H. Li, G. Zeng, J. Tong, L. Wang, Quantitative and qualitative analysis of products formed during co-liquefaction of biomass and synthetic polymer mixtures in sub- and supercritical water, *Fuel Process. Technol.* 90 (2009) 428–434. doi:10.1016/j.fuproc.2008.11.005.
- [26] X. Wu, J. Liang, Y. Wu, H. Hu, S. Huang De, K. Wu, Co-liquefaction of microalgae and polypropylene in sub-/super-critical water, *RSC Adv.* 7 (2017) 13768. doi:10.1039/c7ra01030c.
- [27] X. Pei, X. Yuan, G. Zeng, H. Huang, J. Wang, H. Li, H. Zhu, Co-liquefaction of microalgae and synthetic polymer mixture in sub- and supercritical ethanol, *Fuel Process. Technol.* 93 (2012) 35–44. doi:10.1016/j.fuproc.2011.09.010.
- [28] M. Coma, E. Martinez Hernandez, F. Abeln, S. Raikova, J. Donnelly, T.C. Arnot, M. Allen, D.D. Hong, C.J. Chuck, Organic waste as a sustainable feedstock for platform chemicals, *Faraday Discuss.* 202 (2017) 175–195.

doi:10.1039/C7FD00070G.

- [29] P. Biller, A.B. Ross, Potential yields and properties of oil from the hydrothermal liquefaction of microalgae with different biochemical content, *Bioresour. Technol.* 102 (2011) 215–25. doi:10.1016/j.biortech.2010.06.028.
- [30] J. Wagner, R. Bransgrove, T.A. Beacham, M.J. Allen, K. Meixner, B. Drosig, V.P. Ting, C.J. Chuck, Co-production of bio-oil and propylene through the hydrothermal liquefaction of polyhydroxybutyrate producing cyanobacteria, *Bioresour. Technol.* 207 (2016) 166–174. doi:10.1016/j.biortech.2016.01.114.
- [31] S. Raikova, H. Smith-Baedorf, R. Bransgrove, O. Barlow, F. Santomauro, J.L. Wagner, M.J. Allen, C.G. Bryan, D. Sapsford, C.J. Chuck, Assessing hydrothermal liquefaction for the production of bio-oil and enhanced metal recovery from microalgae cultivated on acid mine drainage, *Fuel Process. Technol.* 142 (2016) 219–227. doi:10.1016/j.fuproc.2015.10.017.
- [32] S.A.A. Channiwala, P.P.P. Parikh, A unified correlation for estimating HHV of solid, liquid and gaseous fuels, *Fuel*. 81 (2002) 1051–1063. doi:10.1016/S0016-2361(01)00131-4.
- [33] L. Wacker, M. Němec, J. Bourquin, A revolutionary graphitisation system: Fully automated, compact and simple, *Nucl. Instruments Methods Phys. Res. Sect. B Beam Interact. with Mater. Atoms.* 268 (2010) 931–934.
- [34] L. Wacker, M. Christl, H.-A. Synal, BATS: A new tool for AMS data reduction, *Nucl. Instruments Methods Phys. Res. Sect. B Beam Interact. with Mater. Atoms.* 268 (2010) 976–979.
- [35] T. Moriya, H. Enomoto, Characteristics of polyethylene cracking in supercritical water compared to thermal cracking, *Polym. Degrad. Stab.* 65 (1999) 373–386. [https://ac.els-cdn.com/S0141391099000269/1-s2.0-S0141391099000269-main.pdf?\\_tid=dcec67c7-0ccf-48bf-926a-526962899a5b&acdnat=1532020397\\_ab7d5d1d0e285f7f4e19803e818ee590](https://ac.els-cdn.com/S0141391099000269/1-s2.0-S0141391099000269-main.pdf?_tid=dcec67c7-0ccf-48bf-926a-526962899a5b&acdnat=1532020397_ab7d5d1d0e285f7f4e19803e818ee590) (accessed July 19, 2018).
- [36] M. Watanabe, H. Hirakoso, S. Sawamoto, T. Adschiri, K. Arai, Polyethylene conversion in supercritical water, 1998. [https://ac.els-cdn.com/S0896844698000588/1-s2.0-S0896844698000588-main.pdf?\\_tid=125be9de-1a3b-464e-bacf-6569c77245ef&acdnat=1535717088\\_35551cc0a82adac56110ad8aa4146f6d](https://ac.els-cdn.com/S0896844698000588/1-s2.0-S0896844698000588-main.pdf?_tid=125be9de-1a3b-464e-bacf-6569c77245ef&acdnat=1535717088_35551cc0a82adac56110ad8aa4146f6d) (accessed August 31, 2018).

- [37] F. Bai, C.-C. Zhu, Y. Liu, P.-Q. Yuan, Z.-M. Cheng, W.-K. Yuan, Co-pyrolysis of residual oil and polyethylene in sub- and supercritical water, *Fuel Process. Technol.* 106 (2013) 267–274. doi:10.1016/j.fuproc.2012.07.031.
- [38] T. Iwaya, M. Sasaki, M. Goto, Kinetic analysis for hydrothermal depolymerization of nylon 6, *Polym. Degrad. Stab.* 91 (2006) 1989–1995. doi:10.1016/j.polymdegradstab.2006.02.009.
- [39] CRC, Physical Constants of Organic Compounds, in: J.R. Rumble (Ed.), *CRC Handb. Chem. Phys. (Internet Version 2018)*, 99th Edition, CRC Press/Taylor & Francis, Boca Raton, FL, 2018.
- [40] H.-S. Shin, H.-S. Ahn, D.-G. Jung, Determination of Phenolic Antioxidants in Spilled Aviation Fuels by Gas Chromatography-Mass Spectrometry, *Chromatographia*. 58 (2003) 495–499. doi:10.1365/s10337-003-0079-6.
- [41] S. Raikova, C.D. Le, T.A. Beacham, R.W. Jenkins, M.J. Allen, C.J. Chuck, Towards a marine biorefinery through the hydrothermal liquefaction of macroalgae native to the United Kingdom, *Biomass and Bioenergy*. 107 (2017) 244–253. doi:10.1016/j.biombioe.2017.10.010.
- [42] S. Raikova, J. Olsson, J. Mayers, G. Nylund, E. Albers, C.J. Chuck, Effect of geographical location on the variation in products formed from the hydrothermal liquefaction of *Ulva intestinalis*, *Energy & Fuels*. (2018) Accepted manuscript. doi:10.1021/acs.energyfuels.8b02374.
- [43] B. Singh, N. Sharma, Mechanistic implications of plastic degradation, *Polym. Degrad. Stab.* 93 (2008) 561–584. doi:10.1016/j.polymdegradstab.2007.11.008.
- [44] J.L. Faeth, P.J. Valdez, P.E. Savage, Fast Hydrothermal Liquefaction of *Nannochloropsis* sp. To Produce Biocrude, *Energy & Fuels*. 27 (2013) 1391–1398. doi:10.1021/ef301925d.
- [45] B. Zhang, M. von Keitz, K. Valentas, Thermal Effects on Hydrothermal Biomass Liquefaction, *Appl. Biochem. Biotechnol.* 147 (2008) 143–150.
- [46] D.K. Ojha, R. Vinu, Copyrolysis of Lignocellulosic Biomass With Waste Plastics for Resource Recovery, in: A. Pandey, T. Bhaskar, S.V. Mohan, D.-J. Lee, S.K. Khanal (Eds.), *Waste Biorefinery Potential Perspect.*, 1st ed., Elsevier B.V., Amsterdam, Netherlands, 2018: p. 381.
- [47] S.L. Wong, N. Ngadi, N.A.S. Amin, T.A.T. Abdullah, I.M. Inuwa, Pyrolysis of low density polyethylene waste in subcritical water optimized by response surface methodology, *Environ. Technol.* 37 (2016) 245–254.

doi:10.1080/09593330.2015.1068376.

- [48] K.R. Arturi, S. Kucheryavskiy, E.G. Søgaaard, Performance of hydrothermal liquefaction (HTL) of biomass by multivariate data analysis, *Fuel Process. Technol.* 150 (2016) 94–103. doi:10.1016/j.fuproc.2016.05.007.
- [49] P. George, E.K. Rideal, A. Robertson, The Oxidation of Liquid Hydrocarbons. I. The Chain Formation of Hydroperoxides and Their Decomposition, *Source Proc. R. Soc. London. Ser. A, Math. Phys. Sci.* 185 (1946) 288–309. <https://about.jstor.org/terms> (accessed July 24, 2018).
- [50] C.T. Barkby, G. Lawson, Analysis of migrants from nylon 6 packaging films into boiling water, *Food Addit. Contam.* 10 (1993) 541–553. doi:10.1080/02652039309374177.
- [51] J. Aguado, D. Serrano, G. San Miguel, European trends in the feedstock recycling of plastic wastes, *Glob. NEST J.* 9 (2007) 12–19. [https://journal.gnest.org/sites/default/files/Journal Papers/12-19\\_SAN\\_MIGUEL\\_432\\_9-1.pdf](https://journal.gnest.org/sites/default/files/Journal_Papers/12-19_SAN_MIGUEL_432_9-1.pdf) (accessed June 20, 2018).
- [52] K. Anastasakis, A.B. Ross, J.M. Jones, Pyrolysis behaviour of the main carbohydrates of brown macro-algae, *Fuel.* 90 (2011) 598–607. doi:10.1016/j.fuel.2010.09.023.



### 4.3 Supplementary information

Table S4.3-1 – Composition of gas phase products of hydrothermal liquefaction of *L. digitata* with plastics

Compound	100 % <i>L. digitata</i>	<i>L. digitata</i> + polyethylene	<i>L. digitata</i> + polypropylene	<i>L. digitata</i> + nylon 6
Methane	0.33	0.42	0.17	0.25
CO <sub>2</sub>	96.49	96.82	96.40	96.81
Ethene	0.15	0.18	0.00	0.11
Ethane	0.20	0.28	0.00	0.11
Ammonia	0.27	0.43	0.46	0.36
Propene	0.41	0.53	0.39	0.40
Propane	0.22	0.27	0.67	0.14
Acetaldehyde	0.27	0.04	0.00	0.49
1-Propene, 2-methyl-	0.23	0.14	0.00	0.05
1,3-Butadiene	0.13	0.52	0.46	0.00
Furan	0.00	0.00	0.16	0.20
Acetone	0.00	0.00	0.11	0.04
2-Pentene, (Z)-	0.19	0.00	0.18	0.00
Cyclopropane, 1,1-dimethyl-	0.12	0.00	0.17	0.00
Cyclopropane, 1,2-dimethyl-, cis-	0.25	0.37	0.25	0.22
Cyclopentene	0.08	0.00	0.14	0.09
Furan, 3-methyl-	0.00	0.00	0.08	0.65
Furan, 2-methyl-	0.43	0.00	0.19	0.00
1,4-Pentadiene, 2-methyl-	0.22	0.00	0.17	0.00

Table S4.3-2 – Identities of compounds identified in volatile portion of bio-crude oils

Plastic blend level	<i>L. digitata</i>		<i>L. digitata</i> + polyethylene			<i>L. digitata</i> + polypropylene		<i>L. digitata</i> + nylon 6	
	10 %	25 %	10 %	25 %	50 %	10 %	25 %	10 %	25 %
Piperidine, 1-ethyl-									
<i>p</i> -Xylene									
Styrene									
2,4-Dimethylfuran									
Butyrolactone									
2-Cyclopenten-1-one, 3-methyl-									
Phenol									
$\alpha$ -Methylstyrene									
2-Cyclopenten-1-one, 3,4-dimethyl-									
2-Cyclopenten-1-one, 2,3-dimethyl-									
Benzyl alcohol									
Phenol, 2-methyl									
<i>p</i> -Cresol									
2-Cyclopenten-1-one, 2,3,4-trimethyl-									
Mequinol (methoxyphenol)									
4-Pyridinol									
Phenylethyl alcohol									
Phenol, 3-amino-									
3-Pyridinol, 2-methyl-									
Phenol, 2-ethyl-									
Phenol, 3,5-dimethyl-									
2(1H)-Pyridinone, 3-methyl-									
Phenol, 2,4-dimethyl-									
3-Pyridinol, 6-methyl-									
Phenol, 4-ethyl-									
Phenol, 2,3-dimethyl-									
3-Pyridinol, 6-methyl-									
Phenol, 4-amino-									
Benzofuran, 2-ethenyl-									



2-Naphthalenamine, 3,4-dihydro-N,N- dimethyl-	█		
Cyclopentane, undecyl-		█	
1-Dodecanol, 2-octyl-		█	
Heptadecane	█	█	
1-Decene			█
Tetradecanoic acid	█	█	█
Tridecane		█	
2-Hexadecanone	█	█	
2-Hexadecene, 3,7,11,15-tetramethyl-, [R-[R*,R*-(E)]]-	█	█	█
Phytol, acetate	█	█	█
Cyclohexene, 1,5,5- trimethyl-6-acetylmethyl-		█	
Nonadecane	█	█	
(2Z,4E)-3,7,11- Trimethyl-2,4- dodecadiene		█	█
Dodecane		█	
n-Hexadecanoic acid	█	█	█
Heptadecane		█	
Eicosane		█	
Methyl n-hexadecyl ketone	█	█	
1-Eicosene		█	
2H-Benzocyclohepten- 2-one, 1,4a,5,6,7,8,9,9a- octahydro-4a-methyl-, trans-		█	
Oleanitrile	█	█	█
Hexadecane	█	█	
Methyl 7,9-tridecadienyl ether			█
1H-Indene, octahydro- 7a-methyl-1- (phenylmethylene)-			█
9-Octadecenoic acid, (E)-	█	█	



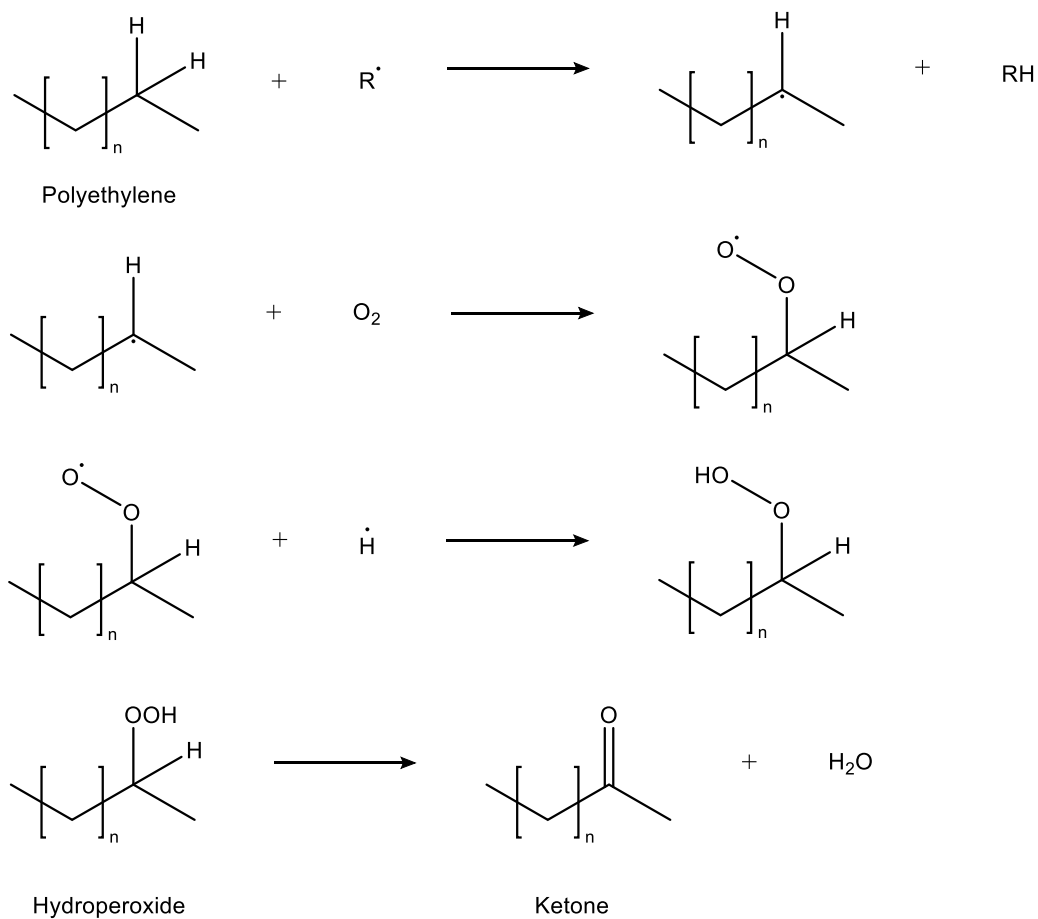
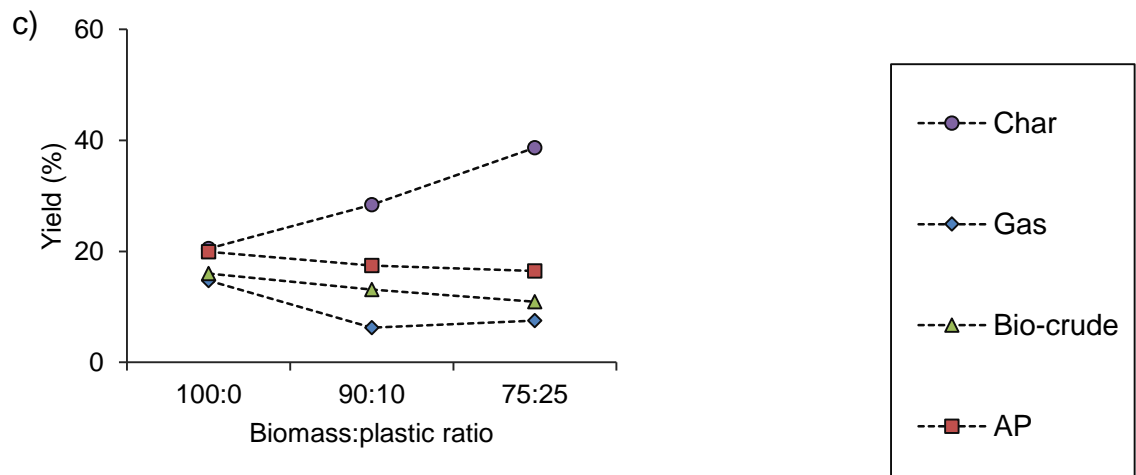
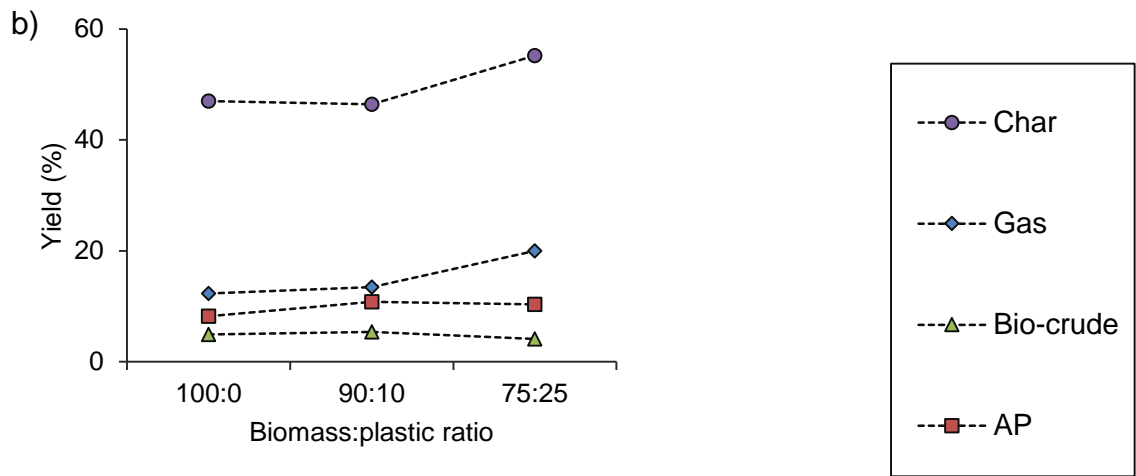
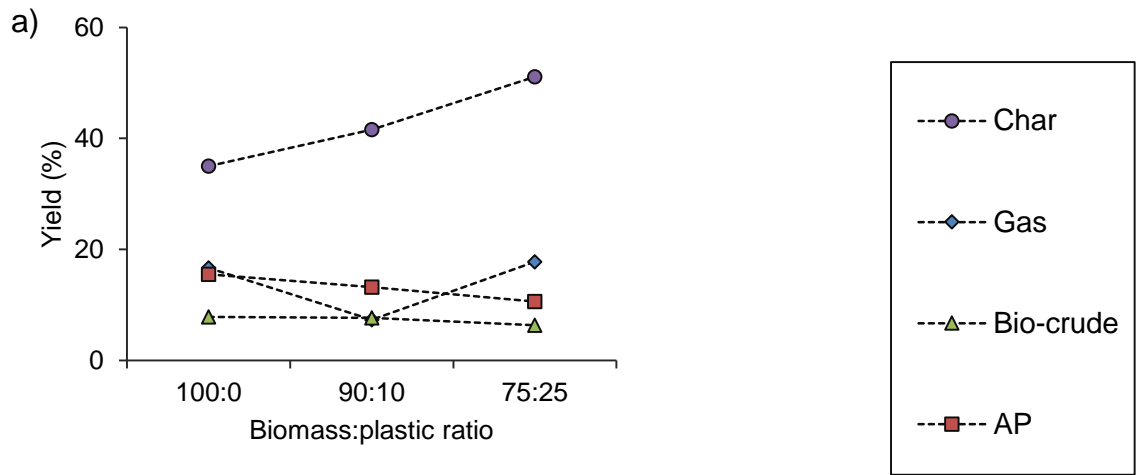
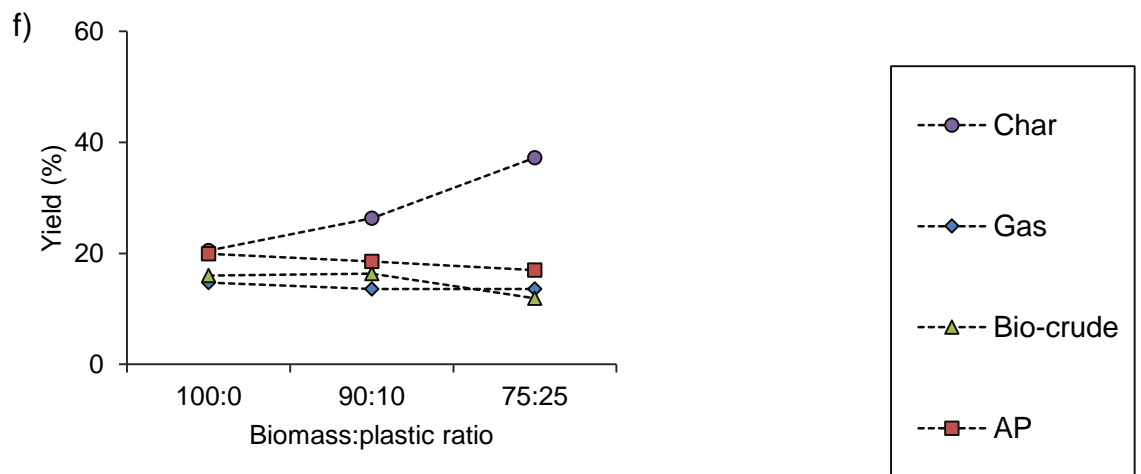
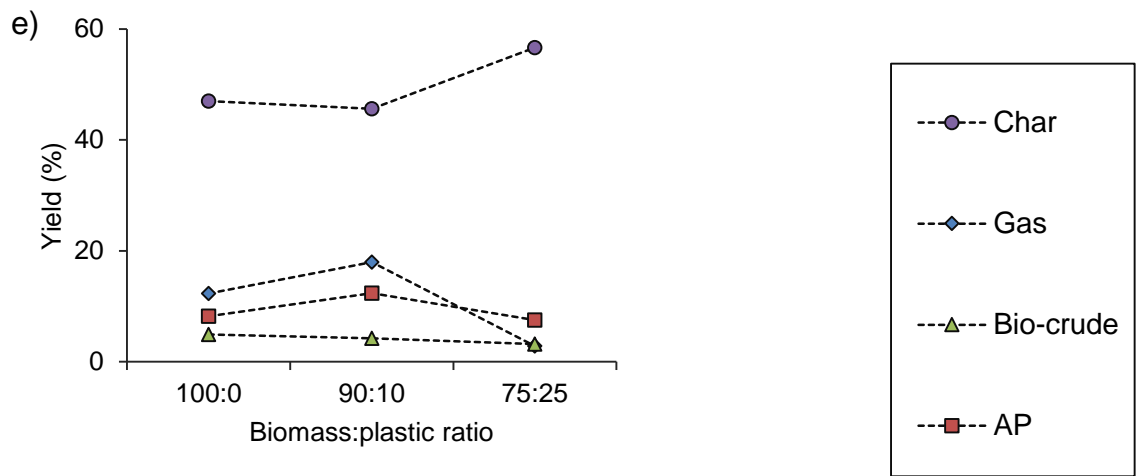
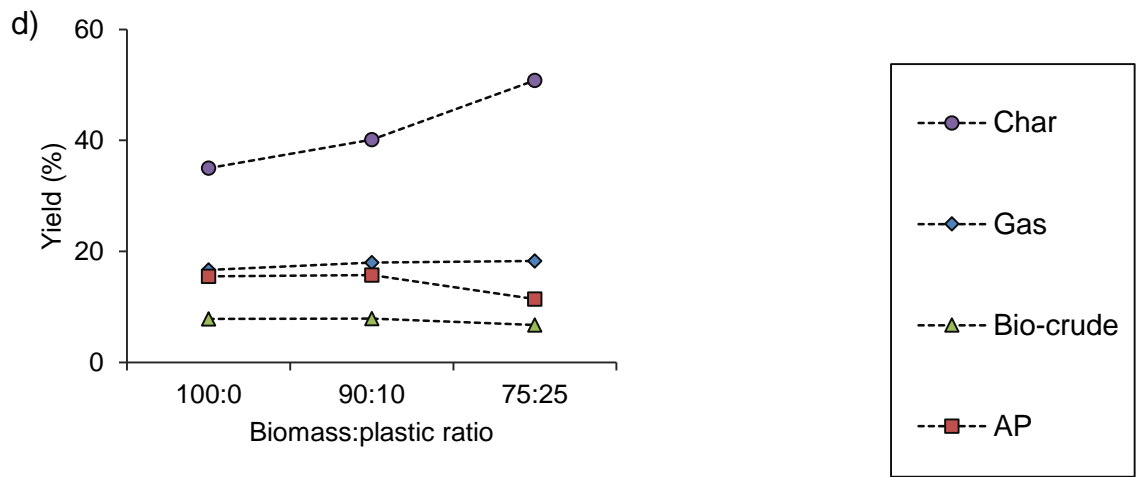


Figure S4.3-1 – Proposed radical mechanism of ketone formation from polyethylene under hydrothermal conditions







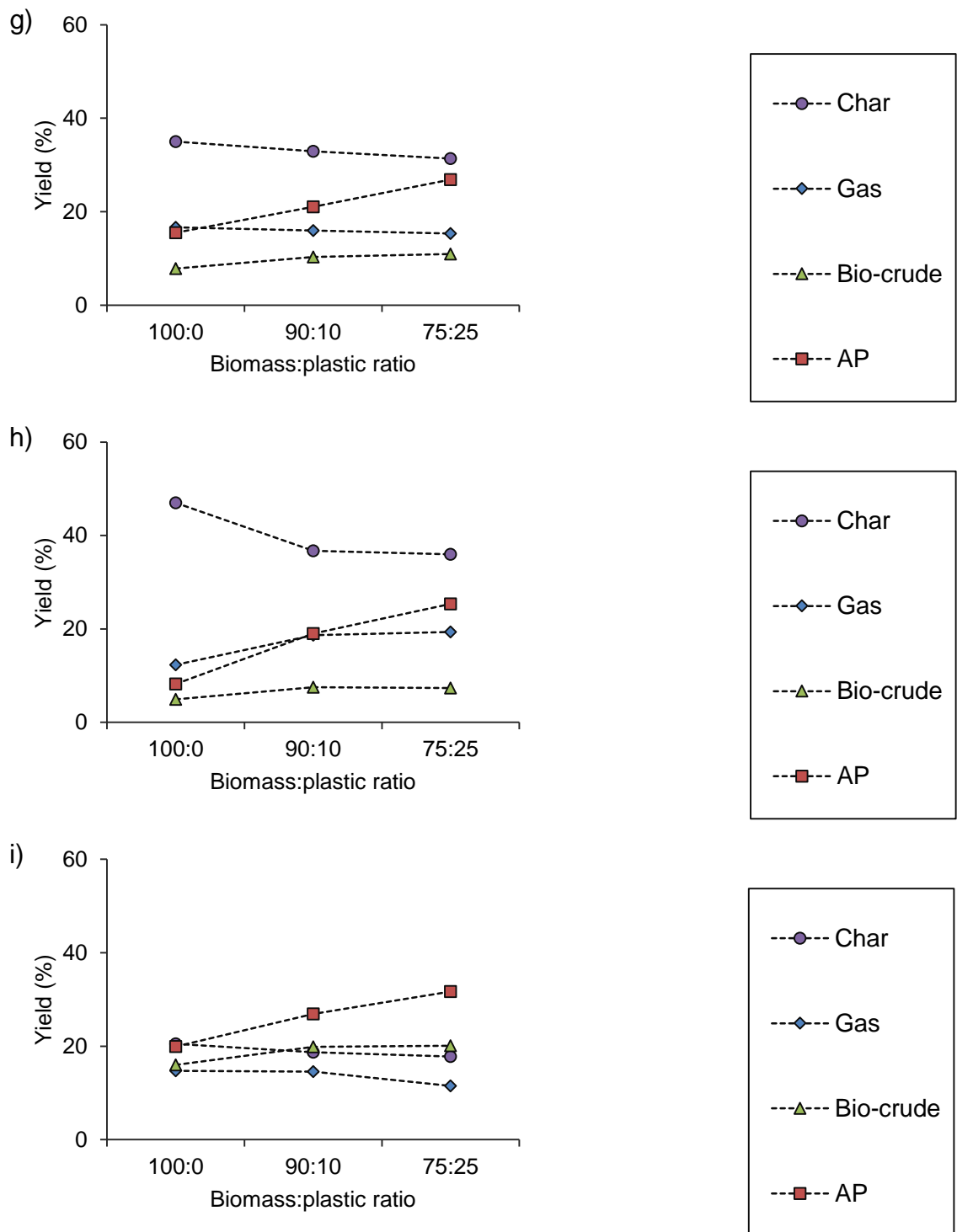


Figure S4.3-2 – Mass balances for hydrothermal liquefaction of marine macroalgae with plastics: a) *F. serratus*, b) *S. muticum* and c) *U. lactuca* with polyethylene; d) *F. serratus*, e) *S. muticum* and f) *U. lactuca* with polypropylene; g) *F. serratus*, h) *S. muticum* and i) *U. lactuca* with nylon 6

## 4.4 Appendices

### 4.4.1 Appendix 4A

Moriya *et al.* [13] propose that for the conversion of aliphatic hydrocarbons in supercritical water, alcohols are formed initially, and are converted to ketones through the liberation of  $\alpha$ -hydrogen from the alcohol intermediates (it is not specified whether the initial alcohol formation proceeds *via* a radical-mediated pathway). However, reaction mechanisms may differ between sub- and supercritical environments.

### 4.4.2 Appendix 4B

The multi-stage degradation of the HTL char observed by TGA may be partially attributable to unreacted biomass. The decomposition temperatures of major components of *L. digitata* are listed in Table 4.4-2.

Table 4.4-1 – Thermal characteristics of major components of *L. digitata* [12]

Component	Onset of degradation (°C)	Degradation peak 1 (°C)	Degradation peak 2 (°C)
Alginate acid	150	225	-
Mannitol	220	336	-
Laminarin	175	342	540
Fucoidan	175	202	710
Cellulose	175	369	-

For the solid phase products from HTL of pure *L. digitata*, degradation peaks at two temperatures: 330 °C and 450 °C. It is possible that the initial degradation peak at 330 °C may be attributable to unreacted laminarin (although unlikely to correspond to mannitol, which is water-soluble, and would have partitioned into the aqueous phase products). However, the second distinct degradation peak at 450 °C is speculated to result from degradation of newly formed species present in the solid phase products.

## 4.5 Context and appendix references

- [1] E. van Sebille, C. Spathi, A. Gilbert, The ocean plastic pollution challenge: towards solutions in the UK (Briefing paper No 19), London, 2016. [www.imperial.ac.uk/grantham/publications](http://www.imperial.ac.uk/grantham/publications) (accessed August 31, 2018).
- [2] UNEP, Press release: Plastic Waste Causes Financial Damage of US\$13 Billion to Marine Ecosystems Each Year as Concern Grows over Microplastics, 2014. <http://get.beatthemicrobead.org/> (accessed August 31, 2018).
- [3] UNEP, Valuing Plastics: The Business Case for Measuring, Managing and Disclosing Plastic Use in the Consumer Goods Industry, 2014. [www.unep.org/pdf/ValuingPlastic/](http://www.unep.org/pdf/ValuingPlastic/).
- [4] A. Dimitriadis, S. Bezergianni, Hydrothermal liquefaction of various biomass and waste feedstocks for biocrude production: A state of the art review, *Renew. Sustain. Energy Rev.* 68 (2017) 113–125. doi:10.1016/j.rser.2016.09.120.
- [5] B. Wang, Y. Huang, J. Zhang, Hydrothermal liquefaction of lignite, wheat straw and plastic waste in sub-critical water for oil: Product distribution, *J. Anal. Appl. Pyrolysis.* 110 (2014) 382–389. doi:10.1016/j.jaap.2014.10.004.
- [6] X. Yuan, H. Cao, H. Li, G. Zeng, J. Tong, L. Wang, Quantitative and qualitative analysis of products formed during co-liquefaction of biomass and synthetic polymer mixtures in sub- and supercritical water, *Fuel Process. Technol.* 90 (2009) 428–434. doi:10.1016/j.fuproc.2008.11.005.
- [7] H. Shui, Q. Jiang, Z. Cai, Z. Wang, Z. Lei, S. Ren, C. Pan, H. Li, Co-liquefaction of rice straw and coal using different catalysts, *Fuel.* 109 (2013) 9–13. doi:10.1016/j.fuel.2012.06.032.
- [8] Y. Shen, H. Wu, Z. Pan, Co-liquefaction of coal and polypropylene or polystyrene in hot compressed water at 360–430°C, *Fuel Process. Technol.* 104 (2012) 281–286. doi:10.1016/j.fuproc.2012.05.023.
- [9] F. Bai, C.-C. Zhu, Y. Liu, P.-Q. Yuan, Z.-M. Cheng, W.-K. Yuan, Co-pyrolysis of residual oil and polyethylene in sub- and supercritical water, *Fuel Process. Technol.* 106 (2013) 267–274. doi:10.1016/j.fuproc.2012.07.031.
- [10] X. Pei, X. Yuan, G. Zeng, H. Huang, J. Wang, H. Li, H. Zhu, Co-liquefaction of microalgae and synthetic polymer mixture in sub- and supercritical ethanol, *Fuel Process. Technol.* 93 (2012) 35–44. doi:10.1016/j.fuproc.2011.09.010.

- [11] B. Gewert, M. Ogonowski, A. Barth, M. MacLeod, Abundance and composition of near surface microplastics and plastic debris in the Stockholm Archipelago, Baltic Sea, *Mar. Pollut. Bull.* 120 (2017) 292–302. doi:10.1016/j.marpolbul.2017.04.062.
- [12] K. Anastasakis, A.B. Ross, J.M. Jones, Pyrolysis behaviour of the main carbohydrates of brown macro-algae, *Fuel*. 90 (2011) 598–607. doi:10.1016/j.fuel.2010.09.023.
- [13] T. Moriya, H. Enomoto, Characteristics of polyethylene cracking in supercritical water compared to thermal cracking, *Polym. Degrad. Stab.* 65 (1999) 373–386. [https://ac.els-cdn.com/S0141391099000269/1-s2.0-S0141391099000269-main.pdf?\\_tid=dcec67c7-0ccf-48bf-926a-526962899a5b&acdnat=1532020397\\_ab7d5d1d0e285f7f4e19803e818ee590](https://ac.els-cdn.com/S0141391099000269/1-s2.0-S0141391099000269-main.pdf?_tid=dcec67c7-0ccf-48bf-926a-526962899a5b&acdnat=1532020397_ab7d5d1d0e285f7f4e19803e818ee590) (accessed December 12, 2018).

## Chapter 5

---

# Co-liquefaction of bloom-forming Vietnamese algae with common marine plastic pollutants

This work was published (as part of a wider co-authored publication) in Faraday Discussions in February 2017. This work was completed in collaboration with Hanoi University of Mining and Geology (HUMG).

Coma, M., Martinez Hernandez, E., Abeln, F., **Raikova, S.**, Donnelly, J., Arnot, T.C., Allen, M., Hong, D.D., Chuck, C.J., 2017. Organic waste as a sustainable feedstock for platform chemicals. *Faraday Discuss.* 202, 175–195. doi:10.1039/C7FD00070G

## 5.1 Declaration

The work described in this chapter was conducted by the author with the exception of the following:

<sup>14</sup>C analysis was carried out externally at Beta Analytic.

Biomass was cultivated or naturally harvested by personnel at HUMG.

## 5.2 Introduction

The preceding chapters were focused on the effects of varying macroalgae species and growing location on the production of HTL bio-crudes within the context of a marine biorefinery. The macroalgal feedstocks for such a biorefinery could be obtained from aquaculture – macroalgae are already cultivated at large scales across Asia – but it may also be possible to obtain industrially relevant quantities of marine biomass opportunistically. Anthropogenic activities are giving rise to global eutrophication, which leads to the emergence of algal blooms. Algal blooms can comprise one or numerous species of both micro- and macroalgae, as well as cyanobacteria, and occur worldwide, in both saline and freshwater environments.

Algal blooms can cause lasting damage to marine ecosystems, pose a risk to human health, and are extremely costly to remediate. For example, a bloom of the green macroalga *Ulva* sp. in an Olympic sailing venue in China is estimated to have cost \$87.3 million to clean up ahead of the 2008 Olympic games [1], whilst collection of *Ulva* along the Atlantic coast of France between 1989–1992 is estimated to have cost €7.60–122 per tonne (not taking into account economic impacts on tourism and local industries) [2]. The predominant drivers for algal bloom clean-up lie in the avoidance of damage to human health and mitigating loss of tourism revenues, but the spontaneous emergence of vast quantities of biomass could also present a lucrative opportunity for simultaneous environmental remediation and biomass processing.

Although the threat of marine plastic pollution discussed in the preceding chapter is a global problem, developing nations in the process of establishing and optimising waste processing and recycling infrastructure, as well as drafting and enforcing the appropriate legislation and waste disposal regulations, tend to suffer more acutely [3]. It has been suggested that marine plastic pollution in South East Asia, in particular, may exceed global averages [4]. Polyethylene, polypropylene, polystyrene, nylon, polyvinyl alcohol and acrylonitrile butadiene styrene have been identified in seawater and sediments in Singapore [5]; plastic contamination has also been highlighted as an important water quality issue in Vietnam [6].

Chapter 3 of this thesis discussed geographical variations in macroalgal HTL outcomes, whilst Chapter 4 examined the possibility of co-liquefaction of marine biomass with common marine plastic pollutants. This chapter, therefore, aimed to expand on these findings by applying the principles of co-liquefaction to bloom-forming micro- and macroalgae from Vietnam.

### 5.3 Aims

The work described in this chapter aimed to examine co-processing of bloom-forming marine micro- and macroalgae common to Vietnam, with the marine plastic pollutants polyethylene and polypropylene in water. The biomasses examined were the microalgae *Arthrospira platensis* (Spirulina) and the macroalgae *Ulva lactuca* (*Ulva*), harvested from the Hanoi region of Vietnam.

## 5.4 Experimental

### 5.4.1 Materials

*Ulva lactuca* Linnaeus (*Ulva*) was collected from Xom Con, Nha Trang, Khanh Hoa province, Vietnam on June 10, 2016. Prior to analysis and conversion, the macroalga was freeze-dried and milled to <1400 µm diameter. *Arthrospira platensis* (Spirulina) was obtained from Hidumi Pharma Green Science Joint – Stock company, Vietnam, and used without subsequent purification.

## 5.4.2 Batch reactions

To enable simultaneous screening of multiple reactions, batch reactors with internal volume ca. 10 cm<sup>3</sup> were fabricated based using Swagelok® components to be used with a Micromeritics FlowPrep 060 6-port furnace (Fig. 5.4-1).

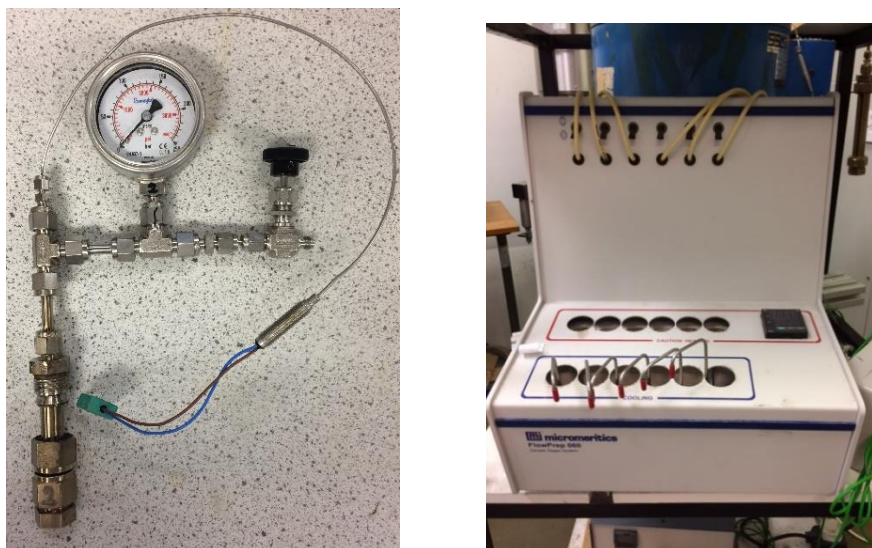


**Figure 5.4-1** – L: batch reactor used for hydrothermal liquefaction; R: six-port Micromeritics FlowPrep 060 furnace

Reactor dimensions were limited by the size of the furnace ports (see Fig. 5.4-1). The reactor body consisted of a length of ½” 316 stainless steel tubing, capped at one end, and connected at the other to a thermocouple, pressure gauge and needle valve to release gaseous products. Stirring occurred through convection within the reactors at high temperatures. At temperatures of 300–350 °C, the expansion of liquid and gaseous water was expected to generate pressures of 86–165 bar, respectively, with an additional contribution from the expansion of air inside the reactor, and gases formed during the reaction. These temperatures and pressures fell within the design pressure ratings of the reactor components (limited by the weakest component: the 1/8” ball valves used to vent the gaseous products – rated to hold a maximum pressure of 172 bar).

In a typical reaction, 0.5 g total feedstock and 5 cm<sup>3</sup> freshly deionised water were used, giving a solid loading of 20 %. Reactors were pre-pressurised to 30 bar with air before reaction.

Reactors were loaded into the pre-heated furnace set to 400 °C and heated within the furnace until the specified reaction temperature (295 °C ± 15 °C) was recorded by a



thermocouple immersed in the reaction mixture. The reactors were then removed from the furnace heating port, and allowed to cool to ambient temperature in the furnace cooling port (see Fig. 5.4-1). This gave an effective time at the maximum reaction temperature of 0 min, and a total time within the HTL range of temperatures of approximately 60 min. Overall heating rates of 4.5–4.9 °C min<sup>-1</sup> were achieved.

### 5.4.3 Extraction

On cooling, gaseous products were vented without further analysis. Gas phase quantification was carried out by subtraction of the remaining product yields from 100 % as described in prior literature [7].

Subsequently, the aqueous phase was decanted from the reactor contents and filtered through a Fisher qualitative filter paper pre-dried overnight at 60 °C. The product yield in the water phase was determined by leaving a 0.2 g aliquot to dry in a 60 °C oven overnight, and scaling the residue yield to the total aqueous phase mass. Aqueous phase residue yield was determined using the following equation:

$$\text{yield}_{\text{AP residue}} = m_{\text{residue}} / (m_{\text{dry biomass}} + m_{\text{plastic}}) \times 100 \% \quad (1)$$

To separate the remaining bio-crude oil and char phase, the reactor was washed repeatedly using chloroform until the solvent ran clear, and filtered through the same filter paper used to separate the aqueous phase (after drying for a minimum of 1 h). The filter paper and collected char were washed thoroughly with chloroform to remove all remaining bio-crude. The filtrate was collected, and solvent removed *in vacuo* (40 °C, 72 mbar) until no further solvent evaporation was observed visually, and bio-crude samples were left to stand in septum-sealed vials venting to the atmosphere *via* a needle for a further 12 h to remove residual solvent. Bio-crude yield was determined using the following equation:

$$\text{yield}_{\text{bio-crude}} = m_{\text{bio-crude}} / (m_{\text{dry biomass}} + m_{\text{plastic}}) \times 100 \% \quad (2)$$

The char yield was calculated from the mass of the retentate collected on the filter paper after drying overnight in an oven at 60 °C.

Solid yield was determined using the following equation:

$$\text{yield}_{\text{solid}} = m_{\text{solid}} / (m_{\text{dry biomass}} + m_{\text{plastic}}) \times 100 \% \quad (3)$$

#### 5.4.4 Characterisation

For macroalgal biomass, bio-crude and char, elemental (CHN) analysis was carried out externally at London Metropolitan University on a Carlo Erba Flash 2000 Elemental Analyser to determine CHN content. (Elemental analyses were carried out at least in duplicate for each sample, and average values are reported.)

GC-MS of bio-crudes was carried out using an Agilent 7890A gas chromatograph fitted with an Agilent HP5-MS capillary column (30 m x 250  $\mu\text{m}$  x 0.25  $\mu\text{m}$ ), and an Agilent 5975C MS detector. Helium (1.2 mL min<sup>-1</sup>) was used as the carrier gas. Samples were injected (splitless injection mode) at 50 °C, held for 1 min, ramped to 290 °C at a rate of 7.5 °C min<sup>-1</sup>, and held for 3 min at 290 °C. Identification of compounds was performed using the NIST mass spectral database.

<sup>1</sup>H NMR of bio-crudes (CDCl<sub>3</sub> solvent) was carried out using a Bruker 400 MHz Bruker Avance III NMR.

<sup>14</sup>C analysis was undertaken by Beta Analytic Inc. (Florida, USA) according to ISO/IEC 17025:2005.

### 5.5 Results and discussion

#### 5.5.1 Hydrothermal co-liquefaction of algal and plastic wastes

Liquefaction of pure *Spirulina* and *Ulva* biomass was carried out and the mass balance calculated (Fig. 5.5-1). A bio-crude yield of 34 % was obtained for *Spirulina*, with a yield of 7 % for *Ulva*. Interestingly, although macroalgae of the genus *Ulva* had been found to be prolific oil producers in previous work described in this thesis, the yield of bio-crude from Vietnamese *Ulva* was substantially lower than from the same species from both the UK [8] or Sweden [9]. This poor yield of bio-crude from the Vietnamese *Ulva* may be a result of its substantially higher proportion of ash – 32.2 %, compared to 17.3 % for *U. lactuca* and 24.5 % for *U. intestinalis* in the UK.

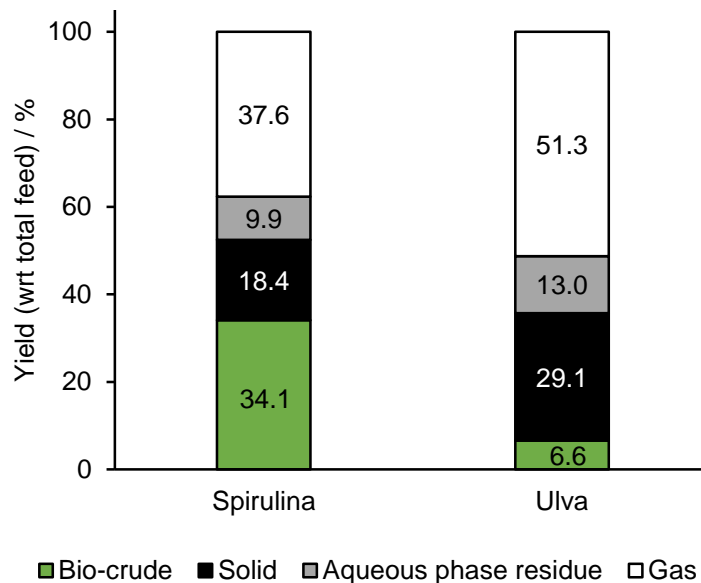


**Figure 5.5-1** – Mass balance of products from HTL of *Spirulina* and *Ulva* (310 °C, 60 min)

Polyethylene and polypropylene processed separately from biomass failed to generate any extractable products. Decomposition of polyethylene in supercritical water has been previously described [10], as well decomposition of polyethylene in water in the presence of organic solvents [11], but neither polyethylene or polypropylene have demonstrated decomposition at subcritical conditions in a purely aqueous medium.

Co-liquefaction of polyethylene with *Spirulina*, and both polyethylene and polypropylene with *Ulva*, led to increases in the overall recovery of bio-crude, despite a smaller quantity of biomass being present in the reaction mixture, suggesting synergistic effects on bio-crude production between biomass and plastics (Fig. 5.5-2). A slight decrease was observed for *Spirulina* with polyethylene, but the bio-crude yield was nonetheless higher than would have been expected from the liquefaction of biomass alone if the plastic had remained entirely inert.

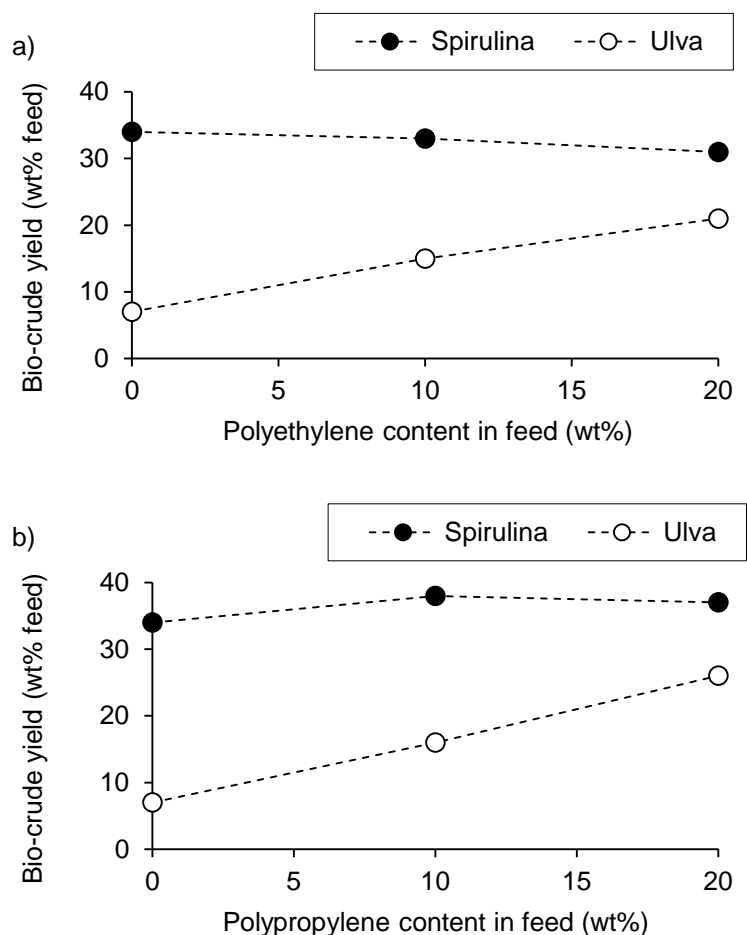


**Figure 5.5-2** – Co-liquefaction bio-crude yields with a) increasing PE content, and b) increasing PP content.

The extent of synergistic effects between the biomass and plastic reactants was calculated using the equation proposed by Wu *et al.* [12]:

$$\text{Synergistic effect (\%)} = Y_{BC} - (X_{macroalgae} \times Y_{macroalgae} + (1 - X_{plastic}) \times Y_{plastic}) \quad (5)$$

where  $Y_{BC}$  represents the yield of bio-crude in a given experiment,  $Y_{\text{component}}$  represents the yield of bio-crude from an individual component when processed in isolation, and  $X_{\text{component}}$  represents the mass fraction of each component in the reaction mixture. A positive value of synergistic effect indicates that a greater yield of bio-crude was obtained from the blended feedstock than the linear sum of the yields expected from each the individual feedstocks, and vice versa.

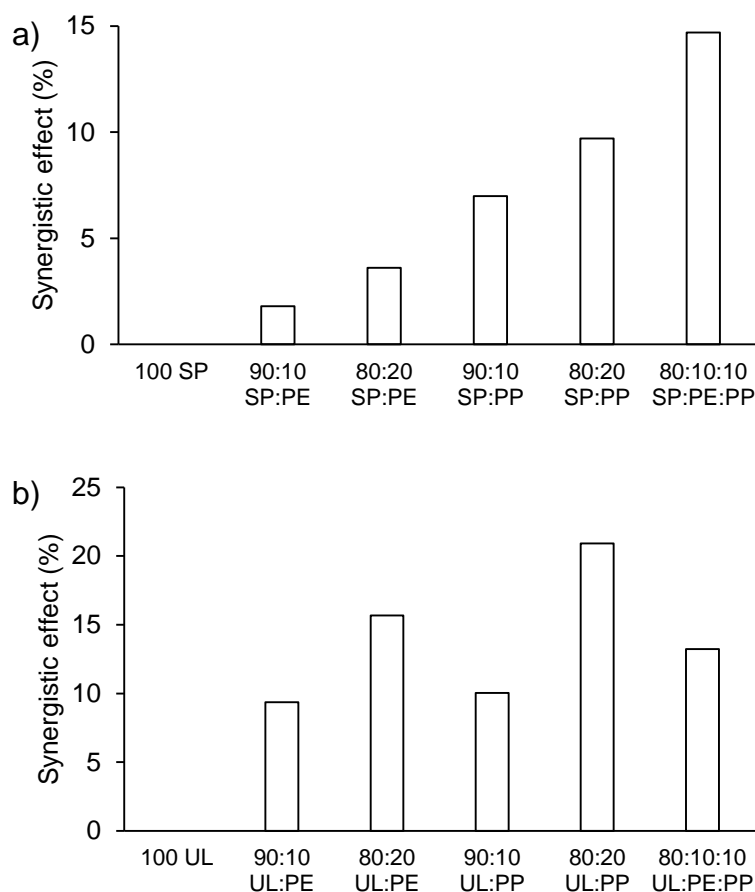


**Figure 5.5-3** – Extent of synergistic effects on bio-crude production during co-liquefaction of a) *Spirulina* and b) *Ulva* with polyethylene (PE) and polypropylene (PP)

Substantial synergistic effects were observed between the conversion of the macroalgae and plastics. For *Spirulina*, synergistic effects with polyethylene were modest, but synergistic effects observed on the addition of polypropylene were more substantial, reaching 7 % and 9.7 % for 20 % blends with polyethylene and polypropylene, respectively. Interestingly, blending polyethylene with polypropylene caused synergistic effects on bio-crude production that amounted to more than the sum of their parts – a total synergistic effect of 14.7 %.

For *Ulva*, synergistic effects were more pronounced. For 10 % blends of polyethylene and polypropylene, synergistic effects were in the region of 10 %, although combining the two plastics only contributed to a 13.2 % synergistic effect, unlike for *Spirulina*. However, the synergistic effects of co-liquefaction with single plastics at a 20 % blend were more pronounced, with a maximum of 20.9 % observed for a 20 % polypropylene blend.

The synergistic effects between the macroalgae and the plastics, compared to the inactivity of the plastics in isolation, suggests that the presence of biomass reactive

fragments affects the thermal stability of the plastics. The greater synergistic effects observed for *Ulva* may also result from the elevated levels of ash within the biomass. The presence of metals in biomass ash can promote plastic decomposition [13], which can, in turn, become hydrogen donors, stabilising biomass radicals to form oil-phase products.

Elemental analysis of the bio-crudes (Fig. 5.5-4) demonstrated that the addition of plastics to the feedstock led to an increase in H/C ratio and a drop in the overall bio-crude nitrogen content, decreasing to a minimum of 3.7 % for *Ulva* co-processed with a blend of polyethylene and polypropylene. These compositional changes amount to an improvement in overall bio-crude fuel properties: higher H/C ratios indicate higher aliphatic content in oils, and heavy oils with a higher H/C have been shown to have better cracking performance in downstream fuel production [14], whilst high bio-crude nitrogen levels would necessitate extensive denitrogenation prior to use as a fuel. High nitrogen levels lead to a range of problems in downstream oil utilisation, impacting on storage stability, and denaturing refinery catalysts [15].

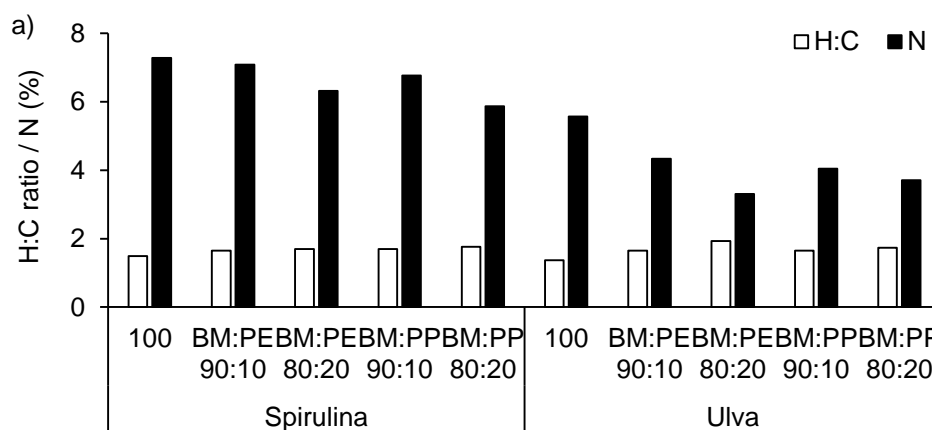


**Figure 5.5-4** – H/C ratio and nitrogen content in bio-crudes

Bio-crudes were analysed using  $^1\text{H}$  NMR, and the ratio of  $\text{CH}_2:\text{CH}_3$  peak areas used as a proxy to gauge the level of branching (Fig. 5.5-5).

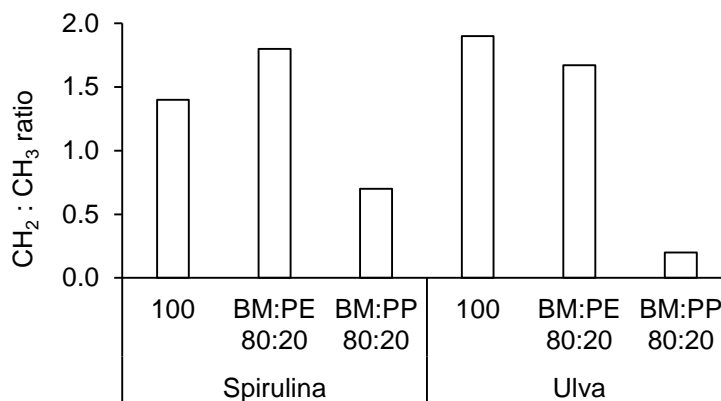


**Figure 5.5-5** – Ratio of CH<sub>2</sub> to CH<sub>3</sub> peak areas quantified using <sup>1</sup>H NMR

Co-liquefaction with polyethylene gave rise to a slight increase in CH<sub>2</sub>:CH<sub>3</sub> ratio (Fig. 5.5-5) for *Spirulina* bio-crudes, with a slight decrease for *Ulva*. However, on addition of polypropylene, a substantial decrease in CH<sub>2</sub>:CH<sub>3</sub> ratio was seen in both cases, suggesting that fragmentation of the polypropylene chain was occurring, and the smaller fragments partitioning to the bio-crude products. Additional signals around  $\delta = 5.4$  ppm suggest the presence of aldehydes or ketones.

Bio-crude composition was analysed in greater detail using GC/MS. *Spirulina* bio-crudes were high in nitrogenous compounds, including heterocycles, due to the high protein content of *Spirulina*. Aromatics are also present, alongside fatty acids presumably originating from lipid decomposition. There was also a significant contribution from long-chain hydrocarbons, with heptadecane dominating. Co-liquefaction with polyethylene and polypropylene gave rise to multiple subtle changes in composition, which could not be unambiguously quantified.

*Ulva* bio-crude was comparatively higher in oxygenated species, with some contribution from sulfurous compounds – *Ulva* macroalgae are known to have high sulfur levels, so this was unsurprising. A number of higher alkanes were also present. Co-processing with plastics gave rise to an increasing level of C<sub>10</sub>–C<sub>20</sub> hydrocarbons, notably, saturated C<sub>20</sub> hydrocarbons formed in the presence of polyethylene (Fig. 5.5-6). The presence of these compounds in the bio-crude suggests that direct fragmentation of polyethylene chains occurs under HTL conditions. Long-chain ketones, also seen for co-liquefaction of polyethylene with *L. digitata* in Chapter 4, confirmed the presence of oxygenated species observed by NMR, which likely originate from oxidative depolymerisation of hydrocarbons. Some nitrogenous compounds, such as dodecanamide, were depleted in the presence of both polyethylene and polypropylene. This decrease is mirrored by the decrease in total N observed by elemental analysis.

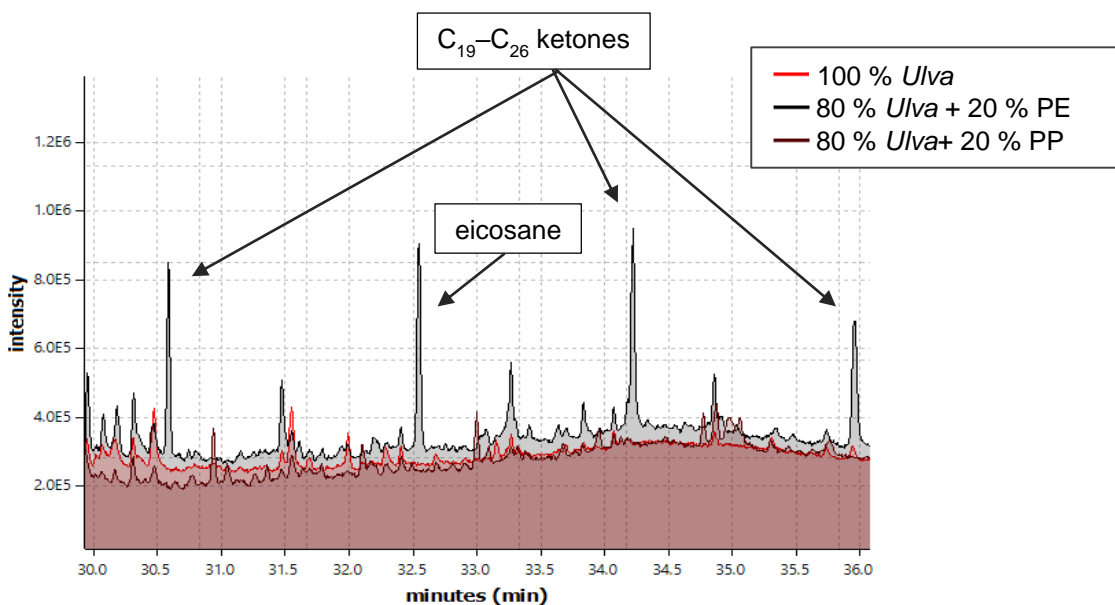


**Figure 5.5-6** – Overlaid GC/MS chromatogram of bio-crudes produced from pure *Ulva* and co-processing with polyethylene and polypropylene

All analysis undertaken suggested that some level of plastic fragmentation was occurring, and fragments were partitioning to the bio-crude phase. To estimate the rate of plastic incorporation into the bio-crudes,  $^{14}\text{C}$  analysis was undertaken. This allowed an estimate of the proportion of the bio-crude oils composed of carbon of fossil origin (in other words, originating from the plastics), compared to the level of biogenic (algal) carbon, as previously described in Chapter 4. The proportion of bio-crude material originating from plastics, scaled to the total bio-crude yields, is presented in Fig. 5.5-7.

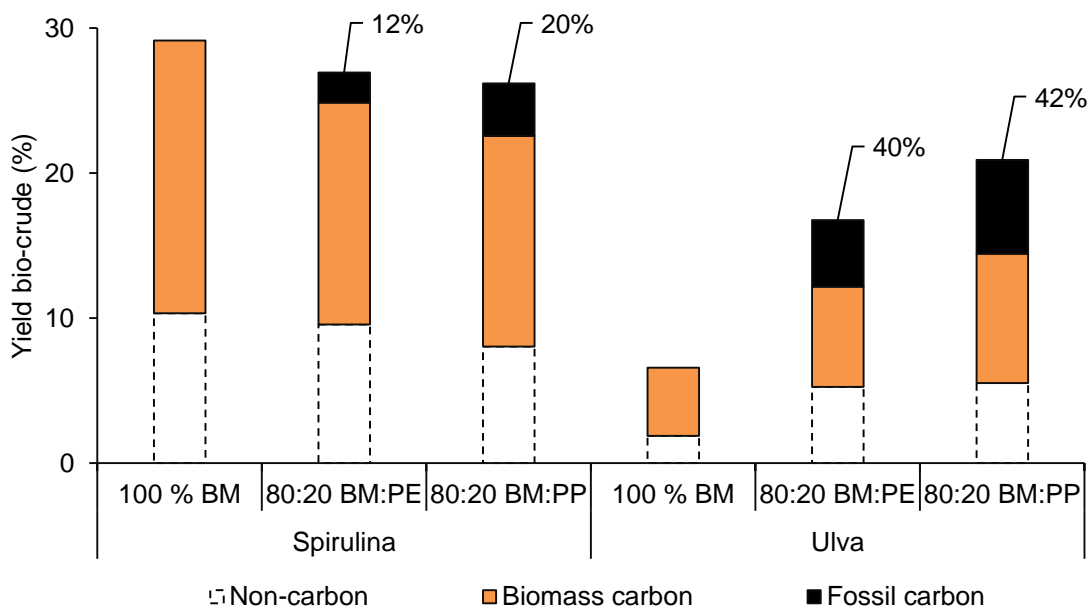


**Figure 5.5-7** – Bio-crude yield and biogenic vs. fossil carbon distribution. Overall percentages of fossil carbon are labelled.



With increasing blend levels of polyethylene and polypropylene, the overall proportion of bio-crude carbon originating from fossil sources increased, indicating that incorporation of plastics into the bio-crude products was occurring, somewhat higher for polypropylene than polyethylene. For *Spirulina*, this was accompanied by a slight decrease in the overall level of biogenic carbon in bio-crudes, suggesting that the presence of plastics had an inhibitory effect on biomass conversion – a similar effect to that observed for *L. digitata*, as described in Chapter 4. However, for the *Ulva* bio-crudes, the opposite was true. The presence of plastics appeared to increase the total levels of biogenic carbon partitioning to the bio-crude phase, as well as contributing to a direct increase in fossil carbon. The presence of plastic leads to higher conversion of biomass to bio-crude products in this case, with the effect slightly more pronounced in the case of polypropylene than polyethylene.

Previous studies have suggested that donation of hydrogen from polypropylene during co-liquefaction may promote the Maillard reaction between carbohydrates and proteins [12], causing higher levels of biogenic material to partition to the oil phase, rather than solid char products. The generation of hydrogen radicals from plastic may also prevent recondensation of organic fragments into larger, insoluble molecules, thus suppressing char formation.

Based on the  $^{14}\text{C}$ , the overall conversion of plastic carbon to bio-crude carbon can be calculated.

**Table 5.5-1** – Distribution of carbon from the initial plastic into the bio-crude phase

	Plastic	Initial plastic loading (wt %)	Plastic C partitioning to bio-crude (%)
Spirulina	PE	20	14.3
	PP	20	21.3
Ulva	PE	20	31.6
	PP	20	38.0

Up to 21 % of the carbon in the plastic feedstock was incorporated into the bio-crude oil for *Spirulina* and up to 38 % was converted to bio-crude products for *Ulva* – substantially higher than for the *L. digitata* examined in Chapter 4, where the highest plastic conversion to bio-crude products was only 7 %. The difference is likely to be attributable to the differing biochemical compositions of different biomass feedstock species, specifically the inorganic fraction.

### **5.5.2 Fate of remaining plastics**

Although it has been shown that a proportion of the plastic feed is incorporated into the bio-crude oil products, the remaining material distributed between the solid and aqueous phases. The solid char phase product yield increased on the incremental addition of plastics (Fig. 5.5-8a), with increasing solid phase carbon content (Fig. 5.5-8b) and depleted nitrogen (Fig. 5.5-8c), indicating some level of plastic deposition in the solid phase, either as unreacted plastics, or fragmented oligomers too large to be chloroform-soluble.

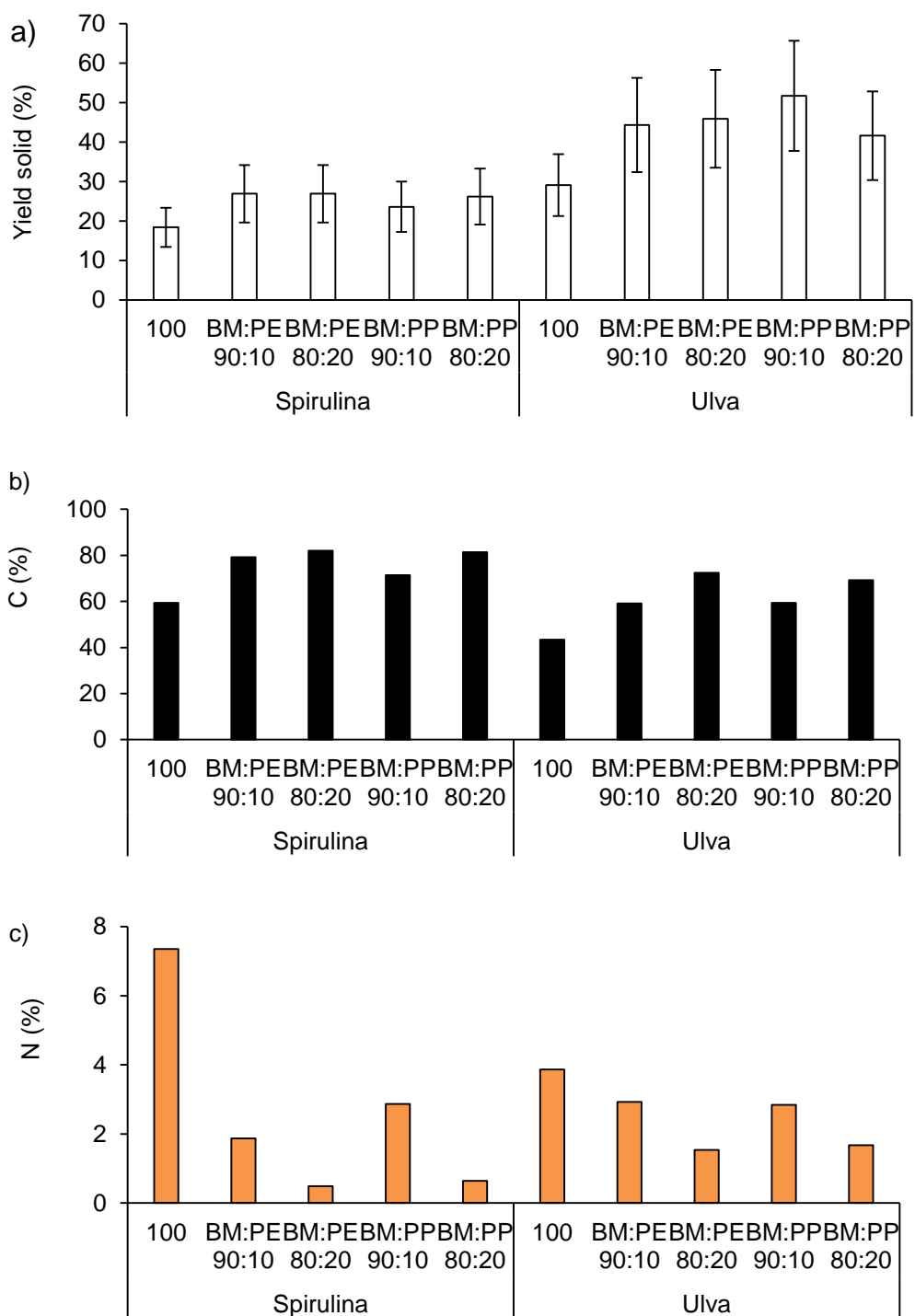


**Figure 5.5-8** – Analysis of the solid residue from the HTL of *Spirulina* and *Ulva* (320 °C, 40 mins) where a) solid residue yield with increasing plastic, b) carbon content (%) of the solid phase products and c) nitrogen content (%) of the solid phase products.

## 5.6 Conclusions

The aim of this chapter was to expand on previous work conducted in the UK and examine co-liquefaction of common marine plastic pollutants with bloom-forming micro-

and macroalgae from Vietnam for simultaneous remediation of marine pollutants and fuel production. Despite polyethylene and polypropylene being inert to HTL processing in isolation, co-processing with biomass promoted plastic decomposition and partitioning of polymer fragments and secondary reaction products to oil phase products. Synergistic effects between biomass and polymers led to substantial improvements in bio-crude yield for the Vietnamese *Ulva* macroalgae, whilst bio-crude fuel properties were improved by co-liquefaction with plastics for both *Ulva* and *Spirulina*. Substantial conversion of plastics to bio-crude products was observed, H/C ratios indicated that aliphatic content increased on co-liquefaction with both polyethylene and polypropylene, and increased levels of chain branching were seen for co-liquefaction with polypropylene. Furthermore, the presence of plastics in the feedstock matrix for *Ulva* caused an increase in biomass carbon partitioning to the bio-crude oil phase products.

## 5.7 References

- [1] X.H. Wang, Economic Cost of an Algae Bloom Cleanup in China's 2008 Olympic Sailing Venue, *Eos* (Washington, DC). 90 (2009) 238–239. <https://agupubs.onlinelibrary.wiley.com/doi/pdf/10.1029/2009EO280002> (accessed August 31, 2018).
- [2] R.H. Charlier, P. Morand, C.W. Finkl, A. Thys, Green tides on the Brittany coasts, *Environ. Res. Eng. Manag.* 3 (2007) 52–59.
- [3] M.S. Islam, M. Tanaka, Impacts of pollution on coastal and marine ecosystems including coastal and marine fisheries and approach for management: a review and synthesis, *Mar. Pollut. Bull.* 48 (2004) 624–649. doi:10.1016/j.marpolbul.2003.12.004.
- [4] P.A. Todd, X. Ong, L.M. Chou, Impacts of pollution on marine life in Southeast Asia, *Biodivers. Conserv.* 19 (2010) 1063–1082. doi:10.1007/s10531-010-9778-0.
- [5] K.L. Ng, J.P. Obbard, Prevalence of microplastics in Singapore's coastal marine environment, *Mar. Pollut. Bull.* 52 (2006) 761–767. doi:10.1016/j.marpolbul.2005.11.017.
- [6] L. Lahens, E. Strady, T.C. Kieu-Le, R. Dris, K. Boukerma, E. Rinnert, J. Gasperi, B. Tassin, Macroplastic and microplastic contamination assessment of a tropical river (Saigon River, Vietnam) transversed by a developing megacity, *Environ. Pollut.* 236 (2018) 661–671. doi:10.1016/j.envpol.2018.02.005.
- [7] H.K. Reddy, T. Muppaneni, S. Ponnusamy, N. Sudasinghe, A. Pegallapati, T. Selvaratnam, M. Seger, B. Dungan, N. Nirmalakhandan, T. Schaub, F.O. Holguin, P. Lammers, W. Voorhies, S. Deng, Temperature effect on hydrothermal liquefaction of *Nannochloropsis gaditana* and *Chlorella* sp., *Appl. Energy.* 165 (2016) 943–951. doi:10.1016/j.apenergy.2015.11.067.
- [8] S. Raikova, C.D. Le, T.A. Beacham, R.W. Jenkins, M.J. Allen, C.J. Chuck, Towards a marine biorefinery through the hydrothermal liquefaction of macroalgae native to the United Kingdom, *Biomass and Bioenergy.* 107 (2017) 244–253. doi:10.1016/j.biombioe.2017.10.010.
- [9] S. Raikova, J. Olsson, J. Mayers, G. Nylund, E. Albers, C.J. Chuck, Effect of geographical location on the variation in products formed from the hydrothermal liquefaction of *Ulva intestinalis*, *Energy & Fuels.* (2018) Accepted manuscript.

doi:10.1021/acs.energyfuels.8b02374.

- [10] T. Moriya, H. Enomoto, Characteristics of polyethylene cracking in supercritical water compared to thermal cracking, *Polym. Degrad. Stab.* 65 (1999) 373–386. [https://ac.els-cdn.com/S0141391099000269/1-s2.0-S0141391099000269-main.pdf?\\_tid=dcec67c7-0ccf-48bf-926a-526962899a5b&acdnat=1532020397\\_ab7d5d1d0e285f7f4e19803e818ee590](https://ac.els-cdn.com/S0141391099000269/1-s2.0-S0141391099000269-main.pdf?_tid=dcec67c7-0ccf-48bf-926a-526962899a5b&acdnat=1532020397_ab7d5d1d0e285f7f4e19803e818ee590) (accessed July 19, 2018).
- [11] S.L. Wong, N. Ngadi, N.A.S. Amin, T.A.T. Abdullah, I.M. Inuwa, Pyrolysis of low density polyethylene waste in subcritical water optimized by response surface methodology, *Environ. Technol.* 37 (2016) 245–254. doi:10.1080/09593330.2015.1068376.
- [12] X. Wu, J. Liang, Y. Wu, H. Hu, S. Huang De, K. Wu, Co-liquefaction of microalgae and polypropylene in sub-/super-critical water, *RSC Adv.* 7 (2017) 13768. doi:10.1039/c7ra01030c.
- [13] B. Singh, N. Sharma, Mechanistic implications of plastic degradation, *Polym. Degrad. Stab.* 93 (2008) 561–584. doi:10.1016/j.polymdegradstab.2007.11.008.
- [14] X. Meng, C. Xu, L. Li, J. Gao, Cracking Performance and Feed Characterization Study of Catalytic Pyrolysis for Light Olefin Production, 25 (2011) 1357–1363. doi:10.1021/ef101775x.
- [15] G.H.C. Prado, Y. Rao, A. de Klerk, Nitrogen Removal from Oil: A Review, *Energy & Fuels.* 31 (2017) 14–36. doi:10.1021/acs.energyfuels.6b02779.

# Chapter 6

---

## Conclusions and future work

## 6.1 Conclusions

The overarching aim of this thesis was to explore the effect of species, location and possible contamination on the hydrothermal liquefaction of macroalgae with a view to developing a model marine biorefinery.

The effect of species on HTL feedstock suitability was examined using thirteen South West U.K. macroalgae species, nine of which were unexplored in previous literature. A detailed assessment of biomass biochemical composition in terms of crude protein, lipid, carbohydrate and ash content was carried out, with a view to understand the correlation between biochemical composition and bio-crude production, and ultimately design a predictive model for bio-crude yield. Although, in agreement with prior work, lipids were found to account for a substantial proportion of the variation in bio-crude yield, the overall relationship between feedstock composition and bio-crude yield was complex, and could not be unilaterally predicted for all species using a single correlation. Secondary interactions between reactive biomass fragments play a significant role in determining HTL outcomes, which are not accounted for using a model based on linearly additive yields from individual biochemical components.

Within the species examined, green macroalgae of the genus *Ulva* (*U. lactuca* and *U. intestinalis*) gave the highest bio-crude yields, albeit at the expense of nitrogen content, which was elevated due to the high protein content. However, feedstock nitrogen contents overall were substantially lower than those seen for microalgae, and correspondingly lower ammonia concentrations were observed in the aqueous phase products for all species examined, potentially limiting their potential for nutrient recovery and utilisation as a fertiliser or growth medium for algae or higher plants.

Having established *Ulva* macroalgae as promising bio-crude producers within a UK context, the effect of geographical variation on feedstock suitability was examined. Three samples of *U. intestinalis* were wild-harvested in each of eight distinct locations spanning 1,200 km around the coast of Sweden, and used as feedstocks for HTL. The bio-crude yields observed were substantially lower than those observed for the same species harvested in the U.K. (9–20 %, *c.f.* 29 %). Furthermore, there was substantial variability in biomass compositions and bio-crude yields between samples, not only between sampling sites, but also between the three samples gathered within the same site. Metal content fluctuated substantially, influenced by different sources of marine contamination at each site. It follows that there is unlikely to be a single 'optimal' species to supply a marine biorefinery, and different species are likely to produce optimal results in different geographical locations.



Within a functioning marine biorefinery, marine pollutants, including plastics, are likely to be present alongside biomass, and play a role in determining HTL product distribution and processing conditions. The effect of plastics commonly found in marine environments (specifically, polyethylene, polypropylene and nylon 6) on HTL was, therefore, examined. Four common U.K. macroalgae species were used. Despite being unreactive under HTL conditions when processed in isolation, polyethylene and polypropylene displayed a degree of degradation when processed alongside macroalgal biomass, forming bio-crude phase products. Modest synergistic effects between the macroalgae and plastics were observed, with improvements in bio-crude fuel properties (increases in HHV and decreases in nitrogen content) observed for polyethylene and polypropylene. Nylon 6, however, originating predominantly from discarded fishing gear within marine environments, depolymerised readily to monomeric caprolactam under hydrothermal conditions, both in the presence of macroalgae and in isolation, although synergistic effects were also observed when the two were processed together. Caprolactam distributed between the bio-crude and aqueous phases, with detrimental effects for bio-crude quality. Hydrothermal liquefaction has, therefore, been shown to be an effective means of processing marine plastics, although the isolation of certain types of plastic for separate processing (e.g. depolymerisation of nylon and other condensation polymers) may present an additional, separate, value stream.

Although HTL at large scales is likely to require cultivated macroalgae, HTL may also be used as an on-demand environmental remediation tool through the use of opportunistically harvested biomass from algal blooms as a feedstock. Hence, the effect of plastic co-processing and geographical variation was examined simultaneously, using bloom-forming micro- and macroalgae harvested in Vietnam. Vietnamese *U. intestinalis* produced a substantially lower yield of bio-crude than the same species from either the U.K. or Sweden, but the synergistic effects of co-processing with polyethylene and polypropylene were substantially stronger. Substantial synergistic effects on bio-crude yield were also observed for *Spirulina* microalgae. The presence of plastics in the feedstock matrix for *U. intestinalis* caused an increase in biomass carbon partitioning to the bio-crude oil phase products.

Through the work described in this thesis, HTL has been demonstrated to be a powerful tool for the processing of macroalgal biomass and simultaneous remediation of marine environments. Species, geography and the presence of marine pollutants play a significant role in determining bio-crude yields and properties, and, as such, no single 'optimal' feedstock or set of processing conditions exist: local environmental conditions must be taken into account in the design of future marine biorefineries.

## 6.2 Future work

The current project has examined the liquefaction of a number of species of macroalgae worldwide, and explored the effect of plastic pollutants on bio-crude production. The bio-crude generated is a highly promising fuel precursor, but cannot function as a fuel without further treatment. Hence, the upgrading of macroalgal bio-crude to generate products suitable for direct use as a fuel, or for co-refining with crude oils in conventional fossil refineries, would constitute a sensible route of further study. Catalytic upgrading has been discussed at length for microalgal bio-crudes, but macroalgal bio-crudes have thus far attracted little attention. Macroalgal crudes are similar, although not identical, to their microalgal analogues, so similar upgrading protocols could be adopted.

This report has focused predominantly on the production of bio-crude; further research focusing on the valorisation of the co-product phases would be beneficial to the development of future marine macroalgal biorefineries. The aqueous phase from HTL of microalgae has already been explored for nutrient recovery *via* microalgae cultivation and energy recovery *via* CHG, but aqueous phases have been less well-characterised for macroalgal HTL. Dissolved nitrogen and phosphorus tend to be comparatively lower for HTL aqueous phases derived from macroalgae than for microalgae, but, given the high dilutions that are typically required for microalgal HTL aqueous phases to be used as a suitable growth medium, macroalgal HTL aqueous phases may still be suitable, albeit at higher concentrations. Hence, the valorisation of macroalgal HTL process waters through the cultivation of microalgae could be explored. Additionally, the use of HTL aqueous phases as fertilisers for terrestrial plants has yet to be assessed – this could be assessed for macroalgal HTL process water using fast-growing plants such as tomatoes or *Arabidopsis*.

The gaseous products of HTL, comprising predominantly CO<sub>2</sub>, have been largely overlooked in previous literature. The potential for utilisation of the gas stream to supplement microalgal cultivation (perhaps in tandem with the use of the aqueous products as a growth medium). With purification of the gas phase, a higher-purity CO<sub>2</sub> stream could potentially be used for synthetic applications, such as the manufacture of sustainable polycarbonates.

Biorefineries produce chemicals and materials alongside fuels and energy. Within a future biorefinery, extraction of high-value, low-volume chemical components (such as salts or alginates for speciality food or personal care markets) from biomass prior to HTL may be beneficial for process economics, although, understandably, this could have substantial impacts on HTL product yields and compositions. The fractionation of bio-

crude to extract high-value molecules, or extraction of organics from the aqueous phase, could also be explored.

The effect of geographical location on macroalgae suitability as a feedstock for HTL was explored in Chapter 3. However, seasonality also plays a role in macroalgae composition, and is likely to affect macroalgae differently in different locations worldwide. A study of macroalgal HTL using the same species harvested at regular intervals over the course of a year would be vital for the design of a functioning marine biorefinery. In order to enable continuous production of bio-crudes and other products, a rotating crop system may be necessary – a comprehensive assessment of feedstock options will be necessary once a location has been selected.

In Chapter 4, the co-processing of macroalgal biomass with plastics, including nylon 6, was examined. Nylon 6 decomposed readily under hydrothermal conditions, generating oil- and aqueous-phase monomeric caprolactam. Its presence is detrimental to bio-crude properties, but its extraction could provide a novel route for value addition. To this end, the fractionation of bio-crudes, and separation protocols for caprolactam specifically, would need to be developed.

In Chapter 5, the synergistic effects on co-processing *Spirulina* and *Ulva* sp. were found to be significantly stronger than those seen for the marine macroalgae discussed earlier in Chapter 4. This is likely to be attributable to differences in the biochemical composition of the algal biomass. In particular, metals in the inorganic fraction of the algal biomass may be playing a catalytic role in plastic conversion to bio-crude products. As such, a more detailed examination of the inorganic composition of the *Spirulina* and *Ulva* would be highly beneficial. If any individual inorganic component conducive to plastic conversion can be isolated, this could potentially inform the development of novel additives, which could improve HTL yields within a marine biorefinery context.

Although cultivated biomass is likely to be the most reliable route to supplying a marine biorefinery, there is scope for utilisation of bloom-forming macroalgae on an opportunistic basis. The design of a portable pilot-scale system able to be deployed to regions experiencing problematic blooms and generate bio-crude and other products *in situ* could form an interesting project further down the line.

Although the production of biofuels reduces reliance on fossil resources, the cultivation and harvesting of macroalgae, as well as the process of HTL, consume a substantial amount of energy. A techno-economic and life cycle assessment for a marine macroalgal HTL biorefinery would need to be carried out. This would help to determine the most financially and energetically favourable cultivation and processing conditions, as well as

a range of valorisation options for the co-product phases. Policy considerations will also play a huge role in the implementation of novel marine biorefineries in the U.K. and elsewhere worldwide, so will need to be taken into consideration.